Quorum sensing and surface attachment in *Acinetobacter baumannii*

Mario López Martín, MSc.

Thesis submitted to the University of Nottingham for the degree of Doctor of Philosophy

April 2020

Declaration of originality

I declare that the work presented here is my own, except where otherwise stated and clearly acknowledged. Neither this work nor any part of it has been submitted for any assessment or award at the University of Nottingham or elsewhere.

Mario López Martín, April 2020.

Abstract

Acinetobacter baumannii is a Gram-negative nosocomial pathogen that causes a wide range of infections, including ventilator-associated pneumonia and soft tissue infections, mostly in seriously ill patients. Even though several virulence-associated factors have been described, the exact mechanisms of infection and the overall regulation of *A. baumannii* virulence are still poorly understood. One of the regulatory systems involved in virulence in many other pathogenic bacteria is quorum sensing (QS), a cell density-dependent bacterial communication system that relies in the accumulation of an extracellular signal. In Gram-negative bacteria, these are usually *N*-acyl-homoserine lactones (AHLs)) and they facilitate coordination of gene expression within a bacterial population. *A. baumannii* possesses a single LuxR/LuxI-type QS locus, named AbaR/AbaI, that, despite being reported in previous publications to be involved in surface motility and biofilm formation, remains poorly characterized.

In this project the role of *ABUW_3775* (here named a*baM*), a gene encoding an RsaM orthologue, was investigated in the hypervirulent *A. baumannii* strain AB5075. RsaM is known to be involved in virulence gene regulation and QS repression in the plant pathogens *Pseudomonas fuscovaginae*, *Burkholderia glumae* and *Burkholderia cenocepacia*, but its role in *A. baumannii* has not been reported. Phenotypic characterization of *abaM* and QS in *A. baumannii* AB5075 was undertaken. Using an *abaM* transposon mutant, we detected and quantified AHLs by LC-MS/MS, revealing a 100 to 875-fold increase in production of the major AHL identified (*N*-(3-hydroxydodecanoyl)-L-homoserine lactone; OHC12) when compared with the wild-type parental strain at different time points throughout growth. This transposon mutant also exhibited significantly greater surface motility on 0.3% Eiken agar and attachment to polystyrene. Additionally, AbaM was required for full virulence in

Galleria mellonella larvae. The role of QS was also examined in these phenotypes, with the *abaI* transposon mutant showing complete lack of AHL production, reduced surface motility, increased attachment to polystyrene in the opaque phase variant and reduced attachment in the translucent phase variant. However, virulence in *G. mellonella* was the same as the wild-type. Exogenous addition of OHC12 increased surface motility and attachment to polystyrene, but did not affect virulence.

The regulatory roles of QS and AbaM, as well as the regulation of their expression, were investigated. A promoter-*lux* fusion showed that *abaM* expression is negatively auto-regulated but positively modulated by QS and OHC12, highlighting the connection between QS and AbaM. Moreover, screening of a diverse range of AHLs and *N*-(3-oxododecanoyl)-L-homoserine lactone-derived compounds showed that AbaR had a high specificity for 3-modified AHLs of 10-14 carbons length, as well as revealing some interesting AbaR inhibitors and agonists. RNA-seq analysis of the opaque phase variants of *abaM* and the QS synthase (*abaI*) mutants comparing them with the wild-type strain revealed that they possess overlapping regulons, with AbaM co-regulating around 22% of the genes differentially expressed by the *abaI* mutant. Moreover, both mutants strongly overexpressed the genes encoding for proteins required for the assembly of the Csu (chaperone-usher) type I pili, which is involved in biofilm formation. The *abaM* mutant also showed increased expression of the putative acinetin 505 biosynthetic operon, which has also been reported to be involved in biofilm formation. Finally, enrichment analysis of the RNA-seq data showed that many of the differentially expressed genes in both *abaM* and *abaI* mutants were involved in metabolism, transport and energy production. The RNA-seq data was validated by quantitative real-time PCR (qPCR).

Given the RNA-seq data, Csu pili were investigated in more detail, as these pili play key roles in *Acinetobacter* attachment and biofilm formation. A promoter-*lux* fusion confirmed that *csuA/BABCDE* was expressed at higher levels in the *abaM* mutant than in the wild-type strain. Attachment assays using *csuA/B* and *csuE* transposon mutants showed a reduction in attachment to polypropylene compared to the wild-type strain, being this reduction higher in the *csuE* mutant than in the *csuA/B* mutant. Using an *E. coli* BL21 recombinant strain expressing the *A. baumannii* ATCC 19606 Csu pili, a library of (meth)acrylates was tested to establish the contribution of this pilus to surface attachment and recognition of chemically diverse polymers, as a previous hypothesis suggested that Csu pili attached preferably to hydrophobic surfaces. However, no correlation was found between the physicochemical properties of the materials and bacterial attachment. Moreover, the recombinant strain strongly attached to ethylene glycol dicyclopentenyl ether acrylate (EGDPEA), a broad spectrum bacterial anti-attachment polymer previously characterized. Interestingly, EGDPEA prevented biofilm formation by the *A. baumannii* AB5075 wild-type.

In summary, the RsaM orthologue AbaM and QS have been phenotypically and genetically characterized in *A. baumannii* AB5075, elucidating their role in attachment, surface motility, AHL production, virulence in *G. mellonella* and gene regulation. Finally, the results of this study involving Csu pili suggest that they might not be the only factor involved in surface sensing and 'deciding' whether a surface is suitable for attachment and formation of biofilm or not. This work provides a deeper understanding of QS, gene regulation, attachment and virulence in *A. baumannii*, but more detailed future investigations will be required for a more comprehensive understanding of the virulence and physiology of this challenging pathogen.

Acknowledgments

First of all, I would like to thank my principal supervisor, Professor Paul Williams, who gave me the opportunity to work in this project and guided me during the last four years. I would also like to thank my other supervisor, Prof. Alexander Morgan, for his help and guidance.

Thanks to all the people I met in the last years and gave me a hand in one or another way: Edu, Matt, Manu, Josh, Maria, Ewan, Jenni, Clair, Ale… the list is quite long, but you who you are. Special thanks to Jean and Carol, who not only shared bench with me for four years, but also shared support, advice, jokes and good times in general. Working in the lab was much easier with them around.

I cannot leave out all the people that gave me technical support in all my experiments: Nigel Halliday (AHL detection by LC-MS/MS), Alex Truman (AHL and other compounds synthesis), Prof. Phil N. Rather (identification of phase variants), Prof. Robert M. Shanks (who kindly provided *A. baumannii* compatible plasmid pMQ557) and Prof. Anton Zavialov (who kindly provided the pBAD_*csu* plasmid).

Everyone who is or has been in this crazy world we call research knows how easy it is to drag the stress and worries out of the lab. Luckily, I had quite a few people that supported me there as well.

Cristina is the main reason I managed to keep going in the moments I felt things were not working out. She was there every time I needed. She gave all the support and confidence (and more) one can dream about. Gràcies.

Thanks to my family. I always loved how they just assumed I was going to do great no matter what. It just makes is much easier to keep going when things get harder having a family that supports you in the good moments and the ones that are not so good.

Thanks to Carol, Ioanna and Miriam, with whom I shared house for two years in which we had lots of fun and dealt with some weird people and situations. One way or another, we made lots of funny memories together.

And last but not least, thanks to my lifelong friends. Never ceases to amaze me how can I go back after being away for months and we can just go out as if we just met the day before. It is unbelievably comforting how we can have fun with anything at any time. Thanks, guys.

Table of Contents

Declaration of originality **1**

Abstract **2**

Acknowledgments **5**

Table of Contents **7**

List of Figures **12**

List of Tables **16**

Abbreviations **17**

A note about phase variation **20**

1. Introduction **21**

1.1. The *Acinetobacte*r genus 21

1.1.1. The *A. baumannii* complex 22

1.1.1.1. Infections caused by *A. baumannii* 25

1.1.1.2. *A. baumannii* environmental persistence 28

1.1.1.3. *A. baumannii* AB5075: an hypervirulent multi-drug resistant strain 30

1.2. Virulence in *A. baumannii* 32

1.2.1. Virulence factors in *A. baumannii* 32

1.2.1.1. OmpA 32

1.2.1.2. Other outer membrane proteins (OMPs) 33

1.2.1.3. Outer membrane vesicles (OMVs) 34

1.2.1.4. Lipopolysaccharide 34

1.2.1.5. Capsule 35

1.2.1.6. Pili 36

1.2.1.7. Secretion systems 38

1.2.1.8. Iron acquisition 41

1.2.1.9. Efflux systems 42

1.2.1.10. Other relevant virulence factors 43

1.2.2. Virulence gene regulation in *Acinetobacter baumannii* 44

1.2.2.1. Two-component systems 44
1.2.2.2. H-NS 49
1.2.2.3. AtfA 50
1.2.2.4. Hfq 50
1.2.2.5. Blue light 51
1.3. Phase variation 51
1.3.1. Phase variation in *A. baumannii* 52
1.4. Attachment and biofilm formation 55
1.4.1. Attachment and biofilm formation in *A. baumanni*i 58
1.5. Quorum sensing 61
1.5.1. Quorum sensing in Gram-negative bacteria 63
1.6. Aims and objectives of the project 67
2. Materials and methods 68
2.1. Strains and growth conditions 68
2.2. Bacterial stocks for long term storage 70
2.2.1. *E. coli* stocks 70
2.2.2. *A. baumannii* stocks 70
2.3. DNA manipulation and gene cloning 71
2.3.1. Genetic constructs based on pUC18T-mini-Tn*7*T 76
2.3.1.1. Hygromycin selectable mini-Tn*7* construction 76
2.3.1.2. *lux*-based P*abaM* and P*abaI* reporter construction 76
2.3.1.3. Insertion of mini-Tn*7* constructs into AB5075 strains 76
2.3.2. Genetic constructs based on pMQ557M 77
2.3.2.1. Complementation plasmids for *abaM*::Tn*26* mutant 77
2.3.2.2. *lux*-based *csu* operon reporter. 77
2.3.3. Construction of plasmids for BACTH assay 77
2.4. Phenotypic assays 78
2.4.1. Growth curves 78
2.4.2. Observation of colonies for phase separation 78
2.4.3. Motility on semi-solid surfaces 79
2.4.4. AHL extraction and detection 79
2.4.5. Liquid-air interphase attachment quantitative assay 80
2.4.6. *lux*-based reporters assays 81
2.4.6.1. AHL activity, agonists assays and dose-response assays 81

2.4.6.2. Screening assays to find OHC12 antagonists 82
2.4.7. *Galleria mellonella* killing assays 82
2.4.8. Survival on dry surfaces 83
2.4.9. BACTH assay 83
2.4.10. mRNA sequencing (RNA-seq) 84
2.4.11. Quantitative real-time PCR (qPCR). 85
2.4.12. TECAN plate reader attachment assay 85
2.4.13. Polymer microarray attachment screening 86
2.4.14. *A. baumannii* attachment to NGPDA and EGDPEA 87
2.4.15. Laser scanning confocal microscopy (LSCM) 87
2.5. Data plotting and statistical analysis 88
3. Role of *abaM* and quorum sensing in AB5075 virulence and attachment to abiotic surfaces 89
3.1. Introduction 89
3.1.1. Quorum sensing in *A. baumannii* and pathogenic *Acinetobacter* spp. 89
3.1.2. AbaM orthologues in other species 91
3.2. Aims of the chapter 94
3.3. Results 94
3.3.1. Separation of opaque and translucent phases 94
3.3.2. Growth curves 96
3.3.3. Survival during desiccation 97
3.3.4. Contribution of *abaM* to AHL production 98
3.3.4.1. Profiling AHL production at different time points 99
3.3.4.2. Complementation of *abaM*::Tn26 AHL production 101
3.3.5. *abaM* and quorum sensing in surface motility in 0.3% Eiken agar 102
3.3.5.1. Characterization of surface motility 102
3.3.5.2. Complementation of *abaM*::Tn*26* motility phenotype 103
3.3.5.3. Contribution of OHC12 to surface motility 103
3.3.6. *abaM* and quorum sensing in attachment to abiotic surfaces 104
3.3.6.1. Attachment to polypropylene 105
3.3.6.2. Complementation of the *abaM*::Tn26 attachment phenotype 105
3.3.6.3. Contribution of OHC12 to attachment to polypropylene 106
3.3.7. *abaM* and quorum sensing in virulence for *G. mellonella* larvae infection model 107

3.3.7.1. Characterization of virulence 107
3.3.7.2. Complementation of *abaM*::Tn26 avirulent phenotype 108
3.3.7.3. Contribution OHC12 to virulence 109
3.3.8. BACTH Two-hybrid protein-protein interaction assay 110
3.4. Discussion 111
3.5. Conclusions and future directions 126
3.5.1. Summary of most important findings 129
4. Regulation of *abaM* expression and transcriptomic analysis of *abaM* and *abaI* mutants 130
4.1. Introduction 130
4.1.1. AbaM and QS regulons in *A. baumannii* and other species 130
4.2. Aims of the chapter 132
4.3. Results 132
4.3.1. Investigating the expression of P*abaM* and P*abaI* 132
4.3.1.1. Validation of *lux*-based reporters 132
4.3.1.2. The expression of *abaM* in AB5075 wild-type, *abaM*::Tn*26* and *abaI*::Tn*26* 133
4.3.1.3. The expression of *abaI* in AB5075 wild-type and *abaI*::Tn*26* and response to exogenous OHC12 133
4.3.2. Study of AbaR agonists and screening for QS competitive antagonists 135
4.3.2.1. Response of P*abaM*::*lux* to different long-chain AHLs 135
4.3.2.2. Dose-curve response of OHC12, OHC10 and OC12 137
4.3.2.3. Screening for competitive inhibitors of AB5075 quorum sensing 139
4.3.2.4. Screening the OC12-derived compounds for AbaR agonists 142
4.3.3. RNA-seq-based comparative transcriptomics between AB5075 wild-type strain, *abaI*::Tn26 and *abaM*::Tn26 143
4.3.3.1. Quality analysis 143
4.3.3.2. Differentially expressed genes 144
4.3.3.3. Comparison of *abaI*::Tn*26* vs wild-type and *abaM*::Tn*26* vs wild-type differentially expressed genes 150
4.3.4. Quantitative real-time PCR (qPCR) 151
4.4. Discussion 152

4.5. Conclusions and future directions 169
4.5.1. Summary of most important findings 170

5. Role of Csu pili in surface recognition and attachment 171

5.1. Introduction 171
5.1.1. Csu pili in *A. baumannii* and their role in attachment 171
5.1.2. Strategies for preventing bacterial biofilms 175
5.1.2.1. High-throughput screening of polymers resistant to attachment 176

5.2. Aims of the chapter 178

5.3. Results 179
5.3.1. Analysis of *lux*-based *csu* operon reporters 179
5.3.2. Role of the Csu pili in AB5075 attachment to polypropylene 180
5.3.3. Construction and validation of recombinant *E. coli* BL21 pBAD_*csu* 181
5.3.4. Screening of materials 183
5.3.5. Attachment of *A. baumannii* to EGDPEA and NGPDA 190

5.4. Discussion 191

5.5. Conclusions and future directions 197
5.5.1. Summary of most important findings 198

6. General discussion and future perspectives 199

6.1. Summary of most important findings in this project 202

6.2. Proposed models 204
6.2.1. AbaM regulation of AB5075 genes and phenotypes 204
6.2.2. Cross-regulation of AbaM and quorum sensing 205

7. References 206

8. Supplementary material 239

8.1. Additional experimental results 253

List of Figures

Figure 1.1: Surface virulence factors in *A. baumannii* 32

Figure 1.2: Diagram representing phase variation 52

Figure 1.3: Biofilm formation and dispersion cycle 57

Figure 1.4: "Canonical quorum sensing (QS) circuits" 62

Figure 1.5: General structure of *N*-acyl homoserine lactones 64

Figure 1.6: Cross-regulation of the three *Pseudomonas aeruginosa* QS systems 66

Figure 3.1: Quorum sensing locus in *A. baumannii* AB5075 90

Figure 3.2: Opaque and translucent colony variants 95

Figure 3.3: Growth curves of AB5075, *abaI*::Tn*26* and *abaM*::Tn*26* opaque and translucent phases 96

Figure 3.4: Desiccation survival of AB5075, *abaI*::Tn*26* and *abaM*::Tn*26* 98

Figure 3.5: Quantification of AHLs production at different time points by AB5075, *abaI*::Tn*26* and *abaM*::Tn*26* 100

Figure 3.6: Quantification of AHL production in the *abaM* mutant complemented strain 102

Figure 3.7: Surface motility on 0.3% Eiken agar 104

Figure 3.8: Attachment to polypropylene 106

Figure 3.9: Attachment to polypropylene in genetically complemented *abaM* mutant and AB5075 supplemented with OHC12 107

Figure 3.10: Killing of *G. mellonella* larvae 108

Figure 3.11: Contribution of OHC12 in virulence in *G. mellonella* larvae 109

Figure 3.13: BACTH Two-Hybrid protein-protein interaction assay 111

Figure 4.1: P*abaM*::*lux* activity assays 134

Figure 4.2: P*abaI*::*lux* activity assays in AB5075 and *abaI*::Tn26 ± exogenous OHC12 135

Figure 4.3: Structure of the AHLs 136

Figure 4.4: Comparative agonist activity of AHLs of different acyl chain length and 3-position modifications 137

Figure 4.5: Dose-response curves of OHC12, OHC10 and OC12 138

Figure 4.6: Screening for AbaR inhibitiors 141

Figure 4.7: Screening for AbaR agonists 142

Figure 4.8: Pearson correlation heat map 144

Figure 4.9: Volcano plot displaying differentially expressed genes between *abaI*::Tn26 (abaI) and AB5075 (WT) 145

Figure 4.10: Volcano plot displaying differentially expressed genes between *abaM*::Tn26 (abaM) and AB5075 (WT) 148

Figure 4.11: Overlapping differentially expressed genes in *abaM*::Tn*26* and *abaI*::Tn*26* 150

Figure 4.12: Quantitative real-time PCR 151

Figure 5.1: *A. baumannii* Csu type I pili 174

Figure 5.2: Analysis of *csu* expression in different backgrounds 179

Figure 5.3: Attachment to polypropylene of *csuA/B*::Tn*26* and *csuE*::Tn*26* 180

Figure 5.4: Effect of recombinant *A. baumannii* ATCC 19606 Csu pili on attachment 182

Figure 5.5: Fluorescence scan of the polymer microarrays slides incubated with the uninduced strain and the induced strain 183

Figure 5.6: Violin plot representing the distribution of polymers with *E. coli* BL21 pBAD_*csu* attachment and no attachment 185

Figure 5.7: Csu attachment to monomers with the highest attachment, plus attachment to EGDPEA and NGPDA 186

Figure 5.8: Correlation between bacterial attachment and flexibility and hydrophobicity.....187

Figure 5.9: Qualitative evaluation of opaque *A. baumannii* AB5075 attachment to EGDPEA and NGPDA.....190

Figure 5.10: Biomass, surface area and surface to biovolume data from opaque AB5075 wild-type strain attachment to EGDPEA and NGPDA.....191

Figure 6.1: Proposed model for the AbaM role in regulation of AB5075 genes and phenotypes.....204

Figure 6.2: Proposed model for the cross-regulation of AbaM and QS.....205

Supplementary Material Figure S1: Colony PCR of pure colony variants stocks. 239

Supplementary Material Figure S2: *abaI*::Tn26/AB5075 differentially expressed genes enrichment analysis. 241

Supplementary Material Figure S3: *abaM*::Tn26/AB5075 differentially expressed genes enrichment analysis. 243

Supplementary Material Figure S4: Heat cluster of differentially expressed genes between AB5075 (WT), *abaI*::Tn26 (abaI) and *abaM*::Tn26 (abaM)..... 244

Supplementary Material Figure S5: AbaR protein sequence alignment between *A. baumannii* AB5075 and *A. nosocomialis* M2. 245

Supplementary Material Figure S6: CsuE protein sequence alignment of *A. baumannii* ATCC19606 and *A. baumannii* AB5075 245

Additional Figure 1: Agonist and antagonist assays using medium-length AHLs 254

List of Tables

Table 2.1: Strains used in this project.....68

Table 2.2: Plasmids and vectors used in this project. 71

Table 2.3: Primers used in this project 73

Table 4.1: Nomenclature and structures of the OC12 analogues used in the screening for AbaR inhibitors.....139

Table 4.2: Differentially expressed genes ($|\log_2(\text{fold change})| \geq 1.5$) in *abaI*::Tn*26* 146

Table 4.3: Differentially expressed genes ($|\log_2(\text{fold change})| \geq 1.5$) in *abaM*::Tn*26*.....148

Table 5.1: Nomenclature and chemical structures for the 20 monomers with the highest attachment, plus NGPDA and EGDPEA 187

Supplementary Table 1: Differentially expressed genes ($\log_2(\text{fold change}) \geq 1$) in *abaI*::Tn26.....246

Supplementary Table 2: Differentially expressed genes ($\log_2(\text{fold change}) \geq 1$) in *abaM*::Tn26.....250

Abbreviations

°C	Degrees Celsius
μg	micrograms
μl	Microlitre
μm	micrometres
μM	Micromolar concentration
A_{585}	Absorbance at 585 nanometres
AHL	*N*-acyl homoserine lactone
Amp	Ampicillin
bp	Base pair
CFU	Colony forming unit
DNA	Deoxyribonucleic acid
EC_{50}	Half maximal effective concentration
eDNA	Extracellular DNA
EGDPEA	ethylene glycol dicyclopentenyl ether acrylate
EPS	Extracellular polysaccharides
g	grams
gDNA	Genomic DNA
h	Hours
hygB	Hygromycin B
ICU	Intensive care units
IPTG	Isopropyl-β-D-1-thiogalactopyranoside
Kan	Kanamycin
kDa	Kilo Daltons
LB	Lysogeny broth media
LC-MS/MS	Liquid chromatograph with tandem mass spectrometry
LS-LB	Low-salt lysogeny broth media
MCS	Multiple cloning site
MDR	Multi-drug resistant
min	Minutes
ml	Millilitre

mm	Millimetre
mM	Minimolar concentration
MS	Mass spectrometer
NGPDA	Neopentyl glycol propoxylate diacrylate
nm	Nanometres
nm	nanometres
nM	Nanomolar concentration
OC12	*N*-3-oxododecanoyl-L-homoserine lactone
OD_{600}	Optical density at 600 nanometres
OH10	*N*-3-hydroxydecanoyl-L-homoserine lactone
OHC12	*N*-3-hydroxydodecanoyl-L-homoserine lactone
OMV	Outer membrane vesicle
PBS	Phosphate-buffer saline solution
PCR	Polymerase chain reaction
pHEMA	poly(hydroxyl ethylmethacrylate)
PO-LB	Phase observation lysogeny broth media
PS	Polystyrene
QS	Quorum sensing
RFU	Relative fluorescent unit
RH	Relative humidity
RLU	Relative light unit
RNA	Ribonucleic acid
RNA-seq	RNA sequencing
s	Seconds
ssDNA	Single stranded DNA
TCS	Two Component System
Tet	Tetracycline
UTI	Urinary tract infection
v/v	Volume by volume
w/v	Weight by volume
xg	Times gravity

X-Gal	5-bromo-4-chloro-3-indolyl-ß-D-galactopyranoside

A note about phase variation

A. baumannii AB5075 possesses two colony variants, named opaque and translucent (see 1.3) (Tipton et al., 2015). Except where otherwise specified, the work with AB5075 in this study was performed using the opaque variant of each strain.

1. Introduction

1.1. The *Acinetobacter* genus

Acinetobacter, from the Greek α- [a] + κινετσ [kineto] + βακτηρ [bacter] (non-motile rod), is a genus of Gram-negative gammaproteobacteria ubiquitously distributed, even though not all *Acinetobacter* species can be commonly found in natural environments (i.e. species belonging to the pathogenic *A. baumannii* complex, discussed below). *Acinetobacter* spp. are defined as strictly aerobic, non-fermenting, non-swimming, twitching, catalase-positive, oxidase negative bacteria with a DNA G+C content of 38-47% that grow well in most complex and defined media with a single carbon and energy source (Juni, 2015).

The genus *Acinetobacter* was discovered in 1911 by the Dutch microbiologist Martinus Beijerinck, who originally named an organism isolated from soil as *Micrococcus calcoaceticus*. As the *Acinetobacter* group was not defined, in the following years several organisms of the group were isolated and assigned to different genera and species, such as *Neisseria winogradkyi*, *Moraxella lwoffii*, *Diplococcus mucosus*, *Bacterium anitratum*, *Achromobacter anitratus*, *Achromobacter mucosus* or *Alcaligenes haemolysans* (Almasaudi, 2018). The genus *Acinetobacter* was not proposed until 1954 by Brisou and Prevot, receiving further experimental support thanks to the biochemical studies published by Baumann *et al* in 1968 (Peleg et al., 2008; Baumann et al., 1968). The official recognition of the genus arrived in 1971 by the Subcommittee on the Taxonomy of Moraxella and Allied Bacteria, appearing in the Bergey's Manual of Systematic Bacteriology in 1974 formally classified in the *Pseudomonadales* order and the *Moraxellaceae* family (Peleg et al., 2008; Almasaudi, 2018). In 1986, Bouvet and Grimont identified 12 new genospecies by DNA-DNA hybridization, including *A. baumannii*, A. *calcoaceticus, A. haemolytitcus*, *A. junii*,

A. johnsonnii and *A. lowffii*. Since then, many new species have been isolated and assigned to the group, reaching the current (April 2020) 59 named species (http://www.bacterio.net/*Acinetobacter*.html).

The different species of *Acinetobacter* can be found in many different habitats. While most of them are saprophytes that live in a wide range of natural habitats (including soil, water, food and human and animal microbiota), pathogenic species (discussed below) are usually found almost exclusively in hospital and health care facilities colonizing most hospital equipment and medical devices, where they can survive for long periods of time (Almasaudi, 2018)

1.1.1. The *A. baumannii* complex

The proposed *A. baumannii* complex include the closely related clinically relevant species *A. baumannii*, *A. nosocomialis* (former *Acinetobacter* genomic species 13TU) and *A. pittii* (former *Acinetobacter* species 3) (Nemec et al., 2011). These three species belong to the *A. calcoaceticus-A. baumannii* complex, which also includes the environmental species *A. calcoaceticus*. Despite to the taxonomical similarities, *A. calcoaceticus* is not considered a pathogenic species, and therefore the term *A. baumannii* complex is more useful from an epidemiological and clinical point of view (Peleg et al., 2008).

The most import representative of this group, *A. baumannii* (which gives the complex its name), has become one of the most important and troublesome human pathogens in hospitals and other health care facilities, especially in intensive care units (ICU). *A. baumannii* is estimated to cause between 2 to 10% of all ICU Gram-negative infections. Moreover, it has been shown to colonize virtually any hospital environment, including furniture, medical equipment and

devices, bedding and staff (Bernards et al., 2004; Gootz and Marra, 2008).

Phylogenetic analysis have revealed that *A. baumannii* strains form a genetically compact monophyletic cluster significantly distant from their closest relatives of the complex, *A. nosocomialis* and *A. pittii*, despite their phenotypical similarities (Diancourt et al., 2010). The low genetic divergence in *A. baumannii* is not common among nosocomial pathogens, and is suggested to be the consequence of an evolutionary model that involved two disjointed waves of expansion. The first wave followed a bottleneck event that took place at some point in the past, while the second wave is developing now as a consequence of the selection and expansion of a limited number of multidrug resistant isolates (Diancourt et al., 2010). Consequently, *A. baumannii* possesses three predominant clonal lineages, commonly named international clones I, II and III (ICL1, ICL2 and ICL3, respectively), with a few other lineages identified in two different MLST studies (Zarrilli et al., 2013; Diancourt et al., 2010). Of those, ICL1 (with representative strains such as AYE or AB5075) and ICL2 (which includes relevant strains such as ACICU) are specially relevant due to their multidrug resistance -mainly due to the presence of large resistance islands- and wide distribution in more than 30 countries (Jacobs et al., 2014; Karah et al., 2012).

A. baumannii excels at two particularly important features that are crucial to explain the success of this pathogen as a nosocomial pathogen: antibiotic resistance and environmental persistence. Environmental persistence will be discussed in more detail below (see 1.1.1.2), so this section will be focused on antibiotic resistance. *A. baumannii* clinical strains have accumulated resistance mechanisms to a wide variety of antibiotics during the last few decades to a point in which, currently, most clinical strains are

considered multi-drug resistant (MDR), with even some pan-resistant strains being identified (Nowak et al., 2017; Roca et al., 2012). *A. baumannii* has accumulated β-lactamases, multidrug efflux pumps, alterations of target sites, aminoglycoside-modifying enzymes and changes in membrane permeability, resulting in clinical strains that are significantly hard to eradicate (Lin and Lan, 2014).

Multiple factors contribute to the rapid acquisition and accumulation of antimicrobial resistance elements. One of the most important is the high genomic plasticity of *A. baumannii*. Many clinical strains have been shown to be capable of natural competence and conjugation, facilitating the horizontal gene transfer of different genetic elements, including antibiotic resistance genes (Perez et al., 2007; Domingues et al., 2019; Traglia et al., 2018). Among these elements, there are many transposons and plasmids that contain integrons. These are genetic elements capable of integrating exogenous DNA by site-specific recombination and drive their expression thanks to a promoter region located upstream the integration site (Roca et al., 2012; Lin and Lan, 2014). This ability to accumulate and express genes in a single cluster usually located in a mobilizable genetic element promotes rapid dissemination of many resistance elements among *A. baumannii* strains. Currently, integrons containing diverse genes involved in antibiotic resistance are detected in many MDR clinical strains, with percentages that vary from 44% to 84% (Lin and Lan, 2014; Perez et al., 2007). This ability to acquire genetic material lead to many *A. baumannii* isolates to possess what are known as 'resistance islands': regions of the genome that accumulate a large number of horizontally transferred elements containing antibiotic resistance genes. A notable example would be the AbaR1 resistance island in *A. baumannii* AYE (not to be confused with the quorum sensing response regulator AbaR, which will be discussed later), a large 86 kb region containing 45 cassettes

encoding antibiotic and heavy metal resistance genes, but many others have been identified and characterized in the last few years (Roca et al., 2012; Fournier et al., 2006). Apart from genomic plasticity, *A. baumannii* also possesses robust efflux pump systems that also play a key role in reducing antibiotic susceptibility, as well as an SOS response that has been shown to contribute to the acquisition of antibiotic resistances (Lin and Lan, 2014; Aranda et al., 2014). Both mechanisms will be discussed in more detail below. Summarizing, *A. baumannii* possesses formidable genomic plasticity and other elements that contributed to the rise of MDR and pan-resistant strains isolated from hospitals over the last few decades.

Overall, these characteristics make *A. baumannii* one of the most important threats to hospitalized worldwide and member of the ESKAPE group, the acronym used for the six pathogens (*Enterococcus faecium*, *Staphylococcus aureus*, *Klebsiella pneumoniae*, *Acinetobacter baumannii*, *Pseudomonas aeruginosa* and *Enterobacter* spp.) causing more trouble in hospitals due to the high number of infections they cause and their ability to 'escape' the antimicrobial treatments (Pendleton et al., 2013). Moreover, in a list published by the World Health Organization in 2017, *A. baumannii* appeared as one of the critical pathogens (alongside *Pseudomonas aeruginosa* and *Enterobacteriaceae*) for which new antibiotics were urgently required, highlining the importance of multi-drug resistance in this bacteria (World Health Organization, 2017).

1.1.1.1. Infections caused by *A. baumannii*

A. baumanni causes a wide range of infections, mostly in severely ill patients, including pneumonia, bacteraemia, skin and soft tissue infections, urinary tract infections (UTI), meningitis and endocarditis.

Hospital-acquired pneumonia, especially ventilator associated pneumonia (VAP), is the most common infection caused by *A. baumannii*, representing at least between 7-8% of all ICU-acquired pneumonia cases according to different surveillance studies (Weinstein et al., 2005; Kalanuria et al., 2014). Other studies, however, suggest that the prevalence could be much higher (up to 35%) in some institutions (Huang et al., 2019; Chaari et al., 2013). Seasonal variation and geographical localization could explain these differences, as *A. baumannii* infections are more common in summer and in countries with higher average temperatures (Hurley, 2016). Infection usually occurs during the intubation process due to a prior colonization of the endotracheal tube, which allows the bacteria to by-pass the host physical defence mechanisms (cough reflex) and access the lower respiratory tract (Kalanuria et al., 2014). Crude mortality of *A. baumannii*-caused pneumonia is difficult to assess, as many infections occur in patients with prolonged ICU stays, but some reports associate *A. baumannii* pneumonia with mortality rates between 40-70% (McConnell et al., 2013).

Bacteraemia is also a common infection caused by *A. baumannii* in hospitals. In many cases these infections have their origin in a lower respiratory tract infection or the presence of intravascular devices, with wound and urinary tract infections being less common causes (McConnell et al., 2013). A detailed and extensive surveillance study in the USA found that *A. baumannii* caused 1.3% of all bloodstream infections, being significantly more common in ICU than non-ICU ward infections (Wisplinghoff et al., 2004). Crude mortality varied between 16.3% in non-ICU ward infections and 43.4% in ICU infections, the third highest among all ICU infections. Interestingly, the mean time between hospital admission and *A. baumannii* bacteraemia was 26 days, the longest among all pathogens reported

in this study, which could partially explain the high mortality observed in ICU patients (Wisplinghoff et al., 2004).

Wound, burn and other traumatic infections caused by *A. baumannii* are becoming more common, especially among military personnel in Iraq and Afghanistan that suffered combat injuries. *A. baumannii* is routinely isolated in military burns units, being one of the most common causes of burn wound infections and with many isolates (53%) displaying multidrug resistance. Soft-tissue and skin infections, such as fasciitis or cellulitis, also represent a problem in military health care units, requiring longer healing times and prolonged antibiotic treatment (McConnell et al., 2013). Osteomyelitis caused by *A. baumannii* has also been reported in military members and civilians as a consequence of war-related wounds in Iraq, Syria, Yemen and Afghanistan. As with other types of infections, many of these A. *baumannii* isolates were associated with high levels of antibiotic resistance (Fily et al., 2019; Weintrob et al., 2018). Less frequently, burn, soft tissue and skin infections have also been reported in ICUs. However, and despite the potential complications (including bacteraemia) that can result from these type of infections, an associated higher risk of mortality for *A. baumannii* traumatic infections has not been reported (McConnell et al., 2013; Peleg et al., 2008).

Although less common, *A. baumannii* is a relevant aetiological agent of post-neurosurgical meningitis with mortality rates ranging between 15% to 71%, with the highest rates associated with neonates and *A. baumannii* carbapenem-resistant strains (Kim et al., 2009a). Risk factors include long invasive procedures, multiple operations, cerebrospinal fluid leakage, external ventricular drain and previous antibiotic treatments. As in other *A. baumannii* infections, MDR

strains are common, making the treatment more challenging (Xiao et al., 2019; Peleg et al., 2008).

Other occasional infections caused by *A. baumannii* include urinary tract infections (UTIs), which usually involve catheter associated infections in ICUs, and endocarditis, that can be associated with prosthetic valves and intravascular catheters (Peleg et al., 2008; McConnell et al., 2013).

Exceptionally, *A. baumannii* can cause community-acquired infections (CAI). Many of these CAIs occur in patients with underlying risk factors, including heavy smoking, alcohol abuse, diabetes mellitus, renal disease or obstructive pulmonary disease (Falagas et al., 2007). Pneumonia, being 85% of all reported CAIs caused by *A. baumannii*, is the most common of these infections. Community-acquired *A. baumannii* pneumonia usually involves secondary bacteraemia, has high mortality (up to 60%) and is usually fulminant within 8 days post-infection (Antunes et al., 2014; Peleg et al., 2008). Other CAIs caused by *A. baumannii* include bacteraemia, meningitis and UTIs (Falagas et al., 2007).

1.1.1.2. *A. baumannii* environmental persistence

One of the main characteristics of *A. baumannii* is its ability to persist in the hospital environment resisting disinfectants, long periods of desiccation and a wide range of temperatures and pH (Gootz and Marra, 2008; Bravo et al., 2019). Specifically, *A. baumannii* is remarkably capable of resisting desiccation conditions, maintaining viability for long periods of time under dry conditions on the surface of different hospital equipment and medical devices with some isolates surviving for more than 100 days (Antunes et al., 2011). Moreover, it has been shown that long-term exposure to dry surfaces does not affect the virulence of *A. baumannii* (Chapartegui-González

et al., 2018). The mechanisms behind this persistence on dry surfaces are not fully understood, but it is generally accepted that this is a multi-factorial process that involves different stress responses, biofilm formation and the polysaccharide capsule (Harding et al., 2018). Studies have suggested that high biofilm and capsule production are linked with longer term survival under desiccation conditions, most likely by protecting the cells from external stresses and retaining water (Espinal et al., 2012; Tipton et al., 2018; Harding et al., 2018). Moreover, another study suggested that *A. baumannii* cells that remain viable after a long period of exposure to desiccation conditions are cells in a 'persistence' state that differentially express different proteins, generating a 'persistence phenotype' specifically adapted to survive under those conditions (Gayoso et al., 2014). Proteomic studies revealed that, compared with the proteome of planktonic cells, bacteria that undergo prolonged desiccation expressed higher levels of ribosomal recycling factor (RRF), stress-induced molecular chaperones, oxidative stress-related proteins, DNA-binding proteins IHF (Integration Host Factor) and HU (Histone U93) (involved in transcription regulation and DNA supercoiling maintenance), antibiotic resistance proteins, proteins of the Cpx pathway (a two-component system involved in envelope stress-response), Csu pili components and the HipA toxin (which is involved in the arrest of the cell cycle and induction of a dormant state). The desiccated cells also possessed a general decrease in protein synthesis, as well as lower expression of proteins involved in DNA replication and cell division (Gayoso et al., 2014).

Despite its remarkable ability to persist in the environment, environmental stress often cause heavy DNA damage to *A. baumannii* cells. To prevent lethal DNA damage, *A. baumannii* possesses a stress-inducible DNA repairing system known as SOS response. This response relies on RecA, a protease that binds single-

stranded DNA (ssDNA), which is generated as a results of DNA damage. RecA-ssDNA cleaves $UmuD_{Ab}$, an error-prone polymerase that contains a domain that represses the expression of several genes. Once cleaved, diverse genes encoding error-prone DNA polymerases are expressed, which can then repair a DNA damage that would be lethal otherwise (Aranda et al., 2013; Hare et al., 2012). Interestingly, the *A. baumannii* SOS response has also been involved in the acquisition of antibiotic resistance through DNA-damage induced mutagenesis, suggesting that exposure to non-lethal stress conditions could promote the emergence of MDR strains (Aranda et al., 2014).

In summary, *A. baumannii* possesses a wide range of resistance mechanisms that allow it to persist in hospital environments, facilitating the transmission from environment to host and making it an exceptionally well-adapted nosocomial pathogen.

1.1.1.3. *A. baumannii* AB5075: an hypervirulent multi-drug resistant strain

One of the main issues in research on *A. baumannii* virulence and its regulation is that most investigations have traditionally used non-multidrug resistant strains. More specifically, two strains from the American Type Culture Collection are the most widely used in *A. baumannii* research: ATCC 19606 and ATCC 17978. These strains, despite being genetically more accessible given their susceptibility to most antibiotics, were isolated more than 50 years ago and do not represent the vast majority of MDR isolates currently been found in hospitals (Wieland et al., 2018).

In a study by Jacobs *et al* in 2014, a screen of 200 isolates from U.S. military health care system patients was performed to find a highly virulent MDR strain that was genetically amenable in order to establish an *A. baumannii* model strain more representative of

current clinical isolates. The strain selected, AB5075, belongs to the international clone 1 (ICL-1), was isolated in 2008 from a case of tibial osteomyelitis and was the most virulent strain in *Galleria mellonella* and mouse pulmonary infection models among all the isolates tested. Moreover, it was the only one capable of establishing an osteomyelitis infection in rat fracture model (including among other osteomyelitis-isolated strains). Furthermore, despite being resistant to most antibiotics (including ampicillin, tobramycin, ciprofloxacin, gentamycin and imipenem), AB5075 is susceptible to tetracycline and high levels of hygromycin and erythromycin. These susceptibilities have been exploited to develop and validate diverse genetic tools including a library of tetracycline-resistant transposon mutants, hygromycin resistance-based plasmids and mini-Tn*7* systems (Jacobs et al., 2014; Kalivoda et al., 2011; Gallagher et al., 2015).

Overall, *A. baumannii* AB5075 is highly virulent in many animal models, resistant to many commonly used antibiotics, with useful genetic tools available and represents current clinical isolates much more accurately than the traditionally used ATCC 19606 and ATCC 17978 strains.

1.2. Virulence in *A. baumannii*

1.2.1. Virulence factors in *A. baumannii*

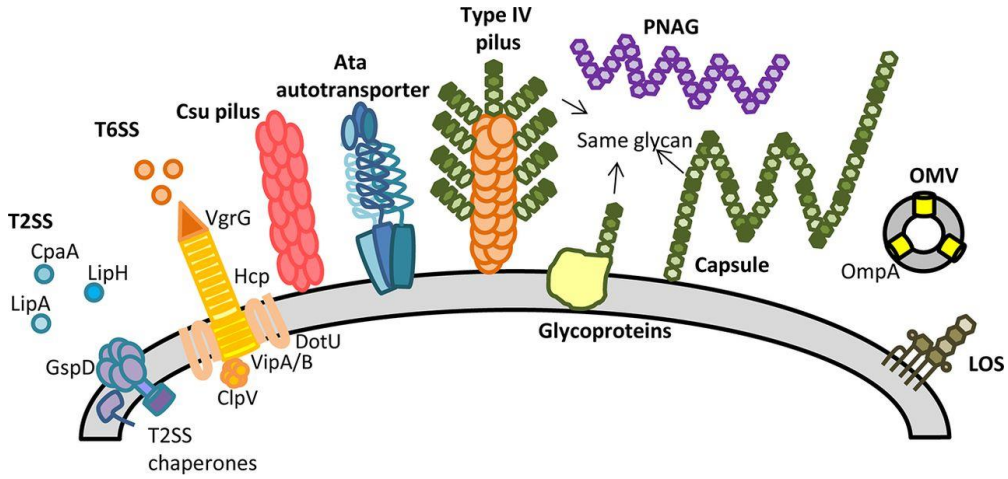


Figure 1.1: Surface virulence factors in *A. baumannii*. Extracted from Weber, Harding and Feldman, 2015. Summary of some of the most relevant virulence factors identified in *Acinetobacter* spp.

1.2.1.1. OmpA

The outer membrane protein A (OmpA) is probably the best known and characterized of all *Acinetobacter baumannii* virulence factors identified to date. OmpA is highly conserved among *A. baumannii* strains and the most abundant porin in the outer membrane with diverse roles in antibiotic resistance and virulence. OmpA possesses eight-stranded anti-parallel β-barrel domain in the outer membrane and a globular C-terminal domain in the periplasm that interacts with the peptidoglycan, which is thought to affect the formation of outer membrane vesicles (OMVs) (Morris et al., 2019; Moon et al., 2012).

In the many published studies, OmpA has been shown to have multiple roles in the virulence of *A. baumannii*. OmpA possesses several mechanisms to induce cell death in eukaryotes: it can interact and activate surface death receptors, translocate into the mitochondria and induce apoptosis through the cytochrome c

pathway and translocate to the nucleus (as it possesses a nuclear translocation signal) to degrade the host DNA in a DNase I-like manner (Morris et al., 2019; Lee et al., 2010). Moreover, OmpA also plays an important role in the survival of *A. baumannii* in human serum by binding soluble complement inhibitors and protecting the bacteria from the alternative complement pathway. Lastly, OmpA is also important for adherence and invasion of eukaryotic cells, as well as being involved in surface motility and biofilm formation (Kim et al., 2009b; Choi et al., 2008; Morris et al., 2019; Gaddy et al., 2009; Clemmer et al., 2011).

With respect to antibiotic resistance, OmpA plays a key role in the low intrinsic permeability of the *A. baumannii* outer membrane. OmpA is selectively permeable to small molecules such as sulbactam or imipenem, but does not uptake other antibiotics like rifampicin, chloramphenicol or tetracycline. Better knowledge of OmpA selectivity could help develop better antimicrobial strategies for the treatment of *A. baumannii* infections (Iyer et al., 2018). Altogether, these studies suggest that OmpA is an important *A. baumannii* virulence factor that also plays a key role in antibiotic resistance, making it a very attractive target for drug development.

1.2.1.2. Other outer membrane proteins (OMPs)

Other OMPs identified in *A. baumannii* include Omp34, which also induces cellular apoptosis in eukaryotic cells, is involved in bacterial persistence in the host through inhibition of autophagy and necessary for full virulence in systemic murine models. Moreover, Omp34 has been shown to be highly immunogenic, which could make it an interesting target for vaccine development. Similarly, OmpW induces a high immune response and is involved in iron acquisition and antibiotic resistance. Both of these OMPs are also abundantly found in OMVs (Morris et al., 2019). Lastly, the 29-kD porin CarO

(carbapenem-associated outer membrane protein) is not directly associated with *A. baumannii* virulence, but plays a key role in its susceptibility to imipenem, one of the most widely used antibiotic to treat *A. baumannii* infections (Mussi et al., 2005; Limansky et al., 2002).

1.2.1.3. Outer membrane vesicles (OMVs)

Outer membrane vesicles are blebs of the outer membrane of Gram-negative bacteria produced by cell lysis and other unknown processes. These vesicles contain, apart from phospholipids and lipooligosaccharides (LOS) that form the outer membrane (OM), proteins from the periplasm and the OM, cytoplasmic components and DNA. Some studies on *Acinetobacter* OMVs have suggested that they are involved in many functions such as delivery of virulence factors inside host cells, modulation of the host immune system, horizontal gene transfer (dissemination of antibiotic resistance) and protection against the immune system (Weber et al., 2015a; Morris et al., 2019). As mentioned above, OmpA is abundantly found in OMVs, and it has been suggested that it may not only be using OMVs as a delivery mechanism into host cells, but also contributing to their formation (Jin et al., 2011; Moon et al., 2012).

1.2.1.4. Lipopolysaccharide

Lipopolysaccharide (LPS) is the main component of the external side of the outer membrane in Gram-negative bacteria and has many roles in stress responses and bacterial physiology. It is composed of an O-antigen (the surface-exposed repeating sugar structure involved in host antibody recognition), a core oligosaccharide and lipid A (Weber et al., 2015a). *A. baumannii* does not produce LPS, but instead biosynthesises a lipooligosaccharide (LOS), which does not contain an O-antigen but has instead an extended core oligosaccharide (Morris et al., 2019).

The lipid A (also known as endotoxin) is highly immunogenic plays a very important role in the virulence of Gram-negative bacteria. It is released into the blood stream when the cells are lysed and can induce fever, diarrhoea and over-activation of immune system cells such as macrophages or monocytes, which can lead to severe inflammation and even cause septic shock (Weber et al., 2015a; Boll et al., 2015). Apart from its role as a toxin, lipid A is very important in antibiotic resistance. More specifically, modifications to the lipid A by lipid A phosphoethanolamine transferases or acyltransferases are associated with increased resistance to polymyxins such as colistin, as well as higher endurance to desiccation (Boll et al., 2015; Arroyo et al., 2011). Interestingly, some of these modifications may have a negative side effect on the bacteria by reducing its virulence. Moreover, lipid A defective strains are routinely found in clinical isolates, which makes *A. baumannii* one of the only three Gram-negative pathogen identified to date capable of surviving without endotoxin (Moffatt et al., 2010). This suggests that the loss of lipid A not only does not induce a biological burden reducing the fitness of *A. baumannii*, but instead confers a selective advantage in an environment of high antibiotic use.

1.2.1.5. Capsule

Acinetobacter baumannii produces an exopolysaccharide surface layer capsule that confers protection against macrophage/neutrophil complement-mediated phagocytosis and other immune system factors, as well as against serum, antibiotics, desiccation and other external threats (Tipton et al., 2018; Russo et al., 2010). The sugar repeating structure in the capsular polysaccharide of *Acinetobacter* species is the same found in the extended core oligosaccharide of the LOS and, more interestingly, also the same as the single repeat carbohydrate unit found in glycosylated proteins. Both carbohydrate subunits found in the capsule/LOS and glycosylated proteins are

synthesized via the same cellular pathway: a glycosyltransferase, PglC, initiates the process attaching the first carbohydrate to the undecaprenyl phosphate (UndP) lipid carrier. Then more sugar monomers are added by different glycosylases until the repeat subunit is complete. The subunit is flipped into the periplasm via the Wzx/Wzy pathway and, once there, there is a bifurcation in which the subunit can be polymerized and transported outside the cell to form the capsule or be linked to the LOS; or otherwise the single subunit is linked to a serine or threonine residue of the protein to be glycosylated by the *O*-oligosaccaryltransferase (*O*-OTase) PglL. This bifurcated pathway is a novel mechanism found in *A. baumannii* that not only provides a very promising target for drug development, as both capsule and glycosylated proteins play important roles in virulence, but also suggests an interesting evolutionary link between the pathways involved in the synthesis of both elements (Weber et al., 2015a; Morris et al., 2019; Kenyon and Hall, 2013).

Moreover, *A .baumannii* also produces and secretes another exopolysaccharide, poly-β-1-6-*N*-acetylglucosamine (PNAG), which is present on almost all clinical strains and is necessary for the correct formation and maturation of biofilm (Choi et al., 2009).

1.2.1.6. Pili

Pili are short surface appendages found in many bacteria that mediate many interactions between bacteria and their environment, including biofilm formation, surface motility, DNA uptake and mechanosensing, among others (Proft and Baker, 2009). Different types of pili, with different structures and characteristics, have been found in many different bacteria, and *Acinetobacter baumannii* strains has shown to have at least two of these pilus types, even though their precise role in *A. baumannii* biology and virulence is only partially known.

Type I Csu pili

The Csu pili is the term used to designate a type I chaperone/usher pili in *Acinetobacter* spp. found in all isolates whose sequence is known. In studies carried out in different *A. baumannii* strains, Csu pili have been shown to be required for biofilm formation and maturation on abiotic surfaces, and the CsuA/B subunit was found to be the most abundant protein in the pellicle matrix (Nait Chabane et al., 2014). Moreover, another two genes of the operon, *csuC* and *csuD*, were shown to be expressed at high levels in the cells of the pellicle, reinforcing the importance of this pilus in biofilms formed on abiotic surfaces. Other putative type I pilus operons have been bioinformatically found in different *A. baumannii* clinical isolates, and mass spectrometry has shown the presence of some non-Csu type I pili subunits in the pellicle matrix, but none of these systems has been properly characterized as yet (Weber et al., 2015a; Eijkelkamp et al., 2014).

Type IV pilus

The Type IV pilus (TFP) has been widely studied in many bacteria, and they have shown to have a critical role in surface motility (specially twitching motility), as well as important roles in horizontal gene transfer and biofilm formation (Weber et al., 2015a). In *Acinetobacter*, diverse studies have revealed that TFP is required for twitching motility, natural transformation, adhesion to host cells and biofilm formation (Eijkelkamp et al., 2014; Wilharm et al., 2013; Harding et al., 2013; Leong et al., 2017; Ronish et al., 2019). Moreover, it has been shown that different *A. baumannii* strains produce PilA pilins (the major pilin subunit of TFP) with different molecular structures, resulting in phenotypic differences between strains in twitching and biofilm formation (Ronish et al., 2019).

1.2.1.7. Secretion systems

Secretion of proteins into the extracellular environment is a process present in all living forms and is required for a wide number of functions, including bacterial virulence. There are diverse systems in bacteria that differ structurally and functionally, with very different roles in virulence depending on the type of effector protein that they secrete or the target of the secretion (environment, eukaryotic host cytoplasm, other bacterial competitors, etc.) (Costa et al., 2015). Some of these secretion systems have been identified in *A. baumannii*, but their role in virulence has been only partially elucidated.

Type II secretion system (T2SS)

This system is the most recent one identified in *Acinetobacter* spp., found in both *A. baumannii* ATCC 17978 and *A. nosocomialis* M2. T2SS secretes effectors (including toxins) outside of the cell from the cytoplasm using a two-step mechanism. The first step is dependent of the Sec or Tat secretory pathways, which translocate the effectors from the cytoplasm to the periplasm, where the T2SS machinery secretes them into the extracellular space. T2SS-dependent substrates (lipases LipA and LipH and metallopeptidase CpaA) were found to be secreted by *A. nosocomalis* M2. Moreover, deletion of *gspD* (a secretin that forms the outer membrane channel of the T2SS) or *lipA* resulted in attenuated virulence in different eukaryotic models such as *G. mellonella* or murine pulmonary infection models (Weber et al., 2015a; Johnson et al., 2015; Morris et al., 2019).

Type V secretion system (T5SS) or autotransporters

Type V secretion systems form channels in the outer membrane and transport to the extracellular space effector proteins previously translocated into the periplasm in a Sec-dependent way (Green and Mecsas, 2016).

A. baumannii possesses three T5SS: two type Vb subclass and one type Vc. The *Acinetobacter* type Vc trimeric autotransporter or Ata is only present in some clinical isolates and has been shown to play roles in adherence to extracellular matrix components such as collagen and laminin and in biofilm formation and maturation. Deletion of this transporter also results in attenuated virulence in mice (Bentancor et al., 2012a). Moreover, *ata* has another gene in the same operon, *tpgA*, which encodes for an OmpA-like lipoprotein that mediates the biogenesis and secretion of Ata to the outer membrane (Ishikawa et al., 2016). FhaB/FhaC, one of the two type Vb secretion systems present in *A. baumannii*, is involved in attachment to A549 eukaryotic cells, in interactions with host fibronectin and is required for full virulence in *C. elegans* fertility model and mice (Pérez et al., 2017). Lastly, the CdiA/CdiB type Vb systems are involved in contact-dependent growth inhibition, where CdiA is the toxin and CdiB is an outer membrane porin. Moreover, *A. baumannii* possesses a third element, CdiI, an immunity protein. Unfortunately, no studies regarding the mechanism of killing of this system are available yet (Morris et al., 2019).

Type VI secretion system (T6SS)

The T6SS is a very recently characterized secretion system with very particular characteristics. It was described for first time in 2006 in *Vibrio cholerae* and *Pseudomonas aeruginosa* as a mechanism for the injection of anti-eukaryotic factors into the host, playing a role similar to type 3 secretion systems. Further research found out that T6SS is involved in many bacterial processes, including the injection of antibacterial toxins into other competitor bacteria, cell-to-cell communication and type I pilus regulation (Weber et al., 2015a; Coulthurst, 2013).

There is only a limited number of studies on *A. baumannii* T6SS, but bioinformatic and laboratory studies have revealed that the *A. baumannii* genome contains a single T6SS operon that is well conserved among all clinical isolates (Eijkelkamp et al., 2014). These studies also found Hcp in *A. baumannii* ATCC 19606 cell free supernatant. This protein polymerizes forming a tubular structure across the bacterial outer membrane that is used to penetrate the target membrane in order to secrete the effectors into the host cytoplasm. Interestingly, *Acinetobacter* spp. does not contain the *vgrG* genes in the T6SS cluster, but they are found spread in different genomic locations, differing in number and structure between the different strains. VgrG is the main effector of T6SS, found in the tip of the Hcp tubular structure, and also plays a crucial role facilitating the secretion of other T6SS-dependent effector proteins. Further bioinformatic studies found that *Acinetobacter* VgrG proteins do not seem to contain effector domains (Weber et al., 2013). Altogether, these studies suggest that VgrG proteins in *Acinetobacter* only facilitate the secretion of toxins and cognate immunity proteins rather than exert any effect on their own, as it occurs in VgrG homologs from other bacteria possessing T6SSs (Coulthurst, 2019).

Another peculiarity of *A. baumannii* T6SS is its regulation. Apart from the major regulator H-NS, which will be described in more detail below, many *A. baumannii* strains carry a resistance plasmid that encodes repressor proteins for T6SS. This plasmid can be spontaneously lost, losing the resistance genes but activating T6SS expression. This suggests that, in environments with high antibiotic selective pressures, *A. baumannii* is less likely to find competitors and therefore maintains the plasmid to resist the antibiotics while repressing T6SS expression, the production of which will cost the cells a high amount of energy. Conversely, environments with low antibiotic selective pressures are more likely to find competitors, so it

is more advantageous to lose the resistance genes and derepress the expression of the T6SS (Weber et al., 2015b).

1.2.1.8. Iron acquisition

Another important factor for the survival of pathogens during infection is iron acquisition. This is due the low bioavailability of free ferric iron in the host environment, as most of it is found in the metalloprotein haemoglobin in erythrocytes, as well as associated with other eukaryotic high iron affinity proteins known as transferrins. In order to obtain enough iron, bacteria have developed a wide range of iron chelating molecules, known as siderophores, that are expressed under iron-limited conditions with the objective of taking up ferric ions from the environment and from the host iron-binding proteins. In the case of *A. baumannii*, acinetobactin is the best studied siderophore, playing a central role in the survival and the ability to successfully infect different animal hosts (Gentile et al., 2014; Shapiro and Wencewicz, 2016; Yamamoto et al., 1994). However, other iron uptake systems have also been identified and/or partially characterized in different *Acinetobacter* strains. In the acinetobactin-deficient strain *A. baumannii* AYE, two hydroxamate siderophores, baumanoferrin A and B, are essential for the growth of this strain in iron-limiting conditions (Penwell et al., 2015). The structure of six other closely related siderophores, named fimsbactins A-F, has also been elucidated, even though their biological role has not been fully characterized (Proschak et al., 2013). Moreover, bioinformatic analysis of different *A. baumannii* genomes led to the identification of two additional putative siderophore clusters, two heme uptake systems clusters (including up to 21 different *tonB*-dependent outer membrane transporter genes) and an homolog of the *E. coli feo* cluster, responsible for the synthesis of ferrous uptake system (Antunes et al., 2011b). Recently, the role of the three different TonB proteins and the Feo system in *A. baumannii*

ATCC 19606 virulence was evaluated. Results revealed that *tonB3* was required for growth under iron-limiting conditions and full virulence in *G. mellonella* larvae and mice, while both TonB3 and Feo systems were necessary for growth in complement-free human serum and resistance to normal human serum killing (Runci et al., 2019). Lastly, disruption of the Fur regulator, which binds to *fur* boxes that have been bioinformatically identified in siderophore clusters and mediates the expression of these proteins in response to iron starvation, results in reduced biofilm and virulence (Morris et al., 2019).

1.2.1.9. Efflux systems

The contribution of efflux systems to antimicrobial resistance is well known in *A. baumannii*. Many pumps have been characterized and are known to reduce the susceptibility of *A. baumannii* to antibiotics and other antimicrobials by transporting those agents from the bacterial cytoplasm to the extracellular space. AdeABC efflux pumps increase the resistance of *A. baumannii* to aminoglycosides and tigecycline, while AdeIJK contribute to resistance to tetracycline, erythromycin, fluoroquinolones, rifampicin, chloramphenicol and β-lactams, among other agents (Damier-Piolle et al., 2008; Morris et al., 2019; Yang et al., 2019).

The role of these systems in virulence, however, is poorly understood. AdeABC has been linked to virulence in murine model and transposon mutants of *adeIJK* showed reduced virulence in *G. mellonella* and murine pneumonia models, but no other systems have been extensively studied (Morris et al., 2019). Very recently, an extensive study using deletion mutants of representatives of the six efflux pump superfamilies was carried out in ATCC 17978, revealing that many other efflux systems could also contribute to virulence and

virulence-related phenotypes. The study revealed that representative knockout mutants of the RND (Resistance Nodulation Division), SMR (Small Multidrug Resistance) and MATE (Multidrug and Toxic Compound Extrusion) efflux pump superfamilies showed impaired surface motility and virulence in *G. mellonella* and *C. elegans* fertility assay. Similarly, mutation of the recently described ABC (Adenosine triphosphate-Binding Cassette) permeases *A1S_1242* and *A1S_2622* also led to similar results for all three phenotypes. Knockout mutations in other previously known ABC efflux pumps and representatives of the PACE (Proteobacterial Antimicrobial Compound Efflux) superfamily did not affect any of these phenotypes (Pérez-Varela et al., 2019). Moreover, many of these efflux systems were involved in resistance to one or more antibiotics, making efflux pumps a very attractive target for therapies that could increase susceptibility to antibiotics and reduce virulence at the same time.

1.2.1.10. Other relevant virulence factors

Acinetobacter baumannii possesses many other virulence factors but these are less well-studied or only bioinformatically predicted, but with a great potential for further research. An example is the biofilm associated (Bap)-like protein, a large protein containing more than 8,500 residues found on the surface of the cell and involved in biofilm formation and attachment to epithelial cells (Loehfelm et al., 2008; Brossard and Campagnari, 2012). Pmt, a major facilitator superfamily transporter supposed to facilitate extracellular DNA secretion, is also involved in adherence and biofilm formation and has been shown to be overexpressed in biofilm cells (Sahu et al., 2012).

Phospholipases, enzymes involved in phospholipid cleavage, are also involved in virulence in many bacteria, breaking host cell membranes or degrading mucus to facilitate cell invasion. The genomes of sequenced *A. baumannii* strains show at least two phospholipases D

and two phospholipases C. One study with one of the phospholipases D showed a role in serum survival, cell invasion and virulence in a pneumonia murine model (Jacobs et al., 2010), while phospholipases C have been found in the supernatant of *A. baumannii* cultures, as well as having a limited effect in virulence in *G. mellonella* and inducing host cell death in epithelial cells (Antunes et al., 2011; Camarena et al., 2010; Fiester et al., 2016).

1.2.2. Virulence gene regulation in *Acinetobacter baumannii*

A good understanding about the virulence factors and infections processes is vital for developing new strategies to fight *Acinetobacter* infections, but a deep knowledge about the mechanisms of regulation of those virulence factors is equally if not more important. Pathogenic bacteria usually find different microenvironments in the host during the infection process. Consequently, they must finely modulate the expression of different virulence determinants in response to environmental and physiological changes in order to respond appropriately adjusting gene expression and maintaining the best fitness for each situation.

There is still very little known about the regulation of virulence in *A. baumannii*, but in the last couple of decades an increasing number of regulatory elements involved in its pathogenesis have been identified and characterized.

1.2.2.1. Two-component systems

Two-component systems (TCSs) are widely spread signal transduction systems involved in the regulation of many different genes in response to environmental changes. In pathogenic bacteria, they usually mediate in many of the adaptations required for a successful infection. A classic TCS consists in two proteins: a membrane-bound histidine kinase (HK) sensor and a response

regulator (RR), usually a transcriptional factor. The HKs can detect a wide range of environmental or physiological stimuli, such as temperature, pH, osmolarity, mechanical contact and other specific ligands. In many cases, however, the specific ligand or activating factor of the HK is unknown. When the sensor domain of the HK detects its activation signal, it triggers the autophosphorylation of a specific histidine in the autokinase domain. This phosphoryl group is then transferred to the receiver domain of the cognate RR, which undergoes a conformational change, activating the regulatory domain. The RR can then modulate different cellular processes, usually through activation or repression of the expression of specific genes (Beier and Gross, 2006; Groisman, 2016).

Many TCSs possess different divergences from this classic view. In some cases, there are hybrid membrane proteins that contain both the HK and RR domains in a single protein. Sometimes, different HKs that detect different signals modify the phosphorylation state of a single RR, modulating its activity in response to different environmental and physiological changes. The opposite can also occur, when a single HK can modulate two or more RRs, which then regulate a different subset of genes/processes. Finally, some phosphorylation cascades present intermediate phosphoryl group transfers between phosphotransferases before phosphorylating the definitive RR, a mechanism well-studied in bacterial sporulation (Groisman, 2016; Hoch, 2000).

A. baumannii AB5075 contains 10 histidine kinases and 17 response regulators annotated in its genome (Gallagher et al., 2015). Most of these have not been characterized yet, but some have been studied in other *A. baumannii* strains and their role in virulence and antibiotic resistance is starting to be elucidated.

BfmR/BfmS

The BfmR/BfmS TCS is involved in the regulation of many phenotypes in *A. baumannii*. It has been shown to be a key virulence regulator, as it is involved in biofilm formation, Csu pili production, attachment to eukaryotic cells and bacterial susceptibility to serum killing. This system promotes the synthesis of the Csu pili through the upregulation of the usher-chaperone system required for its formation and thus indirectly up-regulates biofilm formation on polystyrene surfaces. BfmR/BfmS has also been shown to upregulate the multipurpose virulence mediator OmpA, enhancing attachment to eukaryotic cells and increasing resistance to human serum (Tomaras et al., 2008; Liou et al., 2014).

Interestingly, studies differ in whether the HK, BfmS, is directly involved in biofilm formation. While one study performed in *A. baumannii* ATCC 19606 showed that a knockout of *bfmR* but not *bfmS* abolished biofilm on polystyrene (Tomaras et al., 2008), another study in ATCC 17978 strain revealed that a *bfmS* knockout had a huge impact on biofilm formation (Liou et al., 2014). Similarly, a recent study also demonstrated that BfmR/BfmS modulated exopolysaccharide production in ATCC 17978 through the regulation of the K locus, which encodes several genes involved in the synthesis of surface exopolysaccharides (Geisinger and Isberg, 2015). However, no differences in capsule production were observed in clinical isolates carrying a *bfmR* deletion (Russo et al., 2016). It might be possible that the BfmR/BfmS system cross-interacts with other sensors and/or regulators, and these interactions may differ between strains.

BfmR/BfmS is also involved in regulation of antibiotic resistance. Deletion of *bfmR* in different strains increased susceptibility to meropenem, colistin, rifampicin, imipenem and erythromycin (Geisinger and Isberg, 2015; Russo et al., 2016; Liou et al., 2014).

GacA/GacS

Less is known about the GacA/GacS system in *Acinetobacter baumannii*. In a recent study in ATCC 17978, a GacS homolog was found to regulate 674 genes involved in a number of cellular processes, such as the *csu* pili operon, *ompA/motB*, *algZ* and many other genes involved in motility, biofilm formation and virulence. Phenotypic analysis confirmed that deletion of *gacS* significantly reduced biofilm formation and virulence in *Candida albicans* and mouse septicaemia models (Cerqueira et al., 2014). Moreover, GacS also controls the *paa* (phenylacetic acid pathway) operon, which is involved in the catabolism of aromatic compounds and plays a very important role in virulence and immune system evasion (Cerqueira et al., 2014; Bhuiyan et al., 2016).

Interestingly, the RR *gacA* (*ABUW_3639*) gene is not located adjacent to the HK *gacS* (*ABUW_3306*), as happens in many other TCS. Instead, *gacA* is situated next to two homologous genes of the *pilR*/*pilS* TCS, which has been shown to regulate the expression of T4P in other bacterial species (Mattick et al., 1996), suggesting that the GacA/GacS system cross-talk with other TCS. This has been observed in the much better characterized *P. aeruginosa* GacA/GacS system, where other histidine kinases and regulatory elements modulate the GacA/GacS activity and signalling cascade (Balasubramanian et al., 2013).

AdeR/AdeS

AdeR/AdeS is a well-known TCS that controls antibiotic resistance, virulence and biofilm formation through the direct or indirect regulatation of 579 genes (Richmond et al., 2016). Deletion of *adeR/adeS* results in overexpression of the *adeABC* efflux pump system, leading to reduced susceptibility to many antibiotics, including aminoglycosides, tigecycline and others (Marchand et al.,

2004; Yang et al., 2019). Moreover, deletion of *adeR/adeS* also results in decreased virulence in *G. mellonella*, biofilm formation and cytotoxicity in porcine vaginal mucosa in *A. baumannii* AYE (Richmond et al., 2016).

Other important TCSs

Other TCSs have also been identified and described in *A. baumanii*, but to a lesser extent than the systems described above.

The BaeR/BaeS system upregulates the expression of AdeAB, AdeIJK and MacAB-TolC efflux pumps, which results in reduced susceptibility to tigecycline. It has also been suggested that BaeS responds to osmotic stress, as the *baeR/baeS* genes are overexpressed under high osmotic conditions (Lin et al., 2014, 2015).

The PmrA/PmrB TCS is also linked to antibiotic resistance. In this case, to colistin, a last resort antibiotic used to treat MDR *A. baumannii* infections (Cai et al., 2012). Point mutations in *pmrB* were found in colistin-resistant strains, which also showed higher expression of *pmrA*, *pmrB* and *pmrC* compared to susceptible isolates. PmrC encodes for a lipid A modification enzyme, which catalyses the addition of phosphoethanolamine to the lipid A, conferring resistance to colistin (Arroyo et al., 2011; Beceiro et al., 2011).

The OmpR/EnvZ system has been characterized in many other bacteria and it is known to respond to osmolarity changes in the environment and regulate the expression of outer membrane porins (playing a key role in osmotic stress) and many other genes, as well as being necessary for full virulence in many pathogens (Cai and Inouye, 2002; Reboul et al., 2014; Egger et al., 1997). Similarly, in *A. baumannii* AB5075 OmpR/EnvZ is necessary for adaptation to

osmotic stress, motility and full virulence in *G. mellonella*. Moreover, the system was also found to be involved in regulation of phase variation, which is discussed in detail below (see 1.3) (Tipton and Rather, 2017).

Finally, the most recently described TCS in *A. baumannii* is A1S_2811, an hybrid histidine kinase/response regulator with CheA and CheY-like domains, which are well-studied components of the signal transduction in bacterial chemotaxis, regulating motility (Baker et al., 2006). In *A. baumannii*, deletion of *A1S_2811* resulted in reduced motility, biofilm formation, pili synthesis and exopolysaccharide production. Moreover, transcriptomic analysis revealed that A1S_2811 regulated 197 genes. Among the most interesting downregulated genes there were the *csu* operon, the *abaI* homoserine lactone synthase gene, the *abaM* (*A1S_0110*/*ABUW_3775*) regulator and the acinetin 505 (Ac-505) biosynthetic cluster, among others (Chen et al., 2017). The Ac-505 operon is proposed to be under control of quorum sensing and it has been shown to modulate surface motility, biofilm formation and virulence in *A. baumannii* and *A. nosocomialis* (Clemmer, Bonomo and Rather, 2011; Giles *et al.*, 2015; Brotherton and Greenberg, 2017 (Poster); Rumbo-Feal *et al.*, 2017). However, whether the small molecule synthesised by the operon, Ac-505, is directly responsible for these phenotypes or acts as a signalling molecule that indirectly activates other regulatory mechanisms remains to be elucidated.

1.2.2.2. H-NS

An isolated hyper-motile ATCC 17978 strain had an insertion element disrupting the *hns* gene, which encodes a nucleoid-associated protein that has been shown to regulate hundreds of genes in other bacteria (Wan et al., 2016). Deletion of this gene further confirmed the motility phenotype, as well as increased adherence to A549

human pneumocytes, pellicle formation, cell surface hydrophobicity, resistance to colistin and virulence in *Caenorhabditis elegans*. Transcriptomic analysis showed that H-NS regulates dozens of genes, including a type I pili, the T6SS, *fabG* and *fabF* (encoding for enzymes involved in fatty acid biosynthesis), *abaR*, genes of the *csu* operon, genes involved in the biosynthesis of poly-β-1,6-*N*-acetylglucosamine (PNAG), *eptA* (a *pmrC* homolog) or the *ata* autotransporter adhesin, among others and depending on the strain studied (Eijkelkamp et al., 2013; Deveson Lucas et al., 2018).

1.2.2.3. AtfA

AtfA (acidic transcription factor A) is an RNA polymerase-binding protein that displaces DNA from the RNA polymerase and exerts a global regulatory role, modulating the expression of 522 genes in *Acinetobacter baylyi*. Among the most differentially regulated genes there are genes involved in the T6SS, T4P, DNA transposition, iron acquisition, DNA replication and ethanol and acetate metabolism, among others. Deletion of *aftA* in *A. baylyi* and *A. baumanii* ATCC 19606 results in cell enlargement, reduced twitching motility, decreased biofilm formation and increased susceptibility to ampicillin, gentamycin, spectinomycin and ethanol (Withers et al., 2014).

1.2.2.4. Hfq

The RNA chaperone Hfq is an important mediator of the stress response and virulence in many pathogens, affecting host invasion, motility, biofilm formation and growth in different stress conditions (Kulesus et al., 2008). Hfq promotes the binding of small RNAs (sRNAs) to their target messenger RNAs (mRNAs), which results in positive (by preventing RNase degradation) or negative (by facilitating mRNA degradation or blocking ribosome binding) regulation of the mRNA translation (Kavita et al., 2018). In

A. baumannii ATCC 17978, deletion of *hfq* results in growth defects and reduced cell size, OMV secretion, OmpA levels, adhesion and invasion of A549 epithelial cells, survival in macrophages, biofilm formation and pilus biosynthesis. Moreover, it also promotes enhanced susceptibility to a range of environmental stresses (pH, temperature, ethanol, osmotic pressure and oxidative stress) and affects the expression of *csuA/B* and stress-related genes (Kuo et al., 2017).

1.2.2.5. Blue light

Interestingly, *A. baumannii* is capable of sensing and responding to changes in light, affecting diverse phenotypes. The photoreceptor BlsA is expressed at temperatures lower than 25°C and is capable of sensing blue light, negatively affecting motility and biofilm formation and enhancing killing of *C. albicans* (Golic et al., 2019; Mussi et al., 2010).

1.3. Phase variation

Phase variation is a type of phenotypic switching between different on/off-expressing 'variants' or 'phases' controlled by a genetic or epigenetic mechanism (such as DNA inversion and slipped-strand mispairing of nucleotide repeats, or DNA methylation, among others) that results in a variation in the expression of one or more proteins. Phase variation differs from genetic mutations because of its frequency (higher than random mutagenesis) and reversibility (cells can switch from one variant/phase to the other and vice versa) (van der Woude and Bäumler, 2004). Phase variation is used by many bacteria, including many pathogens, to regulate diverse phenotypes as a mechanism of rapid environmental adaptation. Some examples include regulation of fimbriae and virulence factors by *Bordetella pertussis*, capsule in *Haemophilus influenzae*, fimbriae in *Escherichia*

coli or capsule and outer membrane proteins in *Neisseria meningitidis* (van der Woude and Bäumler, 2004).

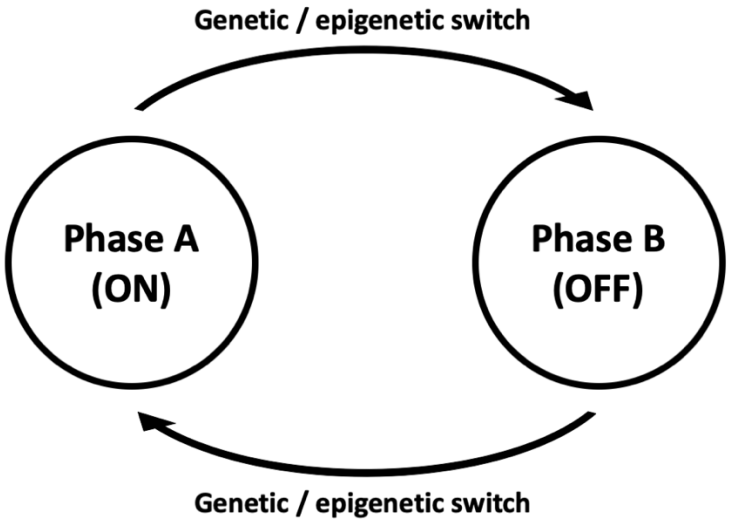


Figure 1.2: Diagram representing phase variation. Bacteria can switch through a reversible mechanism from two different phases that usually involve differential expression of one or more proteins.

1.3.1. Phase variation in *A. baumannii*

In Tipton *et al*, 2015, *A. baumannii* AB5075 was found to produce two colony variants, which were designated opaque and translucent. The two phase variants were capable of switching to the other at high frequency in a cell density-dependent manner not related to quorum sensing, suggesting that the switching was controlled by a phase-variable mechanism (Tipton et al., 2015). Moreover, the two colony variants showed several phenotypic differences. The opaque phase was more virulent in *G. mellonella*, more motile and showed lower susceptibility to tobramycin, amikacin and gentamycin, but produced less biofilm. The translucent phase, on the other hand, was less virulent, less motile and more susceptible to antibiotics, but produced thicker biofilms. This phenotypic heterogenicity was also observed in many other strains excluding ATCC 17978, which showed a different

colony phenotype distinct from the opaque/translucent variants observed in the other strains (Tipton et al., 2015).

Further research also revealed that opaque variants of AB5075 produce 2-fold more capsule than translucent variants, as well as having higher resistance towards hospital disinfectants and desiccation (Chin et al., 2018). The virulent/avirulent phenotypes of the opaque and translucent phases, respectively, were confirmed in pulmonary infections in mice. Interestingly, cells recovered from infected mice after 24 h of infection were almost exclusively opaque colony variants, independently of the composition of the initial inoculum, suggesting that there was strong selective pressure during infection in favour of the opaque variant. Furthermore, more bacteria were recovered from mice (10,000-fold more from lungs and 1,000-fold more from spleen and livers) infected with the opaque phase than in those infected with the translucent variant. The higher resistance of the opaque populations to host innate immune system antimicrobials such as lysozyme, CRAMP (Cathelin-Related Anti-Microbial Peptide) and reactive oxygen species has been proposed as the explanation for this selective pressure (Chin et al., 2018). Consequently, it is not surprising that clinical isolates of *A. baumannii* produce an overwhelming higher proportion of opaque colonies (Ahmad et al., 2019; Chin et al., 2018). The translucent variants, on the other hand, are hypothesised to be better adapted to survival in some specific nutrient-limited environmental conditions outside the host due to the increased ability to form biofilms, better growth in minimal media and higher expression of genes involved in nutrient acquisition and metabolism (Chin et al., 2018)

The exact regulatory mechanism that controls the switch between phases is not fully understood, but some key regulatory elements that strongly affect the frequency of switching have been recently

characterized. Deletion of *ompR* or *envZ* results in a 401 and 281-fold increase (respectively) of the switching frequency from the opaque to the translucent variant when compared with the wild-type AB5075 strain. Deletion of both genes yields a similar result (463-fold increase). This suggests that this TCS strongly represses phase switching in response to environmental factors, presumably osmotic pressure (Tipton and Rather, 2017). The RND-type efflux system, constituted by two membrane transporters named ArpA and ArpB, exerts the opposite effect. Deletion of either *arpA* or *arpB* decreases the frequency of switching from opaque to translucent colony variants by 77 and 1,916-fold, respectively. Interestingly, deletion of a gene encoding a TetR-type regulator located in the same locus as the *arpAB* operon significantly increases the expression of *arpA* and also reduces the opaque to translucent switch frequency by 1,916-fold (Tipton et al., 2017).

Finally, the most important phase switching regulator found to date is ABUW_1645, a TetR-type transcriptional regulator that was found 60 times more expressed in translucent than in opaque variants. Moreover, this regulator modulated the expression of around 70% of the genes differentially expressed between the two variants. Deletion of *ABUW_1645* increases by 18-fold the translucent to opaque switching frequency, while overexpression of the gene in the opaque variant (AB5075-O/1645) induces an irreversible switch to the translucent phenotype. Interestingly, vaccination of mice with the avirulent AB5075-O/1645 strain confers protection against infection with the virulent AB5075 opaque wild-type strain, providing a very interesting precedent for the use of translucent-locked variants of *A. baumannii* as attenuated live vaccines (Chin et al., 2018).

Overall, these studies strongly suggest that opaque variants are responsible for the pathogenesis of *A. baumannii* AB5075, as they are

more virulent and resistant to antibiotics and host defences. The recovery of opaque-dominant *A. baumannii* clinal samples also suggests that these results could be applied to other strains that possess a similar phase switching mechanism. The role of translucent variants on the survival in nutrient-limited natural environments, however, remains to be further characterized.

1.4. Attachment and biofilm formation

Biofilms are communities composed of one or more aggregated microorganisms embedded in a self-produced extracellular matrix formed by extracellular polysaccharides (EPS), proteins, extracellular DNA (eDNA) and lipids. Most bacteria form biofilms as a mechanism of persistence in the environment, as cells in biofilms possess a series of distinctive features that make them much more resistant to external threats such as desiccation, antimicrobial agents, host defences and mechanical forces. In fact, it is now generally accepted that biofilms are the predominant state of bacteria in the natural environment. Cells in biofilms are usually phenotypically distinct from planktonic cells, with differences in gene expression and a much slower metabolism and growth rate. This slow metabolism, along with the protective layer created by the extracellular matrix, confers biofilm cells a much higher tolerance to antimicrobials, including antibiotics, being in some cases up to 1,000 times more resistant than planktonic bacteria. Moreover, the high numbers of bacteria within biofilms aids increased horizontal gene transfer, facilitating the spread on antibiotic resistance and virulence genes (Del Pozo, 2018; Toyofuku et al., 2016; Rabin et al., 2015).

Most pathogens are also capable of forming biofilms not only as a mechanism of persistence in the natural environment, but also to colonise hospital facilities, medical devices and even the human body, causing different biofilm-associated infections such as chronic lung

infections in cystic fibrosis patients, periodontitis, osteomyelitis, sinusitis, endocarditis or urinary tract infections, among others (Del Pozo, 2018). Biofilm formation usually involves several steps (**Figure 1.3**): attachment of planktonic cells to a surface, biofilm maturation and dispersal.

Attachment

The process of attachment is the initial, crucial step in biofilm formation, as this is when the cells decide to either remain in a planktonic state or switch to a sessile lifestyle. Usually, bacterial attachment involves two stages: reversible and irreversible attachment. In the reversible attachment step, flagella and T4P are employed to weakly attach a surface. During this process, different environmental signals, biological factors and forces come into play, ultimately determining whether the bacteria detach from the surface and returns to a planktonic state or proceeds towards irreversible attachment and biofilm formation (Toyofuku et al., 2016). The factors contributing to make a surface suitable for the bacteria to irreversibly attach are still a matter of intense research. The surface chemistry and topography, conditioning, charge or hydrophobicity have all been proposed to play key roles in the process, but more research is still needed to fully understand why bacteria form biofilms preferably on some surfaces rather than others (Palmer et al., 2007).

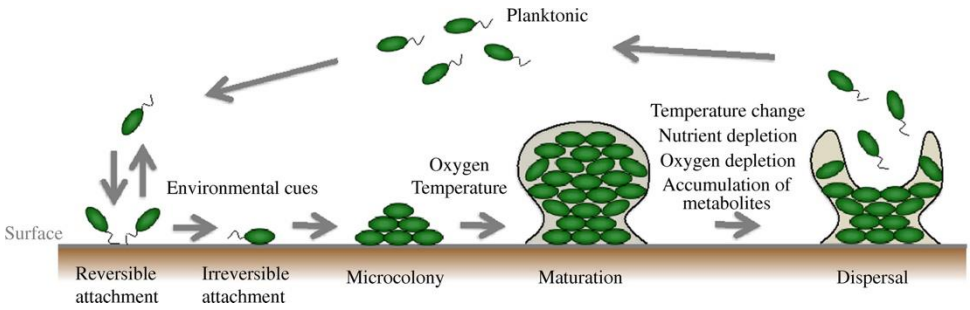


Figure 1.3: Biofilm formation and dispersion cycle. Extracted from Toyofuku *et al.*, 2016. Planktonic cells arrive at the surface and reversibly attach to it. In this phase, the bacteria can either detach and return to the planktonic lifestyle or irreversibly attach and start dividing forming microcolonies. As the microcolony grows, cells undergo physiological changes, losing motility and secreting extracellular elements that constitute the matrix. Diverse environmental signals can trigger the dispersal phase, which consists on a coordinated degradation of the extracellular matrix and return to the planktonic lifestyle.

Biofilm maturation

Once cells are irreversibly attached, physiological changes start to occur. Cells lose motility and start to divide, forming microcolonies. These microcolonies begin to produce the extracellular matrix by secreting proteins, extracellular polysaccharides, eDNA and other biomaterials. The matrix gives the biofilm its three dimensional structure, maintaining the cells together and attached to the surface. During the maturation step, the biofilm undergoes a stratification process, where cells in different areas of the biofilm display different metabolic activities and gene expression profiles. It has also been observed that mature biofilms possess a complex architecture, with water channels that might contribute to nutrient and waste transportation across the biofilm (Donlan and Costerton, 2002; Toyofuku et al., 2016; Rabin et al., 2015). During this stage there is already some passive dispersal, as mechanical forces act on the surface of the biofilm, detaching cells that then leave to seed in a new surface and restart the biofilm cycle.

Dispersal

The last stage of the biofilm cycle is the active dispersal process, where cells co-ordinately and actively degrade the matrix and return to a planktonic lifestyle. During this process, biofilm cells undergo additional physiological changes, expressing once again motility factors, secreting degrading enzymes and repressing genes involved in the synthesis of matrix components and attachment. The list of biological and environmental factors that lead to biofilm dispersal is extensive, with many more still to be identified and most not completely understood. Some of these cues include quorum sensing, bis-(3'-5')-cyclic-diguanosine monophosphate (c-di-GMP), changes in temperature, nutrient availability, oxygen, accumulation of metabolites or detection of host signals, among others (Guilhen et al., 2017; Solano et al., 2014).

1.4.1. Attachment and biofilm formation in *A. baumannii*

As for many other pathogens, *A. baumannii* forms biofilms as an essential part of the colonization process of abiotic surfaces on hospital equipment and medical devices (Bernards et al., 2004; Rocha et al., 2018). Despite the importance of biofilm formation in *A. baumannii* pathogenesis and the well-studied mechanisms involved in attachment and biofilm formation in other human pathogens, very little is known about the process in *A. baumannii*. Nonetheless, some common factors important for attachment and biofilm formation have been identified and characterized. The type I Csu (chaperone-user) pilus is probably the best-known mediator of biofilm formation and attachment in *A. baumannii*, being required for biofilm formation in many strains (Rumbo-Feal et al., 2013; Nait Chabane et al., 2014; Tomaras et al., 2003). The structure and regulation of the Csu pilus will be discussed in detail in Chapter 5 (see 5.1.1). Interestingly, some clinical strains lack the *csu* operon or this is disrupted due to insertions, indicating that the Csu pilus is not

always necessary for biofilm formation. Other bioinformatically predicted type I pili clusters have also been identified in *A. baumannii* and could also play an important role in biofilm formation. Unfortunately, none of these systems has been phenotypically characterized (Eijkelkamp et al., 2014; Harding et al., 2018).

An orthologue of the biofilm-associated protein (Bap), originally identified in *Staphylococcus aureus,* has also been characterized in *A. baumannii*. In *A. baumannii,* Bap is a large protein of more than 8,500 amino acids secreted through the type I secretion system (T1SS) and located in the surface of the outer membrane that plays diverse roles in biofilm formation and adherence (Harding et al., 2018; Goh et al., 2013). Bap was first identified in *A. baumannii* 307-0294 and was involved in biofilm maturation and maintenance, as disruption of the *bap* gene resulted in thinner static biofilms in late stages of development (Loehfelm et al., 2008). Further research revealed that Bap is necessary for biofilm formation on different medically relevant surfaces, including titanium, polystyrene and polypropylene, as well contributing to cell surface hydrophobicity and adherence (but not invasion) on NHBE (Normal and Diseased Bronchial Epithelial) and NHNK (Normal Human Neonatal Keratinocyte) human cells (Brossard and Campagnari, 2012). Extensive bioinformatic analysis revealed that Bap is highly polymorphic, with 3 different variants present in different proportions across the analysed isolates, with type 3 being exclusive to *A. baumannii*. Moreover, 20% of the strains analysed lacked Bap in their genome sequences (De Gregorio et al., 2015).

As mentioned above, EPS are integral elements of the biofilm matrix. *A. baumannii* produces poly-β-1,6-*N*-acetylglucosamine (PNAG), which has also been identified as a major component of biofilm matrix

in other species such as *Bacillus subtilis* and *S. aureus* (Heilmann et al., 1996; Roux et al., 2015). In *A. baumannii*, PNAG is synthesize by proteins encoded in the *pgaABCD* locus. Deletion of this locus leads to a significant reduction in biofilm formation after 24 h and a reduction in biomass and loss of three-dimensional structure after 48 h on glass (Choi et al., 2009). Moreover, antibodies against PNAG mediate *A. baumannii* killing by promoting opsonophagocytosis, suggesting that this polysaccharide could be a potential attractive candidate for vaccine development (Bentancor et al., 2012b).

Protein glycosylation, which is closely related to capsule synthesis (see 1.2.1.4), also affects biofilm formation. Deletion of the *O*-OTase *pglL* leads to a loss glycosylation of different proteins, attenuated virulence and a significant reduction of thickness and biomass in biofilm formation (Iwashkiw et al., 2012).

Biofilm is regulated by different environmental factors in *A. baumannii*. As a strict aerobe, *A. baumannii* forms much thicker biofilms at the liquid-air interface. Temperature is also very important, as *A. bauma*nnii forms better biofilms at 28-30°C than 37°C, probably due to the upregulation of both Bap and Csu pili (Eze et al., 2018; Tomaras et al., 2003). Other regulators of biofilm formation in *A. baumannii* such as QS, TCS, blue light and phase variation have been discussed in more detail above in their respective sections.

1.5. Quorum sensing

Quorum sensing (QS) is a term coined in 1994 (Fuqua et al., 1994) to describe a cell density-dependent communication mechanism used by bacteria (but also archaea and eukaryotes) to coordinate the expression of specific genes according to the presence of other bacteria in the surrounding environment. The mechanism of action involves the synthesis and release of extracellular signalling molecules called autoinducers (Nealson, 1977). These chemical signals accumulate in the local environment as the population grows and, when their concentration reaches a certain threshold, they bind and activate a response regulator, which triggers the modulation of expression of a specific regulon.

Signalling molecules differ in their nature and specificity. Gram-positive bacteria typically secrete oligopeptides that are detected by a two-component system consisting of a membrane-bound sensor kinase and a response regulator (usually a transcriptional regulatory protein) that modulates gene expression (**Figure 1.4A**) (Banerjee and Ray, 2017). In Gram-negative bacteria, a synthase enzyme usually produces acyl-homoserine lactones (AHLs) as autoinducers (or other molecules derived from *S*-adenosylmethionine), which can diffuse freely through the bacterial membrane and bind to a specific response regulator (usually a transcriptional regulator) in the inner membrane or the cytoplasm, which regulates QS-specific gene expression (**Figure 1.4C**) (Papenfort and Bassler, 2016).

In both Gram-negative and Gram-positive bacteria, the autoinducer specificity can range from interspecies, species or even strain-specific, with some strains producing more than one type of signalling molecule. Another feature in common is that QS systems usually possess a positive autoinduction loop: autoinducer-mediated activation of the response regulator results in the synthesis of more

autoinducer, which in turn results in more activation of the response regulator, restarting the loop (Rutherford and Bassler, 2012). Presumably, this feature ensures a sufficiently high concentration of signalling molecules in the environment to co-ordinately activate the QS of the population as a whole, promoting synchronous gene expression in the community.

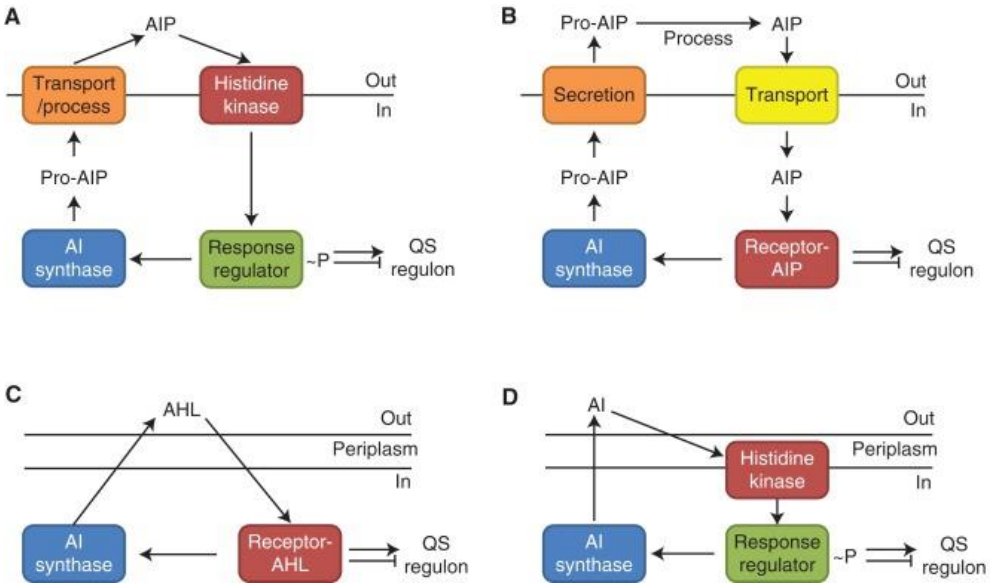


Figure 1.4: "Canonical quorum sensing (QS) circuits". Extracted from Rutherford and Bassler, 2012. Canonical AIP-based Gram-positives QS based in a **(A)** two-component system or **(B)** transport of AIP into the cytoplasm and binding to a response regulator**. (C)** Canonical AHL-based QS system in Gram-negative bacteria. **(D)** Gram-negative QS system based in a two-component system, used by diverse bacteria, most notably *V. cholerae*. A more detailed description of all 4 systems can be found in the original review by Rutherford and Bassler, 2012.

The role of quorum sensing has been shown to be key regulating the production of metabolically costly goods and limit their synthesis to situations in which they will be beneficial for the community in order to adapt to the environmental conditions. In a pathogenicity context, an illustrative example would be the production of virulence factors such as extracellular toxins in *Staphylococcus aureus*. Production of toxins when there is a small number of cells in the host is likely to be a waste of resources and even provoke an early activation of the host immune system that the pathogen is not ready to neutralize. Instead,

when the number of bacteria is low, the QS system of *S. aureus* is inactive, and cells produce more surface-associated components that help in the initial colonization of the host. As their number increase, accumulation of the peptide signalling molecule (known as an autoinducing peptide (AIP)) results in the activation of the QS, which upregulates the expression of toxins and other extracellular virulence factors such as alpha-hemolysin, leukocidins, exotoxins, proteases and lipases, among others. These virulence factors help neutralize the immune response and release more nutrients from host cells. Surface components, on the other hand, are generally downregulated by QS, as they are no longer required for the infection (Rutherford and Bassler, 2012; Dunman et al., 2001; Thoendel et al., 2011; Jenul and Horswill, 2018; Ji et al., 1995; Ky and Otto, 2015). QS has also been shown to regulate many other physiological processes in different bacteria such as biofilm formation, cell motility, antibiotic resistance, conjugation and pigment production (Brackman and Coenye, 2014; Dou et al., 2017; Krašovec et al., 2014; Whitehead et al., 2001).

1.5.1. Quorum sensing in Gram-negative bacteria

Cell-to-cell communication was firstly reported in the early 1960's as a mechanism to regulate the formation of the fruiting body of the *Myxococcus xanthus*. Subsequent studies revealed that other bacteria also used a similar communication mechanism to regulate diverse phenotypes, such as streptomycin biosynthesis in *Streptomyces griseus*, competent state in *Streptococcus pneumoniae* or bioluminescence the Gram-negative *Vibrio fischeri* (Reviewed by Williams *et al.*, 2007). It was in *V. fischeri* where an AHL (*N*-(3-oxohexanoyl)homoserine lactone (OC6)) was isolated and identified as the autoinducer molecule for first time (Eberhard et al., 1981). Further work on this bacteria lead to the characterization of the now widely known LuxR/LuxI QS system (Fuqua et al., 1994).

Since then, many other LuxR/LuxI-like QS systems have been identified and characterized in many different Gram-negative bacteria. These systems produce AHLs of different acyl chain length and 3-position modifications (**Figure 1.5**) that, as previously mentioned, vary between species and strains (Whitehead et al., 2001). One of the best examples and well-studied QS systems in Gram-negative bacteria is *Pseudomonas aeruginosa*'s. *P. aeruginosa* possesses three different QS systems, two LuxI/LuxR-like AHLs-based and one based in alkyl quinolones (AQ) as signalling molecules. The three systems are hierarchically organized and possess a positive auto-induction loop, allowing a high adaptability through tight regulation of gene expression (Williams and Cámara, 2009).

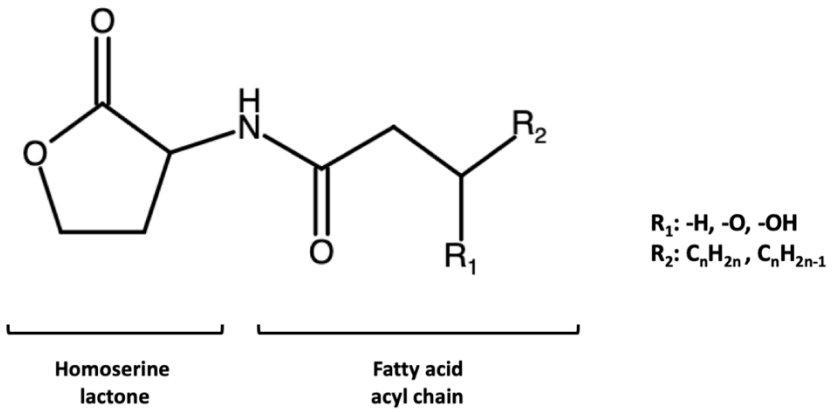


Figure 1.5: General structure of *N*-acyl homoserine lactones (AHLs). R_1 represents the 3-position substitution/modifications: 3-oxo (-O), 3-hydroxy (-OH) or unsubstituted (-H) R_2 represents the length of the acyl chain, where the number of hydrogens is 2*n* for 3-hydroxy and unsubstituted AHLs and 2*n*-1 for 3-oxo AHLs.

The hierarchical AHL system in *P. aeruginosa* depends on LasI/LasR and *N*-(3-oxododecanoyl)-L-homoserine lactone (OC12). This system activates a second AHL system, RhlI/RhlR, as well as the AQ-based QS system (commonly known as PQS system). The RhlI/RhlR, in turn, produces *N*-butanoyl-L-homoserine lactone (C4) and negatively regulates the PQS system. Lastly, the *Pseudomonas* AQ (PQS) system produces PQS (*Pseudomonas* Quinolone Signal, 2-heptyl-3-hydroxy-

4-quinolone) and activates RhlI/RhlR (**Figure 1.6**) (Latifi et al., 1996; McGrath et al., 2004; Coggan and Wolfgang, 2012).

Both AHL systems possess overlapping regulons that include several virulence factors such as elastase, exotoxin A, pyocyanin, proteases, cyanide, RpoS (stress response regulator), rhamnolipids, LecA lectine, type II secretion system (T2SS), siderophores and pyoverdine, among others (Lee and Zhang, 2015; Schuster and Peter Greenberg, 2006). Moreover, these systems are involved in biofilm formation through the indirect regulation of *pel* genes (involved in the synthesis of extracellular polysaccharides) and direct regulation of other biofilm-related factors, such as rhamnolipids (Lee and Yoon, 2017; Sakuragi and Kolter, 2007). Overall, LasI/LasR and RhlI/RhlR systems regulate the expression of around 3-7% (depending on the study and methodology used) of *P. aeruginosa* genome (Schuster and Peter Greenberg, 2006).

The PQS system also regulates many virulence factors such as pyocyanin, elastase, LecA, rhamnolipids and cyanide. This system also plays a very important role in biofilm formation, regulating the production of biofilm-related factors such as extracellular DNA (eDNA), an important element of the biofilm matrix (Dubern and Diggle, 2008; Rampioni et al., 2016; Allesen-Holm et al., 2006).

Due to the importance of QS in the regulation of virulence and adaptation to environmental and host changes, several other regulatory mechanisms interact with the three systems, adding extra layers of regulation that further adjust the bacterial response. QscR, for example, binds LasR and RhlR, delaying their response. Moreover, it can repress *lasI* expression and directly regulate several genes, including those under the control of the LasI/LasR and RhlI/RhlR systems.

RpoS, which is regulated by the RhlI/RhlR system, can also regulate the expression of around 40% of the QS-regulated genes and activate the expression of both AHL systems.

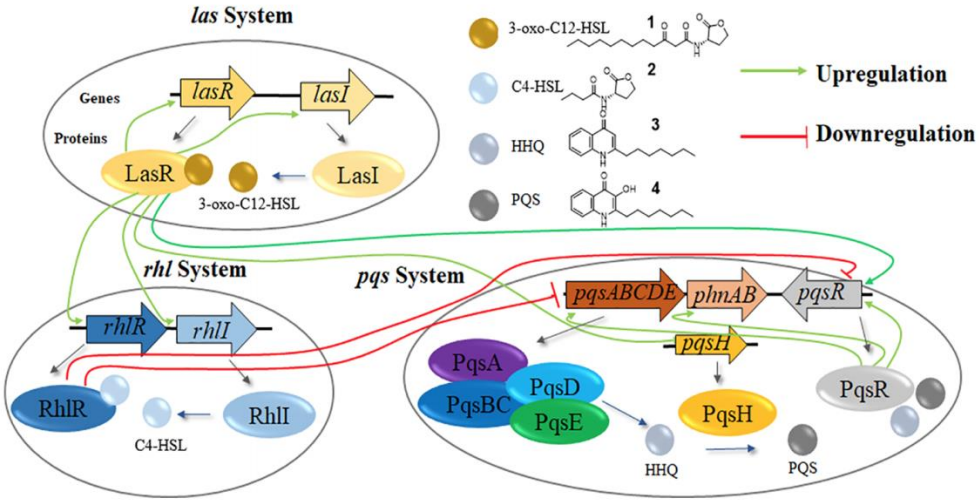


Figure 1.6: Cross-regulation of the three *Pseudomonas aeruginosa* QS systems. Extracted from Soukarieh, Williams, *et al.*, 2018. Green arrows represent up-regulation and blocked red arrows represent down-regulation. All three systems are positively auto-regulated. the las system positively regulates the *rhl* and *pqs* system, while the *rhl* system negatively regulates the *pqs* system.

Under phosphate limitation, PhoB activates the expression of the PQS system regulator, PqsR. PmpR, on the other hand, exerts the opposite effect, repressing *pqsR* expression. Many other regulatory proteins perform a similar role: Vfr, RsmY/RsmZ/RsmA, VqsR, PtxR, RsaL, VqsM and DksA, among others (Coggan and Wolfgang, 2012; Williams and Cámara, 2009). All these regulators, through different mechanisms, have a similar objective: to fine-tune the expression of the QS systems and their regulons to ensure their activation takes places at the best time to optimize the adaption of the bacterial community to the environment.

Overall, *P. aeruginosa* provides a detailed Gram-negative example of the importance of QS in biofilm formation and the colonization and infection process through a fine-tuned regulation of virulence factors involved in different aspects of pathogenesis. Moreover, it also illustrates the interconnections between multiple regulatory systems to provide optimal adaptation to the environment.

1.6. Aims and objectives of the project

- Elucidate the contributions of QS and the uncharacterized *abaM* to AHL production, surface motility, attachment and virulence to *G. mellonella* in *A. baumannii* AB5075.
- Characterize the regulation and nature of the QS and AbaM regulons.
- Identify the selectivity of AbaR for different AHLs.
- Discover activators and inhibitors of AB5075 QS and investigate the moieties and structural properties involved.
- Study the role of the Csu pili in AB5075 attachment and its contribution to surface selectivity by testing polymer surfaces with different physicochemical properties.

2. Materials and methods

2.1. Strains and growth conditions

A. baumannii strains were routinely grown in low-salt lysogeny broth (LS-LB) containing 10 g l^{-1} of Bacto™ tryptone (BD Biosciences), 5 g l^{-1} of yeast extract (Oxoid) and 5 g l^{-1} of NaCl. *E. coli* strains were routinely grown in lysogeny broth (LB) containing 10 g l^{-1} of Bacto™ tryptone (BD Biosciences), 5 g l^{-1} of yeast extract (Oxoid) and 10 g l^{-1} of NaCl.

Hygromycin was added when needed to a final concentration of 125 μg ml^{-1} (*E. coli*) or 250 μg ml^{-1} (*A. baumannii*). Ampicillin was added when needed to a final concentration of 100 μg ml^{-1}; chloramphenicol and tetracycline to a final concentration of 10 μg ml^{-1}. Gentamycin was used as a counterselection for *E. coli* in a final concentration of 100 μg ml^{-1}.

A list of all the strains used in this study can be found in **Table 2.1**.

Table 2.1: Strains used in this project.

Strain	Description	Reference
E.coli		
DH5α	λ^- *φ*80dlacZ*ΔM15 Δ(lacZYA-argF)U169 recA1 endA1 hsdR17*(r_K^- m_K^-) *supE44 thi-1 gyrA relA1*	Lab stock.
BL21	F^- *ompT gal dcm lon hsdS*$_B$($r_B^-m_B^-$) [*malB*$^+$]$_{K-12}$(λ^S)	Lab stock

A. baumannii		
AB5075	Wild-type parental strain of the hypervirulent, multi-drug resistant *A . baumannii* AB5075, isolated from a patient with tibia osteomyelitis.	(Jacobs et al., 2014)
abaM::Tn*26*	AB5075 with the Tn*26* transposon disrupting the RsaM orthologue *ABUW_3775*.	(Gallagher et al., 2015)
abaI::Tn*26*	AB5075 with the Tn*26* transposon disrupting the quorum sensing synthase gene *abaI* (*ABUW_3776*).	(Gallagher et al., 2015)
AB5075 pMQ557M	AB5075 carrying the pMQ557M plasmid.	This study
abaM::Tn*26* pMQ557M	*abaM*::Tn*26* carrying the pMQ557M plasmid.	This study
abaM::Tn*26* pMQ_*abaM*	*abaM*::Tn*26* carrying the pMQ_*abaM* complementation plasmid.	This study
AB5075 P*abaM*::*lux*	AB5075 carrying the mini-Tn*7*T_Hyg^R_P*abaM*::*lux* insertion.	This study
AB5075 P*abaI*::*lux*	AB5075 carrying the mini-Tn*7*T_Hyg^R_P*abaI*::*lux* insertion.	This study
AB5075 Tn*7*::*lux*	AB5075 carrying the mini-Tn*7*T_Hyg^R_*lux* insertion.	This study
abaM::Tn*26* P*abaM*::*lux*	*abaM*::Tn*26* carrying the mini-Tn*7*T_Hyg^R_P*abaM*::*lux* insertion.	This study
abaM::Tn*26* Tn*7*::*lux*	*abaM*::Tn*26* carrying the mini-Tn*7*T_Hyg^R_*lux* insertion.	This study

abaI::Tn*26* P*abaM*::*lux*	*abaI*::Tn*26* carrying the mini-Tn*7*T_Hyg^R_P*abaM*::*lux* insertion.	This study
abaI::Tn*26* P*abaI*::*lux*	*abaI*::Tn*26* carrying the mini-Tn*7*T_Hyg^R_P*abaI*::*lux* insertion.	This study
abaI::Tn*26* Tn*7*::*lux*	*abaI*::Tn*26* carrying the mini-Tn*7*T_Hyg^R_*lux* insertion.	This study
AB5075 pMQ_P*csu*::*lux*	AB5075 carrying the pMQ_P*csu*::*lux* plasmid.	This study
abaM::Tn*26* pMQ_P*csu*::*lux*	*abaM*::Tn*26* carrying the pMQ_P*csu*::*lux* plasmid.	This study
csuA/B::Tn*26*	AB5075 with the Tn*26* transposon disrupting the Csu pili major pilin subunit (CsuA/B) encoding gene, *ABUW_1487*.	(Gallagher et al., 2015)
csuE::Tn*26*	AB5075 with the Tn*26* transposon disrupting the Csu pili adhesive tip (CsuE) encoding gene, *ABUW_1492*.	(Gallagher et al., 2015)

2.2. Bacterial stocks for long term storage

2.2.1. *E. coli* stocks

E.coli stocks were prepared by mixing 1 ml of an overnight culture with 700 µl of sterile 50% glycerol (20% final concentration) in a 2 ml cryogenic vial and stored at -81°C.

2.2.2. *A. baumannii* stocks

A. baumannii stocks were prepared by picking a single colony from a Phase Observation LB (PO-LB) plate (see 2.4.2) of the desired strain and growing it in 1 ml of LS-LB in a 2 ml cryogenic vial overnight at room temperature to an $OD_{600} \approx 0.1$. After that, 700 µl of sterile 50%

glycerol (20% final concentration) were added and mixed with the culture and the vial was stored at -81°C.

All stocked strains were streaked in PO-LB plates and colonies were observed under a SMZ1000 stereo microscope (Nikon) to verify that the correct phase was stocked.

2.3. DNA manipulation and gene cloning

All restriction digests mentioned in this section were carried out using New England Biolab enzymes. Likewise, all ligations were performed at 4°C overnight using a T4 DNA ligase (Promega). Genetic constructs described in this section were confirmed by Sanger sequencing (Source BioScience). Plasmids and primers used in this study can be found below in **Tables 2.2** and **2.3**, respectively.

Table 2.2: Plasmids and vectors used in this project.

Plasmid	Description	Source
pBluelux	pBluescript plasmid containing the promoterless *luxCDABE* operon.	Lab stock
pBluescript-IISK_KO_Multi_HYG_UTRs	pBluescript containing the hygromycin resistance cassette (*hph*).	James Chamberlain
pBAD_*csu*	pBAD cloning vector containing the *A. baumannii* ATCC 19606 *csuA/BABCDE* operon cloned under control of the *araBAD* promoter.	(Pakharukova et al., 2018)

pSW002_*E2-Crimson*	pSW002-Pc-E2-Crimson vector. Used for red fluorescence-tagging *E. coli* BL21.	(Wilton et al., 2018)
pMQ557	Vector replicative and stable in *A. baumannii* containing the *hph* cassette as antibiotic marker.	Prof. Robert M. Q. Shanks (personal communication)
pMQ557M	pMQ557 with the yeast replication genes removed.	This study
pMQ_*abaM*	pMQ557M containing the *abaM* gene and 758 bp of the upstream region.	This study
pMQ_P*csu*::*lux*	pMQ557M containing the *csuA/B* promoter – *luxCDABE* operon fusion.	This study
pUC18T-mini-Tn*7*T	pUC18 plasmid with the mini-Tn*7* containing only terminator regions and a multi-cloning site (MCS).	(Choi et al., 2005)
pUC18T-mini-Tn*7*T_Hyg^R	pUC18T-mini-Tn*7*T with the *hph* cassette cloned in the MCS.	This study
pUC18T-mini-Tn*7*T_Hyg^R_*lux*	pUC18T-mini-Tn*7*T_Hyg^R with the promoterless *luxCDABE* operon cloned in the MCS.	This study
pUC18T-mini-Tn*7*_Hyg^R _P*abaM*::*lux*	pUC18T-mini-Tn*7*T_Hyg^R containing part of the AB5075 QS locus, from the *abaR* gene to the first *abaM* codon for the *abaM* promoter – *luxCDABE* operon fusion, cloned in the MCS.	This study

pUC18T-mini-Tn*7*T_Hyg^R_*PabaI*::*lux*	pUC18T-mini-Tn*7*T_Hyg^R containing part of the AB5075 QS locus, from the *abaR* gene to the first *abaI* codon (including the *abaM* gene) for the *abaI* promoter – *luxCDABE* operon fusion, cloned in the MCS.	This study
pKT25	Vector for the BACTH bacterial two hybrid assay.	Euromedex, (Karimova et al., 1998)
pKNT25	Vector for the BACTH bacterial two hybrid assay.	Euromedex, (Karimova et al., 1998)
pUT18	Vector for the BACTH bacterial two hybrid assay.	Euromedex, (Karimova et al., 1998)
pUT18C	Vector for the BACTH bacterial two hybrid assay.	Euromedex, (Karimova et al., 1998)

Table 2.3: Primers used in this project. Bases corresponding to the restriction sites are underlined.

Primer name	Sequence 5' →3'	Description
*abaM*_check_FW	GAAGAGCTTAAAGATGTGCTA	Confirmation of Tn*26* insertion in *abaM.*
*abaM*_check_RV	GGCCTTCTGAAAAATTGTTTTG	Confirmation Tn*26* insertion in *abaM.*
*abaM*_compl_FW_*Bam*HI	ATATGGATCCTTGCTCTCATTAG ACTCCATTCAC	*abaM*::Tn*26* complementation.

*abaM*_compl_RV	ATATGGTACCGTGCTTCCACTTATTTTTCAAGT	*abaM*::Tn*26* complementation.
*lux*_reporter_FW	CTCCGATTAATTATAATTAACC	Construction of P*abaM*::*lux* and P*abaI*::*lux*
*lux*_reporter_*abaM*_RV	GCGCGGATCCGCGCGGTACCCCATGCTACCTGCTTAAGTACCC	Construction of P*abaM*::*lux*
*lux*_reporter_*abaI*_RV	GGATCCGGTACCCATTACAAGTGCTTCCACTTA	Construction of P*abaI*::*lux*
*lux*_reporter_*csu*_FW	ATAGGTACCCAATTTTGATCATTATCCAGCCTG	Construction of P*csu*::*lux*
*lux*_reporter_*csu*_RV	ATACTCGAGCATATTCATAACCTACATATATAATG	Construction of P*csu*::*lux*
*abaI*_check_FW	CAATACGTCATTAACCGAGTCTTC	Confirmation of Tn*26* insertion in *abaI.*
*abaI*_check_RV	GCAAACTTAAATCTAAAAACCAAG	Confirmation of Tn*26* insertion in *abaI.*
M13F	CCCAGTCACGACGTTGTAAAACG	Sequencing of mini-Tn*7*-based constructs.
Tn*7*L_seq	GGTTGGCCTGCAAGGCCTTCGCG	Sequencing of mini-Tn*7*-based constructs.
pMQ_insertion_RV	CAGACATTGCCGTCACTGCG	Sequencing of pMQ557M-based constructs.
*abaM*_FW_pKT25	AAAGCTCTGCAGGGGTTAGCATACCCCCTC	Cloning of *abaM* in BACTH vectors.
*abaM*_FW_BACTH	AAAGCTCTGCAGGGTTAGCATACCCCCTC	Cloning of *abaM* in BACTH vectors.
*abaM*_RV_BACTH	AAAGCTGGATCCTCAGAGAAGGTTTGACTTAATGAAGACTCGG	Cloning of *abaM* in BACTH vectors.

*abaR*_FW_pKT25	AAAGCTCTGCAGGGGAAAGTTGGCAAGAGGA	Cloning of *abaR* in BACTH vectors.
*abaR*_FW_BACTH	AAAGCTCTGCAGGGAAAGTTGGCAAGAGGA	Cloning of *abaR* in BACTH vectors.
*abaR*_RV_BACTH	AAAGCTGGATCCTCCAAAAGCCCTAGCATTACAGC	Cloning of *abaR* in BACTH vectors.
*abaI*_FW_pKT25	AAAGCTCTGCAGGGAATATTATTGCTGGATTTC	Cloning of *abaI* in BACTH vectors.
*abaI*_FW_BACTH	AAAGCTCTGCAGGAATATTATTGCTGGATTTC	Cloning of *abaI* in BACTH vectors.
*abaI*_RV_BACTH	AAAGCTGGATCCTCGATATCAATCAAGCATGCAAAC	Cloning of *abaI* in BACTH vectors.
Hyg_FW	TCATCACTGCAGATGAAAAAGCCTGAACTCACC	Cloning of *hph* cassette in mini-Tn*7*T.
Hyg_RV	TCATCACTGCAGGGGGGATCGATCCCGGTCGG	Cloning of *hph* cassette in mini-Tn*7*T.
*rpoB*_qPCR_FW	TCGTGTTGAGCGTGCTGTTA	qPCR of the endogenous control gene *rpoB*
*rpoB*_qPCR_RV	TGCAGCAGCAACTGGTTTTG	qPCR of the endogenous control gene *rpoB*
*csuAB*_qPCR_FW	AGCAGCAACAGGTGGCAATA	qPCR of the *csuA/B* gene
*csuAB*_qPCR_RV	GGTCTGTACGTTCACCACCAT	qPCR of the *csuA/B* gene
*3773*_qPCR_FW	AGTGTCACTGCGGGTTACTG	qPCR of the *ABUW_3773* gene
*3773*_qPCR_RV	CTAGGTTGTCCCGCCTCATC	qPCR of the *ABUW_3773* gene

2.3.1. Genetic constructs based on pUC18T-mini-Tn*7*T

The pUC18T-mini-Tn*7*T plasmid was kindly provided by Herbert Schweizer (Addgene plasmid #64957).

2.3.1.1. Hygromycin selectable mini-Tn*7* construction

The *hph* gene, conferring resistance to hygromycin B, was amplified by PCR using pBluescript-IISK_KO_Multi_HYG_UTRs plasmid as a template, the PCR product was digested using *Kpn*I and *Hin*dIII restriction enzymes and ligated in the MCS of the mini-Tn*7* in pUC18T-mini-Tn*7*T.

2.3.1.2. *lux*-based P*abaM* and P*abaI* reporter construction

The upstream region of *abaM* or *abaI* were amplified by PCR and ligated in pGEM®-T Easy using the pGEM®-T Easy Vector System (Promega) following the manufacturer protocols. The resulting plasmid and the promoterless *luxCDABE* operon were digested with *Kpn*I and *Bam*HI and ligated in order to introduce the *lux* operon downstream of the promoter of *abaM*/*abaI*.

After that, the whole construct (upstream region with the *lux* genes) was transferred into the MCS of pUC18T-mini-Tn*7*T-Hyg^R after digesting with *Not*I and *Pst*I and ligating the corresponding fragments.

2.3.1.3. Insertion of mini-Tn*7* constructs into AB5075 strains

Mini-Tn*7*T-based constructs were inserted into *A. baumannii* through four-parental conjugation. Briefly, PBS-washed overnight cultures of the *E. coli* DH5α donor strain (containing the plasmid with the mini-Tn*7* construct to be inserted), the *E. coli* DH5α helper strain (containing pUX-B13, the plasmid carrying the transposase genes), the *E. coli* DH5α mobilizable strain (containing pRK600, the plasmid that can mobilise other plasmids) and the *A. baumanii* recipient

strain were mixed in a 1:1:1:1 proportion (100 µl of each), resuspended in 50 µ of PBS and spotted in a non-selective LB plate for incubation at 30°C for at least 6 hours (ideally overnight). Cells were collected from the LB plate, resuspended in PBS and plated in a selective media containing hygromycin (for mini-Tn*7* selection) and gentamycin (for counterselection of *E. coli*).

2.3.2. Genetic constructs based on pMQ557M

The pMQ557 plasmid was a gift of Robert M.Q. Shanks. The pMQ557M plasmid was obtained by digesting pMQ557 with *Pml*I (to remove the genes required for yeast replication) and religating the resulting large linear product.

2.3.2.1. Complementation plasmids for *abaM*::Tn*26* mutant

The *abaM* gene plus 768 bp from its upstream region (containing the native promoter) were amplified by PCR. The PCR fragments were digested with *Bam*HI and *Kpn*I and ligated in the MCS of pMQ557M.

2.3.2.2. *lux*-based *csu* operon reporter.

The upstream region of the *csuA/BABCDE* operon (containing its native *in silico* predicted promoter) was amplified by PCR, digested with *Kpn*I and *Xho*I and ligated in the MCS of pMQ557M. The resulting plasmid and the *luxCDABE* operon were digested with *Xho*I and *Not*I and ligated to introduce the *lux* genes downstream of the *csuA/BABCDE* operon promoter.

2.3.3. Construction of plasmids for BACTH assay

The *abaM*, *abaR* and *abaI* genes were amplified by PCR. The PCR products and the four Bacterial Adenylate Cyclase Two-Hybrid (BACTH) plasmids (pKT25, pKNT25, pUC18 and pUC18T) were digested with restriction enzymes *Bam*HI and *Pst*I, purified and

ligated so all four genes were inserted in all four plasmids in frame with the T25 (pKT25 and pKNT25) or T18 (pUC18 and pUC18T) fragments of the catalytic domain of *Bordetella pertussis* adenylate cyclase (Karimova et al., 1998; Ladant and Ullmann, 1999).

2.4. Phenotypic assays

2.4.1. Growth curves

Strains were grown in LS-LB to an OD_{600} = 0.3 and then adjusted in fresh media to an OD_{600} = 0.05. A 200 µl aliquot of each strain culture was added, in triplicate, to a 96-well (black, flat clear bottom) microtiter plate (Greiner Bio-One). Unused wells were filled with 200 µl of PBS to avoid evaporation. Plates were incubated at 37°C static in an Infinite 200 PRO (Tecan Diagnostics) plate reader and OD_{600} was measured every 30 minutes.

2.4.2. Observation of colonies for phase separation

Phase-observation LB (PO-LB) plates were prepared as previously described (Tipton et al., 2015). Briefly, a modified LB recipe containing 5 g l^{-1} of Bacto™ tryptone (BD Biosciences), 2.5 g l^{-1} of yeast extract (Oxoid) and 2.5 g l^{-1} of NaCl were mixed with agar (Oxoid) in a concentration of 0.8%, autoclaved at 121°C for 15 min and 20 ml were poured in Petri dishes.

Strains were grown in LS-LB to an OD_{600} = 0.3 and serially diluted in fresh LS-LB. The proper dilutions were streaked in PO-LB plates so each plate contained at least 200 colonies. Colonies were then observed under a SMZ1000 stereo microscope (Nikon) using obliquus light to discriminate between opaque and translucent phases.

2.4.3. Motility on semi-solid surfaces

Motility media plates were prepared by adding Eiken agar to a final concentration of 0.3% (w/v) to the LS-LB recipe (see section 2.1). The media was autoclaved at 121°C for 15 min and then cooled down in a 55°C water bath for 30 min. 20 ml were poured in each Petri dish (90 mm x 15.9 mm, Thermo Fisher Scientific) and solidified by leaving the plates without the lid for 40 min under a Bunsen burner. After that, plates were dried out for 20 min in a laminar flow cabinet. Plates were used within the same day of preparation. For the OHC12 assays, the compound was added at the corresponding final concentration before pouring the media in the plates. Acetonitrile was used as a negative control.

Strains were grown in LS-LB to an OD_{600} = 0.3. A 1-µl drop of each strain was spotted in the centre of a motility media plate and incubated at 30°C for 16 h. After that, motility diameters were measured and the data of 3 independent assays were used for the statistical analysis.

2.4.4. AHL extraction and detection

Strains were grown in LS-LB to an OD_{600} = 0.5 and then diluted 1:10 in 50 ml of fresh LS-LB. Cultures were incubated in static conditions at 37°C for 18 h (single time-point extraction) or for 6, 12, 18 and 24 h (over-time assay). Cultures were centrifuged at 10400 xg for 10 min and supernatants were sterile-filtered using 0.2 a µm pore size membrane filter to obtain cell-free supernatants. AHLs were extracted twice with equal volume of ethyl acetate acidified with 0.1% acetic acid. Extracts were evaporated to dryness using a Rotavap and analysed by liquid chromatography with tandem mass spectrometry (LC-MS/MS) as previously reported (Ortori et al., 2014). Briefly, dried samples were resuspended in 50 µl of methanol (MeOH) and

transferred to LC vials. 20 µl of each sample were injected into the LC instrument (Phenomonex Germini C18, 3.0 µm, 100 x 3.0 mm) and run at a 450 µl/min constant flow rate with mobile phases consisting of aqueous (A) 0.1% (v/v) formic acid and (B) 0.1% (v/v) formic acid in methanol. The binary gradient began at 10% B and run isocratically for 1 min. The gradient was then linearly increased to 99% B over 9 min and maintained at 99% B for 5 min before returning to 10% B over 1 min and maintained at 10% B for 4 min to re-equilibrate the column. The MS (Applied Biosystems Qtrap 4000 hybrid triple-quadrupole linear iron trap mass spectrometer (Foster City, CA, USA)) operating in the positive electrospray (+ES) mode and set up for multiple reaction monitoring (MRM) was used to screen the eluents from the LC column. The system used the Analyst software (Foster City, CA, USA) for automatic peak identification and integration.

For quantification, calibration samples consisting of a serial dilution of the synthetic standard stock solution of the analytes (AHLs) of interest (*N*-3-hydroxydodecanoyl-L-homserine lactone (OHC12) and *N*-3-hydroxydecanoyl-L-homoserine lactone (OHC10)) were run as detailed above to create a straight line calibration graph by plotting the mean ratio of the analyte peak area/internal standard (IS) for three replicates against concentration of the analyte. Quantification was determined by dividing the peak of the AHL of interest of each sample by the IS peak area and interpolating the value in the corresponding straight line calibration graph.

2.4.5. Liquid-air interphase attachment quantitative assay

Strains to be tested were grown in LS-LB to an OD_{600} = 0.3 and 750 µl were inoculated into 1.5 ml microcentrifuge polypropylene tubes. Tubes were incubated in static conditions at 37°C for 24 h. Cell density was determined by measuring the OD_{600}. The media was

removed and tubes were rinsed twice with 1 ml PBS. To visualize attached cells, 850 µl of 0.25% crystal violet were added to each tube, tubes were incubated at room temperature for 15 min and then rinsed three times with PBS. In order to quantify the attachment, 1 mL of 100% ethanol was added to each tube, incubated at room temperature for 10 min and vortexed thoroughly. Quantification was performed by optical absorbance at A_{585}.

For the OHC12 assays, the compound was added to the media at the corresponding final concentration before starting to grow the strains. Acetonitrile was used as a negative control.

2.4.6. *lux*-based reporters assays

All the compounds used in this assay were made by the laboratory chemist, Alex Truman. A list of the OC12-derived compounds used in the agonist/antagonist screening can be found in **Table 4.1**. Details about the synthesis of the compounds can be found in the original studies by Murray *et al.*, 2014 and Jadhav *et al.*, 2011. Stock compounds (10 mM) were prepared in acetonitrile and stored at -20°C. The amount of acetonitrile added to the bacterial cultures never exceeded 2% (v/v).

2.4.6.1. AHL activity, agonists assays and dose-response assays

A. baumannii AB5075 *abaI*::Tn*26* carrying mini-Tn*7*T_Hyg^R_ _*pabaM*::*lux* was grown in LS-LB to an OD_{600} = 0.3. The culture was normalized in fresh media to an OD_{600} = 0.05 and AHLs were added at concentrations ranging between 10 pM to 100 µM. Acetonitrile was used as a negative control. A 200 µl aliquot of each sample was added, in triplicate, to a 96-well (black, flat clear bottom) microtiter plate (Greiner Bio-One). Unused wells were filled with 200 µl of PBS to avoid evaporation. Cultures were incubated at 37°C in an Infinite 200

PRO (Tecan Diagnostics) plate reader for 24 h and OD_{600} and RLUs were measured every 30 min.

To analyse agonist activity of the different AHLs and the OC12-derived compounds, the compounds were added at a 1 μM final concentration.

2.4.6.2. Screening assays to find OHC12 antagonists

The same procedure as above (see 2.4.6.1) was used for the antagonist screening essay but, in addition of OHC12 at a final concentration of 500 nM, the test compound was added at 100 μM final concentration.

2.4.7. *Galleria mellonella* killing assays

Standardised *G. mellonella* larvae (Trularv™) were purchased from BioSystems Technology Ltd. Assays were performed as described previously (Tipton et al., 2015). Briefly, strains were grown in LS-LB to an OD_{600} = 0.6 and serially diluted in fresh LS-LB. Worms were injected with the corresponding amount of cells into the *G. mellonella* hemolymph and incubated at 37°C. Every 24 h, viability was assessed by checking individual worm activity. Worms that exhibited no motility when prodding with a pipette tip and were typically dark brown or black were considered dead. Assays were performed in triplicate and at least 10 worms were used for each condition. An equal number of larvae were inoculated with LS-LB as control (not shown). None of the control larvae died after 5 days.

For the OHC12 assays, the compound was added to the media at the corresponding final concentration before starting to grow the strains. For this assay, OHC12 was resuspended in PBS, so this solution was used as a negative control. This was done because the preliminary assays showed a possible effect of acetonitrile in the ability of

G. mellonella larvae to respond and survive to *A. baumannii* colonization and infection.

2.4.8. Survival on dry surfaces

Assessment of resistance to desiccation was performed as previously described (Jawad et al., 1996) with minor modifications. Briefly, strains were grown in LS-LB to an OD_{600} = 0.3, 1 ml was centrifuged for 5 min in a bench centrifuge at max speed and the supernatant was removed. The pellet was washed twice in PBS and resuspended in 1 ml of PBS. A 20 µl drop was placed in the centre of a 13 mm round glass coverslip previously sterilized by UV radiation. All coverslips were distributed in Petri dishes without lid, which were kept in an air-tight plastic box with a 50 ml beaker containing a saturated solution of $CaCl_2$ and a digital hygrometer to maintain and control (respectively) the relative humidity at 31% ± 3%. The plastic box was kept in an incubator at the desired temperature (37°C or 22°C).

To make the measurements, a coverslip from each sample was picked and put in a universal 20 ml tube with 2 ml of PBS and vortexed three times for 15 s to resuspend attached cells. Then, appropriate dilutions of each resuspension were streaked in LB plates, which were incubated overnight at 37°C. Viable cells were determined by colony counting. Three biological replicates were used for each strain.

2.4.9. BACTH assay

abaM, *abaI* and *abaR* were cloned into pKT25, pKNT25, pUT18 and pUT18C in frame with the C-terminal or N-terminal adenylate cyclase T25 or T18 fragments following the manufacturer instructions. Constructs were checked by PCR and sequencing. The resulting plasmids were transformed into *E. coli* DHM1 by electroporation in pairs to test all possible combinations.

Strains were grown overnight in LB supplemented with 100 μg ml^{-1} ampicillin and 50 μg ml^{-1} kanamycin. A volume equivalent to an OD_{600} = 1 was collected and washed three times with 1 ml of PBS. The pellets were resuspended in 1 ml of PBS and 10 μl were spotted in M63 glucose agar plates (15.3 mM $(NH_4)_2SO_4$, 0.1 M KH_2PO_4, 1.6 μM $FeSO_4 \cdot 7H_2O$, 3.3 μM 100 thiamine, 1 mM $MgSO_4 \cdot 7H_2O$ and 8 g/l glucose) supplemented with 50 μg ml^{-1} ampicillin, 25 μg ml^{-1} kanamycin and 0.4% (v/v) ChromoMax™ IPTG/X-Gal solution (Fisher BioReagents). Plates were incubated overnight at 30°C and then kept at 22°C for 24 h more.

2.4.10. mRNA sequencing (RNA-seq)

Strains were grown in LS-LB to an OD_{600} = 0.5 and then diluted 1:10 in 20 ml of fresh LS-LB. Cultures were incubated in static conditions at 37°C for 18 h. Two millilitres of bacterial culture were pelleted by centrifugation at 4000 xg for 10 min at room temperature. The pellet was resuspended in 1 ml of RNAprotect (Qiagen) and mixed by vortexing. The pellet was reprecipitated by centrifugation at 5000 g for 10 min at room temperature and the supernatant was discarded. Total RNA extraction from cell pellets was performed using the RNeasy minikit (QIAgen) following manufacturer instructions. To remove all DNA contamination, a DNase treatment was performed using DNA-*free* (Invitrogen) following manufacturer instructions. The absence of DNA was confirmed by PCR and the quality and quantity of the RNA samples was assessed by using a 2100 Bioanalyzer (Agilent).

Samples were sent for Illumina paired-end 150 bp sequencing and bioinformatic analysis, performed by NovoGene.

2.4.11. Quantitative real-time PCR (qPCR).

Complementary DNA (cDNA) synthesis and qPCR were carried out using LunaScript RT Supermix and Luna Universal qPCR Master Mix (New England BioLabs), respectively, according to manufacturer's protocol. Oligonucleotides used for qPCR were designed using Primer-BLAST (Ye et al., 2012) and are listed in **Table 2.3**. Primer efficiency was determined by qPCR with serial dilutions of genomic DNA, and analysis of melting curves was used to evaluate their specificity. Following primer validations, qPCRs were carried out in a 7500 Real-Time PCR System (Applied Biosystems) using the manufacturer's recommended thermocycling protocol (1 cycle at 95ºC for 60 seconds followed by 40 cycles of 95 ºC for 15 seconds and 60 ºC for 30 seconds). The qPCR for each sample was carried out in triplicate. Negative controls containing no template or RNA samples incubated with no reverse transcriptase were included. Data was analysed using the Applied Biosystems 7500 software applying the $\Delta\Delta C_T$ method. The housekeeping *rpoB* was used as endogenous control for normalization, as this gene has been used before (Mayer et al., 2018) and was similarly expressed across all strains in the RNA-seq analysis.

2.4.12. TECAN plate reader attachment assay

Strains were grown overnight in LB medium supplemented with ampicillin and tetracycline. Cultures were diluted 1:100 in fresh LB to an OD_{600} = 0.02 and grown at 37°C and 200 rpm for 2 h to an OD_{600} = 0.1. L-(+)-arabinose was added at the corresponding concentrations to induce the *csu* operon and 900 µl were inoculated into a 24-well polystyrene plate. D-(–)-arabinose at a 0.1% concentration was used as the negative uninduced control. The plate was incubated at 37°C with gentle shaking (60 rpm) for 2.5 h. The OD_{600} was measured and wells were washed twice with PBS to remove unattached cells.

The wells were then emptied and dried and the attachment to the bottom of the wells was determined by fluorescence area scan measurement using a SPARK plate reader (Tecan Diagnostics).

2.4.13. Polymer microarray attachment screening

E. coli BL21 pBAD_*csu* pSW002_*E2-Crimson* was grown overnight in LB medium supplemented with ampicillin and tetracycline. Cultures were diluted to an OD_{600} = 0.02 in fresh LB and grown at 37°C and 200 rpm for 2 h to an OD_{600} = 0.1. A library of 283 different acrylate and methacrylate polymers printed in triplicates as 300 μm diameter spots onto a poly(hydroxyl ethylmethacrylate) (pHEMA)-coated glass microscope slide (25x75 mm) was incubated with the *E. coli* BL21 pBAD_*csu* pSW002_*E2-Crimson* cultures supplemented with 0.05% of either D-(–)-arabinose (uninduced negative control) or L-(+)-arabinose (for Csu expression) for 3 h at 37°C shaking at 60 rpm. Prior to incubation, slides were UV-sterilized for 10 min.

The microarray slides were washed once with LB for 5 min at 60 rpm, twice with PBS the same time and shaking conditions and air-dried for 10 min at room temperature. The fluorescence images of each slide were taken using a GenePix 4000B (Molecular Devices, US) and the GenePix Pro 6 Acquisition and Analysis Software (Molecular Devices, US) using a 635 excitation laser and a 660-690 nm emission filter with the following hardware configuration: Pixel Size = 10, Lines to average = 1, Focus position = 20, PMT gain = 600, Power = 100. The fluorescent values obtained from microarray slide incubated with the uninduced culture was subtracted from the fluorescent data obtained from the slide incubated with the induced culture to remove the background fluorescence generated by the unspecific BL21 attachment and the auto-fluorescence of the polymers. The average data of the three replicate spots on each slide from two independent assays was used for the statistical analysis.

Details about the microarray slides printing process, including monomer polymerization, can be found elsewhere (Hook et al., 2012a).

2.4.14. *A. baumannii* attachment to NGPDA and EGDPEA

Opaque AB5075 was grown to an OD_{600} = 0.7 was diluted in 15 ml of fresh LS LB to an OD_{600} = 0.01 and poured in a Petri dish (90 mm x 15.9 mm, Thermo Fisher Scientific) with a pHEMA-coated glass microscopy slides containing three 5 mm spots of either NGPDA or EGDPEA. The slides were UV-sterilized for 10 min prior incubation. The plates were incubated for 2 h at 37°C statically and then at 37°C and 60 rpm for 18 h more. The slides were washed once with PBS for 5 min at 60 rpm, incubated for 20 min with a 1:5000 dilution of SYTO9 stain (Invitrogen), washed again twice with PBS for 5 min at 60 rpm, air-dried for 10 min at room temperature and visualized by confocal microscopy (see below).

2.4.15. Laser scanning confocal microscopy (LSCM)

Visualization of attached cells was carried out with a LSM 700 confocal microscope from ZEISS using the ZEN 2009 software (ZEISS). Settings varied between different assays, but were maintained within samples of the same assay. Generally, the 488 nm laser was selected for green fluorescence, the laser intensity was set between 10-15%, the pinhole was maintained always at 1 AU (air units) and gain was always kept below 700 to avoid background noise. Z-stack images were taken using the 10X objective and setting the first slice at the base of the sample and the last one above the highest fluorescent cell/biofilm that could be visualize. At least five images of each sample were taken.

2.5. Data plotting and statistical analysis

Except the data from the RNA-seq assays, which was analysed and plotted by Novogene (Beijing, China), all the graphs and statistical analysis were made using Prism 8 (GraphPad Software). Statistical analysis to determine significant differences between groups were carried out using the two-tailed T-test included in the Prism 8 software. The biomass, surface area and surface to biovolume data of LSCM biofilm images was obtained using the Comstat2 plugin of ImageJ (*www.comstat.dk*; Givskov *et al.*, 2000; Vorregaard, 2008). At least 5 images of each sample were loaded and only the green fluorescence channel was selected for the analysis. Connected volume filtration was unselected and a constant threshold was used across all the different samples. The data obtained was then statistically analysed with Prism 8 as detailed above.

3. Role of *abaM* and quorum sensing in AB5075 virulence and attachment to abiotic surfaces

3.1. Introduction

This chapter focuses in the characterization of an RsaM orthologue in *A. baumannii* AB5075 (named AbaM) to elucidate its role in the regulation of quorum sensing and *A. baumannii* virulence-related phenotypes, including attachment to abiotic surfaces, surface motility, survival in dry surfaces and virulence in *Galleria mellonella* infection model.

3.1.1. Quorum sensing in *A. baumannii* and pathogenic *Acinetobacter* spp.

Acinetobacter spp. possess a single *luxR*/*luxI*-type quorum sensing system locus containing an AHL synthase gene (*abaI*) and a transcriptional regulator gene (*abaR*) encoded on divergent operons (Niu et al., 2008). Interestingly, the *Acinetobacter* spp. QS locus also contains an additional gene (annotated as *ABUW_3775* in *A. baumannii* AB5075) located immediately upstream of *abaI* and transcribed in the same direction (**Figure 3.1**). This gene possesses a single DUF4902 domain of unknown function. Orthologues of this gene can be found in different species of β- and γ-proteobacteria, including *Burkholderia* spp., *Halothiobacillus neapolitanus*, *Pseudomonas fuscovagin*ae and *Acidithiobacillus ferrooxidans* (Michalska et al., 2014). A more detailed description of the studies performed on some of these orthologues and their role in QS regulation and virulence-related phenotypes can be found below (see 3.1.2).

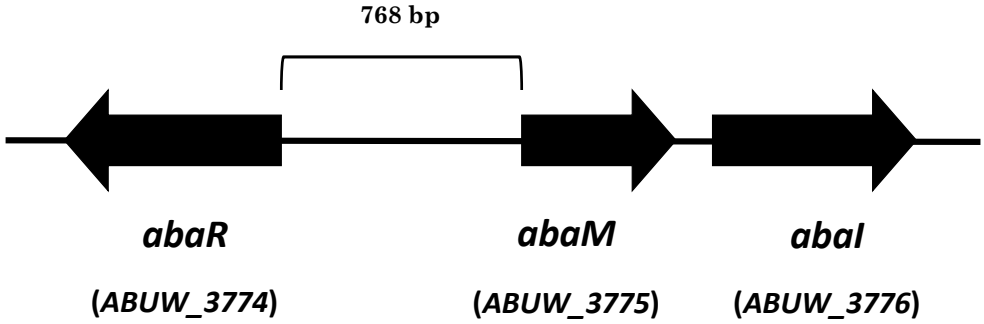


Figure 3.1: Quorum sensing locus in *A. baumannii* AB5075. The distribution and orientation of the three genes is highly conserved among all *Acinetobacter* spp. The spacing region between the response regulator gene *abaR* and *abaM* varies from strain to strain.

Very little is known about quorum sensing in *Acinetobacter* spp. and its role in the biology of this bacterium. Early reports suggested that it might play a role in biofilm formation (Niu et al., 2008; Anbazhagan et al., 2012) and motility on semi-solid surfaces (Clemmer et al., 2011). Some studies also suggested it might also be important in virulence in some animal models (Bhuiyan et al., 2016; Fernandez-Garcia et al., 2018). However, more research is needed to draw a global picture of the role QS in *A. baumanni*, specifically its role in infection, that would help to fully understand the social behaviour of this pathogen.

Most strains of the *Acinetobacter calcoaceticus-baumannii* complex produce AHLs with acyl chain lengths between 10 and 16 carbons, being *N*-(3-hydroxydodecanoyl)-L-homoserine lactone (OHC12) the most common. Some other strains produce medium length acyl chain AHLs with 6 or 8 carbon atoms, but none shorter. Moreover, many strains can produce more than one type of AHL in different quantities (Kamaraju et al., 2019; González et al., 2009; Bitrian et al., 2012). The distribution of these signals, however, is not specific for each *Acinetobacter* species or strain, so the differentiation between species or virulent/non-virulent strains based solely on the AHL production profile is not possible. Finally, the presence of a single QS system

locus in the *Acinetobacter* genomes available strongly suggests that all the AHLs are synthesized exclusively via the AbaI homoserine lactone synthase (Bhargava et al., 2010; Niu et al., 2008).

The regulation of QS in *Acinetobacter* spp. also remains largely unknown. However, in the last years some studies have shed some light on the environmental and genetic factors that affect AHL production. Some studies found that AHL biosynthesis is enhanced in iron-limiting conditions (Modarresi et al., 2015) and on cell-to-surface contact (Mayer et al., 2018; Rumbo-Feal et al., 2013). The nutrient composition of the culture medium has also been shown to affect the type of AHL synthesized (González et al., 2001). A recently described CheY/A-like hybrid TCS was also shown to positively regulate *abaI* expression, as well as QS-controlled genes (Chen et al., 2017). *Acinetobacter* QS, as in many other Gram negative QS systems, also seems to possess a positive feedback loop that further enhances AHL production. This is supported by the putative *lux*-box (CTGTAAATTCTTACAG) found 67 bp upstream the *abaI* gene start codon, which is presumably the binding site for AbaR. Moreover, *abaI* expression is activated in the presence of the native AHL (OHC12) or the supernatant of the cognate *Acinetobacter* strain (Gerdt et al., 2017; Bhargava et al., 2012; Niu et al., 2008).

3.1.2. AbaM orthologues in other species

As briefly described in the Introduction of this thesis, quorum sensing systems are usually regulated by additional factors (see 1.5). In many cases, genes located in different places on the genome encode proteins that modulate QS activity in response to environmental changes such as stress, starvation, host factors, hypoxia or iron/phosphate depletion (Lee and Zhang, 2015). In some other cases, the QS locus encodes one or more additional genes that modulate the QS locus activity. A good example is the RsaL regulator in *P. aeruginosa*, which

is encoded between the *lasR* and *lasI* genes and strongly represses OC12 production and *lasI* expression (Rampioni et al., 2006; de Kievit et al., 1999). The *abaM* gene is encoded in a similar location, between *abaI* and *abaR*, and diverse studies on AbaM orthologues suggest that, as RsaL, AbaM might be a QS negative regulator that also modulates diverse phenotypes in *A. baumannii*.

The first studies on AbaM orthologues were performed in *Pseudomonas fuscovaginae*, where RsaM (as it was named) was shown to negatively regulate AHL production and also control virulence in rice. Interestingly, RsaM not only repressed the promoter activity of the AHL synthase gene *pfsI* within the *psf* QS locus, but also downregulated the activity of the *pfvI* promoter, which encodes the synthase of the second QS system of *P. fuscovaginae* (Mattiuzzo et al., 2011).

In *Burkholderia cenocepacia* H111 the negative regulation of AHL biosynthesis by its RsaM ortholog, *Bc*RsaM, was demonstrated. Moreover, *Bc*RsaM plays a role in controlling swarming motility, biofilm formation, protease and siderophore production, as well as cross-regulation of non-cognate QS systems through modulation of the activity of other LuxR-like transcriptional regulators when expressed in *Escherichia coli*. Interestingly, while the AHL phenotype was rescued by complementation in *trans* of the *BcrsaM* mutation, other phenotypes such as swarming motility or biofilm formation were not, suggesting that *Bc*RsaM might be a *cis*-acting regulator. Structural analysis of *Bc*RsaM showed that the protein, which appears to form dimers in solution, lacks DNA binding sites and/or cavities for ligands such as AHLs. This was further supported by *in vitro* biochemical analysis, which failed to show any interaction with DNA or AHLs, and strongly suggested that RsaM might be a

post-transcriptional and/or post-translational regulator (Michalska et al., 2014).

Similar results have been described for TofM, an RsaM ortholog found in *Burkholderia glumae*. TofM strongly repressed AHL production but positively regulated toxoflavin production and virulence in rice (Chen et al., 2012). Interestingly, complementation of the *tofM* mutation was also found to be complicated. While in the *tofM* mutant toxoflavin production was restored by providing the *tofM* gene in *trans*, the increased AHL production phenotype was not.

Lastly, a recent study described the role of two RsaM orthologues in *Burkholderia thailandensis*. This non-pathogenic bacterium contains three LuxR/LuxI-like QS systems named BtaR1/BtaI1, BtaR2/BtaI2 and BtaR3/BtaI3. Of these, the first two contain an RsaM orthologue. Both RsaM1 and RsaM2 were found to repress their cognate *btaI* gene expression and AHL biosynthesis, albeit the effect on AHL production was much greater than on the *btaI* transcription, indicative of further post-transcriptional/post-translational regulation by RsaM1/2. This hypothesis was further reinforced by the fact that, even though RsaM1 did not regulate the transcription of *btaI3*, it also repressed the production of *N*-(3-hydroxy-octanoyl)-L-homoserine lactone (OHC8), the signal molecule of the QS-3 system. Moreover, both *rsaM1* and *rsaM2* were negatively auto-regulated and positively regulated by their cognate QS systems (Le Guillouzer et al., 2018).

Overall, these studies suggest that RsaM and its orthologues are central regulatory elements that control bacterial QS as well as important phenotypes including biofilm formation, virulence, motility and virulence factors production. While their mechanism of action remains unknown, evidence suggest that they do not bind DNA and

points towards a post-transcriptional/post-translational regulation. Finally, the difficulties described in complementing some phenotypes might indicate that RsaM is, at least partially, as a *cis*-acting regulatory protein.

3.2. Aims of the chapter

The aims of this chapter are to characterize the role of *abaM* and quorum sensing in the biology of *A. baumannii* AB5075 through the phenotypic analysis of the *abaM*::Tn*26* and *abaI*::Tn*26* transposon mutants. More specifically, the main objectives of the chapter are to:

- Separate both opaque and translucent phases of AB5075, *abaM*::Tn*26* and *abaI*::Tn*26*.
- Observe whether there are any differences in growth between the different strains and phases.
- Investigate the impact of *abaM* and *abaI* on AHL production and profile.
- Elucidate the contribution of *abaM* and *abaI* to the regulation of motility, attachment to abiotic surfaces and virulence.
- Investigate the role of OHC12 in the above phenotypes.
- Determine whether AbaM and the proteins of the quorum sensing locus, AbaI and AbaR, interact with each other.

3.3. Results

3.3.1. Separation of opaque and translucent phases

In order to obtain consistent results from the phenotypic assays, it was important to compare equivalent opaque and translucent phases in each mutant. Therefore, it was necessary to check under a stereo microscope the AB5075 stocks of the wild-type, *abaI*::Tn*26* and *abaM*::Tn*26* strains obtained from the University of Washington to isolate pure opaque and translucent phases of each of them (**Figure 3.2A**).

All stocks were a mixed population of opaque and translucent phases (**Figure 3.2B** and **Figure 3.2C**), even though they were present in different proportion. The *abaM*::Tn*26* mutant often formed an hypermotile colony phenotype with an irregular undulate margin instead of the typical round smaller *A. baumannii* colony (**Figure 3.2D**).

Pure phases were isolated and stocked at -81°C, and the purity of each stock was confirmed by observation under obliquus light in a stereo microscope (see Materials and methods, 2.4.2). The colony PCRs performed to confirm that after the phase isolation the strains conserved their corresponding transposon insertions were also positive (**Supplementary Material Figure S1**).

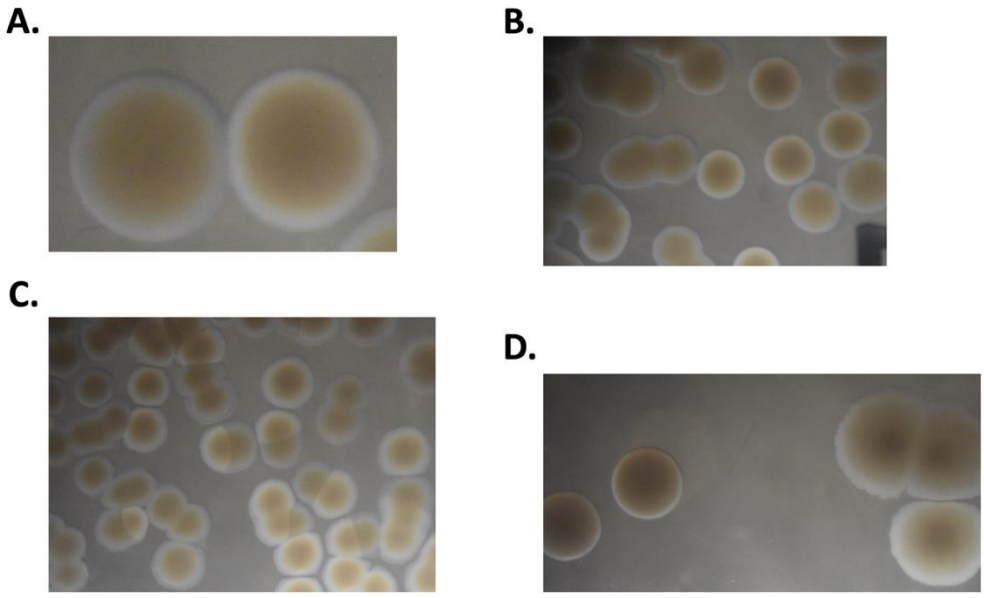


Figure 3.2: Opaque and translucent colony variants (A) Representatives of a translucent (left) and opaque (right) colony variants. **(B)** A mixed population of both variants of the AB5075 wild-type strain. **(C)** A mixed population of both variants of *abaM*::Tn*26*. **(D)** A side-by-side comparison of AB5075 colonies (left) and *abaM*::Tn*26* hypermotile colonies (right) after being incubated the same time in the same conditions. Colonies were photographed under oblique light using a stereo microscope after growing them overnight in PO-LB at 37°C.

3.3.2. Growth curves

Growth curves of all strains for both phases were carried out to confirm that none had any growth defect compared with the others that might affect the interpretation of the phenotypic assays that were carried out afterwards. Comparison of growth curves showed that none of the strains or phases showed any significant difference in growth, all had a similar exponential growth and reached the stationary phase at the same time and showing almost an identical maximum OD_{600} (**Figure 3.3**).

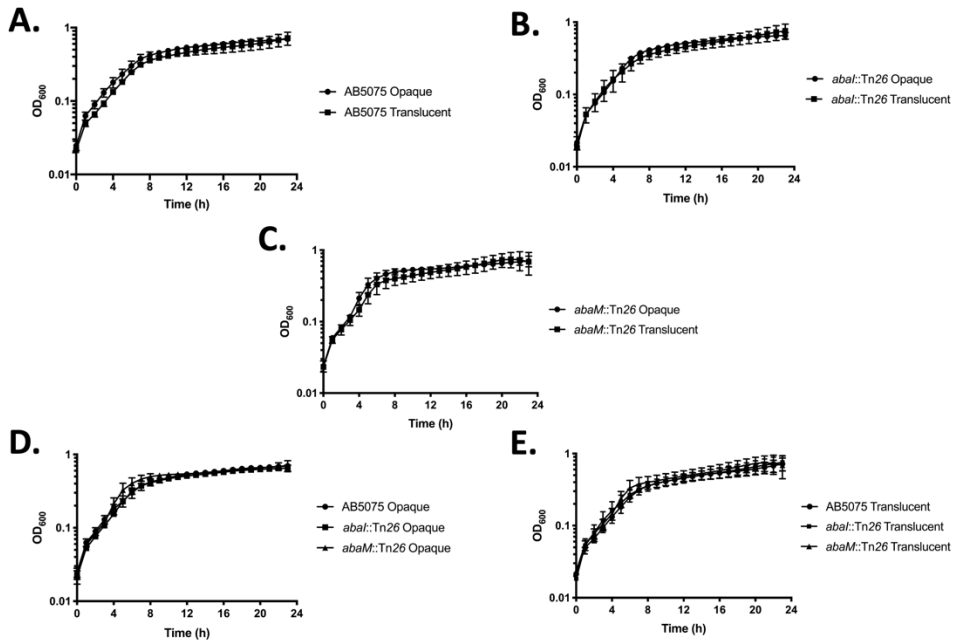


Figure 3.3: Growth curves of AB5075, *abaI*::Tn*26* and *abaM*::Tn*26* opaque and translucent phases growing in 96-well plates. (A, B, C) Comparison of growth between the opaque and translucent variants of AB5075, *abaI*::Tn*26* and *abaM*::Tn*26*, respectively. **(D)** Comparison of growth between the opaque variants of AB5075, *abaI*::Tn*26* and *abaM*::Tn*26*. **(E)** Comparison of growth between the translucent variants of AB5075, *abaI*::Tn*26* and *abaM*::Tn*26*. Cell density (OD_{600}) is plotted in a logarithmic scale. Strains were grown in LS-LB from OD_{600}=0.05 for 24 h at 37°C and OD_{600} was measured every 30 min. Error bars represent the standard deviation of three biological replicates.

3.3.3. Survival during desiccation

To assess the ability of AB5075 to survive desiccation and evaluate whether quorum sensing or *abaM* plays any role in the process, an assay of survival on dry surfaces was performed. However, this assay was performed before the phases were separated and therefore results should be considered as preliminary. It has been previously reported that opaque phases possess a thicker capsule and have a much higher tolerance to desiccation than their translucent counterparts (Chin et al., 2018), so any data where the initial inoculum consists of a mixture of both phases in an unknown proportion should be considered with care.

Neither the *abaI*::Tn*26* nor the *abaM*::Tn*26* showed significant differences in survival compared with the wild-type strain within the same incubation temperature after 12 weeks. Different temperatures, however, seemed to play an important role in survival, as samples incubated at 22°C showed a much higher survival rate than those incubated at 37°C. More specifically, samples incubated at 22°C (standard temperature used for desiccation assays in *A. baumannii*) showed an average survival rate of 22.4% ± 13.84 after 12 weeks of incubation compared with the average 0.29% ± 0.25 of those samples incubated at 37°C (**Figure 3.4).**

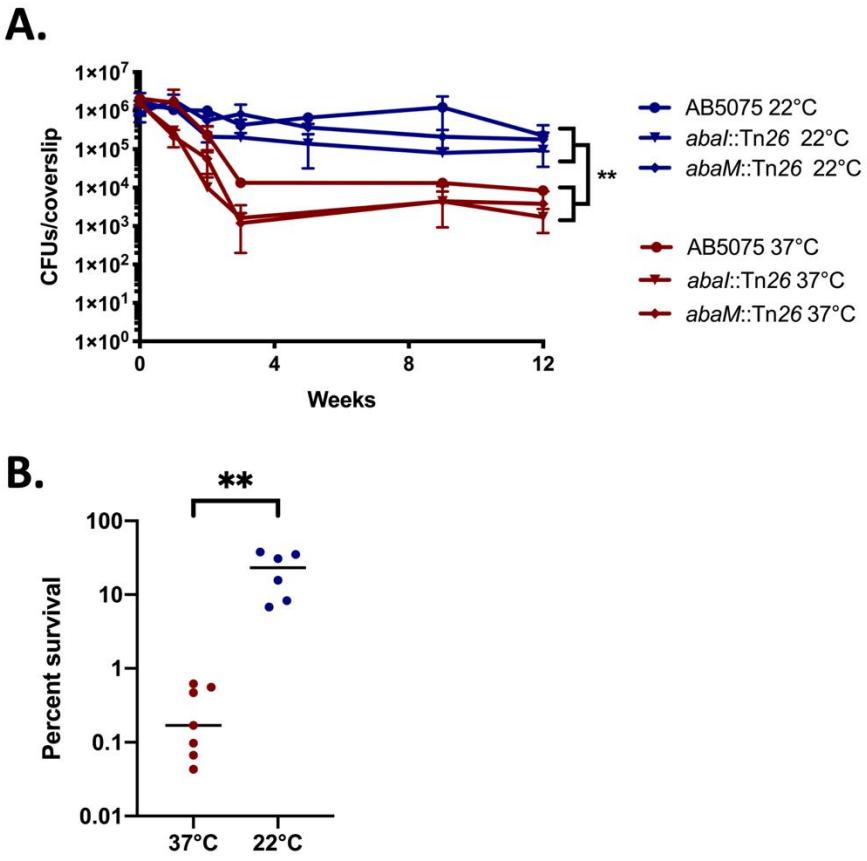


Figure 3.4: Desiccation survival of AB5075, *abaI*::Tn*26* and *abaM*::Tn*26*. (A) Survival curves of AB5075, *abaI*::Tn*26* and *abaM*::Tn*26* incubated at 22°C or 37°C on glass coverslips at 31 ± 3% relative humidity (RH). Error bars represent the standard deviation between three biological replicates. **(B)** Percent survival of all strains at 37°C vs 22°C incubated on glass coverslips at 31 ± 3% RH for 84 days. Data corresponding to the last measurement (week 12) on graph A. Cultures at OD_{600} = 0.3 were washed twice with PBS and resuspended in equal volumes of PBS. 20 µl were poured in a 13 mm round glass coverslip, air-dried and incubated at 22°C or 37°C and at 31 ± 3% RH. CFU counting was performed by plating serial dilutions of the cells recovered from the coverslips. Error bars represent the standard deviation from three biological replicates. Asterisks indicate: **, $p \leq 0.01$.

3.3.4. Contribution of *abaM* to AHL production

To investigate the AHL production profile over time for AB5075 and the contribution of *abaM* to this phenotype, AHL extractions from conditioned media were performed to investigate their production under different conditions

3.3.4.1. Profiling AHL production at different time points

Firstly, AHLs were extracted from AB5075, *abaI*::Tn*26* and *abaM*::Tn*26* supernatants every 6 h over a 24 h growth cycle and detected and characterized by LC-MS/MS. The synthase mutant, *abaI*::Tn*26*, was used as negative control.

The results demonstrate that AB5075 produces OHC12 as the major AHL under the standard growth conditions used in this work (LS-LB, 37°C, static). The AB5075 wild-type strain produced very small amounts of OHC12 in culture (between 0.056 ± 0.053 nM and 0.235 ± 0.117 nM), while the *abaM*::Tn*26* mutant produced significantly higher amounts at all time points (between 5.619 ± 2.634 nM and 188.164 ± 68.305 nM) (**Figure 3.5A**). Specifically, after 6 h incubation, *abaM*::Tn*26* showed an average concentration of OHC12 in culture ~100 times higher than the wild-type. At times 12 h and 18 h the mean OHC12 concentration in the *abaM*::Tn*26* strain was 521 and 834-fold higher, respectively, than the wild-type strain. After 24 h growth, there was a maximum difference of 875-fold between *abaM*::Tn*26* and the wild-type strain. In the samples from the synthase mutant, *abaI*::Tn*26*, no AHLs were detected at any time point.

Another AHL, *N*-(3-hydroxydecanoyl)-L-homoserine lactone (OHC10), was detected at all time points, but only in the *abaM*::Tn*26* mutant in small amounts (between 0.174 ± 0.027 nM and 18.266 ± 5.133 nM) (**Figure 3.6B**). Due to the fact that OHC10 was being produced in much lower amounts than OHC12 in *abaM*::Tn*26* and OHC12 levels in the wild-type strain were already very close to the limit of detection of the mass spectrometer, it is possible to hypothesise that OHC10 is also being produced by wild-type strain, but in such small amounts that detection by mass spectrometry is not possible with the conditions and sample volumes used in this work.

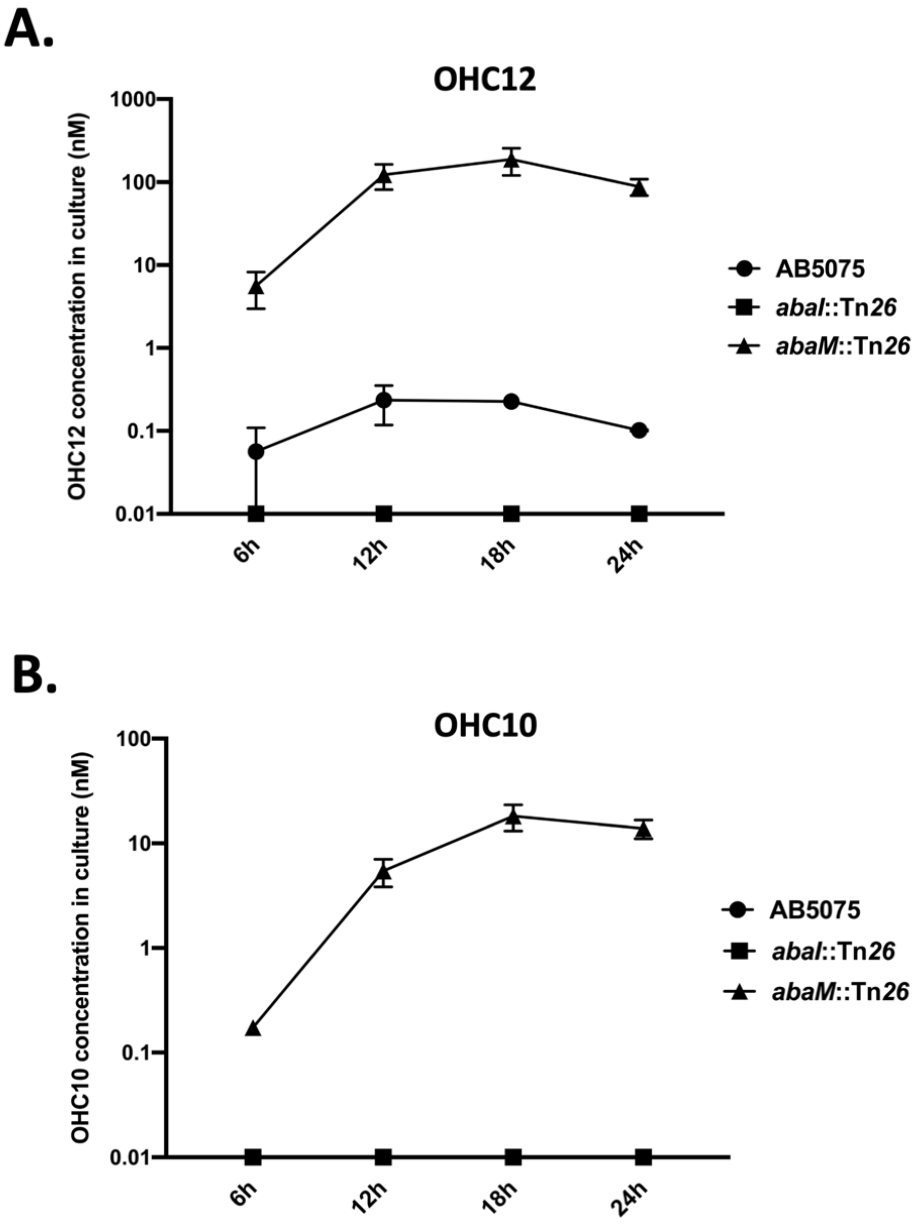


Figure 3.5: Quantification of AHLs production at different time points by AB5075, *abaI*::Tn*26* and *abaM*::Tn*26*. (A) Quantification of OHC12 production. **(B)** Quantification of OHC10 production. Strains were grown in 50 ml LS-LB in 500 ml glass flasks at 37 °C and AHLs were extracted with ethyl acetate acidified with 0.1% acetic acid twice, evaporated and the pellet was sent for LC-MS/MS analysis. Error bars represent the standard deviation between three biological replicates.

3.3.4.2. Complementation of *abaM*::Tn26 AHL production

To further assess the role of *abaM* in the regulation of AHL biosynthesis, supernatants extractions after 18 h static incubation were repeated with the wild-type strain and *abaM*::Tn*26* containing the empty pMQ557M plasmid vector and the *trans* complemented *abaM* mutant, *abaM*::Tn*26* pMQ_*abaM*. As in the previous assays, the synthase mutant, *abaI*::Tn*26*, was used as a negative control.

Biosynthesis of OHC12 in the wild-type and *abaM*::Tn*26* carrying the empty plasmid followed a similar pattern as in the previous extractions, with AB5075 pMQ557M containing an average concentration of OHC12 below 1 nM (0.051 ± 0.008 nM) in culture and *abaM*::Tn*26* pMQ557M producing significantly higher amounts (16.76 ± 6.512 nM). However, the concentration of OHC12 in the supernatant was significantly lower in both the wild-type and the *abaM* mutant carrying the pMQ557M plasmid compared to the amounts observed in the strains not carrying the plasmid, which suggests the plasmid has an effect in AHL production. The complemented strain, *abaM*::Tn*26* pMQ_*abaM* (8.19 ± 5.207 nM), did not reduce the OHC12 production level significantly ($p = 0.305$) below that of the *abaM* mutant (**Figure 3.6A**). Both *abaM*::Tn*26* pMQ557M and *abaM*::Tn*26* pMQ_*abaM* also produced similar amounts of OHC10 (0.501 ± 0.294 nM and 0.241 ± 0.125 nM, respectively), which were also lower than in the strains not carrying the plasmid, while the wild-type did not produce any detectable amounts (**Figure 3.6B**).

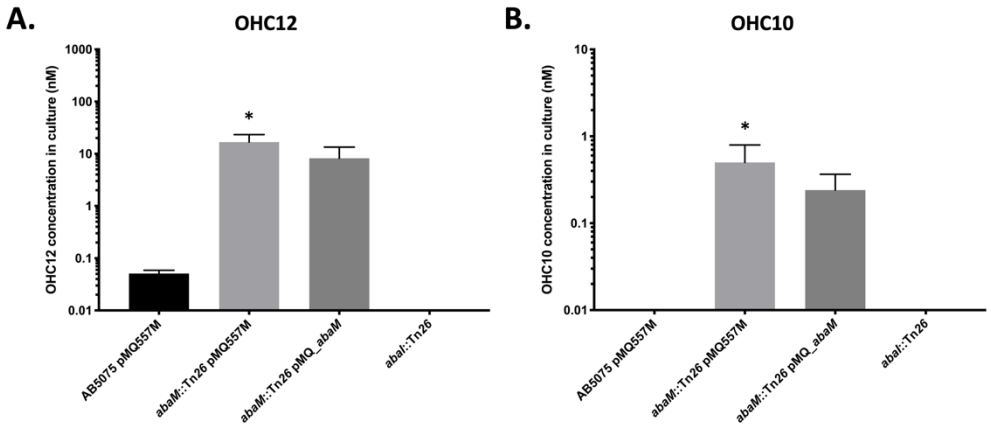


Figure 3.6: Quantification of AHL production in the *abaM* mutant complemented strain. **(A)** Quantification of OHC12 production. **(B)** Quantification of OHC10 production. Strains were grown in 50 ml LS-LB in 500 ml glass flasks at 37 °C for 18 h and AHLs were extracted with ethyl acetate acidified with 0.1% acetic acid twice, evaporated and the pellet was sent for LC-MS/MS analysis. Error bars indicate the standard deviation between three biological replicates. Asterisks indicate: *, $p \leq 0.01$ compared with AB5075 pMQ557M.

3.3.5. *abaM* and quorum sensing in surface motility in 0.3% Eiken agar

3.3.5.1. Characterization of surface motility

The surface motility of AB5075 wild-type, *abaI*::Tn*26* and *abaM*::Tn*26* mutants was examined in LS-LB 0.3% Eiken agar plates using pure phases of each strain.

The opaque wild-type strain exhibited significantly higher motility (59.6 ± 0.7 mm) when compared with the translucent phase strain (34.1 ± 1.7 mm). These differences between phases were not found neither in the *abaI*::Tn*26* nor the *abaM*::Tn*26* mutants. Opaque *abaI*::Tn*26* motility (36.5 ± 1.4 mm) was significantly lower than the opaque wild-type. Moreover, translucent *abaI*::Tn*26* showed no difference compared with the translucent wild-type. Interestingly, both the opaque (76.7 ± 2.4 mm) and translucent *abaM*::Tn*26* (65.3 ± 4.5 mm) were significantly more motile than their wild-type counterpart (**Figure 3.7A**).

3.3.5.2. Complementation of *abaM*::Tn*26* motility phenotype

To confirm the role of *abaM* in surface motility, the same assays were repeated with AB5075 pMQ557M, *abaM*::Tn*26* pMQ557M and *abaM*::Tn*26* pMQ_*abaM*.

As expected, *abaM*::Tn*26* pMQ557M showed a much higher motility (62 ± 4.3 mm) than AB5075 pMQ557M (39.8 ± 1.48 mm). The phenotype was fully restored to levels even lower than the wild-type (30 ± 5.16 mm) by provision of the wild-type *abaM* in *trans* (**Figure 3.7B**).

3.3.5.3. Contribution of OHC12 to surface motility

Since there is little information on the role of quorum sensing in AB5075, it was decided to further characterize the effect of OHC12 on motility. The same assays were repeated using LS-LB 0.3% Eiken agar plates containing either OHC12 in a final concentration of 200 nM in the plate or the same volume of acetonitrile (as a negative control).

Addition of OHC12 significantly increased the motility for both the wild-type strain and the *abaI*::Tn*26* mutant. This increase could not be observed in the *abaM*::Tn*26*, as the mutant migrates to almost the edge of the plate at a much faster rate than the other strains (**Figure 3.7C**). The effect of OHC12 could, however, be observed in *abaM*::Tn*26* pMQ557M, significantly increasing its motility. A similar effect was also noted in AB5075 pMQ557. Interestingly, even though the presence of OHC12 slightly increased the motility of *abaM*::Tn*26* pMQ_*abaM*, the differences where not statistically significant ($p > 0.05$) (**Figure 3.7D**).

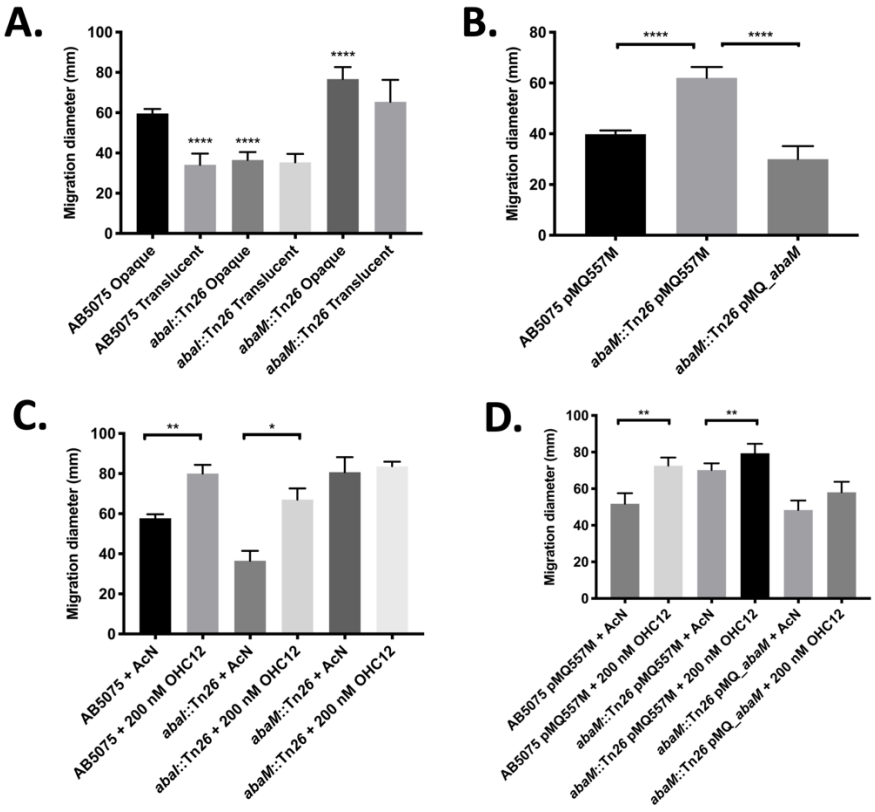


Figure 3.7: Surface motility on 0.3% Eiken agar. (A) Differences in surface motility between opaque and translucent phases of AB5075, *abaI*::Tn*26* and *abaM*::Tn*26*. **(B)** Genetic complementation of opaque *abaM*::Tn*26* hypermotile phenotype. **(C)** Effect of OHC12 on opaque AB5075, *abaI*::Tn*26* and *abaM*::Tn*26*. **(D)** Effect of OHC12 on AB5075 and *abaM*::Tn*26* carrying the empty pMQ557M and the genetically complemented *abaM* mutant. Strains were grown in LS-LB to an OD_{600} = 0.3 and 1 μl was poured in the centre of a freshly prepared LS-LB 0.3% Eiken agar plate. Plates were incubated at 30°C for 16 h. AcN = Acetonitrile. Error bars indicate standard deviation between biological replicates. Asterisks indicate: *, $p \leq 0.05$; **, $p \leq 0.01$; ****, $p \leq 0.0001$.

3.3.6. *abaM* and quorum sensing in attachment to abiotic surfaces

Quantification of attached biomass to an abiotic surface can be challenging, as the many different approaches available possess specific advantages and disadvantages. Crystal violet (CV) biomass quantification is a widely used versatile assay that allows a rapid quantification of attached biomass by staining with CV attached cells and extracellular components such as eDNA, exopolysaccharides and proteins (O'Toole, 2011; Shukla and Rao, 2017; O'Toole and Kolter, 1998). This protocol usually involves the use of 96-well microtiter plates, but here a modified version was used that substitutes the

microtiter plates with 1.5 ml polypropylene tubes. The use of 1.5 ml tubes increases the liquid-air interphase area, where most of the *Acinetobacter* attachment takes place, and also allows individual manipulation of the samples for better handling during the washing and staining processes. This overall reduced the background noise and lead to better reproducibility than the assays performed with 96-well plates (data not shown).

3.3.6.1. Attachment to polypropylene

As previously, the attachment phenotype was firstly characterized by comparing pure separated phases of the wild-type strain, *abaI*::Tn*26* and *abaM*::Tn*26*. No differences between the wild-type opaque (0.8 ± 0.19 A_{585}/OD_{600}) and translucent (0.76 ± 0.1 A_{585}/OD_{600}) strains was observed. In the *abaI*::Tn*26* mutant, the opaque phase showed higher attachment (1.48 ± 0.33 A_{585}/OD_{600}) compared with its wild-type counterpart, while the translucent *abaI* mutant showed the opposite phenotype, with a significant reduction in attached biomass (0.31 ± 0.11 A_{585}/OD_{600}) when compared with the translucent wild-type. In the case of the *abaM* mutant, both phases showed much higher attachment than their isogenic wild-type parent. The opaque *abaM*::Tn*26* showed the biggest difference with a 3.5-fold increase (2.87 ± 0.53 A_{585}/OD_{600}), while the translucent variant showed a 2-fold difference (1.51 ± 0.52 A_{585}/OD600) (**Figure 3.8).**

3.3.6.2. Complementation of the *abaM*::Tn26 attachment phenotype

The opaque wild-type attachment phenotype could be partially restored in the opaque *abaM* mutant in the presence of the pMQ_*abaM* complementation plasmid. As in the previous assay, *abaM*::Tn*26* pMQ557M (3.3 ± 0.32 A_{585}/OD_{600}) showed an amount of attached biomass approximately 2.5-fold higher than AB5075 pMQ557M (1.4 ± 0.54 A_{585}/OD_{600}), while the *abaM*::Tn*26* pMQ_*abaM*

(2.442 ± 0.25 A_{585}/OD_{600}) showed a partial complementation with an amount attachment 1.7-fold higher than the wild-type and 1.3-fold lower than the *abaM* mutant (**Figure 3.9A**).

3.3.6.3. Contribution of OHC12 to attachment to polypropylene

The study of the effect of OHC12 in AB5075 had two objectives: firstly, further characterize the limitedly documented role of quorum sensing in *A. baumannii* attachment to abiotic surfaces. Secondly, investigate whether the lack of full complementation by the presence of pMQ_*abaM* could be due to the *abaM*::Tn*26* pMQ_*abaM* producing levels of OHC12 similar to those found in the *abaM* mutant (see 3.3.4).

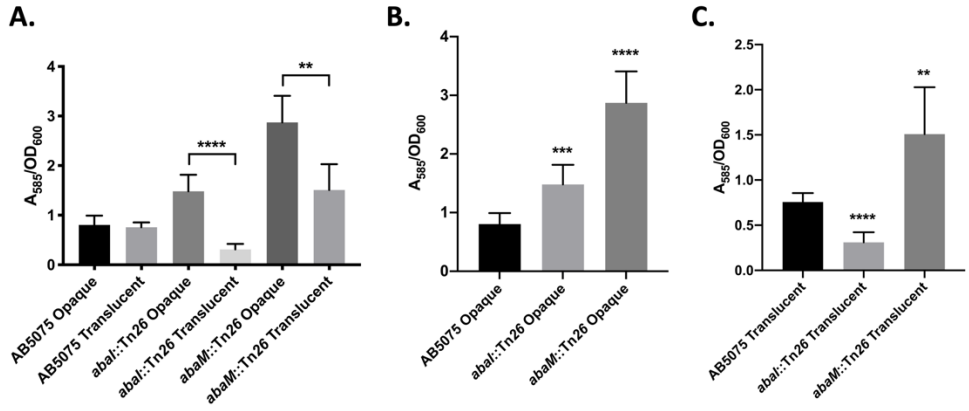


Figure 3.8: Attachment to polypropylene. (A) Differences in attachment between opaque and translucent phases of AB5075, *abaI*::Tn*26* and *abaM*::Tn*26*. **(B)** Differences in attachment between AB5075, *abaI*::Tn*26* and *abaM*::Tn*26* opaque phases. **(C)** Differences in attachment between AB5075, *abaI*::Tn*26* and *abaM*::Tn*26* translucent phases. Both (B) and (C) data is extracted from (A) for a more detailed visualization. Strains grown in LS-LB to an OD_{600} = 0.3 were incubated at 37°C for 24 h in 1.5 ml polypropylene tubes. Attached cells were stained with 0.25% CV and resuspended in 1 ml of 100% ethanol for quantification by absorbance at 585 nm. Error bars indicate standard deviation between biological replicates. Asterisks indicate: **, $p \leq 0.01$; ***, $p \leq 0.001$; ****, $p \leq 0.0001$.

Addition of 200 nM OHC12 increased the amount of attached biomass in the wild-type strain from 0.88 ± 0.26 A_{585}/OD_{600} to 1.523 ± 0.59 A_{585}/OD_{600}. This was approximately a 1.7-fold increase compared with the untreated wild-type, far from the 4-fold increment observed in the *abaM*::Tn*26* (3.65 ± 0.9 A_{585}/OD_{600}). Increasing the amount of exogenous OHC12 to 2 μM (1.47 ± 0.43 A_{585}/OD_{600}) did not induce attachment at higher levels than 200 nM (**Figure 3.9B**).

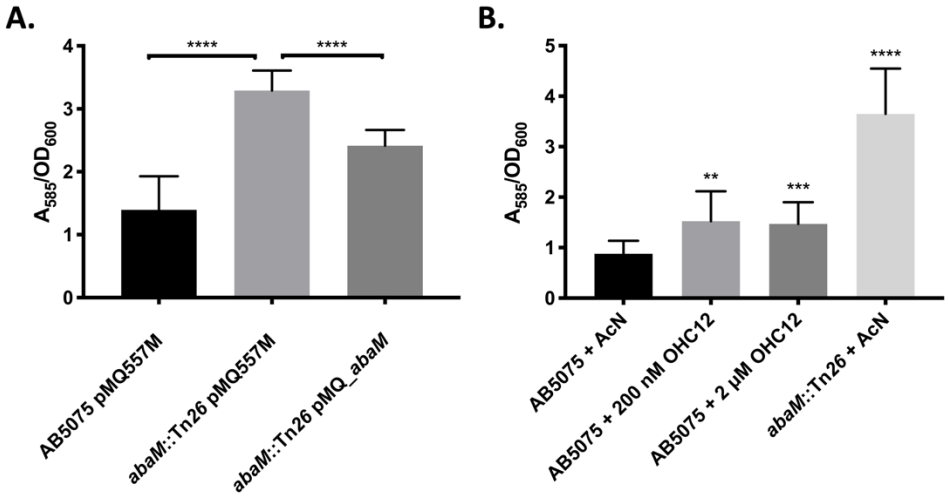


Figure 3.9: Attachment to polypropylene in (A) Genetically complemented *abaM* mutant; and **(B)** AB5075 supplemented with OHC12. Strains grown in LS-LB to an OD_{600} = 0.3 were incubated at 37°C for 24 h in 1.5 ml polypropylene tubes. When needed, OHC12/AcN was added. Attached cells were stained with 0.25% CV and resuspended in 1 ml of 100% ethanol for quantification by absorbance at 585 nm. AcN = Acetonitrile. Error bars indicate standard deviation between biological replicates. Asterisks indicate: **, p ≤ 0.01; ***, p ≤ 0.001; ****, p ≤ 0.0001.

3.3.7. *abaM* and quorum sensing in virulence for *G. mellonella* larvae infection model

3.3.7.1. Characterization of virulence

Results revealed that, while *abaI*::Tn*26* did not affect the virulence (measured as percentage of larvae killed from the total of larvae inoculated with each strain) of AB5075 in *G. mellonella*, the *abaM*::Tn*26* mutant was significantly less virulent than the wild-type strain. In the assay injecting 2 x 10^4 cells/larvae, at t = 24 h, the

wild-type strain and the *abaI*::Tn*26* showed a similar rate of killing (86% and 92%, respectively), while *abaM*::Tn*26* mutant was almost avirulent (6% killing rate). At the end of the assay (t = 120 h), both wild type and *abaI*::Tn*26* showed a 92% killing rate. The *abaM*::Tn*26* mutant, on the other hand, exhibited a much lower pathogenicity (8% killing) at the same time point (**Figure 3.10A**).

Similarly, in the assay injecting 2 x 10^5 cells/larvae, *abaM*::Tn*26* showed a rate of killing at t = 24 h of 57.7%, increasing up to 70% at t = 120 h. The wild-type and *abaI*::Tn*26* both killed all the infected larvae (100% killing rate) within the first 24 hours (**Figure 3.10B**).

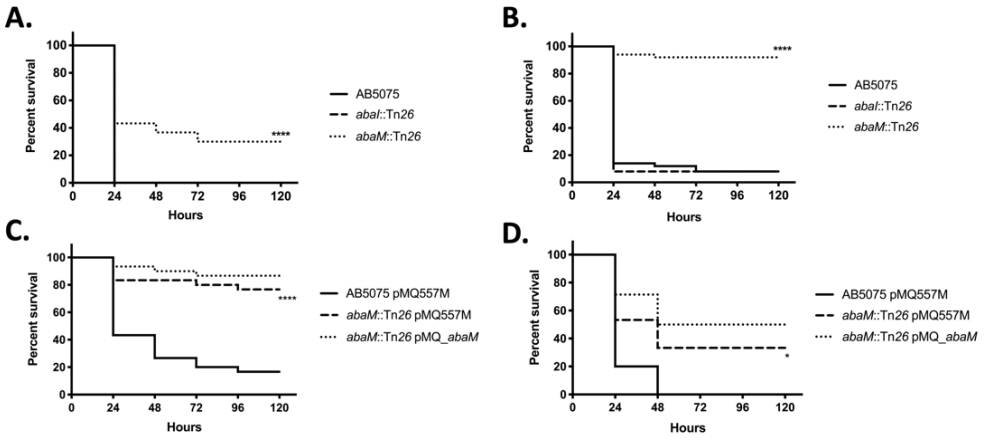


Figure 3.10: Killing of *G. mellonella* larvae. (A) Killing after inoculation of 2 x 10^4 cells/larvae of AB5075, *abaI*::Tn*26* or *abaM*::Tn*26*. **(B)** Killing after inoculation of 2 x 10^5 cells/larvae of AB5075, *abaI*::Tn*26* or *abaM*::Tn*26*. **(C)** Genetic complementation of the *abaM* mutant killing phenotype injecting 2 x 10^4 cells/larvae and **(D)** injecting 2 x 10^5 cells/larvae. Strains grown to an OD_{600} = 0.6 in LS-LB and diluted in fresh media were injected in the last proleg of each *G. mellonella* larvae. Larvae were then incubated in Petri dishes at 37°C and checked every 24 h. Each graph represents the data of three independent experiments together. Asterisks indicate: *, $p \leq 0.05$; ****, $p \leq 0.0001$.

3.3.7.2. Complementation of *abaM*::Tn26 avirulent phenotype

Similar to AHL biosynthesis, the provision in *trans* of the *abaM* wild-type gene through the pMQ_*abaM* did not restore the wild-type phenotype in the *abaM* mutant. AB5075 pMQ557M and *abaM*::Tn*26*

pMQ557M maintained differences similar to those described in the previous section, with the *abaM* mutant being significantly less virulent than the wild-type strain when injecting either 2 x 10^4 cells/larvae or 2 x 10^5 cells/larvae. The complemented strain, however, showed killing rates very similar to *abaM*::Tn*26* pMQ557M at all time points in both assays (**Figure 3.10C** and **D**). Interestingly, it can be observed that the complemented strain seemed to be slightly less virulent than the *abaM* mutant itself in both assays, even though those differences were not statistically significant (p-value > 0.05).

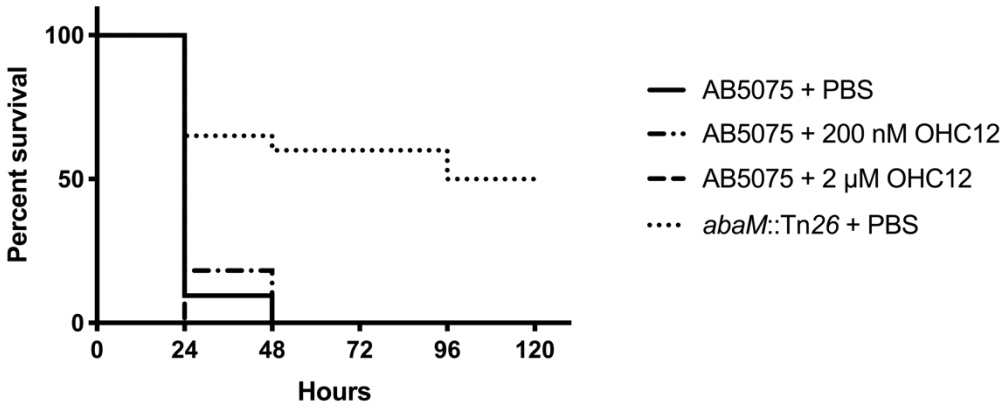


Figure 3.11: Contribution of OHC12 in virulence in *G. mellonella* larvae. Strains grown to an OD_{600} = 0.6 in LS-LB supplemented with OHC12/PBS and diluted in fresh media were injected in the last proleg of each *G. mellonella* larvae. Larvae were then incubated in Petri dishes at 37°C and checked every 24 h. The Asterisks indicate: *, $p \leq 0.05$; ****, $p \leq 0.0001$.

3.3.7.3. Contribution OHC12 to virulence

Although that *abaI*::Tn*26* insertion did not affect AB5075 virulence, it was hypothesised that it could be a consequence of the low levels of OHC12 in the wild-type strain (see 3.3.4), which could not be enough to have an impact in virulence. However, it could be possible that the presence of higher levels of OHC12, such as those produced by the avirulent *abaM*::Tn*26* strain, would reduce *A. baumannii* AB5075 virulence in *G. mellonella*. Interestingly, the presence of 200 nM OHC12 did not alter the virulence of the wild-type in *G. mellonella*. Addition of higher amounts (2 µM) of OHC12 did not result in any

significant changes either. The *abaM*::Tn*26* mutant, which was added as a control, showed the previously observed attenuated virulence phenotype (**Figure 3.11**).

3.3.8. BACTH Two-hybrid protein-protein interaction assay

To elucidate whether AbaM interacts with itself and/or the QS proteins, AbaI and AbaR, a BACTH protein-protein interaction assay was performed. The BACTH two hybrid kit uses the two fragments (T25 and T18, respectively) of the catalytic domain of the adenylate cyclase (CyaA) of *Bordetella pertussis*, which are active only when they are physically close (Karimova et al., 1998; Ladant and Ullmann, 1999). Based on this principle, each of the fragments is fused to a protein of interest and both are co-expressed in the reporter *E. coli* DHM1, an adenylate cyclase-deficient strain. If the two proteins interact, both fragments of the adenylate cyclase will be close enough to become active and produce cAMP. This cAMP is then capable of activating the expression of the reporter gene, *lacZ*. The expression of *lacZ* can then be qualitatively or quantitatively assessed thanks to the presence of X-gal in the medium, which will yields a blue precipitate when hydrolysed by the β-galactosidase enzyme encoded by *lacZ*.

The data obtained did not reveal any interactions between AbaM and AbaI or AbaR in any of the possible combinations for the protein-fragment fusions (**Figure 3.12A**). No AbaM-AbaM dimerization was observed either. Positive controls revealed interactions (i.e. blue colour) in the first 12 hours but none of the tested combinations turned blue before the negative controls after leaving the plates at 22°C for an extra day (**Figure 3.12B).**

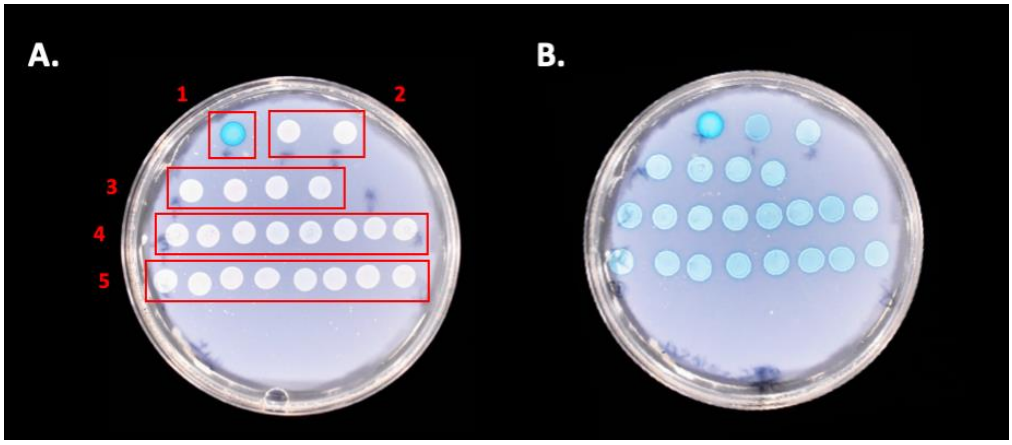


Figure 3.12: BACTH Two-Hybrid protein-protein interaction assay. (A) After 24 h at 30°C. **1)** Positive control (pKT25-zip/pUT18-zip). **2)** Negative controls (left: pKT25/pUT18; right: pKNT15 /pUT18C). **3)** AbaM/AbaM interactions. **4)** AbaM/AbaI interactions. **5)** AbaM/AbaR interactions. **(B)** Same combinations after 24 h at 30°C + 24 h at 22°C. Strains were grown to OD_{600} = 1, washed three times and resuspended in PBS. 10 µl were spotted in M63 glucose plates supplemented with ampicillin, kanamycin and IPTG/X-gal. The assay was performed in triplicate with three technical replicates each, showing the similar results.

3.4. Discussion

In this chapter, an RsaM orthologue (here named AbaM) has been characterized for first time in *A. baumannii* and its role in different phenotypes has been elucidated. Moreover, the contribution of AbaI and OHC12 on some of these phenotypes has also been evaluated, with particular interest in the ability of OHC12 to promote or inhibit *abaM*::Tn*26*-like phenotypes in the wild-type AB5075 in order to clarify whether the difficulties in the genetic complementation of *abaM*::Tn*26* in some assays could be consequence of the inability of pMQ_*abaM* to restore the AHLs production to wild-type levels in the *abaM* mutant.

As previously described, AbaM orthologues have been shown to play important roles in AHL biosynthesis, motility, attachment and virulence in *Pseudomonas fuscovaginae* and *Burkholderia* spp. (Chen et al., 2012; Le Guillouzer et al., 2018; Michalska et al., 2014; Mattiuzzo et al., 2011; Inhülsen, 2011). Therefore, it was decided to test the AB5075 *abaM* mutant for all the same phenotypic

characteristics to elucidate whether this protein played a similar function in *A. baumannii*.

Most *Acinetobacter* isolates produce OHC12 as their major AHL (Niu et al., 2008; Ng et al., 2019; Dou et al., 2017), even though some can produced other signals (Chan et al., 2014; Anbazhagan et al., 2012). Additionally, most strains are capable of producing more than one type of AHL (Kamaraju et al., 2019). In this study, OHC12 was detected as the major AHL produced by *A. baumannii* AB5075, which was also capable of producing OHC10 in smaller amounts. In AB5075, AbaM possessed a similar role as other RsaM-like proteins in other bacteria, with *abaM*::Tn*26* showing levels of OHC12 in culture between 100 and 875 times higher than the wild-type, depending on the time point. Moreover, OHC10, which was undetectable in the wild-type strain, was only found in the *abaM* mutant, suggesting that AB5075 is capable of producing other AHLs, but in such small amounts these are undetectable in the wild-type strain grown under the conditions described. This is further supported by early observations made in some of *abaM* mutant cultures, where other long chain AHLs (OHC14, OHC8, C12 and C10) were occasionally detected in very small amounts, even below OHC10 levels (data not shown). This characteristic have previously been observed in other *A. baumannii* strains and diverse Gram-negative bacteria such as *Y. pseudotuberculosis*, *Serratia* spp. or *P. aeruginosa*, among others, where a single AHL synthase is responsible for the synthesis of multiple AHLs with different acyl chains and/or 3-position modifications (Ortori et al., 2007, 2011; Wei and Lai, 2006).

Interestingly, the levels of OHC12 in the wild-type were below 1 nM in all the assays performed, raising the question of whether AB5075 produces sufficient levels of this quorum sensing signal to activate AbaR and therefore be biologically relevant, a question that will be

addressed in more detail in the Chapter 4. Moreover, the much higher levels of OHC12 at all time points suggest that, at least in the conditions tested, *abaM* is being expressed and constitutively preventing AHL production through an unknown mechanism at all time points during the 24 h growth cycle. The exact purpose of this downregulation is unclear. While the *abaM* mutant exhibits reduced virulence, it does not appear to depend on high levels of OHC12 (see below). It could be an energy-efficiency mechanism where AHLs are synthesized only in environmental conditions where a specific subset of genes needs to be expressed/repressed to ensure optimal fitness. This hypothesis is backed up by a recent transcriptomic study of *A. baumanii* strain 863 that showed that quorum sensing strongly regulated genes involved in carbon source metabolism, energy production, stress response and ribosome structure/maturation (Ng et al., 2019), suggesting that QS might be important in nutrient-limited environments and stress situations. To address this possibility, it would be interesting to study *abaI* and the *abaM* mutants under different nutrient-limited and stress conditions to elucidate whether the absence or overproduction of OHC12 has an impact on growth. No AHLs were detected in any of the assays in the *abaI*::Tn*26* samples, which is consistent with previous studies and bioinformatics predictions that suggested that *A. baumannii* only possesses a single AHL-based QS locus where AbaI is the sole AHL synthase (Bhargava et al., 2010).

An important stage in the characterization of the *abaM*::Tn*26* was to genetically complement the mutant to demonstrate restoration to the wild-type phenotypes. However, the provision in *trans* of the *abaM* gene in the mutant did not restore the wild-type AHL levels and the strain showed instead a phenotype very similar to the *abaM*::Tn*26* containing the empty vector alone. Different reasons can be evoked to explain the difficulty of complementing the AHL phenotype. A polar

effect caused by the transposon insertion on the synthase gene (*abaI*), which is located downstream *abaM*, cannot be discarded. However, this problem has been previously reported in studies of *abaM* orthologues where clean in-frame deletion mutants were used. Specifically, this same problem was described trying to complement the overproduction of AHL in an *abaM* orthologue knockout mutant in *Burkholderia glumae* (*tofM*), as the complementation in *trans* of an in-frame deletion was unable to restore the wild-type phenotype nor to significantly reduce the AHL production back to the wild-type levels (Chen et al., 2012). In other studies, genetic complementation restored the AHL production to wild-type levels, but failed to complement other phenotypes such as motility or biofilm formation (Inhülsen, 2011), which will be discussed below. These repeated complications in the complementation have led to suggestions that AbaM-like proteins could be *cis*-acting regulatory elements (Michalska et al., 2014). Finally, it is important to mention that the presence of the empty pMQ557M vector significantly reduced the AHL production in the wild-type strain and the *abaM*::Tn*26* compared to the extractions made with the strains not containing the plasmid. This reduction might have rendered the differences in AHLs production more difficult to appreciate. Nonetheless, it seems certain that, under the conditions used in this study, the amounts of OHC12 and OHC10 produced by the complemented *abaM*::Tn*26* strain are more similar to those produced by the uncomplemented *abaM* mutant and significantly higher than those produced by the wild-type strain.

Motility is a phenotype often closely linked to pathogenicity and in many pathogenic species is a key virulence factor necessary for the colonization of the host tissues and establishing a successful infection. This has been observed in non-motile mutants of several pathogenic bacteria, including *Proteus mirabilis*, *P. aeruginosa*, *Campylobacter jejuni*, *Salmonella* spp. or *Helicobacter pylori,* which

showed reduced virulence or invasion/colonization of the host (Josenhans and Suerbaum, 2002; Burrows, 2012).

Even though *A. baumannii* was firstly described as a non-motile bacterium, it was later discovered that it was capable of twitching motility (Henrichsen, 1975) and performing a swarming-like motility on semi-solid surfaces (Barker and Maxted, 1975). This type of motility has not been fully characterized, but seems to be regulated by quorum sensing, extracellular stress, osmolarity, lipopolysaccharide production and blue light (Mussi et al., 2010; McQueary et al., 2012; Clemmer et al., 2011; Tipton and Rather, 2017). Despite the fact that a link between this type of motility and virulence has not been clearly established, several studies have observed that *A. baumannii* mutants that displayed altered motility in semi-solid surfaces also showed significant changes in virulence. Specifically, hypermotile phenotypes have been associated with increased virulence (Eijkelkamp et al., 2013; Tipton et al., 2015), while motility-deficient phenotypes have been linked with an attenuated pathogenicity (Pérez-Varela et al., 2017, 2019).

In AB5075, phase variation regulates motility through an unknown mechanism (Tipton et al., 2015), in which the opaque phase is significantly more motile than the translucent variant. In this study, the wild-type strain showed these exact same differences between both phases. Conversely, the synthase mutant did not show any differences between the phases. Both phases showed a low motility, similar to the wild-type translucent, making the opaque *abaI*::Tn*26* significantly less motile than the opaque wild-type. This result confirms that, at least in the opaque variants, QS positively influences surface motility, an observation consistent with previous studies (Clemmer et al., 2011).

Motility was also strongly affected in the *abaM* mutant. Both phases of *abaM*::Tn*26* were significantly more motile than their wild-type counterparts. Moreover, translucent *abaM*::Tn*26* did not show a significant reduction in motility compared with the opaque *abaM*::Tn*26* and both variants showed instead a very similar migration distance after 16 h of incubation. Unlike in the AHL production assays, genetic complementation of the mutation in *trans* restored the wild-type phenotype. Interestingly, in the only previous work with an AbaM orthologue where motility was assessed, in *B. cenocepacia*, the mutant motility phenotype could not be rescued by *trans*-complementation (Inhülsen, 2011). The motility assessed, however, is not the same. In the *B. cenocepacia* study, swarming motility was studied, which is mediated by flagellar rotation (Kearns, 2010). *A. baumanii*, as a non-flagellated bacteria, is incapable of swarming and performs instead a completely different uncharacterized surface motility (Barker and Maxted, 1975). For that reason, it is possible that the different factors involved in the two types of motility are differentially regulated by AbaM/RsaM, explaining why the mutant phenotypes can be genetically complemented in *trans* in one case and not in the other.

To further assess the role of AHLs in AB5075 motility, the effect of OHC12 was evaluated on the surface motility of different AB5075 mutant strains. Addition of OHC12 increased the motility in all strains tested except *abaM*::Tn*26* and the complemented *abaM* mutant, *abaM*::Tn*26* pMQ557M. In the first case, the *abaM* mutant migrated to the edge of the plate after the 16 h incubation. Therefore, addition of exogenous OHC12 did not result in an observable increase of surface motility under the conditions used, but a possible positive effect of OHC12 cannot be discarded under other environmental conditions. However, in the complemented strain it can be hypothesised that AbaM exerts its effect in a OHC12-independent

manner. This is supported by previous observations that also suggest that the regulation of motility by the AbaM orthologue in *B. cenocepacia* is QS-independent (Inhülsen, 2011). As AbaM and OHC12 exert opposite effects on AB5075 motility and the presence of more than one copy of the *abaM* gene (due to the number of copies of the pMQ557M plasmid) will further reduce migration counteracting the inducing effect of OHC12, leading to a greater attenuation of OHC12-induced motility than in the AB5075 pMQ557M and *abaM*::Tn*26* pMQ447M strains. Moreover, the fact that the hypermotyle phenotype of the *abaM*::Tn*26* mutant could be rescued by pMQ557M_*abaM* while the AHL production phenotype could not in the previous assays further supports the hypothesis that AbaM regulates motility independently of QS.

Overall, these results are consistent with previous data suggesting that both *Acinetobacter* QS and AbaM orthologues, as well as phase variation, all play an important role in regulating motility on semis-solid surfaces (Clemmer et al., 2011; Inhülsen, 2011). Moreover, this is the first time this phenotype has been characterized in an *abaM* mutant in *A. baumannii*.

After assessing the role of *abaM* in AHLs synthesis and motility in 0.3% Eiken agar, it was decided to analyse the effect of *abaM* and QS in attachment to abiotic surfaces. QS has been widely linked to attachment and biofilm formation in many pathogenic bacteria (Solano et al., 2014; Rutherford and Bassler, 2012), including *Acinetobacter* species (Niu et al., 2008; Rumbo-Feal et al., 2013). Moreover, AbaM orthologues have also been implicated in biofilm formation on polystyrene (Inhülsen, 2011). For that reason, it was hypothesised that both *abaM* and QS could play an important role mediating *A. baumannii* AB5075 surface attachment and biofilm development on abiotic surfaces.

Even though the translucent phase variant of AB5075 has been reported to attach to surfaces at a significantly greater extent than the isogenic opaque variant (Tipton et al., 2015), this was not observed in the assays described in this thesis, where both showed very similar levels of attachment. This variation could be explained by the differences in the protocols employed. First of all, the material used in this work was polypropylene, while in the Tipton *et al* study it was polystyrene. Moreover, the 96-well plate format was substituted with 1.5 ml tubes, which also require higher volumes of culture than in the Tipton *et al* assays. Overall, these changes may be sufficient to account for the different results obtained.

Comparing equivalent phases of the wild-type and the mutants, *abaI*::Tn*26* opaque showed higher amounts of attached biomass compared with the wild-type opaque strain. This was also surprising, as mutations in the synthase gene in *Acinetobacter* have usually been linked to a decrease in attachment (Niu et al., 2008; Kang and Park, 2010; Anbazhagan et al., 2012). When assessing the translucent variants, however, it was observed that the translucent *abaI*::Tn*26* exhibited ~60% lower attachment than its wild-type counterpart, a reduction similar to the reported previously. Due to the fact that previous work has been done with *Acinetobacter* strains that are either not phase variable or not known to be, and therefore samples used might have consisted of a mixture of phase variants, it is difficult to interpret these results and the role of the AHL synthase and quorum sensing in attachment and biofilm formation in *A. baumannii*. Moreover, no work has been published on the role of QS in AB5075, and therefore its contribution to attachment and biofilm formation might differ from those previously reported in other *A. baumannii* strains (Niu et al., 2008; Mayer et al., 2018; Luo et al., 2015).

In the case of AbaM, its orthologue in *B. cenocepacia* was shown to positively regulate biofilm formation (Inhülsen, 2011). In these assays, the opposite was observed. Both phases of *abaM*::Tn*26* showed significantly higher amounts of attached biomass than their equivalent wild-type variants. The biggest difference was observed in the opaque *abaM*::Tn*26*, which also showed attachment levels significantly higher than the isogenic translucent variant. Addition of *abaM* in *trans* to the opaque *abaM* mutant partially restored the wild-type phenotype, suggesting that there might be more two or more AbaM-dependent regulatory pathways involved in the regulation of attachment.

As previously mentioned in the attachment results section, the assays testing the effect of exogenous OHC12 to the attachment of AB5075 had the objective of further investigating the role of QS in this process, but also elucidate whether the high levels of OHC12 in the *abaM*::Tn*26* complemented strain might be the responsible for the inability to fully complement the *abaM* mutation. Interestingly, addition of OHC12 to the wild-type strain increased the attachment in the wild-type to similar levels to those observed in *abaM*::Tn*26* pMQ_*abaM*. No differences were observed between the samples containing 200 nM and the samples containing 2 μM OHC12, suggesting that, under the conditions used in this study, QS positively regulates the amount of attached biomass to abiotic surfaces, but only to a certain limit. It can be speculated that OHC12 may responsible for the lack of full complementation in *abaM*::Tn*26* pMQ_*abaM*. Therefore, it seems reasonable to propose, based on all the data analysed, that AbaM might exert its regulation on attachment in two or more ways. At least one of these pathways seems to be QS-dependent, while the other is QS-independent and can be genetically complemented in *trans*.

In conclusion, attachment to abiotic surfaces and biofilm formation is a complex, multiregulated process linked to QS in many bacteria. For example, QS plays a key role in biofilm maturation in *P. aeruginosa,* while *B. cenocepacia* QS seems to be required for both initial attachment and correct biofilm maturation (Williams and Cámara, 2009; Tomlin et al., 2005). These results suggest that QS plays a key role in attachment in AB5075, with OHC12 having a positive but limited impact on the process. Moreover, AbaM was characterized as a negative regulator of attachment and it is proposed that exerts its regulatory role in parallel with both QS-dependent and QS-independent pathways. Finally, the interplay between QS, AbaM and phase variation indicates that changes in any of these may lead to alternative phenotypic outcomes, hinting at a fine-tuned and adaptable regulation of attachment and subsequent biofilm formation.

Even though phenotypes like AHL production, motility and attachment are linked to virulence, experiments using relevant animal models are necessary to characterize the pathogenicity of any strain and elucidate the role of specific gene products as a virulence factors. Different animal models mimic different aspects of human infections with more or less fidelity, and the selection of any model will have advantages and disadvantages. In the case of *A. baumannii*, different animal models have been used. Mammalian models (mostly employing mice, rats, rabbits and guinea pigs) mimic human infections more closely than non-mammalian models approaches given that that they possess both innate and acquired immunity and can report on specific types of infections (sepsis, burns, meningitis, endocarditis, etc.). However, these models are costly, not easy to handle and usually involve ethical issues. Non-mammalian models, on the other hand, are cheaper, easy to use, widely available and not subject to ethical problems (McConnell et al., 2013). Among

the available non-mammalian models recently used for *A. baumannii* infection studies there is *Galleria mellonella* larvae. *Galleria* larvae have been widely used to determine the virulence of different strains showing excellent reproducibility. However, despite possessing cellular and humoral innate immune response, *G. mellonella* does not have an adaptive immune response, and therefore cannot replace mammal infection models (Jacobs et al., 2014; Peleg et al., 2009; Tipton et al., 2015; Wand et al., 2012). Nonetheless, *G. mellonella* is a cheap, easy to handle infection model to do initial assessments of bacterial virulence prior using more expensive mammalian models. For that reason, this model was selected to determine the role on virulence of AbaM and QS in AB5075.

Virulence for *G. mellonella* was initially assessed for the opaque variants of the wild-type strain, *abaI*::Tn*26* and *abaM*::Tn*26*. Even though the differences in motility and attachment suggested that QS might affect virulence, no differences between the synthase mutant and the parental strain were found for the two inoculum sizes tested. Moreover, addition of OHC12 did not alter the virulence. This result is not unprecedented. In the study where *G. mellonella* larvae was established as a suitable virulence model for *A. baumannii*, an *A. nosomialis* M2 *abaI* knockout mutant also showed no difference in killing when compared with the wild-type strain (Peleg et al., 2009). However, in another study, this time using zebrafish and a mice murine septicaemia model, the synthase gene was necessary for full virulence in *A. nosocomialis* M2 (Bhuiyan et al., 2016). Similarly, *A. baumannii* ATCC 17978 showed significant differences in virulence between the wild-type and the *abaI* mutant in *G. mellonella* (Fernandez-Garcia et al., 2018). It is also important to consider that *A. baumannii* AB5075 is highly virulent strain compared with other clinical isolates and laboratory strains such as *A. baumannii* ATCC 17978 and *A. nosocomialis* M2, mentioned above

(Jacobs et al., 2014). It is possible that, in such a hypervirulent background, the contribution of *abaI* inactivation or exogenous OHC12 addition in virulence could not be significant enough to be detected in the model and under conditions used in this study. Overall, these discrepancies between studies might raise the question of whether different *Acinetobacter* strains require or not the active participation of quorum sensing depending on the type of infection and animal model used.

The *abaM* mutant, on the other hand, showed a significant decrease in virulence compared with the wild-type strain. Notably, the virulence of the *abaM* mutant was so attenuated that the inoculum of 2 x 10^5 cells/larvae showed less killing that the wild-type inoculum of 2 x 10^4 cells/larvae. This was particularly interesting because, as previously mentioned, increased motility and biofilm formation in *Acinetobacter* has traditionally been linked to increased virulence (Wand et al., 2012; Eijkelkamp et al., 2013). Nonetheless, orthologues of AbaM in the rice pathogens *P. fuscovaginae* and *B. glumae* were described to positively regulate virulence in those bacteria, with a significant decrease in pathogenicity and toxoflavin synthesis (in *B. glumae*) when the corresponding genes were disrupted or knocked out (Chen et al., 2012; Mattiuzzo et al., 2011). However, attempts to genetically complement the *abaM*::Tn*26* phenotype were unsuccessful. The complemented *abaM*::Tn*26* strain killed similar numbers of larvae to the uncomplemented mutant, being both significantly attenuated when compared with the wild-type strain. To determine whether this problem was a direct consequence of the high AHLs levels in the *abaM*::Tn*26* pMQ_*abaM*, a new assay was performed adding either 200 nM or 2 μM of OHC12 to the wild-type strain. Interestingly, it seems that the high levels of OHC12 in the complemented strain cannot explain its *abaM*::Tn*26*-like phenotype, as exogenous addition of OHC12 did not attenuate the wild-type

strain. This is not unexpected, as QS does not seem to play a differential role in AB5075 pathogenicity in *G. mellonella* under the conditions used in this study, as discussed above. Moreover, in *B. glumae*, the mechanism of action of TofM with respect to virulence and toxoflavin production appears to be QS-independent (Chen et al., 2012). These data collectively, despite clearly showing an impact of AbaM in virulence, are not able to explain how AbaM exerts a regulatory role in virulence or why it is not possible to complement the mutation in *trans*.

Summarizing, AbaM seems to be required for full virulence in *G. mellonella* infection model, while the role of QS during *A. baumannii* infection remains elusive. The fact that the wild-type AB5075 produced low levels of OHC12, along with the virulence assays results here presented, suggest that it might not be a key virulence regulatory factor in AB5075, at least under the conditions used in this study. Nonetheless, this observation might not be true for other *A. baumannii* strains and in other infection models.

Despite the fact that neither *abaM* nor QS affected the ability of AB5075 to survive in dry conditions, the assay revealed some interesting information. *A. baumannii* AB5075 showed an extreme resistance to desiccation at 22°C, with an averagege survival of 22% after 12 weeks of exposition to 31% ± 3% relative humidity. Previous studies have reported diverse *Acinetobacter* strains capable of surviving under dry condition for very long periods of time (Wang et al., 2020; Farrow et al., 2018; Bravo et al., 2018; Chaparteguí-González et al., 2018), but the results in AB5075 are particularly interesting for the long duration of the assay (84 days) and the relative low loss of viable cells. It could be interesting to further examine the exceptional resistance to desiccation displayed by

AB5075 to determine what mechanisms are involved in this process and better understand the ability of this pathogen to survive for such long periods of time on unanimated objects, a key aspect of the success of this organism as a nosocomial pathogen. Furthermore, the cells incubated at 37°C showed a significantly lower tolerance (77-fold difference) towards desiccation than the ones incubated at 22°C, which could also lead to more in deep research to better understand the environmental factors are involved in desiccation survival in *Acinetobacter*.

Lastly, the possible interactions between AbaM and QS proteins were evaluated. The exact molecular mechanism of action of AbaM-like regulators has remained elusive since this protein family was first characterized. Sequence alignment of AbaM and orthologues of other species and the crystal structure of one of these orthologues, *Bc*RsaM, revealed that AbaM-like proteins possess three conserved regions: a unique hydrophobic core of four highly conserved tryptophan residues and two surface-exposed regions. However, none of these conserved regions contains any known motif or functional domain that suggested any specific activity. Moreover, biochemical analyses strongly suggest that *Bc*RsaM does not bind AHLs or DNA (via electrophoretic mobility shift assays (EMSAs)) (Michalska et al., 2014). It has also been considered that *Bc*RsaM might be acting by affecting the activity of LuxR-like regulators (Inhülsen, 2011), even though a mechanism for this functionality has not been proposed.

Based on this last hypothesis, the BACTH two hybrid system was used to test the possible protein-protein interactions between AbaM and the QS proteins AbaR and AbaI. No protein-protein interactions were detected between AbaM and either of the QS proteins.

Interestingly, the dimer state in solution previously observed *in vitro* in *Bc*RsaM, the AbaM orthologue in *B. cenocepacia* (Michalska et al., 2014), was not detected in AbaM using this *in vivo* approach.

It is important to note that, as in all techniques, the Bacterial Adenylate Cyclase Two-Hybrid assay has a series of limitations that could have affected the results. First of all, the translational fusion of the target proteins with the T25/T18 fragments might affect the correct folding of the proteins, as well as interfere with the interaction, leading to false negatives. Secondly, the pKT25/pKNT25 and pUT18/pUT18C plasmids, despite possessing the same P_{lac} promoter driving the expression of the protein fusions, possess different replication origins (p15A and ColE1, respectively), which leads to different copy numbers (low copy and high copy number, respectively). This unbalance in the number of plasmid copies generates a different amount of protein fusions being expressed. In protein-protein interactions, stoichiometry can be a crucial factor and these differences in protein amounts might affect the interaction, altering the results. Finally, the BACTH assay is performed in a compatible *E. coli* strain (in this study, DHM1). While both *A. baumannii* and *E. coli* are Gram-negative γ-proteobacteria, it cannot be discarded that the differences between the native and the BACTH assay host could influence in the tested proteins synthesis, folding, stability and interactions (Battesti and Bouveret, 2012).

3.5. Conclusions and future directions

The research around the virulence and its regulation in *Acinetobacter* have gained increasing interest in the recent years, leading to the identification and characterization of novel regulators and their roles in infection (Morris et al., 2019; Weber et al., 2015a). Even so, the mechanisms of *A. baumannii* pathogenesis remain poorly understood. As no set of virulence factors have been unequivocally associated with the ability of *A. baumannii* to cause disease, other hypothesis have been considered, including differential regulation of those virulence factors (Antunes et al., 2014). This highlights the importance of finding new regulators and fully characterize those which are still poorly or not studied in *A. baumannii* but have been already described in more detail in other bacteria, such as quorum sensing and AbaM.

In this chapter, the RsaM orthologue AbaM has been characterized in *A. baumannii* for first time. The data here provided is enough to confirm that its role is similar to the one described in other bacterial species: AbaM is a AHLs synthesis negative regulator that is also involved in the regulation of attachment, surface motility and virulence in *G. mellonella* larvae model. Moreover, the results also suggest that the regulation of these phenotypes can be, at least partially, QS-independent. Unfortunately, not all *abaM*::Tn*26* phenotypes could be genetically complemented. This problem has been described before even in in-frame deletion mutants in other species (Inhülsen, 2011; Le Guillouzer et al., 2018), leading to the hypothesis that AbaM-like proteins might be *cis*-acting regulators. The mechanism of action of these regulators remains unknown, as previous studies discarded AHLs or DNA/RNA binding (Michalska et al., 2014) and the protein-protein two hybrid assays with QS proteins performed in this chapter could not shed any light on the problem.

There are several aspects that, due to the limiting time, have not been fully answered in this chapter and will require further research. The construction of an inducible AbaM mutant would help to understand better its *cis*-acting role and study many phenotypes without the problems associated to the genetic complementation in *trans*. It would also be interesting to see whether AbaM plays a similar role in other *Acinetobacter* strains, as well as to study if it is required for virulence in other infection models. Finally, a wider screening for protein-protein interactions between AbaM and putative targets such as sigma factors, RNA polymerases or other transcriptional regulators might help to elucidate the elusive mechanism of action of this protein.

With respect to quorum sensing, the results described here confirm previous observations that suggested that QS is involved in attachment and motility (Clemmer et al., 2011; Niu et al., 2008). The role of QS in virulence, on the other hand, remains elusive. Results here suggest that it is not necessary for full virulence in *G. mellonella*, but previous studies suggest otherwise depending on the strain and model used (Bhuiyan et al., 2016; Fernandez-Garcia et al., 2018). A more in depth study with a wide range of *A. baumannii* strains isolated from different types of infection in different models is required to determine what is the exact role of QS in the pathogenesis of *Acinetobacter*. Moreover, even though it has been proposed that attachment and iron starvation induce AHL production (Mayer et al., 2018; Modarresi et al., 2015), the exact environmental factors that affect the synthesis of quorum sensing signals remain mostly unknown. Other factors such as nutrient limitation, cellular stress, stringent response or host response have been previously described to modulate QS activity in other species such as *P. aeruginosa* (Lee and Zhang, 2015; Venturi, 2006), so it would be safe to assume that some of them might regulate QS in *Acinetobacter* as well.

Lastly, it is important to highlight the role of phase variation in all these phenotypes. Phase variation has been reported to regulate motility, attachment and virulence in AB5075 wild-type (Tipton et al., 2015). In this study, it has been showed that phase variation affected motility in AB5075 wild-type. However, while phase variation did affect attachment in *abaI*::Tn*26*, no effect was observed in the wild-type strain. Differences in methodology might be responsible for these differences and therefore further research is required to better characterize attachment and biofilm in both colony variants. Due to time limitations, the AHL production and virulence of the translucent phases of AB5075, *abaI*::Tn*26* and *abaM*::Tn*26* were not characterized. It has been recently reported that translucent AB5075 wild-type produces significantly lower amounts of AHL (Rather, 2019), so it would be interesting to characterize the translucent variants of *abaM*::Tn*26* for this phenotype as well as for virulence in *G. mellonella*. It would also be interesting to determine whether QS or *abaM* affect the the opaque to translucent or translucent to opaque phase variation frequency. Despite it has been shown that exogenous addition of OHC12 does not affect the variation frequency, it is possible that QS/AbaM could exert a OHC12-independent regulatory role in the phase switching. Moreover, it has been shown that RsaM-like proteins can regulate genes and phenotypes independently from QS (Uzelac et al., 2017; Inhülsen, 2011), so it would be interesting to know whether AbaM could be playing a similar QS-independent regulatory role in *A. baumannii* phase variation.

3.5.1. Summary of most important findings

- AB5075 possesses a high tolerance to desiccation.
- AB5075 produces OHC12 as the major AHL together with lower levels of OHC10.
- AbaM negatively regulates AHL production, attachment to abiotic surfaces and motility.
- AbaM is required for full virulence in *G. mellonella* larvae model.
- QS positively regulates motility. It also regulates attachment positively or negatively depending on the nature of the phase variant.
- QS is not required for full virulence in *G. mellonella* larvae model in AB5075, at least under the conditions used in this study.
- The *abaM* mutant phenotypes can be *trans*-complemented in some cases (motility, attachment), but not in others (AHL production, virulence).
- AbaM, QS and phase variation might overlap with each other in the regulation of specific phenotypes.
- AbaM does not show any protein-protein interactions with itself or the QS proteins AbaR and AbaI in the BACTH *in vivo* bacterial two-hybrid system.

4. Regulation of *abaM* expression and transcriptomic analysis of *abaM* and *abaI* mutants

4.1. Introduction

The phenotypic characterization carried out in the previous chapter suggested a very important contribution of AbaM to surface motility, attachment, AHL production and virulence in the *G. mellonella* infection model, with QS also involved in each of these processes (with the exception of virulence). To further understand the role of AbaM and QS in *A. baumannii*, it was decided to analyse their regulation, the specificity of the AbaR response regulator to different AHLs and their regulons (by RNA-seq) in attachment-like (static growth) conditions. The RNA-seq data was validated using quantitative real-time PCR.

4.1.1. AbaM and QS regulons in *A. baumannii* and other species

In the previous chapter it was noted that very little is known about the role of QS in *A. baumannii*, apart from its role in attachment and surface motility (Niu et al., 2008; Clemmer et al., 2011). A very recent RNA-seq analysis comparing an *abaI* deletion mutant with the wild-type strain of *A. baumannii* strain 863 during late log phase of growth is the only transcriptomic analysis that has been published to date on *A. baumanii* QS. This study showed that QS in *A. baumannii* is involved in metabolism, energy production, stress response and ribosome biogenesis (Ng et al., 2019). Unfortunately, the current knowledge about *A. baumannii* QS does not go much further. While in other human pathogenic bacteria, such as *P. aeruginosa*, QS is very well characterized and its involvement in bacterial virulence, gene regulation, physiology and metabolism is very well established, there is a long way to reach that level of knowledge in *A. baumannii*.

In the case of AbaM, this is the first time it has been characterized in *A. baumannii*, so there is no previous data regarding its regulon in this species. However, two transcriptomic analysis have been performed in orthologues present in other bacteria. A RNA-seq study of *P. fuscovaginae* (which contains two QS systems, PfsI/R and PfvI/R) *rsaM* mutant suggested that RsaM plays a major regulatory role, upregulating 260 genes and downregulating 206 (Uzelac et al., 2017). As expected, the *pfsI/R* genes were strongly repressed by RsaM, which also negatively controlled the expression of the *pfvI/R genes*, in line with phenotypic observations reported in a previous study (Mattiuzzo et al., 2011). Consequently, the regulons of RsaM and both QS systems were partially overlapped, with 53% of the genes regulated by PfsI/R and 65% by PfvI/R being also part of the pool of genes regulated by RsaM. Among the genes differently regulated in the *rsaM* deletion mutant there were many transporters (32% of the regulon) involved in the transport of carbohydrates, lipids, amino acids, nucleotides and inorganic ions, genes involved in cell wall and membrane processing (6.96%), transcriptional regulators (6%) and genes involved in motility (3.4%) (Uzelac et al., 2017). Another transcriptomic analysis (using a DNA microarray) comparing a mutant of the *rsaM* orthologue *BcrsaM* in *B. cenocepacia* with the wild-type strain showed that controls a regulon that also overlaps with the QS, with around 50% of the differentially expressed genes also present in the CepR (QS response regulator) regulon, consistently with what was previously described in *P. fuscovaginae*. Many of the genes in the *Bc*RsaM operon were involved in metabolism, transport, iron acquisition and transcriptional regulation (Inhülsen, 2011).

4.2. Aims of the chapter

The main aims of the work described in this chapter were to:

- Determine whether *abaM* is auto-regulated and controlled by QS.
- Elucidate whether OHC12 can activate the *abaM* promoter.
- Investigate the AHL structure activity relationship (SAR) for AbaR.
- Screen for AbaR competitive inhibitors and determine their SARs.
- Perform a transcriptomic analysis (RNA-seq) of the opaque phases of the wild-type strain compared with *abaM*::Tn*26* and *abaI*::Tn*26* mutants in static growth conditions.
- Validate the RNA-seq data with qPCR analysis.

4.3. Results

4.3.1. Investigating the expression of P*abaM* and P*abaI*

4.3.1.1. Validation of *lux*-based reporters

The first step before using any promoter - reporter fusion (P*abaM*::*luxCDABE*/P*abaI*::*luxCDABE*) is to correctly validate the constructs to ensure the output observed (in this case, luminescence) is exclusively a consequence of the activity of the target promoter. To assess this, a mini-Tn*7* containing either the P*abaM*::*lux* fusion or the promoterless *lux* operon (mini-Tn*7*::*lux*) was inserted in AB5075, *abaI*::Tn*26* and *abaM*::Tn*26* strains. To each reporter either OHC12 or acetonitrile (negative control) was added and luminescence output was quantified using a TECAN plate reader.

None of the promoterless *lux* strains increased their luminescence in the presence of OHC12, while the P*abaM*::*lux* fusions responded to OHC12, significantly increasing *lux* expression and, in consequence, the luminescence detected. Moreover, the levels of luminescence of promoterless *lux* constructs were much lower (between 35 and

400-fold) than in the same strain containing the P*abaM*::*lux* fusion. Lastly, luminescence in the promoterless strains was very similar among the three strains, while P*abaM* showed different expression levels depending on the genetic background: the synthase mutant showed the lowest levels (8.1 x 10^5 RLUs), followed by the wild-type strain (3.9 x 10^6 RLUs) and the *abaM* mutant (1 x 10^7 RLUs) (**Figure 4.1A**).

4.3.1.2. The expression of *abaM* in AB5075 wild-type, *abaM*::Tn*26* and *abaI*::Tn*26*

To evaluate the differences in *abaM* expression observed between the three strains, assays were repeated with the three reporters without the addition of acetonitrile to avoid any possible effect on growth and/or *lux* expression. As observed in the previous assay, the *abaI* mutant showed much lower P*abaM* expression than the wild-type strain, with a 3-fold reduction when comparing the OD_{600}-normalized RLU values. Similarly, the *abaM* mutant showed an approximate 50% increase in luminescence compared with the parental strain (**Figure 4.1B**).

4.3.1.3. The expression of *abaI* in AB5075 wild-type and *abaI*::Tn*26* and response to exogenous OHC12

To confirm that QS in *A. baumannii* AB5075 follows a positive feedback loop, a similar construct was made containing the *lux* operon under control of the putative *abaI* promoter. The *abaI* promoter showed a 50-fold reduced activity in the *abaI* mutant, while addition of OHC12 increased the activity more than 10-fold, suggesting that *A. baumannii* QS is positively auto-regulated. (**Figure 4.2**).

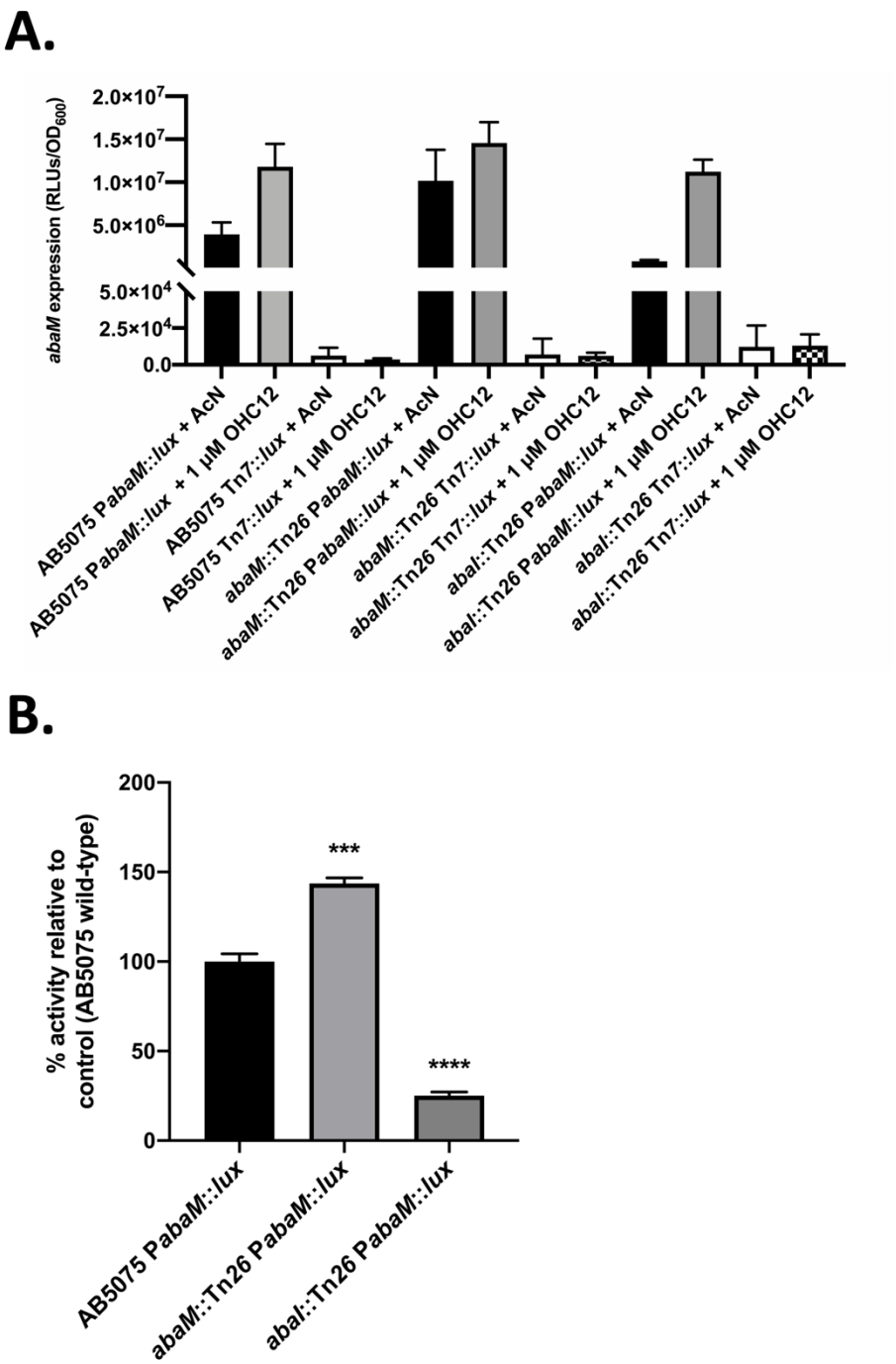


Figure 4.1: P*abaM*::*lux* activity assays. (A) Validation of P*abaM* reporters by comparison of light production with promoterless *lux* operon and response to exogenous OHC12. **(B)** P*abaM* activity in AB5075, *abaM*::Tn*26* and *abaI*::Tn*26* (data expressed as % activity relative to AB5075 p*abaM*::*lux*). Strains were grown to an OD_{600} = 0.5 and diluted 1:10 in 96-well plates. The RLUs and OD_{600} were measured every 30 min and the maximum normalized ($RLUs/OD_{600}$) value was used for the statistical analysis. AcN = Acetonitrile. Error bars indicate standard deviation between three biological replicates. Asterisks indicate: ***, $p \leq 0.001$; ****, $p \leq 0.0001$.

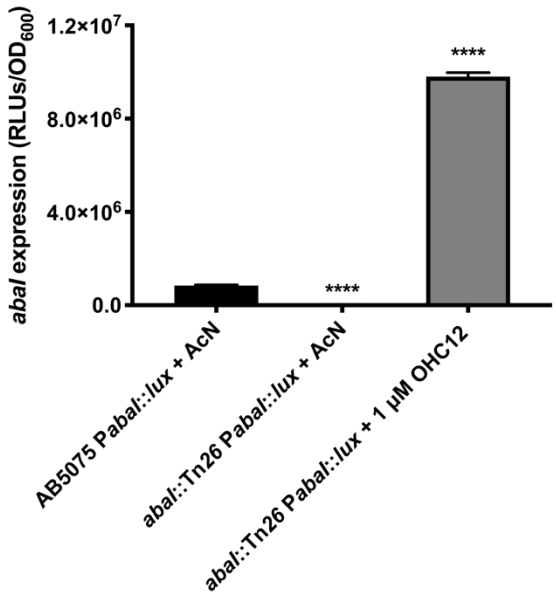


Figure 4.2: P*abaI*::*lux* activity assays in AB5075 and *abaI*::Tn26 ± exogenous OHC12. Strains were grown to an OD_{600} = 0.5 and diluted 1:10 in 96-well plates. The RLUs and OD_{600} were measured every 30 min and the maximum normalized (RLUs/OD_{600}) value was used for the statistical analysis. AcN = Acetonitrile. Error bars indicate standard deviation between three biological replicates. Asterisks indicate: ****, $p \leq 0.0001$.

4.3.2. Study of AbaR agonists and screening for QS competitive antagonists

4.3.2.1. Response of P*abaM*::*lux* to different long-chain AHLs

With the aim of elucidating the specificity of AbaR for AHLs of different acyl chain lengths and oxidation state in the 3-position, a range of hydroxy-, oxo- and unsubstituted AHLs of C10 (*N*-decanoyl-L-homoserine lactone), C12 (dodecanoyl-L-homoserine lactone), C13 (*N*-tridecanoyl-L-homoserine lactone), C14 (*N*-tetradecanoyl-L-homoserine lactone) and C16 (*N*-hexadecanoyl-L-homoserine lactone) acyl chain length were tested in the *abaI*::Tn*26* P*abaM*::*lux* reporter at 10 μM, using OHC12 to normalize the data of the other signalling molecules (being OHC12 100% relative luminescence). The uninduced reporter was used as the negative control to enable subtraction of the background luminescence.

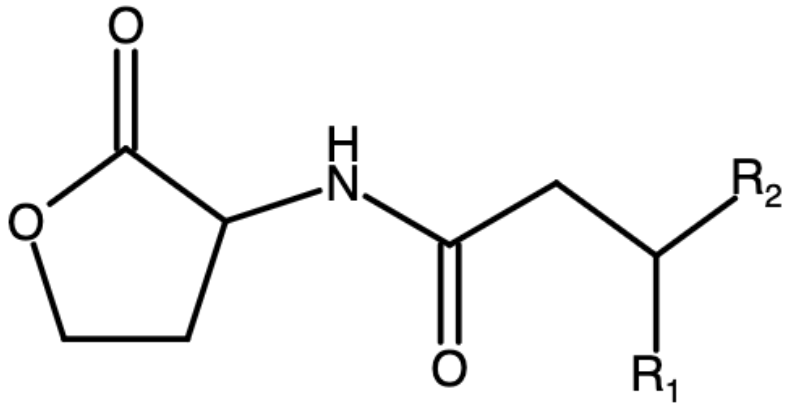


Figure 4.3: Structure of the AHLs used in this assay. Oxidation state in the 3-position (R_1) included 3-oxo (=O), 3-hydroxy (-OH) and unsubstituted (-H) AHLs. Acyl chain length of the AHLs used in this work included C10, C12, C13, C14 and C16, where $R_2 = C_{n-3}H_{2(n-3)+1}$ (for 3-hydroxy and unsubstituted AHLs) or $R_2 = C_{n-3}H_{2(n-3)}$ (for 3-oxo AHLs). *n* = total number of carbons in the acyl chain (e.g. 10 in C10 AHLs).

The results presented in **Figure 4.4** show that both acyl chain length and 3-position modifications greatly affected the ability to activate AbaR. In terms of acyl chain length, the C12 analogues were the strongest activators of AbaR, closely followed by C13, while C14 and C10 were less active. Interestingly, none of the C16 AHLs were capable of inducing P*abaM*::*lux* expression. In relation to 3-position oxidation state, 3-hydroxy modified AHLs were the most active AbaR ligands, followed by the 3-oxo analogues, which activated P*abaM* expression at a lower but still significant levels, with the exception of OC10. None of the unsubstituted AHLs were capable of activating AbaR (**Figure 4.4**).

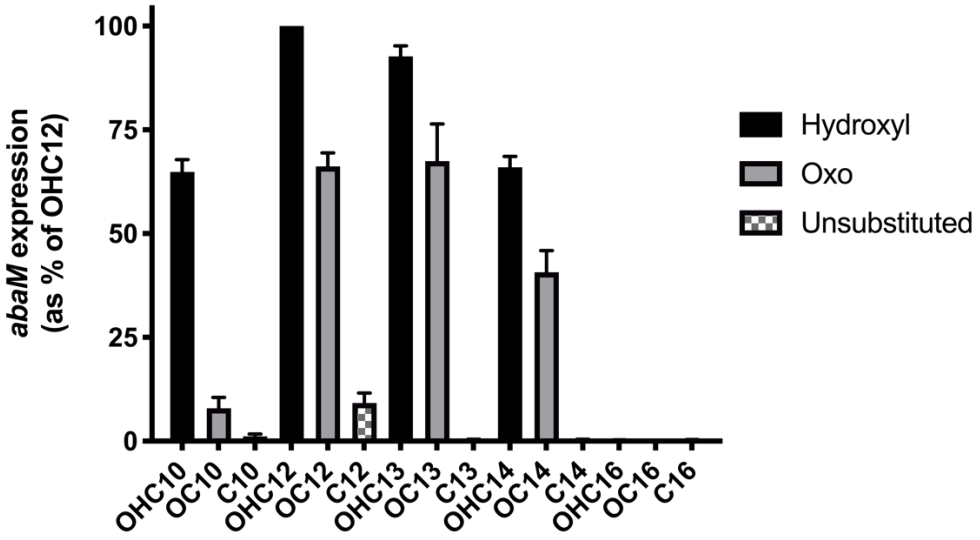


Figure 4.4: Comparative agonist activity of AHLs of different acyl chain length and 3-position modifications. Data expressed as % activity relative to the native ligand, OHC12. Strains were grown to an OD_{600} = 0.5, diluted 1:10 in 96-well plates and AHLs were added at a 100 nM concentration. Plates were incubated at 37°C for 24 h The RLUs and OD_{600} were measured every 30 min and the maximum normalized (RLUs/OD_{600}) value was used for the statistical analysis. Error bars indicate standard deviation between three biological replicates.

4.3.2.2. Dose-curve response of OHC12, OHC10 and OC12

In order to asses more accurately the activity of OHC12, OHC10 and OC12, a dose-response curve for each AHL was performed. OHC12 and OHC10 were selected as both are naturally produced by *A. baumannii* AB5075. OC12 was selected because it had a significant agonist activity (66 ± 3% of OHC12 activity), it is the native signal molecule of the *P. aeruginosa* LasR/LasI QS system and has been reported to enhance biofilm formation in *A. nosocomialis* M2 (Williams and Cámara, 2009; Bhargava et al., 2012). Therefore, assessing the activity of OC12 in *A. baumannii* could give some insights in the cross-regulation of *A. baumannii* QS by other bacterial species. The objective was to determine the EC_{50} of each of the AHLs, which in turn will provide information about the potency of each of the compounds as AbaR activators.

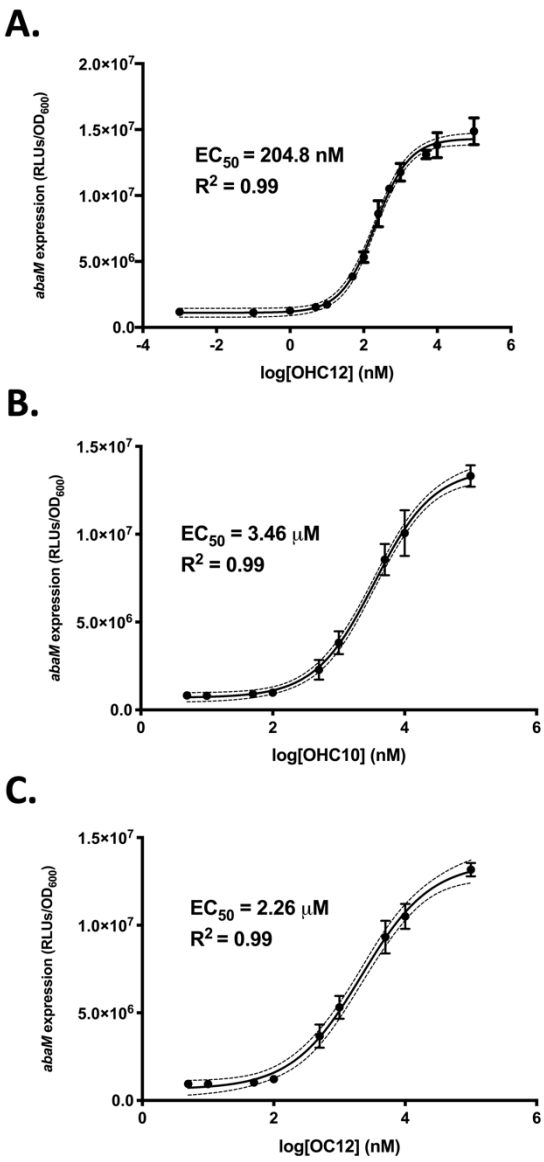


Figure 4.5: Dose-response curves of (A) OHC12, (B) OHC10 and (C) OC12. Strains were grown to an OD_{600} = 0.5, diluted 1:10 in 96-well plates and AHLs were added at the corresponding concentrations. Plates were incubated at 37°C for 24 h. The RLUs and OD_{600} were measured every 30 min and the maximum normalized ($RLUs/OD_{600}$) value was used for the statistical analysis. Error bars indicate standard deviation between three biological replicates. Dashed lines indicate the confidence interval of the line of best fit (black line).

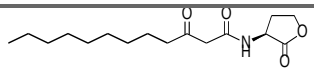
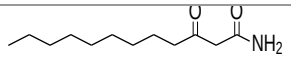
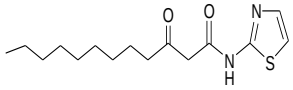
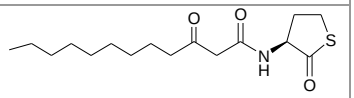
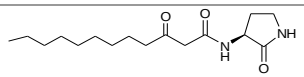
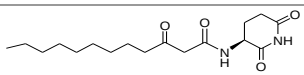
The native ligand of AB5075 AbaR, OHC12, was the most potent agonist, with an EC_{50} = 204.8 nM. Both OHC10 and OC12 were much weaker ligands, showing an EC_{50} 10-fold (2.26 μM) and 17-fold (3.46 μM) higher than OHC12, respectively (**Figure 4.5**).

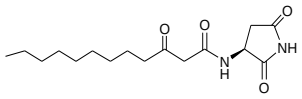
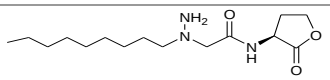
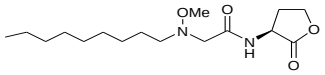
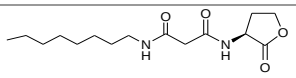
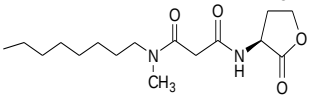
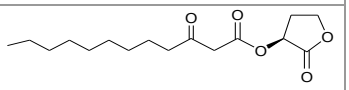
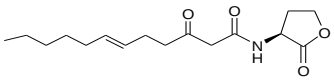
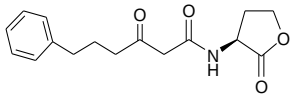
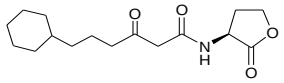
4.3.2.3. Screening for competitive inhibitors of AB5075 quorum sensing

A small library of 14 OC12-derived compounds (**Table 4.1**), in addition to the unsubstituted C10, C12, C13, C14 and C16 AHLs (**Figure 4.3**) were tested as competitive inhibitors of AB5075 QS.

For these experiments, each of the candidates was added at a 100 μM concentration to an *abaI*::Tn*26* Pa*baM*::*lux* culture containing 500 nM of OHC12. The activity of the compounds was expressed as a percentage variation from the positive control (containing only 500 nM of OHC12) activity.

Table 4.1: Nomenclature and structures of the OC12 analogues used in the screening for AbaR inhibitors

Compound	Abbreviation	Name	Chemical structure
OC12	3-oxo-C_{12}-HSL	*N*-(3-Oxododecanoyl)-L-homoserine lactone	
1	3-oxo-C_{12}-NH_2	3-Oxododecanamide	
2	3-oxo-C_{12}-AT	2-(3-Oxododecanoyl amino)thiazole	
3	3-oxo-C_{12}-HTL	*N*-(3-Oxododecanoyl)-L-homocysteine thiolactone	
4	3-oxo-C_{12}-AP	3-(3-Oxododecanoyl amino)-L-2-pyrrolidone	
5	3-oxo-C_{12}-GM	3-(3-Oxododecanoyl amino)-L-piperidine-2,6-dione	

6	3-oxo-C_{12}-Am	3-(3-Oxododecanoyl amino)-L-pyrrolidine-2,5-dione	
7	3-NH_2-3-aza-C_{12}-HSL	*N*-(3-Amino-3-azadodecanoyl)-L-homoserine lactone	
8	3-MeO-3-aza-C_{12}-HSL	*N*-(3-Methoxy-3-azadodecanoyl)-L-homoserine lactone	
9	4-aza-3-oxo-C_{12}-HSL	*N*-(4-Aza-3-oxododecanoyl)-L-homoserine lactone	
10	4-Me-3-oxo-C_{12}-HSL	*N*-(4-Methyl-3-oxododecanoyl)-L-homoserine lactone	
11	3-oxo-C_{12}-HBL	(*S*)-Tetrahydro-2-oxofuran-3-yl 3-oxododecanoate	
12	Δ^{6E}-3-oxo-C_{12}-HSL	*N*-(Trans-6-3-oxododecenoyl)-L-homoserine lactone	
13	6-Ph-3-oxo-C_6-HSL	*N*-(6-Phenyl-3-oxohexanoyl)-L-homoserine lactone	
14	6-Cy-3-oxo-C_6-HSL	*N*-(6-Cyclohexyl-3-oxohexanoyl)-L-homoserine lactone	

All the unsubstituted AHLs (C10, C12, C13, C14 and C16) showed antagonist activity against OHC12 and inhibited QS at a different degree. The best inhibitors were C10, C12 and C13 with approximately 40% inhibition, followed by C16 (32%). The lowest activity was showed by C14, with barely a 23% inhibition (**Figure 4.6A**).

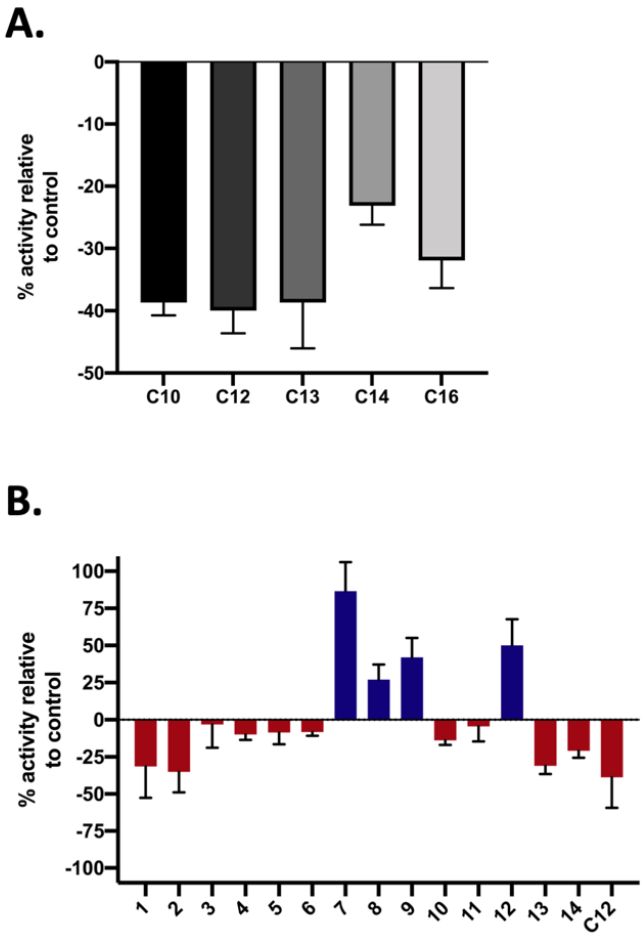


Figure 4.6: Screening for AbaR inhibitiors. (A) Screening inhibition activity of unsubstituted AHLs of different acyl chain length (indicated in the *x*-axis). **(B)** Screening activity of OC12-based compounds. Data is expressed as % of increased or decreased activity relative to the positive control (*abaI*::Tn*26* p*abaM*::*lux* + 500 nM OHC12). The black line at 0% represents positive control activity. Strains were grown to an OD_{600} = 0.5, diluted 1:10 in 96-well plates. OHC12 was added at 500 nM final concentration and the compound to be tested at 100 μM. Plates were incubated at 37°C for 24 h. The RLUs and OD_{600} were measured every 30 min and the maximum normalized (RLUs/OD_{600}) value was used for the statistical analysis. Error bars indicate standard deviation between three biological replicates.

The small library of OC12-derived compounds showed a more heterogenous outcome. Some of the compounds possessed significant inhibitory activity (1, 2, 13, 14), with an 25-35% reduction compared to the positive control, very close to the C12 used as a reference. Most of the compounds, however, showed very low or no inhibition activity (3-14%) (3, 4, 5, 6, 10, 11). Finally, a third group of compounds (7, 8, 9, 12) showed enhanced promoter activities with levels between 27-87% higher than the positive control (**Figure 4.6B**).

4.3.2.4. Screening the OC12-derived compounds for AbaR agonists

To confirm the agonist activity of some of the OC12-derived compounds (7, 8, 9 and 12), an agonist assay with all the OC12-derived compounds was performed. Consistently with the previous assay, compounds 7, 8, 9 and 12 displayed a significant agonist activity. The best agonist was compound 7, which showed an activity very similar to OHC12. Compound 12 also possessed a significant but lower agonist activity (64.3% of OHC12), while compounds 8 and 9 were weaker agonists (23.6% and 30.5% of OHC12 activity, respectively). Interestingly, compound 3, which did not display an enhanced P*abaM* activity in the inhibition assay, was also capable of strongly activate AbaR (71.2% of OHC12 activity). None of the other compounds showed any AbaR agonist activity. OHC12 was used as a positive control and OC12, the original molecule all the compounds are based on, was added as a reference (**Figure 4.7**).

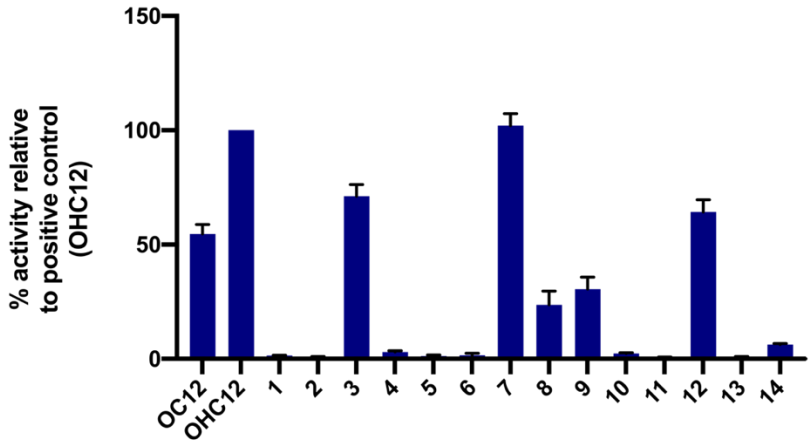


Figure 4.7: Screening for AbaR agonists. Screening activity of OC12-based compounds. Data is expressed as % of increased or decreased activity relative to the positive control (*abaI*::Tn*26* p*abaM*::*lux* + 1 μM OHC12). Strains were grown to an OD_{600} = 0.5, diluted 1:10 in 96-well plates. Compounds to be tested were added at 1 μM final concentration. Plates were incubated at 37°C for 24 h. The RLUs and OD_{600} were measured every 30 min and the maximum normalized (RLUs/OD_{600}) value was used for the statistical analysis. Error bars indicate standard deviation between three biological replicates.

4.3.3. RNA-seq-based comparative transcriptomics between AB5075 wild-type strain, *abaI*::Tn26 and *abaM*::Tn26

4.3.3.1. Quality analysis

Quality control analysis ensures that the transcriptomic data produced is reliable in terms of quality of the reads, genome coverage and reproducibility between biological replicates. In this case, all samples had more than 99% of clean reads (reads remaining after removing reads containing adapters, with > 10% of unidentified bases and other low quality reads) over the total raw reads, leaving most of the reads available for analysis. In terms of genome coverage, more than 96% of the clean reads in all samples were able to be mapped in the AB5075 genome, which is an excellent coverage (data not shown). Finally, the heat map in **Figure 4.8** indicates how the Pearson correlation coefficients of the different samples clearly form three distinct types of clusters depending of the degree of correlation between the samples. The three biological replicates of each of the samples (AB5075 wild-type strain, *abaI*::Tn*26* and *abaM*::Tn*26*) show, between them, the higher level correlation, indicating a good reproductivity between replicates. Between different samples, the wild-type and *abaI*::Tn*26* show a closer correlation than the *abaM*::Tn*26* with either the wild-type or *abaI*::Tn*26*, indicating that *abaM*::Tn*26* has higher differences in gene expression with the wild-type than *abaI*::Tn*26*.

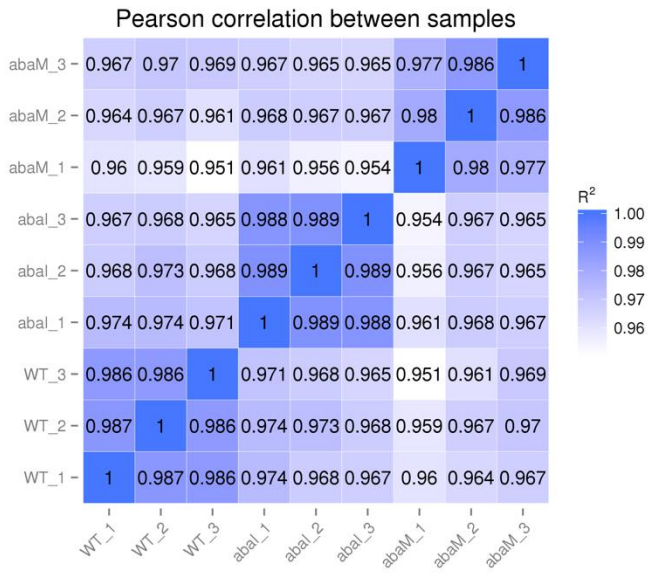


Figure 4.8: Pearson correlation heat map. The heat map represents the Pearson correlation coefficients between the different samples. A $R^2 = 1$ implies a total positive correlation and $R^2 = 0$ implies no correlation. The closer the R^2 value is to 1, the higher is the similarity between the two samples.

4.3.3.2. Differentially expressed genes

abaI::Tn*26* vs AB5075 wild-type

The primary data obtained from Novogene showed 651 differentially expressed genes. Of those, 414 were upregulated in the *abaI* mutant and 237 were downregulated (**Figure 4.9**). The Gene Ontology (GO) enrichment analysis of these genes revealed that most were involved in metabolism. In relation to of biological processes, many genes were involved in ion transport, oxidation-reduction processes and ATP metabolism, with some also involved in carbohydrate and nucleic acid metabolism. Expectedly, the molecular function classification revealed that many genes were related to channel and transporter activity, with also some ATPases and regulators (**Supplementary Material Figure S2B**). Similarly, the Kyoto Enyclopedia of Genes and Genomes (KEGG) enrichment analysis also showed that most of the regulated genes were involved in different aspects of metabolism, including carbohydrate, amino acid and fatty acid metabolism, as well as the biosynthesis of secondary metabolites (**Supplementary Material Figure S2A**).

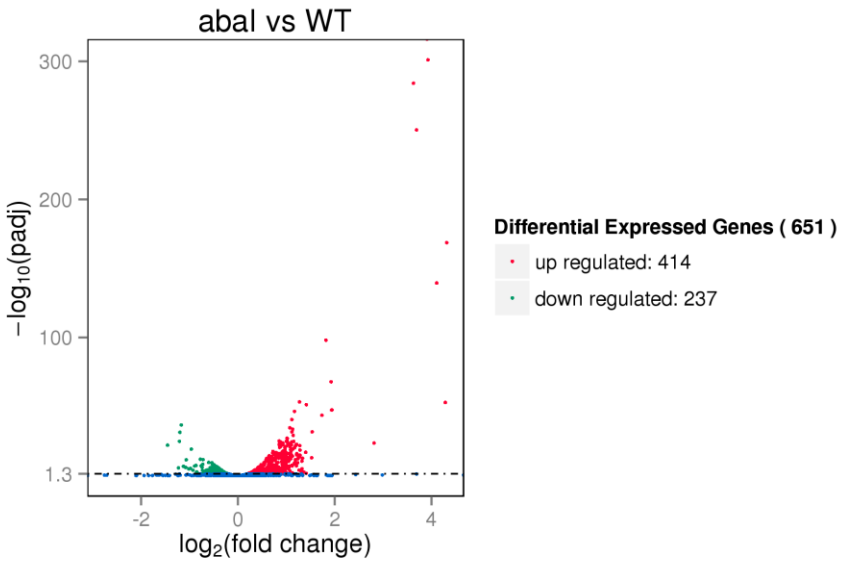


Figure 4.9: Volcano plot displaying differentially expressed genes between *abaI*::Tn26 (abaI) and AB5075 (WT). The horizontal axis (*x*-axis) corresponds to the $\log_2$ fold change value between the expression of the gene in *abaI*::Tn*26* and AB5075. The vertical axis (*y*-axis) displays the additive inverse of the $\log_{10}$ of the adjusted p-value (p_{adj}). Red dots represent genes with higher expression in *abaI*::Tn*26*. Green dots represent genes with reduced expression in *abaI*::Tn*26*. Blue dots represent all the genes with a $-\log_{10}(p_{adj}) < 1.3$ (marked with a doted black line), which indicates that the differential expression is not statistically significant.

To find the most highly expressed genes, a $|\log_2(\text{fold-change})| \geq 1.5$ cut-off was applied, leaving 15 genes upregulated in *abaI*::Tn*26* and none downregulated (**Table 4.2**). A table applying a wider cut-off of $|\log_2(\text{fold-change})| \geq 1$, which showed 88 upregulated and 9 downregulated genes, can be found in **Supplementary Table 1**.

Table 4.2: Differentially expressed genes (|log_2(fold change)| ≥ 1.5) in *abaI*::Tn*26* (compared with AB5075 wild-type).

Gene id	Log_2(Fold change)	Description	Gene name
ABUW_RS18385	4.3142	N-acylhomoserine lactone synthase	*abaI*
ABUW_RS07260	4.2853	SCPU domain-containing protein	*csuB*
ABUW_RS07255	4.1072	protein CsuA	*csuA*
ABUW_RS07265	3.9262	molecular chaperone	*csuC*
ABUW_RS07250	3.9062	SCPU domain-containing protein	*csuA/B*
ABUW_RS07275	3.692	protein CsuE	*csuE*
ABUW_RS07270	3.6287	fimbrial biogenesis outer membrane usher protein	*csuD*
ABUW_RS07245	2.8129	TetR/AcrR family transcriptional regulator	-
ABUW_RS07925	1.9432	alcohol dehydrogenase	-
ABUW_RS01970	1.9355	flavohemoprotein	-
ABUW_RS07910	1.9263	aldehyde dehydrogenase	-
ABUW_RS07630	1.8189	hypothetical protein	-
ABUW_RS07640	1.7361	hypothetical protein	-
ABUW_RS07620	1.5361	hypothetical protein	-
ABUW_RS07905	1.5245	ethanolamine permease	-

abaM::Tn*26* vs AB5075 wild-type

Primary data revealed a total of 977 differentially expressed genes, with 452 upregulated in the *abaM* mutant and 525 downregulated (**Figure 4.10**). The enrichment analysis of the data revealed that, as in *abaI*::Tn*26*, many genes were involved in different metabolic pathways. The most abundant type of genes, according to their biological role, were related in ion transport and energy production, as in *abaI*::Tn*26*, but in this case most of them were downregulated. There was also an significant number of genes involved in proteolysis and protein folding which were not observed in *abaI*::Tn*26*. Classification by molecular function showed, as in *abaI*::Tn*26*, many channel and transporter-related differentially expressed genes, but mostly downregulated. Different peptidases and protein-related genes were also present (**Supplementary Material Figure S1B**). The KEGG enrichment analysis revealed a similar profile to *abaI*::Tn*26*, with many differentially expressed genes related with the metabolism of carbohydrate and amino acid, as well as biosynthesis of secondary metabolites. No genes involved in fatty acid metabolism were found but two genes related to beta-lactam resistance were downregulated (**Supplementary Material Figure S3A**). The application of the $|\log_2(\text{fold-change})| \geq 1$ cut-off left 52 genes upregulated and 24 downregulated. The full list of these genes can be found in **Supplementary Table 2**. Applying the $|\log_2(\text{fold-change})| \geq 1.5$ cut-off revealed 19 upregulated and 5 downregulated genes in the *abaM* mutant compared with the wild-type (**Table 4.3**).

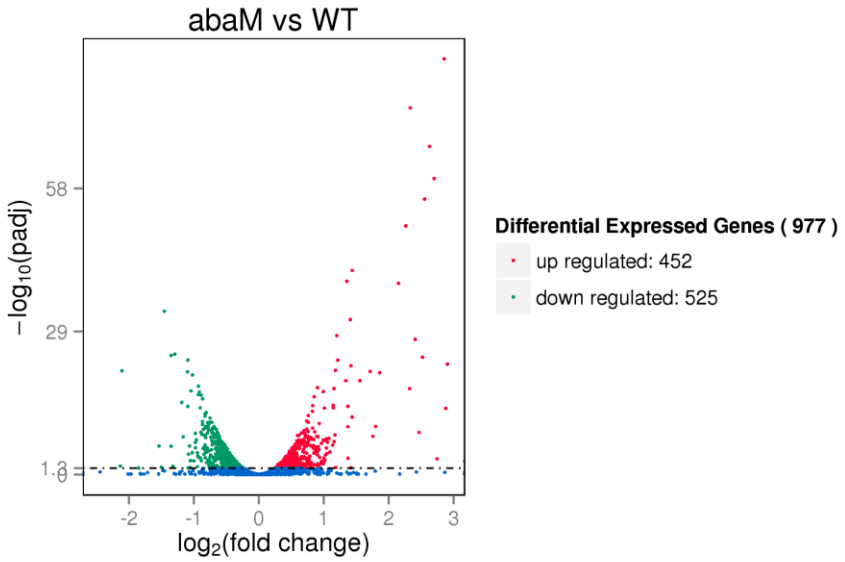


Figure 4.10: Volcano plot displaying differentially expressed genes between *abaM*::Tn*26* (abaM) and AB5075 (WT). The horizontal axis (*x*-axis) corresponds to the $\log_2$ fold change value between the expression of the gene in *abaM*::Tn*26* and AB5075. The vertical axis (*y*-axis) displays the additive inverse of the $\log_{10}$ of the adjusted p-value (p_{adj}). Red dots represent genes with higher expression in *abaM*::Tn*26*. Green dots represent genes with reduced expression in *abaM*::Tn*26*. Blue dots represent all the genes with a $-\log_{10}(p_{adj}) < 1.3$ (marked with a doted black line), which indicates that the differential expression is not statistically significant.

Table 4.3: Differentially expressed genes ($|\log_2(\text{fold change})| \geq 1.5$) in *abaM*::Tn*26* (compared with AB5075 wild-type).

Gene id	Log_2(Fold change)	Description	Gene name
ABUW_RS07245	2.9052	TetR/AcrR family transcriptional regulator	-
ABUW_RS07260	2.878	SCPU domain-containing protein	*csuB*
ABUW_RS18365	2.8531	acyl-CoA dehydrogenase	-
ABUW_RS11870	2.7441	hypothetical protein	-
ABUW_RS18350	2.6991	RND transporter	-

ABUW_RS18355	2.6293	non-ribosomal peptide synthetase	-
ABUW_RS18375	2.554	LuxR family transcriptional regulator	*abaR*
ABUW_RS07265	2.5191	molecular chaperone	*csuC*
ABUW_RS07250	2.4684	SCPU domain-containing protein	*csuA/B*
ABUW_RS18385	2.4087	N-acylhomoserine lactone synthase	*abaI*
ABUW_RS18370	2.3341	acyl-CoA synthetase	-
ABUW_RS07255	2.323	protein CsuA	*csuA*
ABUW_RS07270	2.2652	fimbrial biogenesis outer membrane usher protein	*csuD*
ABUW_RS07275	2.1508	protein CsuE	*csuE*
ABUW_RS07145	1.8615	DUF2171 domain-containing protein	-
ABUW_RS11840	1.7989	stress-induced protein	-
ABUW_RS08050	1.7574	hypothetical protein	-
ABUW_RS11875	1.7165	hypothetical protein	-
ABUW_RS19150	1.5586	hypothetical protein	-
ABUW_RS03380	-1.5003	entericidin EcnA/B family	-
ABUW_RS17200	-1.5374	Na+/H+ antiporter subunit C	*mrpC*
ABUW_RS02775	-1.8507	phage tail assembly protein	-
ABUW_RS12990	-2.1063	hypothetical protein	-
ABUW_RS00585	-2.1307	hypothetical protein	-

4.3.3.3. Comparison of *abaI*::Tn*26* vs wild-type and *abaM*::Tn*26* vs wild-type differentially expressed genes

Both *abaI*::Tn*26* and *abaM*::Tn*26* showed several differentially expressed genes compared with the wild-type strain. However, with these data is not possible to know how many differentially expressed genes are shared between the mutants and how many are exclusively regulated by AbaI or AbaM. For that reason, a comparative analysis between the *abaM*::Tn*26* and *abaI*::Tn*26* differentially expressed genes with an expression difference $|\log_2(\text{fold change})| \geq 1$ compared with AB5075 wild-type was performed. Results revealed that AbaM and AbaI coregulate 21 genes (**Figure 4.11**), which corresponds to 27% of the AbaM and 22% of the AbaI regulons, respectively. The heat cluster in **Supplementary Material Figure S4** shows in more detail the differences in gene expression between the wild-type strain, *abaI*::Tn*26* and *abaM*::Tn*26*.

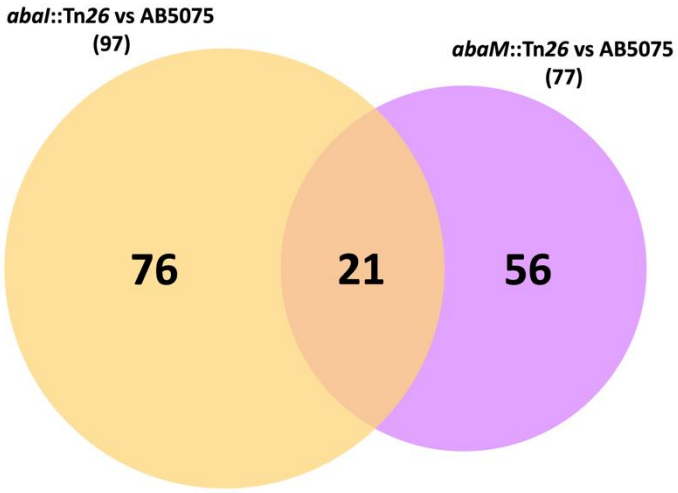


Figure 4.11: Overlapping differentially expressed genes in *abaM*::Tn*26* and *abaI*::Tn*26*. Venn diagram showing exclusively differentially expressed genes in *abaI*::Tn*26* vs AB5075 (orange) and *abaM*::Tn*26* vs AB5075 (purple) and the 21 genes differentially expressed in both (intersection).

4.3.4. Quantitative real-time PCR (qPCR)

To validate the data obtained by RNA-seq, a qPCR was performed using the same RNA extractions used for the transcriptomic analysis to evaluate the level of expression of *csuA/B* and *ABUW_3773*, the first genes of the *csu* and the Ac-505 biosynthesis operons, respectively. When compared with the wild-type strain, a biologically significant ($|\log_2(\text{fold change})| \geq 1$) increase of *csuA/B* expression was observed in the *abaI*::Tn*26* (4.02 ± 0.21 $\log_2$(fold change)) and the *abaM*::Tn*26* (3.03 ± 0.19 $\log_2$(fold change)) mutants, while the expression of *ABUW_3773* was significantly higher in the *abaM*::Tn*26* mutant (2.06 ± 0.22 $\log_2$(fold change)), but not in the *abaI*::Tn*26* mutant (0.51 ± 0.17 $\log_2$(fold change)) (**Figure 4.12**). These results are consistent with the data obtained from the RNA-seq analysis, showing a similar expression pattern for both genes with small $\log_2$(fold change) differences.

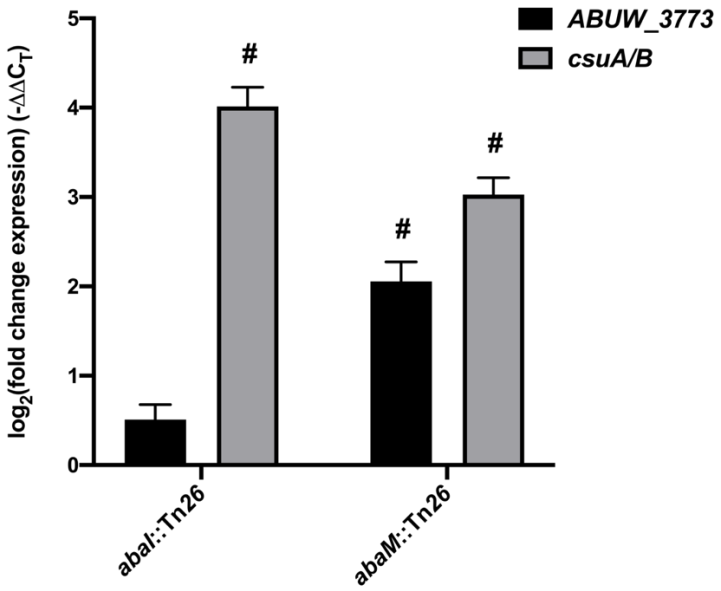


Figure 4.12: Quantitative real-time PCR. Relative increase of expression of *ABUW_3773* and *csuA/B* in *abaI*::Tn*26* and *abaM*::Tn*26* compared to the AB5075 wild-type strain. The expression was normalized in relation to an endogenous control gene (*rpoB*). Error bars indicate the standard deviation between 3 independent biological replicates. Hashtags (#) indicate a biologically significant difference ($|\log_2(\text{fold change})| \geq 1$) compared to the wild-type.

4.4. Discussion

In this chapter, the regulation and regulon of AbaM and QS in *A. baumannii* has been further characterized employing promoter-*lux* fusions and RNA-seq analysis. Comparison with other transcriptomic and regulation analysis performed in AbaM orthologues in other bacteria revealed that AbaM possesses a similar regulatory pattern in *A. baumannii*, showing a negative regulation of QS and itself, as well as regulating dozens of genes, some of them also coregulated by AbaI. Moreover, both the *abaM* and *abaI* mutants displayed significantly higher expression levels of the genes of the *csu* operon, which encodes the proteins responsible for the assembly of the Csu pilus, a type I pilus strongly involved in attachment to abiotic surfaces in *A. baumannii*.

In order to study the regulation of *abaM* and *abaI* expression, promoter fusions with the *lux* operon were analysed (as described in Materials and Methods, see 2.3.1.2). The use of promoter fusions using the *luxCDABE* operon from *Photorhabdus luminiscens* as a reporter of expression is widely used for the study of different bacterial promoters, including promoters of QS genes (Winson et al., 1998). This technique is particularly useful for its efficiency, simplicity and the real-time expression data provided. The fusions can then be delivered through different mechanisms. Among all of them, the mini-Tn*7* transposon was selected for this study for its particular characteristics: it is easy to use and well understood, in contrast with other transposon systems, it is single inserted in a very specific neutral region of the genome (downstream the *glmS* gene); the insertion is stable without antibiotic selection and, finally, it has been successfully tested in *A. baumannii* AB5075 (Jacobs et al., 2014; Choi and Schweizer, 2006; Kumar et al., 2010).

The P*abaM*::*lux* construct was inserted through an hygromycin-marked mini-Tn*7* into *A. baumannii* AB5075 wild-type strain, *abaM*::Tn*26* and *abaI*::Tn*26* to study the effect of QS and the own AbaM in the expression this regulator. In parallel, a promoterless *luxCDABE* operon was inserted via mini-Tn*7* in the same strains as negative controls to demonstrate that any expression observed in the assays was due to the activity of P*abaM* and therefore none of the genes surrounding the insertion site of mini-Tn*7* were affecting the expression of the *lux* operon. Moreover, the *abaM* gene has a predicted *lux*-box 68 bp upstream the start codon (CTGTTAAATATAACAG), 203 bp and 178 bp downstream the -35 and -10 promoter boxes predicted with BPROM (www.softberry.com), This *lux*-box is very similar to the *lux*-box located 67 bp upstream the start codon of the *abaI* gene (CTGTAAATTCTTACAG) (305 bp and 277 bp downstream the predicted *abaI* -35 and -10 boxes, respectively) and the previously identified in the *abaI* locus of *A. nosocomialis* M2 (CTGTAAATTCTTACAG) (Niu et al., 2008). Moreover, these sequences fit in the proposed consensus sequences of *lux* boxes found in other bacteria, such as *V. fischeri* LuxR binding site ([N_3]YR[N_{10}]YRDNB) or *P. aeruginosa* LasR/RhlR binding sites (CT[N_{12}]AG) (where N is any nucleotide, Y is C or T, R is A or G, D is A/G/T and B is C/G/T) (Schuster and Greenberg, 2007; Antunes et al., 2008). The *lux* boxes are specific sequences containing inverted repeats situated upstream QS-regulated genes where the response regulator (in this case, AbaR) binds once they have been activated by AHLs, regulating the expression of the corresponding gene (Papenfort and Bassler, 2016). Finally, a previous study of two *abaM* orthologues (named *rsaM1* and *rsaM2*) in *B. thailandensis* showed that both were positively regulated by their cognate QS systems and negatively auto-regulated (Le Guillouzer et al., 2018). For all these reasons, it was hypothesised that the *abaM* promoter should be responsive to the addition OHC12, the native ligand of AB5075 AbaR.

As expected, the strains containing the *lux* operon under the *abaM* promoter showed much higher luminescence than the promoterless *lux* (mini-Tn*7*::*lux*) control strains. Moreover, the P*abaM*::*lu*x reporter showed significant differences between the wild-type strain, the *abaI* mutant and the *abaM* mutant, while the promoterless *lux* showed similar RLU values between the three strains. Lastly, the addition of OHC12 at 1 μM concentration induced higher *lux* expression only in the P*abaM*::*lux* constructs, while the controls remained with a basal level of luminescence that showed no difference with their uninduced counterparts. Overall, these data is enough to validate the P*abaM*::*lux* reporters and confirm that the *lux* expression in driven by the *abaM* promoter and is not significantly affected by any other promoter or genetic element in the mini-Tn*7* or surrounding its insertion site.

The differential expression of P*abaM*::*lux* in the wild-type strain, *abaM*::Tn*26* and *abaI*::Tn*26* was confirmed by replicating the previous assay without the addition of acetonitrile. Expectedly, P*abaM* showed a lower activity in the *abaI* mutant than in the wild-type, while in the *abaM* mutant it showed a significantly higher expression. Both cases match previous observations in this study: P*abaM* is positively regulated by OHC12 and it was demonstrated by LC-MS/MS that *abaM*::Tn*26* produce significantly higher amounts of OHC12 compared with the wild-type (see 3.3.3), which could explain the higher P*abaM* expression observed in the *abaM* mutant. On the other hand, *abaI*::Tn*26* is uncapable of producing any AHLs, thus negatively affecting P*abaM* expression. Moreover, the data is consistent with the previously mentioned study on *B. thailandensis rsaM1* and *rsaM2* (Le Guillouzer et al., 2018). This regulatory pattern is very similar to the *P. aeruginosa* RsaL transcriptional regulator, which also negatively regulates its own expression and the LasR/LasI QS, affecting both the *lasI* expression and AHL production, as well as

being encoded in a gene situated in a similar location as *abaM*, between the *lasR* and the *lasI* genes (de Kievit et al., 1999). However, while RsaL exerts its effect by directly binding promoters and directing gene expression, AbaM-like regulators do not seem to bind DNA (Michalska et al., 2014). In terms of effect on the physiology of *P. aeruginosa*, RsaL is proposed to exert an homeostatic effect on AHL production, maintaining the levels at a plateau from late logarithmic growth phase onwards. Moreover, it has been characterized as a global regulator that modulates the expression of dozens of genes, including diverse virulence-related genes, and also affecting several phenotypes (biofilm formation, hydrogen cyanide production and pyocyanin biosynthesis, among others) in both a LasR/LasI-dependent and independent way (de Kievit et al., 1999; Rampioni et al., 2006; Kang et al., 2017; Rampioni et al., 2007). The work here presented does not support an homeostatic maintenance role for AbaM, as the *abaM* mutant produced higher levels of AHL from early growth points (see 3.3.4). However, the AHL production characterization performed in Chapter 3 was carried out in static growth conditions, which is known to enhance AHL synthesis in *A. baumannii* (Mayer et al., 2018). Therefore, it is possible that AbaM exerts a different regulation of AHL production under different growth conditions.

The P*abaI*::*lux* construct was inserted in the same way in AB5075 and *abaI*::Tn*26*, but not *abaM*::Tn*26*. This was due to the fact that the constructs were made with all the upstream region including the *abaR* ORF. This means that the P*abaI*::*lux* construct contains the intergenic region between *abaM* and *abaI*, the full *abaM* gene, the intergenic region between *abaR* and *abaM* and the full *abaR* gene. Thus, inserting the P*abaI*::*lux* construct in *abaM*::Tn*26* would mean introducing also a wild-type copy of *abaM*, possibly complementing the mutation and affecting the results obtained from that reporter

strain. Despite the efforts to remove or inactivate the *abaM* gene from the P*abaI*::*lux* construct, all the attempts resulted in a P*abaI*::*lux* reporter unresponsive to the exogenous addition of OHC12 (data not shown), which made the reporter not reliable for further analysis. Removal of either the full *abaM* gene or parts not containing the predicted *abaI* promoter both resulted in the reporter not being responsive to OHC12, which suggests that there could be either some unpredicted/undetected regulatory elements in the *abaM* sequence or some specific spacing DNA required for the correct transcription of *abaI*. A full characterization of the *abaI* promoter would require a more in depth analysis of the *abaM* sequence and the intergenic region between *abaM* and *abaI*, possibly removing or changing specific parts of it to determine what parts are required for the transcription of *abaI*.

Nonetheless, the data obtained from the P*abaI*::*lux* reporter strains constructed in this study showed that *abaI* expression is positively auto-regulated and enhanced by OHC12, thus confirming that *A. baumannii* AB5075 QS possesses the classical positive feedback loop present in the QS systems of most bacterial species (Papenfort and Bassler, 2016). It is important to remark that *abaM* and *abaI* are predicted to be transcribed independently and each possesses transcriptional terminators (data not shown), which strongly suggests that the *luxCDABE* expression from P*abaI*::*lux* reporters is actually mediated by the *abaI* promoter rather than being a readthrough from the upstream *abaM* promoter.

A study published in 2017 using a P*abaI*::*lacZ* fusion in *A. nosocomialis* M2 showed that the AbaR of this strain was very sensitive to changes in the chain length and oxidation state in 3-position (Gerdt et al., 2017). Following the results of that study and knowing that P*abaM* is QS regulated, it was decided to perform a

similar characterization of the selectivity of AB5075 AbaR to AHLs of different acyl chain length and modifications in 3-position. The results of these assays were very similar to those reported in the 2017 study (Gerdt et al., 2017). Consistently with the AbaR of *A. nosocomialis* M2, the AbaR of AB5075 also showed high specificity for 3-hydroxy or 3-oxo AHLs with an acyl chain length close to the native ligand, OHC12. Particularly, 3-hydroxy AHLs of all chain lengths except OHC16 were capable of inducing P*abaM* expression. Not surprisingly, the best inducer was the native ligand, OHC12, closely followed by OHC13. OHC10 and OHC14 induced a significant but much lower P*abaM* expression, around 65% of the OHC12 levels. Of all 3-oxo AHLs, only OC12, OC13 and OC14 were capable of activating AbaR, with OC14 being slightly worse agonist (40%) than OC12 and OC13 (66% and 67%, respectively). Finally, none of the unsubstituted AHLs were able to induce P*abaM* expression. Both *A. nosocomialis* M2 and *A. baumannii* AB5075 AbaR are highly similar (**Supplementary Material Figure S5**), with AB5075 AbaR conserving the 4 residues (A38, N56, Q63, T131) proposed to form hydrogen bonds with the ligand in the *A. nosocomialis* M2 AbaR-ligand binding model (Gerdt et al., 2017), which could explain the similarity between the two studies.

The next step to further characterize the best AbaR agonists was to perform a dose-response curves of OHC12, OC12 and OHC10 to determine their EC_{50}, which allows a better understating of their potency as QS agonists. As expected, the most potent agonist was OHC12, the native ligand of AbaR in AB5075. OHC10, which is produced in much lower amounts (see 3.3.4), was a much weaker agonist, showing a 17-fold increase in the EC_{50} compared with OHC12. Finally, OC12 was also evaluated for different reasons. Firstly, it showed a significant induction of P*abaM*::*lux* in the screening, with levels comparable to OHC10. Secondly, it is a

naturally occurring AHL produced by the *lasI*/*lasR* QS system of *Pseudomonas aeruginosa*, among others. Finally, it has been shown previously that *A. nosocomialis* M2 can coexist with *P. aeruginosa* and use OC12 to promote *abaI* expression and biofilm formation (Bhargava et al., 2012). Interestingly, even though the initial screening showed that at 1 μM both OHC12 and OC12 have a similar activity, the dose-curve response revealed that the EC_{50} of OC12 was significantly lower (about 40%) than the OHC10. Nonetheless, it was still much weaker (10-fold difference) than the native agonist, OHC12.

Next, it was decided to perform an inhibition assay using unsubstituted C10, C12, C13, C14 and C16 by mixing 100 μM of each compound with 500 nM of OHC12 to find the best competitive antagonist. All compounds showed inhibition activity, with C12, C13 and C10 being the best antagonists with an approximately 40% reduction compared to the positive control. A significant but lower amount inhibition was also achieved by C16 (32%) and C14 (23%). This results are similar to the Gerdt *et al*. study, but differ in some points: firstly, C12 and C10 showed similar inhibition activity, while in the 2017 study C10 was a significantly better competitive antagonist than C12. Secondly, C16 showed in this case a significant decrease in P*abaM* activity, while in *A. nosocomialis* M2 barely affected the activity of P*abaI*::*lacZ* compared with the positive control. Lastly, C14 was the weakest inhibitor, while in the *A. nosocomialis* M2 possessed a similar inhibitory activity as C12. Despite the similarity between in the AbaR proteins and the *lux* box sequences between both strains discussed above, it is possible that differences in the type of reporter (*lacZ* vs *lux* operon) and methodology (plus the small differences between AbaR and *lux* boxes) could explain these small discrepancies.

In previous work in our laboratory, a series of OC12-based analogues were synthetized with the original objective of inhibiting *Staphylococcus aureus* quorum sensing (Murray et al., 2014; Jadhav et al., 2011). This library contains compounds carrying out different modifications of OC12 in either the 3-position, the 4-position, the homoserine lactone ring or the acyl chain. Based on the high selectivity of AbaR and the ability of some non-native AHLs to act as competitive inhibitors, it was suggested that some of these compounds might possess interesting activities as a antagonists of AB5075 AbaR. To test the compounds the same inhibition assay was performed using a final concentration of 100 μM of each compound with 500 nM of OHC12 in the *abaI*::Tn*26* P*abaM*::*lux* reporter and results were displayed as a percentage of the difference in activity relative to the positive control (*abaI*::Tn*26* P*abaM*::*lux* + 500 nM OHC12). The unsubstituted C12 was used as a reference.

Interestingly, none of these compounds was a better inhibitor than C12, but three of them showed similar reduction in luminescence: compounds 1, 2 and 13. Compounds 1 (3-oxo-C12-NH_2 or *N*-(3-Oxododecanamide)) and 2 (3-oxo-C12-AT or 2-(*N*-(3-Oxododecanoylamino)) thiazole) were both ring-modified variants of OC12. Compound 13 (6-Ph-3-oxo-C6-HSL or *N*-(3-oxo-6-phenylhexanoyl)-L-homoserine lactone), on the other hand, was a OC12 analogue that contains a phenyl group in the 6-position of the acyl chain substituting the remaining 6-carbon linear chain. Interestingly, the compound 14 (6-Cy-3-oxo-C6-HSL or *N*-(3-oxo-6-cyclohexylhexanoyl)-L-homoserine lactone), which is structurally very similar to compound 13, showed some inhibition, but it was significantly lower. The activity of the other compounds can be divided in two groups: those that did not have any inhibitory or induction activity (compounds 4, 5, 6, 10 and 11), and those that displayed AbaR agonist activity (compounds 7, 8, 9 and 12). The

testing these compounds alone in the absence of OHC12 confirmed the AbaR agonist activity of the second group. Moreover, compound 3, which did not show increased P*abaM*::*lux* activity in the antagonist assay, also displayed an intrinsic AbaR agonist activity when tested alone.

It is important to notice that all the compounds with significant antagonist activity possessed important changes either in the ring (compounds 1 and 2) or in the acyl chain (compounds 13 and 14). Interestingly enough, other compounds with modifications in the ring (compounds 4, 5 and 6), even though they did not act as strong inhibitors, did not possessed AbaR agonist activity either. The exception is compound 3, which did indeed strongly activate the P*abaM*::*lux* reporter. Compound 3 possesses a substitution of the oxygen in the lactone ring for a sulphur atom, which has similar physicochemical properties. This could explain why compound 3 possesses agonist activity while the none other compounds containing ring modifications does. Overall, these results suggest that the structure of the lactone ring might be very important for the correct binding and activation of AbaR.

On the other hand, even though the compound 12 can be classified as an acyl chain-modified derivative of OC12, the modification does not change the structure of the molecule as significantly as the modifications in compounds 13 and 14, in which were the last 6 carbons of the acyl chain were substituted by a phenyl or a cyclohexyl group, respectively. In compound 12, the single covalent bond between carbon 6 and 7 is replaced for a double bound, losing one hydrogen atom in each of these carbons. However, the overall structure of the molecule is very similar to OC12, which could explain why this molecule possesses AbaR agonist activity.

Finally compounds 7, 8 and 9 all had modifications in either the 3- (compounds 7 and 8) or 4-position (compound 9) carbons of the acyl chain. While all three compounds possessed different agonist activity, being compound 7 the strongest AbaR activator with a similar activity to OHC12, the data obtained is not sufficient to exactly evaluate the effect of modifications in carbons 3 and 4 of the acyl chain. These results might suggest that AbaR possesses a high degree of tolerance to these modifications, but more data with other compounds with different 3 and 4-carbon substitutions is required to evaluate the exact selectivity of AbaR for these changes. Moreover, further research screening of other compounds with different changes in the acyl chain and the homoserine lactone ring would also help to find better agonists/antagonists of AbaR and better understand the structural properties required for this activation/inhibition.

Summarizing, the unsubstituted long chain AHLs were confirmed as strong inhibitors of *Acinetobacter* QS. Moreover, the screening of the small library of compounds revealed some very interesting details about the specificity of AbaR and structural properties of AHL-based compounds required to act as inhibitors or activators of AbaR. This data could be utilized in further research to refine the compound screening and find better antagonists that then could be tested as inhibitors of biofilm formation, motility and virulence in *A. baumannii* and other pathogenic species.

RNA-seq is an extremely powerful transcriptomic tool that allows the sequencing of all the RNA in a sample, allowing the identification and quantification of the full transcriptome with high resolution. Further bioinformatic analysis of the raw data using a reference genome allows to identify the genes associated to a given set of reads, giving precise information about the level of expression of any specific gene in the sample (Wang et al., 2009).

Moreover, the data output can also be used to identify novel genes and small RNAs, make promoter predictions and detect single nucleotide polymorphisms (SNPs), among others. Overall, it is a high-throughput technique that requires little sample preparation and provides a huge amount of information about the physiological state of any biological sample, allowing comparative transcriptomic analysis in a vast range of different studies.

In this work, RNA-seq was used in AB5075 to study the transcriptome of the opaque phases of *abaI*::Tn*26* and *abaM*::Tn*26* and the wild-type strain in attachment-like conditions (static growth). Based on the phenotypic data presented in the previous chapter, both opaque *abaI*::Tn*26* and *abaM*::Tn*26* showed higher attachment than the wild-type strain in abiotic surfaces, with the *abaM* mutant showing, by far, the highest level of attachment of the three. Moreover, the static growth during 18 h were the best conditions and time-point for AHLs synthesis in the wild-type strain while maintaining a significant difference with the *abaM* mutant, according to the LC-MS/MS data showed in the previous chapter (see 3.3.4). Due to the low amount of AHLs produced by the wild-type strain, these conditions were very attractive to observe the biggest differences in gene expression between the wild-type and the *abaI* mutant.

Overall, the objectives were to identify the common changes that allowed those mutants to perform better than the wild-type in surface adhesion, to find differences between the *abaM* and the *abaI* mutant that could explain the highest attachment phenotype in the first and, finally, to have a more global vision of the differences and similarities (overlapping) between the regulons of QS and AbaM in AB5075.

Enrichment analysis permits to have a general vision of the differentially regulated genes between two samples in a functional context. In this study, it was observed that both the largest proportion of genes in both the QS and the AbaM regulons in a static growth attachment-related conditions were related with metabolism, and more specifically in ion transport and cellular respiration/energy production-related processes. The synthase mutant, moreover, also showed several differentially expressed genes involved in carbohydrates metabolism. A previous transcriptional analysis in an *A. baumannii* synthase mutant, despite employing a different strain (863) and culturing conditions (shaking in normal LB), also revealed that QS regulated many metabolism-related genes, including the expression of many proteins involved in cellular respiration/energy production and carbon metabolism (Ng et al., 2019). Studies in other bacteria, such as *P. aeruginosa* or *Burkholderia* spp., also reported similar observations (Davenport et al., 2015; Goo et al., 2012).

Apart from metabolism related-genes, a good number of peptidases and protein folding enzymes were also found both up and downregulated in *abaM*::Tn*26*, including several stress-related protein chaperones such as DnaJ, DnaK, GroE and GroES, as well as the RNA chaperone Hfq (Voth and Jakob, 2017; Brown and Elliott, 1996; Guisbert *et al.*, 2007). Many of these chaperones were also found upregulated in desiccation stress conditions in *A. baumannii* clinical strain AbH12O-A2 (Gayoso et al., 2014).

Among the 15 most differentially expressed ($|\log_2(\text{fold-change})| \geq 1.5$) genes in *abaI*::Tn*26*, which were all upregulated, there were some particularly interesting. First of all, the six genes of the *csu* operon (*ABUW_RS07250* to *ABUW_RS07275*) were among the most overexpressed, with an increased expression between 16 to 18-fold compared to the wild-type strain. As previously mentioned,

the *csu* operon encodes the proteins responsible for the synthesis and structure of the Csu pilus, a type I chaperone-usher pilus strongly linked to attachment and biofilm formation (Tomaras et al., 2003; Luo et al., 2015; Rumbo-Feal et al., 2013). Along with the phenotypic characterization of the *abaI* mutant performed in section 3.3.5, that revealed that the opaque synthase mutant produced higher levels of attachment than the opaque wild-type strain, the presence of the *csu* operon among the most overexpressed genes in *abaI*::Tn*26* is consistent with the key role assigned for the Csu pili in attachment and biofilm formation. Moreover, another gene situated upstream the *csu* operon was also found among top upregulated in *abaI*::Tn*26*: an uncharacterized TetR/AcrR-like transcriptional regulator (*ABUW_RS07245*). Based on its location and similar differential expression it would interesting to experimentally characterize the role of this regulator to elucidate if it plays a role in the regulation of the *csu* operon expression.

Interestingly, *abaI* was the most upregulated gene in *abaI*::Tn*26* compared with the wild-type. This could seem contradictory, as previous studies and the promoter fusion data previously shown in this chapter have shown that, as in many QS systems, the *Acinetobacter* spp. QS possesses a positive feedback loop (Gerdt et al., 2017). Therefore, it could be expected that *abaI* would be significantly down-regulated in the absence of OHC12. However, it is important to notice that a recent transcriptomics study in a *abaI* mutant in *A. baumannii* strain 863 (late log-phase cultures grown in shaking conditions) showed that the synthase gene was not among the most downregulated genes compared to the wild-type strain (Ng et al., 2019). Moreover, other studies have correlated an increased expression of *abaI* to attachment and biofilm formation (Mayer et al., 2018; Rumbo-Feal et al., 2013). In consequence, the higher *abaI* expression here observed could be consequence of the increased

attachment in *abaI*::Tn*26* described previously in this study (see 3.3.5), that would have a much higher impact on the expression than the lack of AHLs caused by the *abaI* mutation. None of the other QS-locus genes, *abaR* and *abaM*, were found to be differentially expressed in *abaI*::Tn*26*. This also seems to contradict the previous P*abaM*::*lux* reporter data (see 4.3.1.1), which showed a significative decrease in *abaM* expression. However, the reporters data was calculated by picking the maximum expression point over a 24 h period, while the RNA-seq was performed using a single time-point (18 h). Moreover, the regulation of *abaM* expression remains largely unknown and there could be other mechanisms involved, apart from QS, that could be affecting the expression in different growth conditions. Taking everything into consideration, comparison of these two different assays is complicated and is not surprising that they could result in small discrepancies like the ones presented here.

In the transcriptomics study mentioned above (Ng et al., 2019), *abaR* was not found to be differentially expressed either. However, *abaM* showed a 4-fold increased expression in the *abaI* mutant compared with the wild-type strain (Ng et al., 2019). This is surprising because, as it was demonstrated by the *abaM* promoter fusions assays described above (see 4.3.1.1), *abaM* is positively regulated by QS and OHC12. Once more, the differences between the culture conditions used for the total RNA extraction and the time point of analysis (as well as the strain studied) might be the reason of these discrepancies.

Among the 24 most differentially expressed ($|\log_2(\text{fold-change})| \geq 1.5$) genes in *abaM*::Tn*26*, the full *csu* operon appears again at the top of the list, along with the TetR/AcrR-like transcriptional regulator also shown in the *abaI* vs wild-type comparative above.

Unfortunately, due to the limited amount of information regarding the regulon of AbaM-like proteins and about the Csu and orthologue pili systems in other species, it is difficult to contextualize these results in the current knowledge of these regulators. Nonetheless, as in *abaI*::Tn*26*, *abaM*::Tn*26* showed an increased attachment phenotype compared with the wild-type strain (see 3.3.6), so it is not surprising that attachment and biofilm-related genes such as the *csu* operon are upregulated in the *abaM* mutant.

The QS genes were also among the most differentially expressed in the *abaM* mutant. In this case, however, not only *abaI* was overexpressed compared with the wild-type strain, but also the response regulator, *abaR*, which showed a similar upregulation too. It has been discussed above that the increased expression of the synthase gene could be consequence of the higher attachment on the mutant strain rather than a direct effect of the mutation. Something similar could argued here for the *abaI* gene. The overexpression of *abaR*, however, does not seem to follow the same pattern. Even though a small increase in expression of *abaR* was observed in the *abaI* mutant comparative analysis, it did not seem to be biologically significant (1.5 fold-change) and was insignificant compared with the 6-fold change observed in the *abaM* mutant. Moreover, the AbaM orthologue RsaM has been previously shown to also regulate the expression of the QS response regulator gene in a similar way, as well as the homoserine lactone synthase (Uzelac et al., 2017). However, whether this regulation is QS-dependent or independent (or both) remains to be studied in more detail.

Interestingly, *abaM* was not among the most upregulated genes in the *abaM* mutant. In this case, however, the transcriptomic data and the P*abaM*::*lux* assays were fairly consistent. In the RNA-seq data of *abaM*::Tn*26*, *abaM* showed a 1.9-fold increase in expression compared

with the wild-type strain, while the P*abaM*::*lux* expression in the *abaM* mutant was about 50% higher than the wild-type in the reporter assays.

Another set of genes upregulated (exclusively) in the *abaM* mutant are also very interesting to discuss. These genes (*ABUW_RS18370* to *ABUW_RS18350*) are part of a larger biosynthetic operon (*ABUW_RS18370* - *ABUW_RS18335*) that has been briefly characterized in *A. baumannii* AB5075/ATCC 17978 and *A. nosocomialis* M2. This operon is proposed to be QS-regulated, responsible for the synthesis and secretion of a small molecule named acinetin 505 (Ac-505) and has been involved in pellicle formation, motility in semi-solid surfaces and virulence (Clemmer, Bonomo and Rather, 2011; Giles *et al.*, 2015; Brotherton and Greenberg, 2017 (Poster); Rumbo-Feal *et al.*, 2017). A similar operon studied in *Mehtylobacter tundripaludum* was also shown to be regulated by QS and possessed a very similar structure (Puri et al., 2017), but no further characterization was performed. Similarly, some of the genes of this operon were upregulated in the presence of OHC12 in *A. baumannii* ST-2_clon_2010 (López et al., 2017). Finally, a previously mentioned transcriptomic study that compared gene expression in biofilm vs planktonic cells in *A. baumannii* ATCC 17978 also reported this operon as one of the most upregulated in biofilm cells. A knock-out in one of the genes of the operon, *A1S_0114* (homolog of *ABUW_RS18360*), completely abolished biofilm formation, and further characterization of this gene revealed it played a critical role in adhesion, virulence and regulation of biofilm-related genes (Rumbo-Feal et al., 2013, 2017).

Overall, even though the role of this operon and Ac-505 remains to be fully characterized, the transcriptomic data presented here and previous studies suggest that it could have an important role in

attachment and virulence. Therefore it could have been a key player in the high level of attachment and reduced virulence observed during the phenotypic characterization of the *abaM* mutant. Moreover, the operon seems to be AHL-upregulated (Brotherton and Greenberg, 2017), which is consistent with the *abaM*::Tn*26* AHL-hyperproducing phenotype (see 3.3.4).

A comparison between the regulons ($|\log_2(\text{fold-change})| \geq 1$) of AbaM and AbaI revealed a significant overlap (21 genes), with 22% of the AbaI regulon being also controlled by AbaM, an observation also made in the RsaM of *P. fuscovaginae* with its cognate QS system (PfvI/R) (Uzelac et al., 2017). Among the genes coregulated by AbaI and AbaM there were the *csu* operon, two transcriptional regulators, an aminoglycoside O-phosphotransferase (involved in resistance against aminoglycosides) and diverse hypothetical proteins.

Finally, a validation of the RNA-seq data by a analysing the expression of *csuA/B* and *ABUW_3773* (the first gene of the Ac-505 biosynthetic operon) by qPCR allowed was performed. The qPCR results strongly supported the RNA-seq data, as the expression patterns of both genes in the wild-type strain, the *abaM*::Tn*26* mutant and the *abaI*::Tn*26* were consistent with the differences in expression observed in the RNA-seq data.

4.5. Conclusions and future directions

In this chapter the regulation of *abaM* expression has been characterized, including the role of QS. The specificity of AbaR has been confirmed and some key advances have been done in identifying the key features in the AHLs molecules that affect the activation/inhibition of AbaR. Some of the compounds tested possessed significant inhibitory activity against AbaR. Further research testing the effect of these compounds in different *A. baumannii* phenotypes (such as motility, attachment/biofilm formation and virulence) could provide new insights into the control and treatment of *A. baumannii* infections, as this strategy (QS inhibition) has been used to reduce virulence and/or biofilm formation in other pathogenic bacteria such as *P. aeruginosa* or *S. aureus* (Soukarieh et al., 2018; Rutherford and Bassler, 2012). Some other of these compounds showed AbaR agonist activity, which might help to understand the selectivity of AbaR and the structural properties required for its activation. Moreover, the RNA-seq analysis revealed a partial overlap of AbaM and AbaI regulons, in which the *csu* operon was present, being upregulated by both mutants. The biofilm-related Ac-505 biosynthetic operon was also upregulated in *abaM*::Tn*26*. Along with the increased attachment showed by opaque *abaM*::Tn*26* and *abaI*::Tn*26* (see 3.3.6) and the limited knowledge regarding attachment and biofilm formation in *A. baumannii*, it would be interesting to further characterize these two operons to elucidate their role in biofilm, their connection with AbaM/QS, what is their contribution to environmental persistence and their overall role in the biology of *A. baumannii*.

4.5.1. Summary of most important findings

The promoter-*lux* fusions showed that:

- *abaM* expression is positively regulated by AHLs/QS.
- *abaM* expression is negatively auto-regulated.
- OHC12 is the most potent AbaR agonist among all AHLs tested.
- AbaR is selectively activated by 3-hydroxy and 3-oxo AHLs of acyl chain length between 10 and 14 carbons.
- Unsubstituted long chain AHLs cannot activate AbaR and are strong competitive inhibitors of QS.
- Modifications in the AHL 3-position and 4-position, as well as small changes in the acyl chain or the amide might have a smaller effect on AbaR activation than changes in the homoserine lactone ring or major changes in the acyl chain, which can result in compounds that possess a competitive antagonist activity on AbaR.

The RNA-seq data, validated by qPCR, showed that, in static growth conditions:

- AbaM and QS regulons partially overlapped.
- AbaM regulates the expression of many genes in a QS-independent way.
- AbaM and AbaI regulate the expression of the *csu* operon.
- AbaM regulates the expression of a biosynthetic operon that produces Ac-505, a putative compound involved in attachment and motility.

5. Role of Csu pili in surface recognition and attachment

5.1. Introduction

Following the RNA-seq data obtained in the previous chapter, it was decided to further analyse the role of Csu pili in attachment and biofilm formation, as previous publications suggested they play a very important role in both processes. Specifically, this Chapter is focused on the ability of Csu pili to discriminate between different surfaces to assess whether they are responsible for the 'decision' of the bacteria to attach or not to an specific surface. Bacteria can attach to virtually any abiotic surface, but the strength and robustness of the biofilms formed in each vary from surface to surface . Therefore, defining the properties of an 'ideal' attachment or anti-attachment surface is complicated, mostly due to the diverse factors involved in the process of attachment, many of them still poorly understood. Consequently, understanding the contribution of the Csu pili to *Acinetobacter* attachment would have a major scientific and medical relevance, as it could help to design materials and strategies that inhibit Csu pili-mediated attachment and prevent the colonization of medical devices and hospital equipment.

5.1.1. Csu pili in *A. baumannii* and their role in attachment

As described in the section 1.4.1, Csu pili have been identified by several studies as being required for attachment and biofilm formation in abiotic surfaces and remains as one of the best-known *A. baumannii* factors involved (Rumbo-Feal et al., 2013; Tomaras et al., 2003).

The Csu pilus is synthetized by the products of the *csuA/BABCDE* operon via the archaic chaperone-usher (CU) pathway. The *csuA/B*, *csuA*, *csuB* and *csuE* encode for the structural elements of the pilus,

while *csuD* and *csuC* encode for the chaperone and the usher protein that mediate the secretion and assembly of the pilus structure, respectively (Pakharukova et al., 2015). The archaic clade of CU pilus is the most common and widely spread among all the CU superfamily, with orthologues in α-, β-, γ-, δ-proteobacteria, Cyanobacteria and *Deinococcus-Thermus* (Nuccio and Bäumler, 2007). However, unlike the classical CU pili, the mechanisms involved in the synthesis and assembly of the archaic CU pilus are poorly understood. Structural characterization of the *A. baumannii* Csu pilus revealed that CsuA/B is the major subunit of the Csu pilus and it is capable of self-polymerization by donor strand polymerization in the presence of the CsuC chaperone. The crystal structure of the CsuA/B pilin revealed that it possesses an incomplete immunoglobulin-like fold missing a β-sheet that leaves an hydrophobic region where the N-terminal of another CsuA/B subunit is inserted during the polymerization process. The CsuE, on the other hand, is the adhesive tip of the pilus and is incapable of self-polymerization (Pakharukova et al., 2015). Further structural and phenotypical characterization showed that the CsuE adhesive tip possesses three highly flexible hydrophobic finger-like loops that are crucial for biofilm formation and proposed to mediate the attachment to abiotic surfaces *via* a flexible novel binding mechanism (**Figure 5.1B**) (Pakharukova et al., 2018). The hydrophobic nature of the CsuE finger-like loops is proposed as the reason many *A. baumannii* strains attach better to hydrophobic surfaces such as polystyrene or polypropylene than hydrophilic surfaces, including glass or cellophane, something already observed in other studies (Tomaras et al., 2003).

The earliest report of the role of Csu pili in *A. baumannii* attachment and biofilm formation is a transposon mutagenesis study where the disruption of *csuC* and *csuE* resulted in a total loss of pilus formation and attachment to abiotic surfaces (Tomaras et al., 2003). Subsequent

research confirmed the important role of these pili in biofilm formation. Several genes of the the *csu* operon were overexpressed in biofilm cells compared to non-attached cells in *A. baumannii* ATCC 17978 (Rumbo-Feal et al., 2013). Similarly, a proteomics study found that the CsuA/B pilin was the most abundant protein in the pellicle matrix in three different clinical isolates, with CsuA and CsuB also being highly produced (Nait Chabane et al., 2014). Moreover, AHL-mediated enhancement of Csu pilus synthesis has also been reported to result in increased biofilm formation in *A. baumannii* ATCC 19606 (Luo et al., 2015). Another interesting study used subinhibitory concentrations of trimethoprim and sulfamethoxazole in *A. baumannii* ATCC 17978 to repress *csu* expression, which abolished biofilm formation (Moon et al., 2017). Blocking the tip adhesin CsuE or the CsuA/B pilin using anti-CsuE or anti-CsuA/B (respectively) antibodies also resulted in loss of biofilm formation, with the anti-CsuE antibody being much more effective than the anti-CsuA/B (Pakharukova et al., 2018). Lastly, the transcriptomic analysis presented in the previous chapter also showed that the entire *csu* operon was overexpressed in the high-attachment opaque *abaI*::Tn*26* and *abaM*::Tn*26* mutants (see 3.3.5). Interestingly, it seems that these pili are not necessary for attachment to biotic surfaces, as a study using human epithelial cells revealed (de Breij et al., 2009). Overall, the data suggests that Csu pili may play a very important role in the substrate recognition, initial attachment and biofilm formation on abiotic surfaces, even though many aspects such the exact specificity of CsuE finger-like loops for different substrates has not been fully characterized.

The regulation of *csu* expression is still largely unknown. However, some systems and factors have been recently identified. The BfmRS two-component system was found to regulate the expression of the *csu* operon and biofilm formation (Tomaras et al., 2008; Liou et al.,

2014). Another TCS, the GacSA, was also shown to modulate the expression of some *csu* genes (*csuB* and *csuC*), as well as moderately regulate biofilm formation (Cerqueira et al., 2014). Lastly, the disruption of *A1S_0114* (*ABUW_RS18360*), a gene belonging to the Ac-505 biosynthetic operon which encodes an acyl carrier protein, increased expression of the *csuA/B* pilin-encoding gene (Rumbo-Feal et al., 2017).

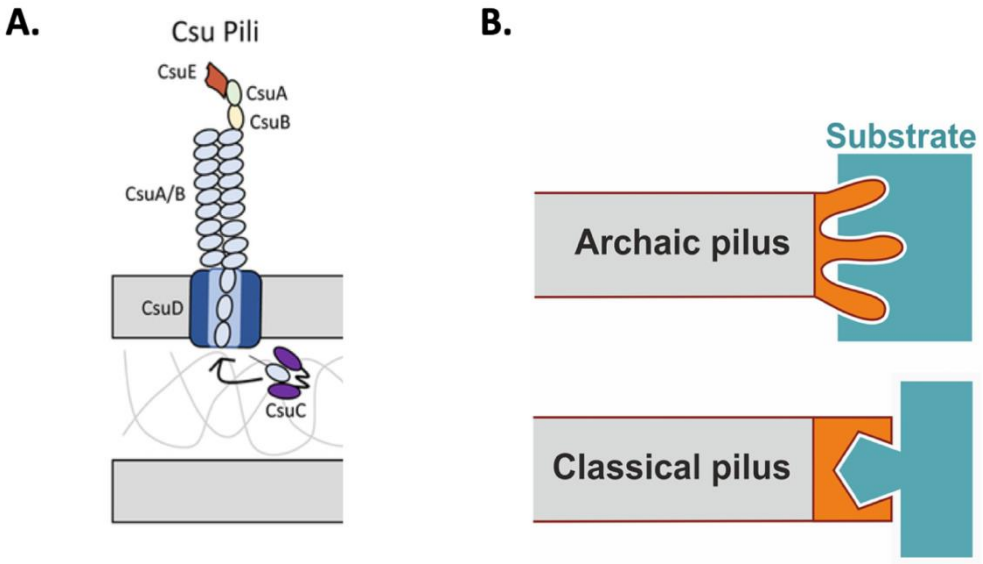


Figure 5.1: *A. baumannii* Csu type I pili. (A) Proposed assembly model of the Csu pilus. The CsuA/B, CsuA, CsuB and CsuE form the structural body of the pilus, with CsuA/B as the major pilin, CsuA and CsuB as minor pilins and CsuE as the adhesive tip protein. The pilins are secreted through the CsuD usher protein, which is embedded to the outer membrane forming a channel that also catalyses the polymerization of the pilus subunits. Lastly, there is the CsuC chaperone, which is located in the periplasm and binds the subunits to stabilize them, ensure the correct folding and mediate in the polymerization process. Adapted from Harding *et al*, 2018. **(B)** "Conceptual difference in substrate recognition between archaic (Csu) and classical pili". The three flexible hydrophobic CsuE 'fingers' would adapt to the surface cavities, permitting a less specific attachment to a variety of substrates. In comparison, the 'classical' pilus displays a more typical substrate-receptor recognition, where the pilus relies in a cavity complementary to a specific surface structure. Extracted from Pakharukova *et al*., 2018.

5.1.2. Strategies for preventing bacterial biofilms

A high percentage of hospital infections are associated with biofilms (see 1.4), which in turn result in increased economic costs and worse prognosis. Biofilm infections associated with implanted medical devices (such as catheters, prosthetics, artificial heart valves, pacemakers or breast implants, among others) are especially relevant, as they represent the 50-70% of all nosocomial infections and usually lead to many problems such as chronic infections and device failures, significantly increasing mortality and morbidity rates of the patients. Moreover, the treatment of these infections is extremely complicated, usually requiring the replacement of the device and an aggressive antibiotic treatment, which are not always successful owing to the risk of re-infection and antibiotic resistance (Khatoon et al., 2018).

Due to the importance of device-associated biofilm infections and the difficulty to treat them once the biofilm has been established, a great amount of effort has been put into researching novel methods for the treatment of these infections. While some strategies have focused on the developing of new alternative treatments to synergically act with antibiotics and enhance their activity in mature biofilms (bacteriophages, QS inhibitors, proteases, etc), there is an increasing interest in developing materials resistant to bacterial attachment, preventing the formation biofilms (Römling and Balsalobre, 2012). This strategy has been used for some time, usually involving coating the devices with antibiotics or other antimicrobials to kill the colonizing bacteria. Despite the efficacy of this approach, the increasing concern regarding the development of resistant strains and the possible tissue toxicity of some of these compounds opens the door to find alternative anti-attachment approaches (Cyphert and Recum, 2017).

One of these alternative approaches is the development of novel materials intrinsically resistant to bacterial attachment. This approach presents several advantages over traditional antimicrobial-based coatings: as only prevent the attachment without killing the bacteria, the risk of developing resistance to the material is much lower, they do not contribute to the emergence of antibiotic-resistant strains and they do not require continuous release of potentially cytotoxic compounds to the patient's body (Cyphert and Recum, 2017). Several studies have investigated a wide variety of materials with anti-attachment properties, including trimethylsilane plasma nanocoatings, zwitterionic polymers, polymer brush coatings or submicron surface textures, among many others (Chen et al., 2013).

5.1.2.1. High-throughput screening of polymers resistant to attachment

One of the main limitations for the discovery of novel anti-attachment materials is the poor comprehension of all the chemical, physical and biological factors involved in the bacteria-surface interactions, limiting the rational development of new materials. In order to overcome this limitation, our group developed a high-throughput screening method based on the incubation of hundreds of polymers printed in a microscope slide on a microarray format with bacterial cultures to identify novel materials resistant to attachment (Hook et al., 2012b). Using this strategy, a library of over 118 acrylates and methacrylates was tested as homo and copolymers with *P. aeruginosa*, *S. aureus* and uropathogenic *E. coli*, which led to the discovery of several 'hit' polymers that efficiently prevented bacterial attachment. Polymer-coated catheters significantly reduced the bacterial coverage *in vitro* in coated silicone catheters, in most cases outcompeting the commercially available silver-hydrogel (BactiGuard)-coated latex catheter (Bardex) by up to 30-fold.

The polymer that gave the best result, ethylene glycol dicyclopentenyl ether acrylate (EGDPEA), was also tested in *in vivo* in a murine catheter implant model as a co-polymer with di(ethylene glycol) methyl ether methacrylate (DEGMA) (which increases the flexibility of the material without affecting its anti-attachment properties (Adlington et al., 2016)), reducing the number of bacteria in the coated catheter, the surrounding tissue and in other organs when compared with the uncoated silicone catheter. Moreover, a high throughput surface characterization of all polymers suggested that the presence polar hydrophilic ester groups and hydrophobic pendant cyclic hydrocarbon groups, forming weakly amphiphilic structures, was associated with higher resistance to bacterial attachment (Hook et al., 2012a). Further research applying the same methodology in a larger library of (meth)acrylates showed results consistent with this hypothesis, identifying new hit monomers resistant to bacterial attachment with similar amphiphilic characteristics and confirming the anti-attachment properties of four of the previously identified monomers, including EGDPEA (Hook et al., 2013). A subset of the library of (meth)acrylates used in the above mentioned studies was used in a surface chemistry and bacterial attachment characterization to generate a model that predicts *P. aeruginosa* attachment to (meth)acrylates with hydrocarbon pendant groups, which was associated with the hydrophobicity and molecular flexibility. Polymers with rigid amphiphilic moieties, on the other hand, where associated with higher resistance to attachment (Sanni et al., 2015)

Overall, these studies not only identified novel materials with anti-attachment/biofilm properties, but also demonstrated that polymer microarrays are a powerful methodology to screen hundreds of materials simultaneously with bacterial cultures, greatly accelerating the discovery of polymers with new and interesting

properties. Moreover, the high-throughput screening of materials provides large amounts of data that can be systematically analysed to find structure-performance relationships (Sanni et al., 2015). None of these materials have ever been tested with *A. baumannii*. Due to the ability of the hit polymers to prevent attachment of both Gram-negative and Gram-positive bacteria, suggesting either non-specific or well-conserved mechanism of action, it would be interesting to test whether these materials also prevent biofilm formation by *A. baumanii* and, more interestingly, whether Csu pili plays a role in that process.

5.2. Aims of the chapter

The aims of the work described in this chapter were to further characterize the importance of Csu pili in the attachment of *A. baumannii* to abiotic surfaces with special interest in the structural basis of surface selection. Specifically, this chapter aims to:

- Confirm differential expression of the *csu* operon in the wild-type strain and *abaM*::Tn*26*.
- Analyse the role of the Csu pili in AB5075 attachment.
- Validate a recombinant *E. coli* BL21 pBAD_*csu* that expresses *A. baumannii* ATCC 19606 Csu pili.
- Test the ability of the Csu pilus to discriminate between hydrophobic (polystyrene) and hydrophilic (borosilicate glass) surfaces.
- Find materials Csu pili attach preferably through a microarray attachment assay and generate a structure-function relationship.
- Test the attachment of AB5075 to EGDPEA (anti-attachment) and NGPDA (pro-attachment) polymers previously described in our laboratory.

5.3. Results

5.3.1. Analysis of *lux*-based *csu* operon reporters

To confirm the observations made in the RNA-seq, a P*csu*::*lux* fusion was constructed by cloning the 600 bp region upstream the *csuA/B* gene (and including the first four codons of the *csuA/B* gene) followed by the promoterless *luxCDABE* operon into the *Acinetobacter*-compatible plasmid pMQ557M. The plasmid containing the promoter fusion was introduced into the opaque phases of the wild-type strain and *abaM*::Tn*26* by electroporation. The construct showed a significantly higher (2-fold) *csu* expression in *abaM*::Tn*26* than in the isogenic parental strain (**Figure 5.2**). The addition of OHC12 did not affect the P*csu* activity in the wild-type strain.

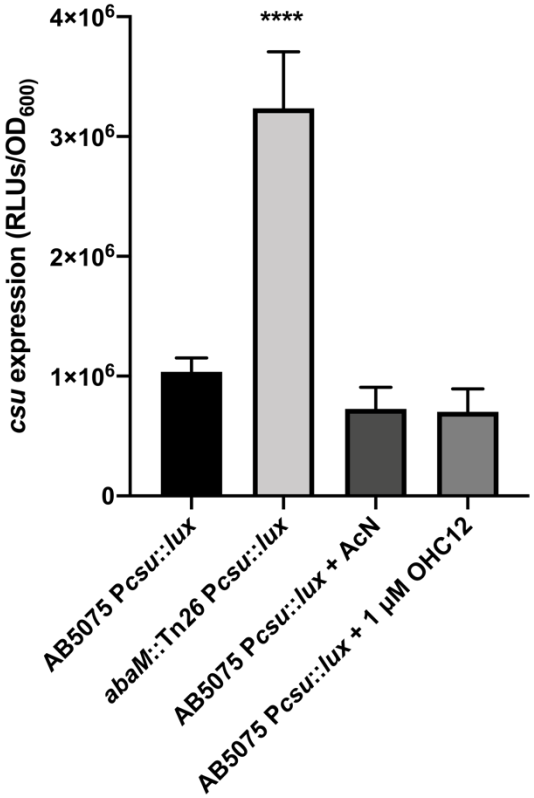


Figure 5.2: Analysis of *csu* expression in different backgrounds. Strains were grown to an OD_{600} = 0.5 and diluted 1:10 in 96-well plates. Plates were incubated at 37°C for 24 h. The RLUs and OD_{600} were measured every 30 min and the maximum normalized ($RLUs/OD_{600}$) value was used for the statistical analysis. AcN = Acetonitrile. Error bars indicate standard deviation between three biological replicates. Asterisks indicate: ****, $p \leq 0.0001$.

5.3.2. Role of the Csu pili in AB5075 attachment to polypropylene

In order to evaluate the role of the Csu pili in AB5075 attachment and confirm it plays an important role in this process (as suggested by the RNA-seq data and previous studies), a simple liquid-air interphase quantitative attachment assay in polypropylene was performed using the opaque phases of transposon mutants of the major pilin (*csuA/B*) the adhesive tip (*csuE*) encoding genes. Both mutants showed a significantly reduced attachment when compared to the wild-type strain (**Figure 5.3**). The *csuE*::Tn*26* mutant was the one with higher reduction, showing an average 60% decrease in biomass compared to the wild-type, while the *csuA/B*::Tn*26* mutant displayed 40% less attachment that the wild-type strain.

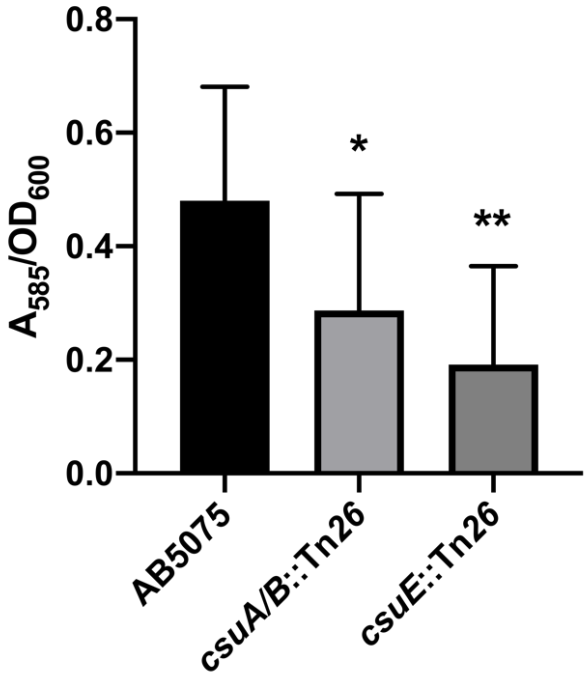


Figure 5.3: Attachment to polypropylene of *csuA/B*::Tn*26* and *csuE*::Tn*26*. Differences in attachment between AB5075, *csuA/B*::Tn*26* and *csuE*::Tn*26* opaque phases. Strains grown in LS-LB to an OD_{600} = 0.3 were incubated at 37°C for 24 h in 1.5 ml polypropylene tubes. Attached cells were stained with 0.25% CV and resuspended in 1 ml of 100% ethanol for quantification by absorbance at 585 nm. Error bars indicate standard deviation between three biological replicates. Asterisks indicate: *, $p \leq 0.05$; **, $p \leq 0.01$.

5.3.3. Construction and validation of recombinant *E. coli* BL21 pBAD_*csu*

The first step for the validation of the recombinant *E. coli* BL21 pBAD_*csu* was to confirm that BL21 significantly attached to abiotic surfaces when the *csu* operon was being expressed through induction of the P_{BAD} promoter with L-(+)-arabinose. In other words, it was necessary to discard any effect of the pBAD plasmid or the L-(+)-arabinose in BL21 attachment to ensure the differences in attachment observed were caused exclusively by Csu pili expression. With that aim in mind, a simple attachment assay was performed using BL21 carrying either the empty pBAD or the pBAD_*csu* vector, both fluorescence-tagged with pSW002_*E2-Crimson*. Results showed that *E. coli* BL21 attached to the polystyrene bottom of the wells only when the *csu* operon expression was induced, discarding any effect by the plasmid or the arabinose (**Figure 5.4A**). Finally, Csu pili attached significantly better to polystyrene than borosilicate glass bottom plates when samples were grown and washed in the same conditions (**Figure 5.4B**).

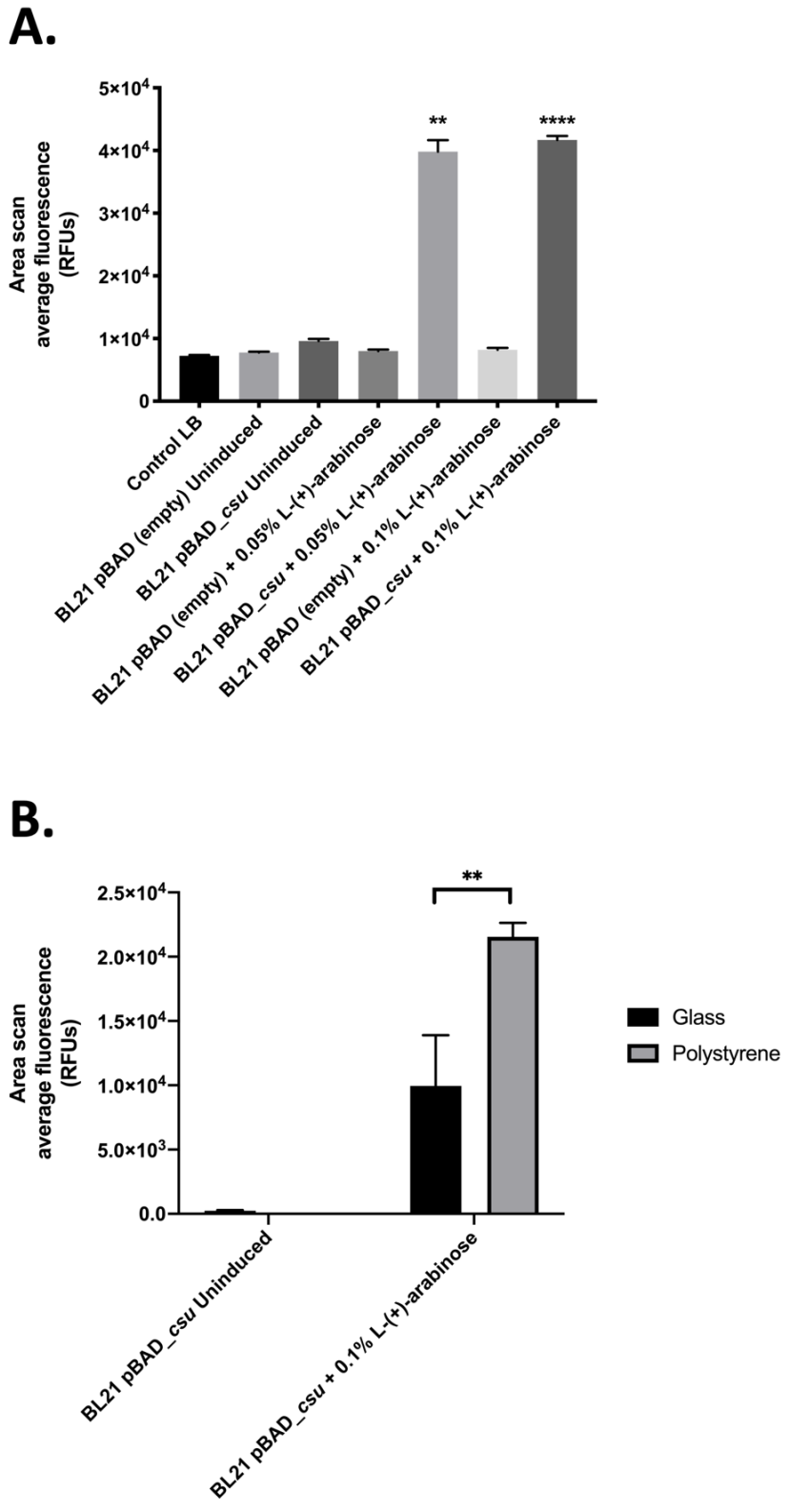


Figure 5.4: Effect of recombinant *A. baumannii* ATCC 19606 Csu pili on attachment. (A) Validation of BL21 pBAD_*csu* pSW002_*E2-Crimson*. **(B)** Assay to test differential attachment of the Csu pili to glass and polystyrene. Strains grown to an OD_{600} = 0.1 were incubated in a 24-well plate at 37°C and 60 rpm for 2.5 h. Wells were washed and the average fluorescence bottom of each well was measured and used for analysis. Error bars indicate standard deviation between three biological replicates. Asterisks indicate: **, $p \leq 0.01$; ****, $p \leq 0.0001$.

5.3.4. Screening of materials

Once the recombinant BL21 pBAD_*csu* pSW002_*E2-Crimson* was validated, it was decided to screen a library of 283 different acrylates and methacrylates printed as 300-μm diameter spots in a (pHEMA)-coated glass microscope slide to generate a structure-function relationship for the Csu pilus by detecting those materials that Csu pili expression-induced recombinant strain would attach significantly more than the uninduced strain (**Figure 5.5**).

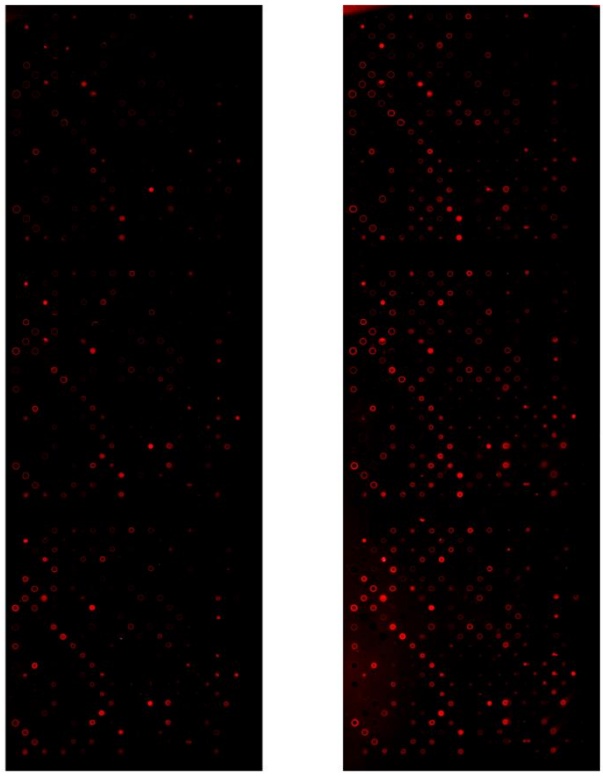


Figure 5.5: Fluorescence scan of the polymer microarrays slides incubated with the uninduced strain (left) and the induced strain (right). *E.coli* BL21 pBAD_*csu* pSW_*E2-Crimson* cultures at OD_{600} = 0.1 were incubated with the polymer microarray slides for 3 h at 37°C and 60 rpm with or without arabinose induction. Slides were washed to remove non-attached bacteria and air-dried. Images of the fluorescence were taken using a GenePix 4000B scanner. Images are representative of two independent assays.

Overall, *E. coli* BL21 expressing Csu pili showed attachment to 178 different polymers (fluorescence value for the polymer spot was higher than the fluorescence of the equivalent spot in the uninduced sample), while it did not attach to 103 polymers (fluorescence value for the polymer spot was equal or lower than the uninduced sample) (**Figure 5.6**). A further analysis of the 20 polymers that showed the highest amount of attachment (**Figure 5.7**) did not reveal any

particular chemical property in common among the different materials. Interestingly, Csu pili-expressing BL21 showed a significant attachment (around the average) on EGDPEA, the 'hit' material that prevented most efficiently the attachment in *P. aeruginosa*, *E.coli* and *S. aureus* in previous studies (Hook et al., 2013). Contrarily, in NGPDA, which is routinely used as a positive control 'pro-attachment' polymer in our laboratory, Csu pili-expressing BL21 did not show attachment compared with the uninduced strain (**Figure 5.7**). Finally, Csu pili attachment to meth(acrylates) with hydrocarbon pendant groups was not correlated with the α value ($\alpha = 0.44n\text{RoTB} - c\log P$, where nRoTB is the number of rotatable bonds of each monomer and $c\log P$ is the logarithm of the octanol/water partition coefficient), a parameter developed by our group (Sanni et al., 2015) that relates hydrophobicity and flexibility of (meth)acrylates with hydrocarbon pendant groups, as can be observed in **Figure 5.8**. The nomenclature and chemical structures of the 20 monomers with more attachment, plus NGPDA and EGDPEA is detailed in **Table 5.1**.

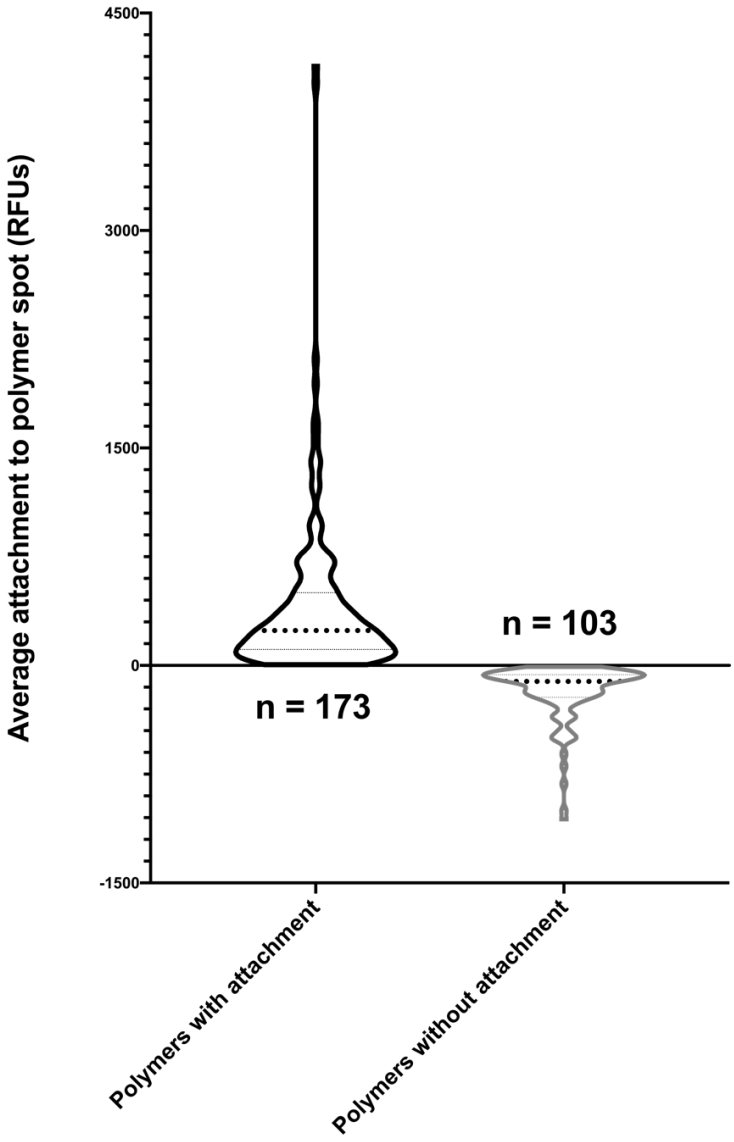


Figure 5.6: Violin plot representing the distribution of polymers with *E. coli* BL21 pBAD_*csu* attachment (left) and no attachment (right) according to the normalized RFUs. *E.coli* BL21 pBAD_*csu* pSW_*E2-Crimson* cultures at OD_{600} = 0.1 were incubated with the polymer microarray slides for 3 h at 37°C and 60 rpm with or without arabinose induction. Slides were washed to remove non-attached bacteria and air-dried. Images of the fluorescence were taken using a GenePix 4000B scanner and RFUs values were obtained with GenePix Pro 6 Microarray Acquisition and Analysis Software. Data from uninduced samples was subtracted from the corresponding spot of the polymers incubated with the induced *E.coli* BL21 pBAD_*csu* to remove background fluorescence and unspecific attachment of BL21. Values use for the plotting are the average of two independent assays. The width of the plot represents the number of polymers within a given range of attachment (expressed in RFUs). The dotted line in each plot represents the mean attachment of all polymers with or without attachment, respectively.

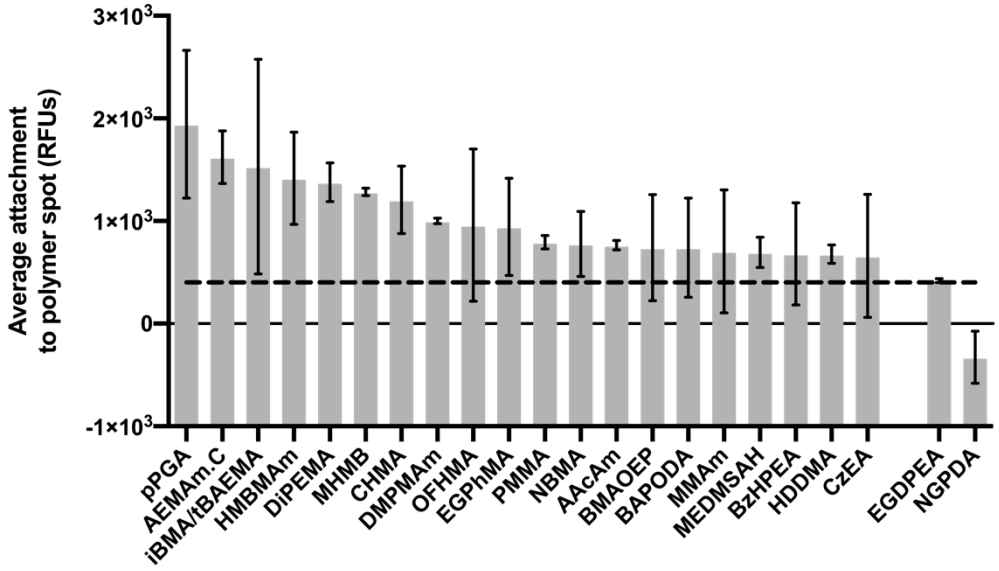


Figure 5.7: Csu attachment to monomers with the highest attachment, plus attachment to EGDPEA and NGPDA. *E.coli* BL21 pBAD_*csu* pSW_*E2-Crimson* cultures at OD_{600} = 0.1 were incubated with the polymer microarray slides for 3 h at 37°C and 60 rpm with or without arabinose induction. Slides were washed to remove non-attached and air-dried. Images of the fluorescence were taken using a GenePix 4000B scanner and fluorescence values for each spot was obtained using GenePrix Pro 6 Acquisition and Analysis Software. The average fluorescence of the three technical replicates for each material were used for the statistical analysis and the values from the uninduced sample were subtracted from the induced sample to remove background noise. Error bars represent the standard deviation of two independent assays, each with three technical replicates. Black dashed line represents the average attachment (402 RFUs) to the 178 (meth)acrylates with *E.coli* BL21 pBAD_*csu* pSW_*E2-Crimson* attachment.

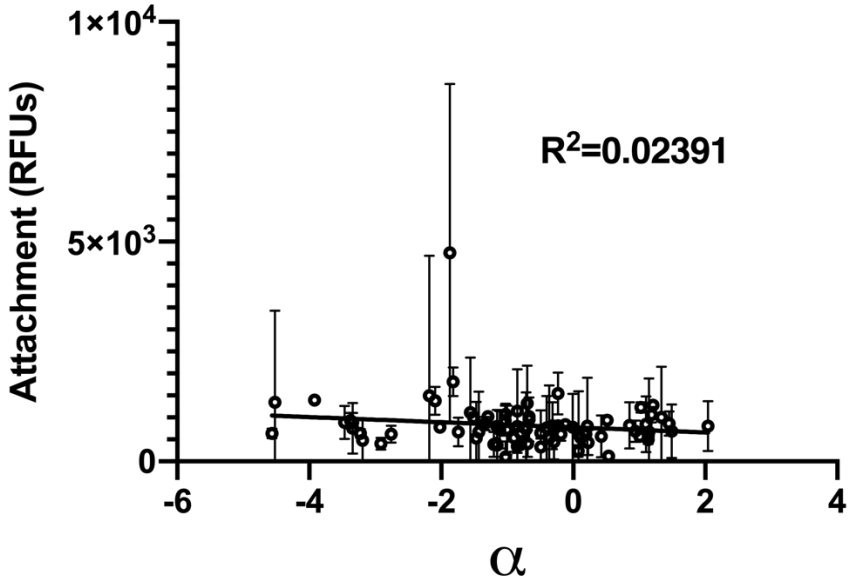
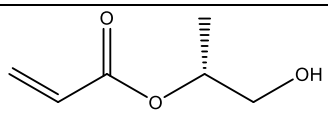
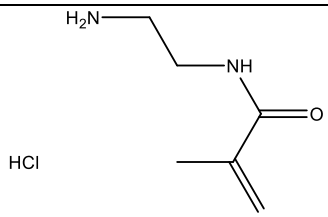
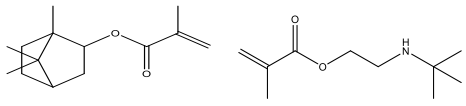
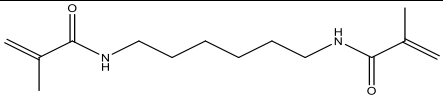
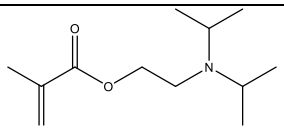
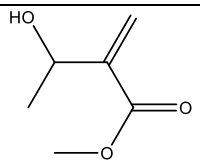
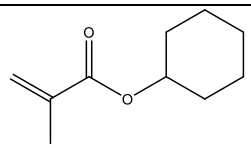
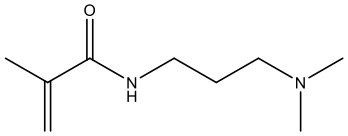
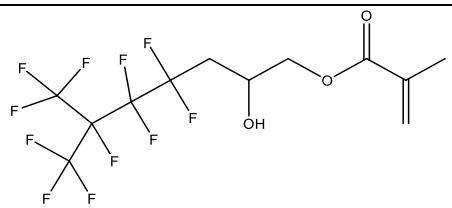
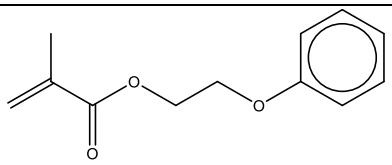
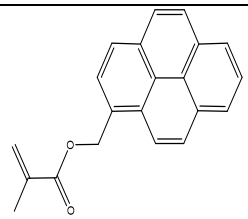
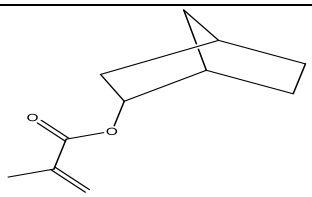
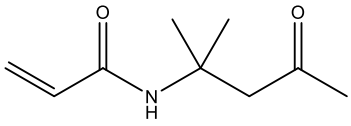
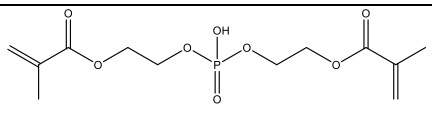
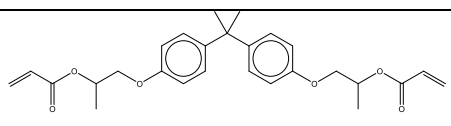
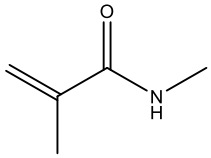
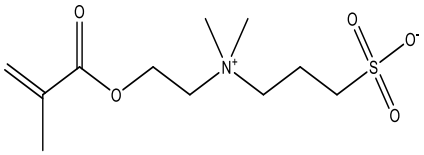
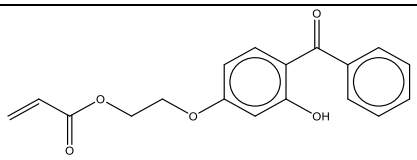
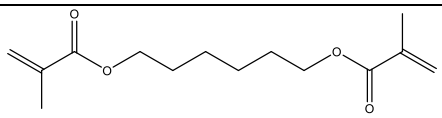
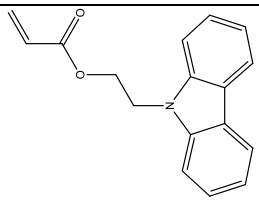
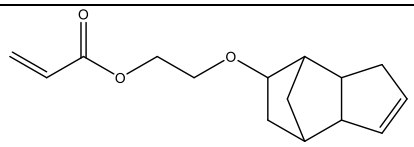
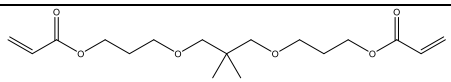


Figure 5.8: Correlation between bacterial attachment and flexibility and hydrophobicity. The attachment of *E. coli* BL21 pBAD_*csu* (RFUs) to each polymer is plotted against the α parameter of the corresponding polymer. The linear regression shows no correlation (R^2=0.02391) between attachment and the α parameter. Error bars represent standard deviation from two independent assays, each with three technical replicates.

Table 5.1: Nomenclature and chemical structures for the 20 monomers with the highest attachment, plus NGPDA and EGDPEA, from the microarray screening assay.

Acronym	Full name	Chemical structure
pPGA	Poly(propylene glycol) acrylate	
AEMAm.C	N-(2-aminoethyl) methacrylamide hydrochloride	
iBMA/ tBAEMA	Isobornyl methacrylate / Tert-butylaminoethyl methacrylate	
HMBMAm	N,N'-Hexamethyl enebis(methacrylamide)	
DiPEMA	2-Diisopropylaminoethyl methacrylate	

MHMB	Methyl 3-hydroxy-2-methylenebutyrate	
CHMA	Cyclohexyl methacrylate	
DMPMAm	N-[3-(Dimethylamino) propyl]methacrylamide	
OFHMA	Octafluoro-2-hydroxy-6-(trifluoromethyl)heptyl methacrylate	
EGPhMA	Ethylene glycol phenyl ether methacrylate	
PMMA	1-Pyrenylmethyl methacrylate	
NBMA	Norbornyl methacrylate	
AAcAm	Diacetone acrylamide	
BMAOEP	Bis[2-(methacryloyloxy) ethyl] phosphate	
BAPODA	Bisphenol A propoxylate diacrylate	

MMAm	N-Methylmethacrylamide	
MEDMSAH	[2-(Methacryloyloxy) ethyl]dimethyl-(3-sulfopropyl) ammonium hydroxide	
BzHPEA	Benzoyl-3-hydroxy-phenoxy)ethyl acrylate	
HDDMA	1,6-Hexanediol dimethacrylate,	
CzEA	Carbazol-9-yl ethyl acrylate	
EGDPEA	Ethylene glycol dicyclopentenyl ether acrylate	
NGPDA	Neopentyl glycol propoxylate diacrylate	

5.3.5. Attachment of *A. baumannii* to EGDPEA and NGPDA

To confirm whether Csu pili were responsible of the surface selectivity in the attachment process of *A. baumannii*, a scale-up attachment/biofilm assay was performed using microscope slides containing three 6-10 mm spots of either NGPDA or EGDPEA and incubated with opaque *A. baumannii* AB5075 opaque.

Interestingly, the results were contrary to the data obtained in the microarray attachment assay, with AB5075 showing a high degree of attachment to NGPDA and very low attachment to EGDPEA (**Figure 5.9** and **5.10**).

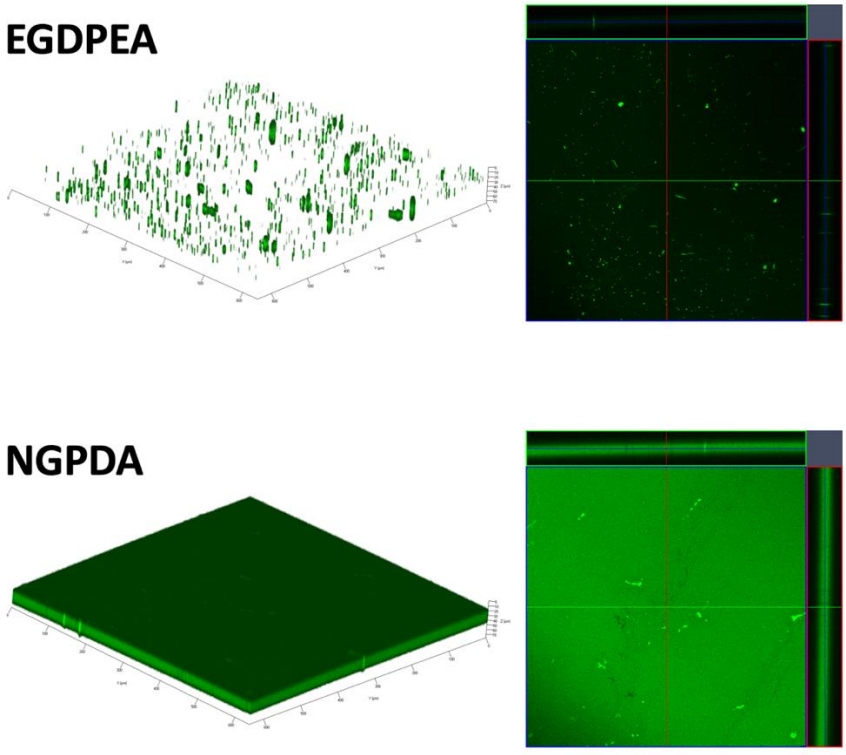


Figure 5.9: Qualitative evaluation of opaque *A. baumannii* AB5075 attachment to EGDPEA (up) and NGPDA (down). An OD_{600} = 0.01 15 ml culture of opaque AB5075 was incubated with a pHEMA-coated glass microscopy slide containing three 5 mm spots of either NGPDA or EGDPEA at 37°C for 2 h at 60 rpm and then for 18 h statically. Cells were stained with SYTO9 and images were obtained with a LSM 700 confocal microscope using ZEN 2009 software. The images are representative of the attachment observed in the polymer spots. Assay were performed in duplicate.

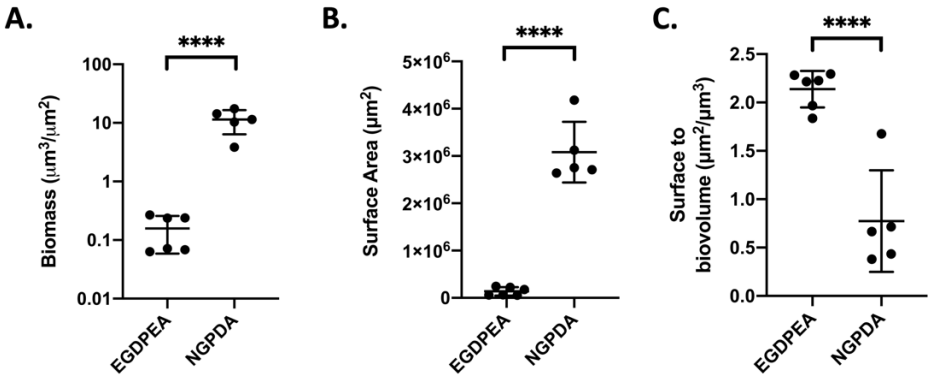


Figure 5.10: Biomass, surface area and surface to biovolume data from opaque AB5075 wild-type strain attachment to EGDPEA and NGPDA. An OD_{600} = 0.01 15 ml culture of opaque AB5075 was incubated with a pHEMA-coated glass microscopy slide containing 3 spots of either NGPDA or EGDPEA at 37°C for 2 h at 60 rpm and then for 18 h statically. Cells were stained with SYTO9 and images were obtained with a LSM 700 confocal microscope using ZEN 2009 software. Quantification of biomass, surface area and surface to biovolume was performed using the Comstat2 plugin from ImageJ software using at least 5 images from two independent assays. Error bars indicate the standard deviation of the measurements obtained from the 5 images. Asterisks indicate: ****, $p \leq 0.0001$.

5.4. Discussion

Following the RNA-seq data, it was hypothesised that the increased expression of the genes of the *csu* operon could be one of the differential factors that explained the higher attachment phenotype in opaque *abaM*::Tn*26* and *abaI*::Tn*26*. In consequence, it was decided to further investigate the role of this type I pilus in substrate recognition and attachment to abiotic surfaces. The first step of the process was constructing a *csu* promoter fusion with the *lux* operon (P*csu*::*lux*) to confirm the RNA-seq data and further investigate the role of OHC12 in Csu pili expression. This construct was introduced through the pMQ557M plasmid into AB5075 and *abaM*::Tn*26*. However, the attempts to obtain a reliable *csu* promoter reporter in the *abaI*::Tn*26* mutant were unsuccessful. When electroporating the pMQ557M_P*csu*::*lux* plasmid into the *abaI* mutant, the different clones obtained showed very different levels of light between them, indicating no consistency in *luxCDABE* expression, therefore making

the resulting data unreliable. This did not happen with neither the wild-type strain nor the *abaM*::Tn*26* mutant.

Consistent with the RNA-seq data, the *abaM* mutant showed an enhanced activity of the P*csu*::*lux* construct compared with the wild-type strain. To elucidate whether this increased expression was a consequence of the higher levels of OHC12 in the *abaM* mutant or was QS-independent, 1 μM of OHC12 was added to the wild-type strain. Interestingly, no differences were observed between the 'induced' and the control (acetonitrile) strain. A previous study, however, suggested that Csu expression could be enhanced in ATCC 19606 using a non-native AHL (*N*-hexanoyl-L-homoserine lactone (C6)), but no information was presented as to whether this enhancement was through an activation of AbaR or mediated by another mechanism (Luo et al., 2015). Moreover, C6 has been shown to be a potent inhibitor of *A. nosocomialis* M2 AbaR (Gerdt et al., 2017). Overall, to date there is no published study that conclusively demonstrates the regulation of *csu* expression by QS, thus it cannot be claimed that AbaM regulates Csu pili expression independently from QS based solely in the data presented in this study. Furthermore, during the construction of the P*abaM*::*lux* and P*abaI*::*lux* reporters in Chapter 3, it was observed that the attempts to remove the *abaR* gene from the constructs led to a loss of responsiveness to OHC12, so there is also the possibility that *abaR* needs to be present close to the promoter under study for assays employing these type of constructs. In conclusion, AbaM negatively regulates *csu* expression, apparently in a QS-independent manner, but this would need to be further confirmed using more sensitive methods, such as RT-qPCR.

Previous studies have shown that the Csu pili plays a central role in attachment and biofilm formation in abiotic surfaces in diverse *A. baumannii* strains (Tomaras et al., 2003; Luo et al., 2015; Moon et al., 2017; Pakharukova et al., 2018). Similarly to what has been reported in other *A. baumannii* strains, the Csu pili seems to be important for attachment and biofilm formation in AB5075. Disruption of the major pilin subunit gene, *csuA/B*, resulted in 40% reduction of attachment compared to the wild-type strain, while inactivation of the *csuE* gene, which encodes for the adhesin tip of the pili, reduced attachment by 60% compared to the parental strain. A similar assay in *A. baumannii* ATCC 19606, where the cells were incubated with antibodies against either CsuA/B or CsuE, showed a similar pattern. Incubation of ATCC 19606 with a 1:100 dilution of the antibodies significantly reduced attachment to polystyrene, with the anti-CsuE antibody incubated cells showing a higher reduction in biofilm formation than the cells incubated with the anti-CsuA/B antibody. Moreover, only the anti-CsuE antibody was capable of abolishing biofilm formation even when diluted 1:1000 (Pakharukova et al., 2018). Overall, these suggests that the Csu pili is important for AB5075 attachment to abiotic surfaces, while highlighting the key role of the CsuE tip adhesin in the Csu pili-mediated biofilm formation.

To further elucidate the role of Csu pili in attachment, it was decided to use a recombinant *E. coli* strain carrying the *csu* operon from *A. baumannii* ATCC 19606 under control of the P_{BAD} promoter. This construct was kindly provided by Dr. Zavialov (University of Turku, Finland), who collaborated in the structural characterization of the Csu pilus and identification of the hydrophobic finger-like loop structures of the CsuE adhesive tip that promotes attachment to hydrophobic surfaces (see 5.1.1) (Pakharukova et al., 2018). The results from the validation assays were consistent with part of the

observations made by Pakharukova *et al.*, 2018 confirming the preference of the Csu pili for hydrophobic surfaces (polystyrene) rather than hydrophilic surfaces (borosilicate glass). Moreover, the extra validation steps performed in this chapter discarded any possible effect of the vector or the arabinose in the attachment of the recombinant *E. coli* BL21 strain and exposed that even small amounts of L-(+)-arabinose are enough to effectively induce Csu-mediated attachment.

However, after the validation of the recombinant *E. coli* strain the objective was to test more exhaustively the hypothesis that the CsuE pili preferably attaches hydrophobic surfaces. To do so, a polymer microarray containing 283 different acrylates and methacrylates with a wide range of different chemical and physical properties was incubated with *E.coli* BL21 expressing Csu pili. Previous work in our group using these materials led to the observation that bacteria avoid attachment to acrylates and methacrylate polymers containing amphile (ester) together with a hydrophobic, mechanically rigid cyclic hydrocarbon pendant group (Sanni et al., 2015), so the assay would also help to test whether the Csu pili possessed a similar selectivity. The results, however, showed that the Csu pili promoted attachment to polymers with a wide variety of structures without any particular correlation between them. Among the different pendant moieties found in the monomers that showed more attachment there were esters, fluorocarbon groups and cyclic, aromatic and linear hydrocarbons. Many monomers possessed amphiphilic polar groups, which were correlated with low attachment in previous studies (Hook et al., 2012a, 2013). Moreover, analysis of the combined hydrophobicity and flexibility of the materials using the parameter α ($\alpha = 0.44n\text{RoTB} - c\log P$, where nRoTB is the number of rotatable bonds of each monomer and $c\log P$ is the logarithm of the octanol/water partition coefficient), which was previously established

and used in our laboratory to combine the hydrophobicity and flexibility in materials with hydrocarbon pendant groups in a single parameter (Sanni et al., 2015), revealed that there was no correlation between the α values of materials with hydrocarbon pendant groups and Csu attachment. This observation, nonetheless, has also been made in *Proteus mirabilis* and *S. aureus*, in which the α value was weakly or not correlated with bacterial attachment, respectively (Dundas *et al.*, 2019 (unpublished manuscript)). Furthermore, high levels of attachment were observed to EGDPEA, the lead monomer that prevented attachment of *P. aeruginosa*, *S. aureus* and uropathogenic *E. coli*, while no significant attachment was detected in NGPDA, the 'pro-attachment' monomer routinely used as a positive control for attachment in our group (Hook et al., 2012a). However, is important to remark that this assay aimed to identify the selectivity of the Csu pili, rather than the selectivity of *A. baumannii*, to different surfaces. Therefore, is possible that the Csu pili is not particularly selective for NGPDA, but other *A. baumannii* biofilm/attachment-associated factors could promote biofilm formation on this surface.

Consistently with this hypothesis, when testing *A. baumannii* AB5075 attachment to EGDPEA and NGPDA, the reverse result was observed. Similarly to the results in other bacteria, AB5075 formed biofilm in NGPDA, while in EGDPEA biofilm formation was greatly reduced in both surface coverage and total biomass. These differences between the recombinant BL21 expressing *A. baumannii* ATCC 19606 Csu pili and *A. baumannii* AB5075 do not seem to be caused by differences in the Csu adhesive tip protein CsuE, as this is highly conserved between the two strains (**Supplementary Material Figure S6**). Instead, the results suggest that, as briefly discussed above, while the Csu pili (and more specifically, CsuE) might be important for the initial interactions with the surface that

lead to attachment and biofilm formation, it is probably not the (only) deciding factor used by the bacteria to choose whether stay in the surface and form a biofilm or return to the planktonic lifestyle. This complex process is better studied in *P. aeruginosa*, in which some of these factors have been characterized, including cAMP, TFP, c-di-GMP, PilY1, AlgZ/AlgR or PilJ (O'Toole and Wong, 2016).

It is also important to mention that both assays were performed under very different conditions and it is possible that the differences in methodology might have had an impact in the results. While the recombinant *E. coli* pBAD_*csu* attachment assays were performed with microarrays in Petri dishes, the *A. baumannii* AB5075 attachment assays were carried out the 'wheel' system using 5-mm polymer dots (see Material and methods 2.4.13 and 2.4.14, respectively). The biological differences between *E. coli* and *A. baumannii* might also have contributed to the conflicting data between both assays. Differences in composition and/or length of the saccharide A of the LPS/LOS of *E. coli* and *A. baumannii* (respectively), the capsule thickness/composition, and surface charge/hydrophobicity, as well as the presence of other pili or OM proteins, could all have contributed to the attachment of both bacteria to the different polymers.

Nonetheless, there is still a long way to go to fully understand all the factors and processes involved in surface sensing and attachment in bacteria. For that reason, while the work presented here stablishes some novel data and hypothesis, more exhaustive research is needed to fully elucidate the exact role of Csu pili in the initial steps of attachment and biofilm formation in *A. baumannii*.

5.5. Conclusions and future directions

In this chapter, an investigation of the expression and function of *A. baumannii* Csu pili is described. Promoter fusion analysis validated the RNA-seq that showed that *abaM*::Tn*26* expressed higher levels of expression of the *csu* operon. Moreover, attachment assays with *csuA/B* and *csuE* transposon mutants revealed that the Csu pili plays an important role in AB5075 biofilm formation, as suggested by previous assays in other strains (Tomaras et al., 2003; Rumbo-Feal et al., 2013; Nait Chabane et al., 2014). Future work should focus on confirming this data by more sensitive assays. A quantitative or semi-quantitative protein assay would confirm whether the higher promoter activity and RNA levels correlate with a higher levels of Csu pili expression. Transmission electron microscopy, which has been previously used to visualize *A. baumannii* Csu pili (Luo et al., 2015; Pakharukova et al., 2018), would also further confirm the presence of higher levels of Csu pili on *abaM*::Tn*26*, as well as to observe whether the pili expression is abolished in *csuE*::Tn*26* and *csuA/B*::Tn*26* or their structure is modified by the loss of some of their structural subunits. Attachment assays with mutants of genes encoding other elements of the Csu pili (or deletion of the entire *csu* operon) would also help to fully characterize the role of this pili in AB5075.

The exacts mechanisms involved in the bacterial 'decision' to attach or not to an abiotic surface are still a matter of intense debate and research. While Pakharukova *et al.*, 2018 observations suggested that the Csu pili attached better to hydrophobic surfaces than hydrophilic and the initial observations here performed using borosilicate glass and polystyrene were consistent with this hypothesis, the screening with a large library of materials revealed that the *E. coli* expressing *A. baumannii* Csu pili attached to polymers of with different chemical compositions, including our lead anti-attachment polymer, EGDPEA.

Unfortunately, these assays could only be performed in duplicate, as the materials required (microarray polymer slides and scaled up polymer slides) were not available for a long time due to technical issues. Therefore, repetition of these assays is required to confirm the observations made. If the results from the repeated assays are consistent, it would be interesting to scale up the 'top attachment' polymers and test them with both the *E. coli* BL21 pBAD_*csu* and *A. baumannii* AB5075, plus other *A. baumanii* strains. This way, it would be possible to confirm whether the surface selectivity mediated by Csu pili and the surface selectivity of *A. baumannii* are coincident or not, as well as validate EGDPEA as a suitable anti-attachment material for *A. baumannii*. Lastly, testing AB5075 mutants of the *csu* operon (more specifically, *csuE* and/or *csuA/B* mutants), as well as the *csu* operon-overexpressing *abaM*::Tn*26* mutant, in different polymers in attachment assays could also help to shed more light on the contribution of Csu pili in surface discrimination, attachment and biofilm formation, as well as the role of the CsuE tip in the discrimination and selection between different abiotic surfaces.

5.5.1. Summary of most important findings

- Csu pili seem to be negatively regulated by AbaM.
- Csu pili expression does not seem to be regulated by OHC12.
- Csu pili is important for attachment to polypropylene in AB5075.
- The CsuE adhesive tip seems to have a bigger impact in the Csu pili-mediated attachment process than the CsuA/B pilin.
- Csu pili promote attachment to polymers with diverse structures and properties.
- The Csu pili attach to EGDPEA, the leading anti-attachment material identified and characterised in our laboratory.
- *A. baumannii* AB5075, however, does not attach to EGDPEA but forms biofilms on NGPDA.

6. General discussion and future perspectives

QS is a well-known regulatory system that modulates virulence and biofilm formation in many Gram-negative and Gram-positive bacterial pathogens (Castillo-Juárez et al., 2015; Papenfort and Bassler, 2016; Rutherford and Bassler, 2012) but remains poorly studied in *A. baumannii*. The aim of this project was to expand the current knowledge about *A. baumannii* QS by characterizing the AB5075 AHL synthase mutant, as well as an orthologue of the QS negative regulator RsaM, here named AbaM, which has never been studied in *A. baumannii*. The work presented in this thesis showed that AbaM negatively regulates AHL production, surface motility, attachment/biofilm formation to polypropylene and is required for full virulence in *G. mellonella*. Moreover, AbaI was shown to positively contribute to surface motility and also affect attachment in polypropylene in a phase variation-dependent manner, with the opaque *abaI*::Tn*26* mutant displaying increased levels of attachment and the translucent isogenic strain showing reduced attachment when compared with the equivalent wild-type phase variant. However, neither AbaI nor OHC12 had any impact on virulence in *G. mellonella*. Lastly, the RNA-seq analysis, along with the assays with promoter-*lux* reporter strains, revealed that AbaM and AbaI possess overlapping regulons, QS positively regulates its own and *abaM* expression and AbaM negatively regulates QS and its own expression. All these observations are consistent with transcriptomic and promoter fusion studies performed in other bacteria possessing QS systems with an *abaM*-like gene, such as *P. fuscovaginae* and *B. cenocepacia* (Inhülsen, 2011; Uzelac et al., 2017). Overall, these data show that both QS and AbaM play important roles in the biology of *A. baumannii*. Some of the limitations of the work presented in this thesis that should be addressed in future research include further characterization of the *abaM*::Tn*26* avirulent phenotype in rodent infection models, characterization of the *abaM*::Tn*26* translucent

variants for AHL production and virulence and evaluation of the contribution of *abaM* in other relevant phenotypes, such as phase switching frequency or antibiotic resistance.

The testing of long-chain AHLs in the *abaI*::Tn*26* P*abaM*::*lux* reporter strain revealed some interesting data about the selectivity of AB5075 and the screening of unsubstituted long chain AHLs and a library of OC12-based compounds led to the finding of some promising AbaR inhibitors. Testing the effect of these compounds on diverse *A. baumannii* phenotypes could open an interesting line of research towards finding effective agents that disrupt virulence or biofilm formation through the inhibition of QS. Moreover, screening of other OC12/OHC12-derived compounds for agonist/antagonist AbaR activity could also help to characterize in more detail the structural characteristics required for AbaR activation/inhibition.

The RNA-seq also revealed another interesting piece of information: in both the opaque *abaI*::Tn*26* and *abaM*::Tn*26* mutants the *csu* operon genes were among the most upregulated compared with the wild-type strain. Csu pili have been reported to be involved in initial attachment and biofilm formation in different studies (Pakharukova et al., 2018; Tomaras et al., 2003; Rumbo-Feal et al., 2013; Luo et al., 2015). The presence of this operon among the most upregulated genes in two strains that showed increased attachment to polypropylene compared with the opaque wild-type strain (see 3.3.6) and the reduction of attachment to polypropylene in *csuA/B* and *csuE* transposon mutants in AB5075 (see 5.3.2) raised the question of what is the precise role of Csu pili in the attachment process. Specifically, our group is particularly interested in the elements involved in surface selectivity and has developed diverse assays to study this process. A previous study using a recombinant *E. coli* BL21 pBAD_*csu* strain expressing Csu pili suggested that the Csu pili

attaches preferably to hydrophobic surfaces (Pakharukova et al., 2018). Moreover, previous work in our laboratory led to a model that correlates *P. aeruginosa* attachment with hydrophobicity and flexibility of the material in (meth)acrylates with hydrocarbon pendant groups (Sanni et al., 2015). The results of the assays performed in this work did not support either of these hypotheses for the Csu pili, as these showed attachment to very different materials without any correlation between their structures or physicochemical properties. Moreover, Csu pili, when expressed in *E. coli*, strongly attached to the lead anti-attachment polymer EGDPEA identified and characterized in our group as resistant against biofilm formation by diverse pathogens such as *P. aeruginosa*, *E. coli* and *S. aureus* (Hook et al., 2012a). However, EGDPEA did prevent biofilm formation by *A. baumannii* AB5075, which might indicate that the anti-biofilm properties of EGDPEA are mediated through a more generic mechanism highly conserved in different bacteria rather than Csu pili-mediated selectivity alone. Further research is necessary to confirm these observations, which would also help to elucidate whether the surface selection and initial attachment of *A. baumannii* is mediated by other factors apart from Csu pili and could help to better understand the initial steps of attachment, as well as provide very useful structural information for the rational development of more efficient anti-attachment materials that might help to prevent the colonization of medical surfaces/devices by *A. baum*annii and other important nosocomial pathogens.

6.1. Summary of most important findings in this project

- AbaM is an RsaM orthologue that negatively regulates AHL production, surface motility and attachment to polypropylene. Moreover, it is required for full virulence in *G. mellonella* infection model.
- QS positively regulates surface motility. Phase variation and QS seem to co-regulate attachment/biofilm formation
- Based on BACTH bacterial two-hybrid assays, AbaM does not appear to interact with AbaR or AbaI, nor form dimers *in vivo* when expressed in *E. coli*.
- AbaM is negatively auto-regulated and negatively regulates *abaR* and *abaI* expression.
- QS is positively auto-regulated and positively regulates *abaM* expression.
- AbaR is highly selective for 3-hydroxy and 3-oxo AHLs with an acyl chain length between 10 and 14 carbons. The most potent agonist tested was the native ligand, OHC12.
- Unsubstituted AHLs of 10 to 16 carbons length are AbaR antagonists.
- Some changes in the homoserine lactone ring and the acyl chain of OC12 can result in strong AbaR inhibitory compounds.
- AbaM and AbaI regulons are partially overlapped.
- The opaque *abaM* and *abaI* mutants significantly overexpress genes encoding proteins of the Csu pilus compared with the wild-type strain. Moreover, the *abaM* mutant also overexpressed genes of the Ac-505 biosynthetic operon. Both are involved in attachment and biofilm formation.
- Csu promoter-*lux* fusions also showed higher levels of activity in the *abaM* mutant compared with the wild-type strain.
- The Csu pili is required for biofilm formation in opaque AB5075.

- The hypothesis that Csu pili attach preferably to hydrophobic surfaces was not supported by the attachment screening to a library of (meth)acrylates with different chemical and physical properties.
- Csu pili attached the anti-attachment polymer EGDPEA, but *A. baumannii* AB5075 did not, suggesting that more factors are involved in the surface sensing, attachment and biofilm formation.

6.2. Proposed models

6.2.1. AbaM regulation of AB5075 genes and phenotypes

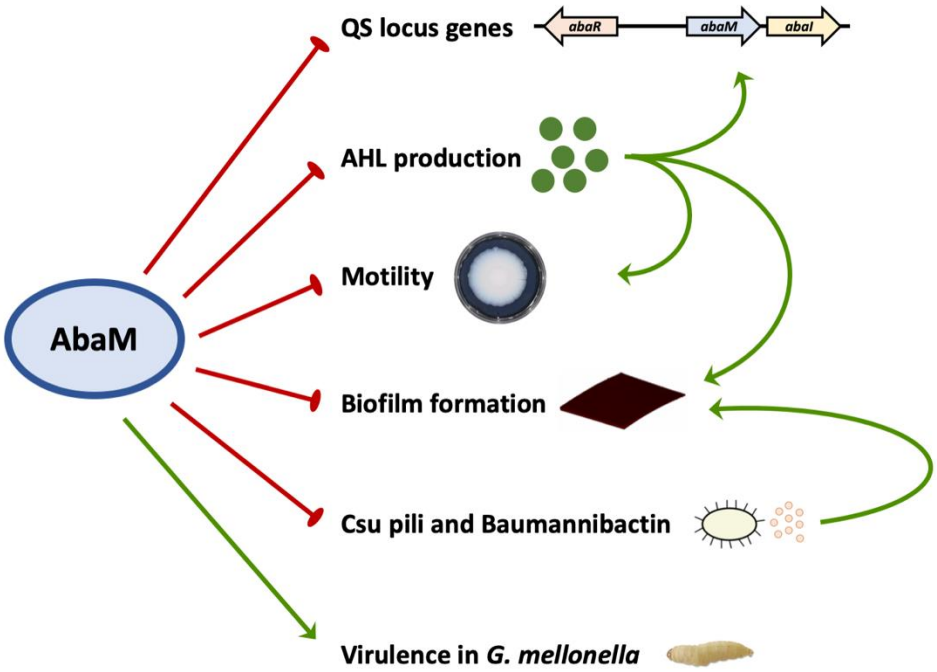


Figure 6.1: Proposed model for the AbaM role in regulation of AB5075 genes and phenotypes. AbaM, through and unknown mechanism, negatively regulates the expression of QS locus genes (including its own encoding gene), AHL production, motility, attachment and biofilm formation and expression of Ac-505 and Csu pili, but positively affects virulence in *G. mellonella*. At the same time, AHL production has been shown to positively impact the expression of *abaM* and *abaI*, as well as positively regulate motility and biofilm formation, in which Csu pili and Ac-505 have also been involved in other studies. Red arrows indicate negative regulation or contribution. Green arrows indicate positive regulation or contribution.

6.2.2. Cross-regulation of AbaM and quorum sensing

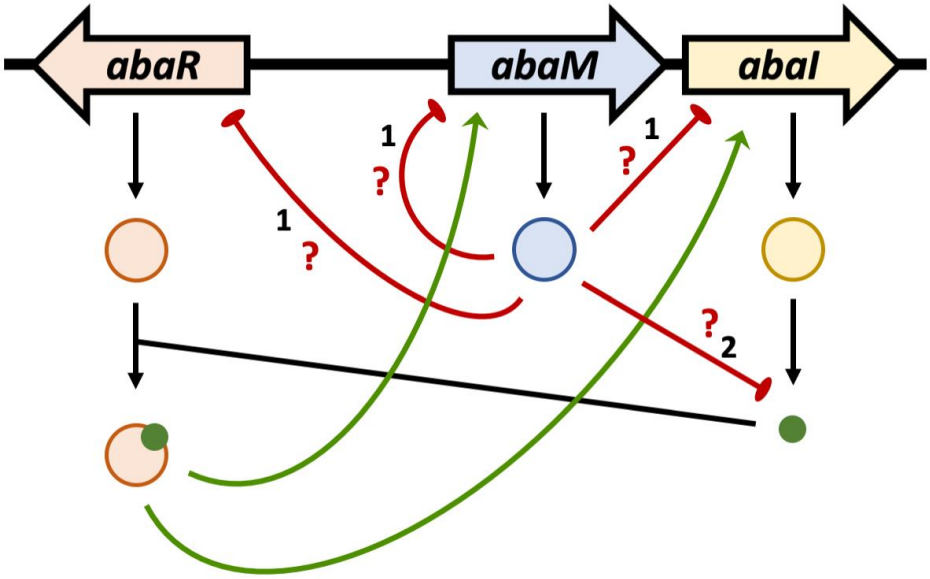


Figure 6.2: Proposed model for the cross-regulation of AbaM and QS. Based on the RNA-seq and *lux*-based reporters data obtained in this piece of work and previous studies in QS and in AbaM orthologues, the following model for *A. baumannii* AbaM/QS cross-regulation is proposed: The AHL synthase produces *A. baumannii* AB5075 main signal, OHC12, which binds AbaR. The AbaR-OHC12 complex can enhance the expression of *abaM* and *abaI*. AbaM, on the other hand, is capable of **(1)** negatively regulate the expression of its own gene, *abaR* and *abaI* through an unknown **(?)** mechanism and **(2)** negatively regulate the production of OHC12, either as a consequence of downregulating *abaI* expression or through another unknown **(?)** mechanism. Red arrows indicate negative regulation. Green arrows indicate positive regulation.

7. References

Adlington, K., Nguyen, N.T., Eaves, E., et al. (2016) Application of targeted molecular and material property optimization to bacterial attachment-resistant (meth)acrylate polymers. Biomacromolecules, 17 (9): 2830–8.

Ahmad, I., Karah, N., Nadeem, A., et al. (2019) Analysis of colony phase variation switch in *Acinetobacter baumannii* clinical isolates. *PloS one*, 14 (1): e0210082.

Allesen-Holm, M., Barken, K.B., Yang, L., et al. (2006) A characterization of DNA release in *Pseudomonas aeruginosa* cultures and biofilms. *Molecular Microbiology*, 59 (4): 1114–1128.

Almasaudi, S.B. (2018) *Acinetobacter* spp. as nosocomial pathogens: Epidemiology and resistance features. *Saudi journal of biological sciences*, 25 (3): 586–596.

Anbazhagan, D., Mansor, M., Yan, G.O.S., et al. (2012) Detection of quorum sensing signal molecules and identification of an autoinducer synthase gene among biofilm forming clinical isolates of *Acinetobacter* spp. de Crécy-Lagard, V. (ed.). *PLoS ONE*, 7 (7): e36696.

Antunes, L.C.M., Ferreira, R.B.R., Lostroh, C.P., et al. (2008) A mutational analysis defines *Vibrio fischeri* LuxR binding sites. *Journal of bacteriology*, 190 (13): 4392–7.

Antunes, L.C.S., Imperi, F., Carattoli, A., et al. (2011a) Deciphering the multifactorial nature of *Acinetobacter baumannii* Pathogenicity Adler, B. (ed.). *PLoS ONE*, 6 (8): e22674. d

Antunes, L.C.S., Imperi, F., Towner, K.J., et al. (2011b) Genome-assisted identification of putative iron-utilization genes in *Acinetobacter baumannii* and their distribution among a genotypically diverse collection of clinical isolates. *Research in Microbiology*, 162 (3): 279–284.

Antunes, L.C.S., Visca, P. and Towner, K.J. (2014) *Acinetobacter baumannii*: Evolution of a global pathogen. *Pathogens and Disease*, 71 (3): 292–301.

Aranda, J., López, M., Leiva, E., et al. (2014) Role of *Acinetobacter baumannii* UmuD homologs in antibiotic resistance acquired through DNA damage-induced mutagenesis. *Antimicrobial agents and chemotherapy*, 58 (3): 1771–3.

Aranda, J., Poza, M., Shingu-Vazquez, M., et al. (2013) Identification of a DNA-ramage-inducible regulon in *Acinetobacter baumannii*. *Journal of Bacteriology*, 195 (24): 5577–5582.

Arroyo, L.A., Herrera, C.M., Fernandez, L., et al. (2011) The *pmrCAB* operon mediates polymyxin resistance in *Acinetobacter baumannii* ATCC 17978 and clinical isolates through phosphoethanolamine modification of lipid A. *Antimicrobial Agents and Chemotherapy*, 55 (8): 3743–3751.

Baker, M.D., Wolanin, P.M. and Stock, J.B. (2006) Signal transduction in bacterial chemotaxis. *BioEssays*, 28 (1): 9–22.

Balasubramanian, D., Schneper, L., Kumari, H., et al. (2013) A dynamic and intricate regulatory network determines *Pseudomonas aeruginosa* virulence. *Nucleic Acids Research*, 41 (1): 1–20.

Banerjee, G. and Ray, A.K. (2017) Quorum-sensing network-associated gene regulation in Gram-positive bacteria. *Acta Microbiologica et Immunologica Hungarica*, 64 (4): 439–453.

Barker, J. and Maxted, H. (1975) Observations on the growth and movement of *Acinetobacter* on semi-solid media. *Journal of Medical Microbiology*, 8 (3): 443–446.

Battesti, A. and Bouveret, E. (2012) The bacterial two-hybrid system based on adenylate cyclase reconstitution in *Escherichia coli*. *Methods*, 58 (4): 325–334.

Baumann, P., Doudoroff, M. and Stanier, R.Y. (1968) A study of the *Moraxella* group. II. Oxidative-negative species (genus *Acinetobacter*). *Journal of bacteriology*, 95 (5): 1520–41.

Beceiro, A., Llobet, E., Aranda, J., et al. (2011) Phosphoethanolamine modification of lipid A in colistin-resistant variants of *Acinetobacter baumannii* Mediated by the *pmrAB* Two-Component Regulatory System. *Antimicrobial Agents and Chemotherapy*, 55 (7): 3370–3379.

Beier, D. and Gross, R. (2006) Regulation of bacterial virulence by two-component systems. *Current Opinion in Microbiology*, 9 (2): 143–152.

Bentancor, L. V., Camacho-Peiro, A., Bozkurt-Guzel, C., et al. (2012a) Identification of Ata, a multifunctional trimeric autotransporter of *Acinetobacter baumannii*. *Journal of Bacteriology*, 194 (15): 3950–3960.

Bentancor, L. V, O'Malley, J.M., Bozkurt-Guzel, C., et al. (2012b) Poly-N-acetyl-ß-(1-6)-glucosamine is a target for protective immunity against *Acinetobacter baumannii* infections. *Infection and immunity*, 80 (2): 651–6.

Bernards, A.T., Harinck, H.I.J., Dijkshoorn, L., et al. (2004) Persistent *Acinetobacter baumannii?* Look Inside Your Medical Equipment. *Infection Control & Hospital Epidemiology*, 25 (11): 1002–1004.

Bhargava, N., Sharma, P. and Capalash, N. (2010) Quorum sensing in *Acinetobacter* : an emerging pathogen. *Critical Reviews in Microbiology*, 36 (4): 349–360.

Bhargava, N., Sharma, P. and Capalash, N. (2012) *N*-acyl homoserine lactone mediated interspecies interactions between *A. baumannii* and *P. aeruginosa*. *Biofouling*, 28 (8): 813–822.

Bhuiyan, M.S., Ellett, F., Murray, G.L., et al. (2016) *Acinetobacter baumannii* phenylacetic acid metabolism influences infection outcome through a direct effect on neutrophil chemotaxis.

Proceedings of the National Academy of Sciences of the United States of America, 113 (34): 9599–604.

Bitrian, M., Solari, C.M., González, R.H., et al. (2012) Identification of virulence markers in clinically relevant strains of *Acinetobacter* genospecies. *International microbiology : the official journal of the Spanish Society for Microbiology*, 15 (2): 79–88.

Boll, J.M., Tucker, A.T., Klein, D.R., et al. (2015) Reinforcing lipid A acylation on the cell surface of *Acinetobacter baumannii* promotes cationic antimicrobial peptide resistance and desiccation survival. Sperandio, V. (ed.). *mBio*, 6 (3): e00478-15.

Brackman, G. and Coenye, T. (2014) Quorum sensing inhibitors as anti-biofilm agents. *Current Pharmaceutical Design*, 21 (1): 5–11.

Bravo, Z., Chapartegui-González, I., Lázaro-Díez, M., et al. (2018) *Acinetobacter pittii* biofilm formation on inanimate surfaces after long-term desiccation. *Journal of Hospital Infection*, 98 (1): 74–82.

Bravo, Z., Orruño, M., Navascues, T., et al. (2019) Analysis of *Acinetobacter baumannii* survival in liquid media and on solid matrices as well as effect of disinfectants. *Journal of Hospital Infection*.

de Breij, A., Gaddy, J., van der Meer, J., et al. (2009) CsuA/BABCDE-dependent pili are not involved in the adherence of *Acinetobacter baumannii* ATCC19606T to human airway epithelial cells and their inflammatory response. *Research in Microbiology*, 160 (3): 213–218.

Brossard, K.A. and Campagnari, A.A. (2012) The *Acinetobacter baumannii* biofilm-associated protein plays a role in adherence to human epithelial cells. *Infection and immunity*, 80 (1): 228–33.

Brotherton, C.A. and Greenberg, E.P. (2017) "The chemistry of collective behavior in *Acinetobacter baumannii*." In *Poster presented at: 6th ASM Conference on Cell-Cell Communicaton in Bacteria (Athens, GA)*. 2017. University of Washington.

Brown, L. and Elliott, T. (1996) Efficient translation of the RpoS sigma factor in *Salmonella typhimurium* requires host factor I, an RNA-binding protein encoded by the hfq gene. *Journal of bacteriology*, 178 (13): 3763–70.

Burrows, L.L. (2012) *Pseudomonas aeruginosa* twitching motility: Type IV Pili in action. *Annual Review of Microbiology*, 66 (1): 493–520.

Cai, S.J. and Inouye, M. (2002) EnvZ-OmpR interaction and osmoregulation in *Escherichia coli*. *The Journal of biological chemistry*, 277 (27): 24155–61.

Cai, Y., Chai, D., Wang, R., et al. (2012) Colistin resistance of *Acinetobacter baumannii*: clinical reports, mechanisms and antimicrobial strategies. *Journal of Antimicrobial Chemotherapy*, 67 (7): 1607–1615.

Camarena, L., Bruno, V., Euskirchen, G., et al. (2010) Molecular mechanisms of ethanol-induced pathogenesis revealed by RNA-sequencing. *PLoS Pathogens*, 6 (4): 1–14.

Castillo-Juárez, I., Maeda, T., Mandujano-Tinoco, E.A., et al. (2015) Role of quorum sensing in bacterial infections. *World journal of clinical cases*, 3 (7): 575–98.

Cerqueira, G.M., Kostoulias, X., Khoo, C., et al. (2014) A global virulence regulator in *Acinetobacter baumannii* and Its control of the phenylacetic acid catabolic pathway. *The Journal of Infectious Diseases*, 210 (1): 46–55.

Chaari, A., Mnif, B., Bahloul, M., et al. (2013) *Acinetobacter baumannii* ventilator-associated pneumonia: epidemiology, clinical characteristics, and prognosis factors. *International journal of infectious diseases*, 17 (12): e1225-8.

Chan, K.-G., Cheng, H.J., Chen, J.W., et al. (2014) Tandem mass spectrometry detection of quorum sensing activity in multidrug resistant clinical isolate *Acinetobacter baumannii*. *TheScientificWorldJournal*, 2014: 891041.

Chapartegui-González, I., Lázaro-Díez, M., Bravo, Z., et al. (2018) *Acinetobacter baumannii* maintains its virulence after long-time starvation. *PloS one*, 13 (8): e0201961.

Chen, M., Yu, Q. and Sun, H. (2013) Novel strategies for the prevention and treatment of biofilm related infections. *International journal of molecular sciences*, 14 (9): 18488–501.

Chen, R., Barphagha, I.K., Karki, H.S., et al. (2012) Dissection of quorum-sensing genes in *Burkholderia glumae* reveals non-canonical regulation and the new regulatory gene *tofM* for toxoflavin production. *PLoS ONE*, 7 (12).

Chen, R., Lv, R., Xiao, L., et al. (2017) A1S_2811, a CheA/Y-like hybrid two-component regulator from *Acinetobacter baumannii* ATCC17978, is involved in surface motility and biofilm formation in this bacterium. *MicrobiologyOpen*, 6 (5).

Chin, C.Y., Tipton, K.A., Farokhyfar, M., et al. (2018) A high-frequency phenotypic switch links bacterial virulence and environmental survival in *Acinetobacter baumannii*. *Nature microbiology*, 3 (5): 563–569.

Choi, A.H.K., Slamti, L., Avci, F.Y., et al. (2009) The *pgaABCD* locus of *Acinetobacter baumannii* encodes the production of Poly-1-6-*N*-Acetylglucosamine, which is critical for biofilm Formation. *Journal of Bacteriology*, 191 (19): 5953–5963.

Choi, C.H., Lee, J.S., Lee, Y.C., et al. (2008) *Acinetobacter baumannii* invades epithelial cells and outer membrane protein A mediates interactions with epithelial cells. *BMC Microbiology*, 8 (1): 216.

Choi, K.-H., Gaynor, J.B., White, K.G., et al. (2005) A Tn*7*-based broad-range bacterial cloning and expression system. *Nature Methods*, 2 (6): 443–448.

Choi, K.-H. and Schweizer, H.P. (2006) mini-Tn*7* insertion in bacteria with single *att*Tn*7* sites: example *Pseudomonas aeruginosa*. *Nature Protocols*, 1 (1): 153–161.

Clemmer, K.M., Bonomo, R.A. and Rather, P.N. (2011) Genetic analysis of surface motility in *Acinetobacter baumannii*. *Microbiology*, 157 (Pt 9): 2534.

Coggan, K.A. and Wolfgang, M.C. (2012) Global regulatory pathways and cross-talk control *Pseudomonas aeruginosa* environmental lifestyle and virulence phenotype. *Current Issues in Molecular Biology*, 14 (2): 47–70.

Costa, T.R.D., Felisberto-Rodrigues, C., Meir, A., et al. (2015) Secretion systems in Gram-negative bacteria: structural and mechanistic insights. *Nature Reviews Microbiology*, 13 (6): 343–359.

Coulthurst, S. (2019) The Type VI secretion system: a versatile bacterial weapon. *Microbiology*, 165 (5): 503–515.

Coulthurst, S.J. (2013) The Type VI secretion system – a widespread and versatile cell targeting system. *Research in Microbiology*, 164 (6): 640–654.

Cyphert, E.L. and Recum, H.A. von (2017) Emerging technologies for long-term antimicrobial device coatings: advantages and limitations. *Experimental Biology and Medicine*, 242 (8): 788.

Damier-Piolle, L., Magnet, S., Brémont, S., et al. (2008) AdeIJK, a resistance-nodulation-cell division pump effluxing multiple antibiotics in *Acinetobacter baumannii*. *Antimicrobial agents and chemotherapy*, 52 (2): 557–62.

Davenport, P.W., Griffin, J.L. and Welch, M. (2015) Quorum sensing is accompanied by global metabolic changes in the opportunistic human pathogen *Pseudomonas aeruginosa*. *Journal of bacteriology*, 197 (12): 2072–82.

Deveson Lucas, D., Crane, B., Wright, A., et al. (2018) Emergence of high-level colistin resistance in an *Acinetobacter baumannii* clinical isolate mediated by inactivation of the global regulator H-NS. *Antimicrobial agents and chemotherapy*, 62 (7).

Diancourt, L., Passet, V., Nemec, A., et al. (2010) The population structure of *Acinetobacter baumannii*: Expanding multiresistant clones from an ancestral susceptible genetic pool. *PLoS ONE*, 5 (4).

Domingues, S., Rosário, N., Cândido, Â., et al. (2019) Competence for natural transformation is common among clinical strains of resistant *Acinetobacter* spp. *Microorganisms*, 7 (2): 30.

Donlan, R.M. and Costerton, J.W. (2002) Biofilms: survival mechanisms of clinically relevant microorganisms. *Clinical microbiology reviews*, 15 (2): 167–93.

Dou, Y., Song, F., Guo, F., et al. (2017) *Acinetobacter baumannii* quorum-sensing signalling molecule induces the expression of drug-resistance genes. *Molecular medicine reports*, 15 (6): 4061–4068.

Dubern, J.-F. and Diggle, S.P. (2008) Quorum sensing by 2-alkyl-4-quinolones in *Pseudomonas aeruginosa* and other bacterial species. *Molecular BioSystems*, 4 (9): 882.

Dundas, A.A., Sanni, O., Dubern, J.-F., et al. (2019) Validating a predictive structure-property relationship by discovery of novel polymers which reduce bacterial biofilm formation. *Advanced Materials*, (Unpublished)

Dunman, P.M., Murphy, E., Haney, S., et al. (2001) Transcription profiling-based identification of *Staphylococcus aureus* genes regulated by the *agr* and/or *sarA* loci. *Journal of bacteriology*, 183 (24): 7341–53.

Eberhard, A., Burlingame, A.L., Eberhard, C., et al. (1981) Structural identification of autoinducer of *Photobacterium fischeri* luciferase. *Biochemistry*, 20 (9): 2444–2449.

Egger, L.A., Park, H. and Inouye, M. (1997) Signal transduction via the histidyl-aspartyl phosphorelay. *Genes to Cells*, 2 (3): 167–184.

Eijkelkamp, B.A., Stroeher, U.H., Hassan, K.A., et al. (2013) H-NS plays a role in expression of *Acinetobacter baumannii* virulence features. *Infection and Immunity*, 81 (7): 2574.

Eijkelkamp, B.A., Stroeher, U.H., Hassan, K.A., et al. (2014) Comparative analysis of surface-exposed virulence factors of *Acinetobacter baumannii*. *BMC Genomics*, 15 (1): 1020.

Espinal, P., Martí, S. and Vila, J. (2012) Effect of biofilm formation on the survival of *Acinetobacter baumannii* on dry surfaces. *Journal of Hospital Infection*, 80 (1): 56–60.

Eze, E.C., Chenia, H.Y. and El Zowalaty, M.E. (2018) *Acinetobacter baumannii* biofilms: effects of physicochemical factors, virulence, antibiotic resistance determinants, gene regulation, and future antimicrobial treatments. *Infection and drug resistance*, 11: 2277–2299.

Falagas, M.E., Karveli, E.A., Kelesidis, I., et al. (2007) Community-acquired *Acinetobacter* infections. *European Journal of Clinical Microbiology & Infectious Diseases*, 26 (12): 857–868.

Farrow, J.M., Wells, G. and Pesci, E.C. (2018) Desiccation tolerance in *Acinetobacter baumannii* is mediated by the two-component response regulator BfmR. *PLoS ONE*, 13 (10).

Fernandez-Garcia, L., Ambroa, A., Blasco, L., et al. (2018) Relationship between the quorum network (sensing/quenching) and clinical features of pneumonia and bacteraemia caused by *A. baumannii*. *Frontiers in Microbiology*, 9: 3105.

Fiester, S.E., Arivett, B.A., Schmidt, R.E., et al. (2016) Iron-regulated phospholipase C activity contributes to the cytolytic activity and virulence of *Acinetobacter baumannii*. *PLoS ONE*, 11 (11).

Fily, F., Ronat, J.-B., Malou, N., et al. (2019) Post-traumatic osteomyelitis in Middle East war-wounded civilians: resistance to first-line antibiotics in selected bacteria over the decade 2006–2016. *BMC Infectious Diseases*, 19 (1): 103.

Fournier, P.E., Vallenet, D., Barbe, V., et al. (2006) Comparative genomics of multidrug resistance in *Acinetobacter baumannii*. *PLoS Genetics*, 2 (1): 62–72.

Fuqua, W.C., Winans, S.C. and Greenberg, E.P. (1994) Quorum sensing in bacteria: the LuxR-LuxI family of cell density-responsive transcriptional regulators. *Journal of bacteriology*, 176 (2): 269–75.

Gaddy, J.A., Tomaras, A.P. and Actis, L.A. (2009) The *Acinetobacter baumannii* 19606 OmpA protein plays a role in biofilm formation on abiotic surfaces and in the interaction of this pathogen with eukaryotic cells. *Infection and Immunity*, 77 (8): 3150–3160.

Gallagher, L.A., Ramage, E., Weiss, E.J., et al. (2015) Resources for genetic and genomic analysis of emerging pathogen *Acinetobacter baumannii*. *Journal of bacteriology*, 197 (12): 2027–35.

Gayoso, C.M., Mateos, J., Méndez, J.A., et al. (2014) Molecular mechanisms involved in the response to desiccation stress and persistence in *Acinetobacter baumannii*. *Journal of Proteome Research*, 13 (2): 460–476.

Geisinger, E. and Isberg, R.R. (2015) Antibiotic modulation of capsular exopolysaccharide and virulence in *Acinetobacter baumannii*. *PLoS pathogens*, 11 (2): e1004691.

Gentile, V., Frangipani, E., Bonchi, C., et al. (2014) Iron and *Acinetobacter baumannii* Biofilm Formation. *Pathogens (Basel, Switzerland)*, 3 (3): 704–19.

Gerdt, J.P., Wittenwyler, D.M., Combs, J.B., et al. (2017) Chemical interrogation of luxr-type quorum sensing receptors reveals new insights into receptor selectivity and the potential for interspecies bacterial signaling. *ACS chemical biology*, 12 (9): 2457–2464.

Giles, S.K., Stroeher, U.H., Eijkelkamp, B.A., et al. (2015) Identification of genes essential for pellicle formation in *Acinetobacter baumannii*. *BMC microbiology*, 15: 116.

Givskov, M., Hentzer, M., Ersbøll, B.K., et al. (2000) Quantification of biofilm structures by the novel computer program Comstat. *Microbiology*, 146 (10): 2395–2407.

Goh, H.M.S., Beatson, S.A., Totsika, M., et al. (2013) Molecular analysis of the *Acinetobacter baumannii* biofilm-associated protein. *Applied and environmental microbiology*, 79 (21): 6535–43.

Golic, A.E., Valle, L., Jaime, P.C., et al. (2019) BlsA is a low to moderate temperature blue light photoreceptor in the human pathogen *Acinetobacter baumannii*. *Frontiers in Microbiology*, 10: 1925.

González, R.H., Dijkshoorn, L., Van Den Barselaar, M., et al. (2009) Quorum sensing signal profile of *Acinetobacter* strains from nosocomial and environmental sources. *Revista Argentina de Microbiologia*, 41 (2): 73–78.

González, R.H., Nusblat, A. and Nudel, B.C. (2001) Detection and characterization of quorum sensing signal molecules in *Acinetobacter* strains. *Microbiological Research*, 155 (4): 271–277.

Goo, E., Majerczyk, C.D., An, J.H., et al. (2012) Bacterial quorum sensing, cooperativity, and anticipation of stationary-phase stress. *Proceedings of the National Academy of Sciences of the United States of America*, 109 (48): 19775.

Gootz, T.D. and Marra, A. (2008) *Acinetobacter baumannii:* an emerging multidrug-resistant threat. *Expert Review of Anti-infective Therapy*, 6 (3): 309–325.

Green, E.R. and Mecsas, J. (2016) Bacterial secretion systems: An overview. *Microbiology spectrum*, 4 (1).

De Gregorio, E., Del Franco, M., Martinucci, M., et al. (2015) Biofilm-associated proteins: news from *Acinetobacter*. *BMC Genomics*, 16 (1): 933.

Groisman, E.A. (2016) Feedback control of two-component regulatory systems. *Annual Review of Microbiology*, 70 (1): 103–124.

Guilhen, C., Forestier, C. and Balestrino, D. (2017) Biofilm dispersal: multiple elaborate strategies for dissemination of bacteria with unique properties. *Molecular Microbiology*, 105 (2): 188–210.

Le Guillouzer, S., Groleau, M.-C. and Déziel, E. (2018) Two *rsaM* homologues encode central regulatory elements modulating quorum sensing in *Burkholderia thailandensis* O'Toole, G. (ed.). *Journal of Bacteriology*, 200 (14).

Guisbert, E., Rhodius, V.A., Ahuja, N., et al. (2007) Hfq modulates the sigmaE-mediated envelope stress response and the sigma32-mediated cytoplasmic stress response in *Escherichia coli*. *Journal of bacteriology*, 189 (5): 1963–73.

Harding, C.M., Hennon, S.W. and Feldman, M.F. (2018) Uncovering the mechanisms of *Acinetobacter baumannii* virulence. *Nature Reviews Microbiology*, 16 (2): 91–102.

Harding, C.M., Tracy, E.N., Carruthers, M.D., et al. (2013) *Acinetobacter baumannii* strain M2 produces type IV Pili which play a role in natural transformation and twitching motility but not surface-associated motility. *mBio*, 4 (4).

Hare, J.M., Adhikari, S., Lambert, K. V., et al. (2012) The *Acinetobacter* regulatory UmuDAb protein cleaves in response to DNA damage with chimeric LexA/UmuD characteristics. *FEMS Microbiology Letters*, 334 (1): 57–65.

Heilmann, C., Schweitzer, O., Gerke, C., et al. (1996) Molecular basis of intercellular adhesion in the biofilm-forming *Staphylococcus epidermidis*. *Molecular Microbiology*, 20 (5): 1083–1091.

Henrichsen, J. (1975) The occurence of twitching motility among Gram-negative bacteria. *Acta Pathologica Microbiologica Scandinavica Section B Microbiology*, 83 B (3): 171–178.

Hoch, J.A. (2000) Two-component and phosphorelay signal transduction. *Current Opinion in Microbiology*, 3 (2): 165–170.

Hook, A.L., Chang, C.-Y., Yang, J., et al. (2012a) Combinatorial discovery of polymers resistant to bacterial attachment. *Nature Biotechnology*, 30 (9): 868–875. doi:10.1038/nbt.2316.

Hook, A.L., Chang, C.-Y., Yang, J., et al. (2012b) Polymer microarrays for high throughput discovery of biomaterials. *Journal of visualized experiments : JoVE*, (59): e3636.

Hook, A.L., Chang, C.-Y., Yang, J., et al. (2013) Discovery of novel materials with broad resistance to bacterial attachment using combinatorial polymer microarrays. *Advanced Materials (Deerfield Beach, Fla.)*, 25 (18): 2542.

Huang, Y., Zhou, Q., Wang, W., et al. (2019) *Acinetobacter baumannii* ventilator-associated pneumonia: Clinical efficacy of combined antimicrobial therapy and in vitro drug sensitivity test results. *Frontiers in Pharmacology*, 10: 92.

Hurley, J.C. (2016) World-wide variation in incidence of *Acinetobacter* associated ventilator associated pneumonia: a meta-regression. *BMC Infectious Diseases*, 16 (1): 577.

Inhülsen, S. (2011) Investigations on the quorum sensing circuitry in *Burkholderia cenocepacia* H111. PhD Thesis, University of Zurich. Zurich.

Ishikawa, M., Yoshimoto, S., Hayashi, A., et al. (2016) Discovery of a novel periplasmic protein that forms a complex with a trimeric autotransporter adhesin and peptidoglycan. *Molecular Microbiology*, 101 (3): 394–410.

Iwashkiw, J.A., Seper, A., Weber, B.S., et al. (2012) Identification of a general O-linked protein glycosylation system in *Acinetobacter baumannii* and its role in virulence and biofilm formation. *PLoS pathogens*, 8 (6): e1002758.

Iyer, R., Moussa, S.H., Durand-Réville, T.F., et al. (2018) *Acinetobacter baumannii* OmpA is a selective antibiotic permeant porin. *ACS Infectious Diseases*, 4 (3): 373–381.

Jacobs, A.C., Hood, I., Boyd, K.L., et al. (2010) Inactivation of phospholipase D diminishes *Acinetobacter baumannii* pathogenesis. *Infection and Immunity*, 78 (5): 1952–1962.

Jacobs, A.C., Thompson, M.G., Black, C.C., et al. (2014) AB5075, a highly virulent isolate of *Acinetobacter baumannii*, as a model strain for the evaluation of pathogenesis and antimicrobial treatments. *mBio*.

Jadhav, G.P., Chhabra, S.R., Telford, G., et al. (2011) Immunosuppressive but non-LasR-inducing analogues of the *Pseudomonas aeruginosa* quorum-sensing molecule *N*-(3-oxododecanoyl)- L -homoserine lactone. *Journal of Medicinal Chemistry*, 54 (9): 3348–3359.

Jawad, A., Heritage, J., Snelling, A.M., et al. (1996) Influence of relative humidity and suspending menstrua on survival of *Acinetobacter* spp. on dry surfaces. *Journal of clinical microbiology*, 34 (12): 2881–7.

Jenul, C. and Horswill, A.R. (2018) Regulation of *Staphylococcus aureus* virulence. *Microbiology Spectrum*, 6 (1).

Ji, G., Beavis, R.C. and Novick, R.P. (1995) Cell density control of staphylococcal virulence mediated by an octapeptide pheromone. *Proceedings of the National Academy of Sciences of the United States of America*, 92 (26): 12055–9.

Jin, J.S., Kwon, S.-O., Moon, D.C., et al. (2011) *Acinetobacter baumannii* secretes cytotoxic outer membrane protein A via outer membrane vesicles. Bereswill, S. (ed.). *PLoS ONE*, 6 (2): e17027.

Johnson, T.L., Waack, U., Smith, S., et al. (2015) *Acinetobacter baumannii* is dependent on the type II secretion system and its substrate LipA for lipid utilization and *in vivo* fitness. *Journal of bacteriology*, 198 (4): 711–9.

Josenhans, C. and Suerbaum, S. (2002) The role of motility as a virulence factor in bacteria. *International Journal of Medical Microbiology*, 291 (8): 605–614.

Juni, E. (2015) "*Acinetobacter*." In *Bergey's Manual of Systematics of Archaea and Bacteria*. Chichester, UK: John Wiley & Sons, Ltd. pp. 1–26.

Kalanuria, A.A., Ziai, W., Zai, W., et al. (2014) Ventilator-associated pneumonia in the ICU. *Critical care (London, England)*, 18 (2): 208.

Kalivoda, E.J., Horzempa, J., Stella, N.A., et al. (2011) New vector tools with a hygromycin resistance marker for use with opportunistic pathogens. *Molecular biotechnology*, 48 (1): 7–14.

Kamaraju, S., Ch, S., Ratnakar, K.S., et al. (2019) Quorum sensing system in *Acinetobacter baumannii* : a potential target for new drug development. *Journal of Applied Microbiology*, p. jam.14330.

Kang, H., Gan, J., Zhao, J., et al. (2017) Crystal structure of *Pseudomonas aeruginosa* RsaL bound to promoter DNA reaffirms its role as a global regulator involved in quorum-sensing. *Nucleic acids research*, 45 (2): 699–710.

Kang, Y.-S. and Park, W. (2010) Contribution of quorum-sensing system to hexadecane degradation and biofilm formation in *Acinetobacter* sp. strain DR1. *Journal of Applied Microbiology*, 109 (5): no-no.

Karah, N., Sundsfjord, A., Towner, K., et al. (2012) Insights into the global molecular epidemiology of carbapenem non-susceptible clones of *Acinetobacter baumannii*. *Drug Resistance Updates*, 15 (4): 237–247.

Karimova, G., Pidoux, J., Ullmann, A., et al. (1998) A bacterial two-hybrid system based on a reconstituted signal transduction pathway. *Proceedings of the National Academy of Sciences of the United States of America*, 95 (10): 5752.

Kavita, K., de Mets, F. and Gottesman, S. (2018) New aspects of RNA-based regulation by Hfq and its partner sRNAs. *Current Opinion in Microbiology*, 42: 53–61.

Kearns, D.B. (2010) A field guide to bacterial swarming motility. *Nature reviews. Microbiology*, 8 (9): 634–44.

Kenyon, J.J. and Hall, R.M. (2013) Variation in the complex carbohydrate biosynthesis loci of *Acinetobacter baumannii* genomes. *PloS one*, 8 (4): e62160.

Khatoon, Z., McTiernan, C.D., Suuronen, E.J., et al. (2018) Bacterial biofilm formation on implantable devices and approaches to its treatment and prevention. *Heliyon*, 4 (12): e01067.

de Kievit, T., Seed, P.C., Nezezon, J., et al. (1999) RsaL, a novel repressor of virulence gene expression in *Pseudomonas aeruginosa*. *Journal of bacteriology*, 181 (7): 2175–84.

Kim, B.-N., Peleg, A.Y., Lodise, T.P., et al. (2009a) Management of meningitis due to antibiotic-resistant *Acinetobacter* species. *The Lancet Infectious Diseases*, 9 (4): 245–255.

Kim, S.W., Choi, C.H., Moon, D.C., et al. (2009b) Serum resistance of *Acinetobacter baumannii* through the binding of factor H to outer membrane proteins. *FEMS Microbiology Letters*, 301 (2): 224–231.

Krašovec, R., Belavkin, R. V, Aston, J.A.D., et al. (2014) Mutation rate plasticity in rifampicin resistance depends on *Escherichia coli* cell-cell interactions. *Nature communications*, 5: 3742.

Kulesus, R.R., Diaz-Perez, K., Slechta, E.S., et al. (2008) Impact of the RNA chaperone Hfq on the fitness and virulence potential of uropathogenic *Escherichia coli*. *Infection and immunity*, 76 (7): 3019–26.

Kumar, A., Dalton, C., Cortez-Cordova, J., et al. (2010) Mini-Tn*7* vectors as genetic tools for single copy gene cloning in *Acinetobacter baumannii*. *Journal of Microbiological Methods*, 82 (3): 296–300.

Kuo, H.-Y., Chao, H.-H., Liao, P.-C., et al. (2017) Functional characterization of *Acinetobacter baumannii* lacking the RNA chaperone Hfq. *Frontiers in microbiology*, 8: 2068.

Ky, L. and Otto, M. (2015) Quorum-sensing regulation in staphylococci - an overview. *Front. Microbiol*, 6: 1174.

Ladant, D. and Ullmann, A. (1999) *Bordatella pertussis* adenylate cyclase: a toxin with multiple talents. *Trends in microbiology*, 7 (4): 172–6.

Latifi, A., Foglino, M., Tanaka, K., et al. (1996) A hierarchical quorum-sensing cascade in *Pseudomonas aeruginosa* links the transcriptional activators LasR and RhlR (VsmR) to expression of the stationary-phase sigma factor RpoS. *Molecular Microbiology*, 21 (6): 1137–1146.

Lee, J. and Zhang, L. (2015) The hierarchy quorum sensing network in *Pseudomonas aeruginosa*. *Protein & cell*, 6 (1): 26–41.

Lee, J.S., Choi, C.H., Kim, J.W., et al. (2010) *Acinetobacter baumannii* outer membrane protein a induces dendritic cell death through mitochondrial targeting. *The Journal of Microbiology*, 48 (3): 387–392.

Lee, K. and Yoon, S.S. (2017) *Pseudomonas aeruginosa* biofilm, a programmed bacterial life for fitness. *Journal of microbiology and biotechnology*, 27 (6): 1053–1064.

Leong, C.G., Bloomfield, R.A., Boyd, C.A., et al. (2017) The role of core and accessory type IV pilus genes in natural transformation and twitching motility in the bacterium *Acinetobacter baylyi*. Cascales, E. (ed.). *PLOS ONE*, 12 (8): e0182139.

Limansky, A.S., Mussi, M.A. and Viale, A.M. (2002) Loss of a 29-kilodalton outer membrane protein in *Acinetobacter baumannii* is associated with imipenem resistance. *Journal of Clinical Microbiology*, 40 (12): 4776–4778.

Lin, M.-F. and Lan, C.-Y. (2014) Antimicrobial resistance in *Acinetobacter baumannii*: From bench to bedside. *World journal of clinical cases*, 2 (12): 787–814.

Lin, M.-F., Lin, Y.-Y. and Lan, C.-Y. (2015) The role of the two-component system BaeSR in disposing chemicals through regulating transporter systems in *Acinetobacter baumannii*. Gao, F. (ed.). *PLOS ONE*, 10 (7): e0132843.

Lin, M.-F., Lin, Y.-Y., Yeh, H.-W., et al. (2014) Role of the BaeSR two-component system in the regulation of *Acinetobacter baumannii adeAB* genes and its correlation with tigecycline susceptibility. *BMC microbiology*, 14: 119.

Liou, M.-L., Soo, P.-C., Ling, S.-R., et al. (2014) The sensor kinase BfmS mediates virulence in *Acinetobacter baumannii*. *Journal of Microbiology, Immunology and Infection*, 47 (4): 275–281.

Loehfelm, T.W., Luke, N.R. and Campagnari, A.A. (2008) Identification and characterization of an *Acinetobacter baumannii* biofilm-associated protein. *Journal of Bacteriology*, 190 (3): 1036–1044.

López, M., Mayer, C., Fernández-García, L., et al. (2017) Quorum sensing network in clinical strains of *A. baumannii*: AidA is a new quorum quenching enzyme. *PloS one*, 12 (3): e0174454.

Luo, L., Wu, L., Xiao, Y., et al. (2015) Enhancing pili assembly and biofilm formation in *Acinetobacter baumannii* ATCC19606 using non-native acyl-homoserine lactones. *BMC microbiology*, 15: 62.

Marchand, I., Damier-Piolle, L., Courvalin, P., et al. (2004) Expression of the RND-type efflux pump AdeABC in *Acinetobacter baumannii* is regulated by the AdeRS two-component system. *Antimicrobial Agents and Chemotherapy*, 48 (9): 3298–3304.

Mattick, J.S., Whitchurch, C.B. and Alm, R.A. (1996) The molecular genetics of type-4 fimbriae in *Pseudomonas aeruginosa* - a review. *Gene*, 179 (1): 147–155.

Mattiuzzo, M., Bertani, I., Ferluga, S., et al. (2011) The plant pathogen *Pseudomonas fuscovaginae* contains two conserved quorum sensing systems involved in virulence and negatively regulated by RsaL and the novel regulator RsaM. *Environmental Microbiology*, 13 (1): 145–162.

Mayer, C., Muras, A., Romero, M., et al. (2018) Multiple quorum quenching enzymes are active in the nosocomial pathogen *Acinetobacter baumannii* ATCC17978. *Frontiers in cellular and infection microbiology*, 8: 310.

McConnell, M.J., Actis, L. and Pachón, J. (2013) *Acinetobacter baumannii*: Human infections, factors contributing to pathogenesis and animal models. *FEMS Microbiology Reviews*, 37 (2): 130–155.

McGrath, S., Wade, D.S. and Pesci, E.C. (2004) Dueling quorum sensing systems in *Pseudomonas aeruginosa* control the production of the *Pseudomonas* quinolone signal (PQS). *FEMS Microbiology Letters*, 230 (1): 27–34.

McQueary, C.N., Kirkup, B.C., Si, Y., et al. (2012) Extracellular stress and lipopolysaccharide modulate *Acinetobacter baumannii* surface-associated motility. *Journal of Microbiology*, 50 (3): 434–443.

Michalska, K., Chhor, G., Clancy, S., et al. (2014) RsaM: a transcriptional regulator of *Burkholderia* spp. with novel fold. *The FEBS journal*, 281 (18): 4293–306.

Modarresi, F., Azizi, O., Shakibaie, M.R., et al. (2015) Iron limitation enhances acyl homoserine lactone (AHL) production and biofilm formation in clinical isolates of *Acinetobacter baumannii*. *Virulence*, 6 (2): 152–61.

Moffatt, J.H., Harper, M., Harrison, P., et al. (2010) Colistin resistance in *Acinetobacter baumannii* is mediated by complete loss of lipopolysaccharide production. *Antimicrobial agents and chemotherapy*, 54 (12): 4971–7.

Moon, D.C., Choi, C.H., Lee, J.H., et al. (2012) *Acinetobacter baumannii* outer membrane protein a modulates the biogenesis of outer membrane vesicles. *The Journal of Microbiology*, 50 (1): 155–160.

Moon, K.H., Weber, B.S. and Feldman, M.F. (2017) Subinhibitory concentrations of trimethoprim and sulfamethoxazole prevent biofilm formation by *Acinetobacter baumannii* through inhibition of Csu pilus expression. *Antimicrobial Agents and Chemotherapy*, 61 (9).

Morris, F.C., Dexter, C., Kostoulias, X., et al. (2019) The mechanisms of disease caused by *Acinetobacter baumannii*. *Frontiers in Microbiology*, 10: 1601.

Murray, E.J., Crowley, R.C., Truman, A., et al. (2014) Targeting *Staphylococcus aureus* quorum sensing with nonpeptidic small molecule inhibitors. *Journal of medicinal chemistry*, 57 (6): 2813–9.

Mussi, M.A., Gaddy, J.A., Cabruja, M., et al. (2010) The opportunistic human pathogen *Acinetobacter baumannii* senses and responds to light. *Journal of bacteriology*, 192 (24): 6336–45.

Mussi, M.A., Limansky, A.S. and Viale, A.M. (2005) Acquisition of resistance to carbapenems in multidrug-resistant clinical strains of *Acinetobacter baumannii*: Natural insertional inactivation of a gene encoding a member of a novel family of ß-barrel outer membrane proteins. *Antimicrobial Agents and Chemotherapy*, 49 (4): 1432–1440.

Nait Chabane, Y., Marti, S., Rihouey, C., et al. (2014) Characterisation of pellicles formed by *Acinetobacter baumannii* at the air-liquid interface. *PloS one*, 9 (10): e111660.

Nealson, K.H. (1977) Autoinduction of bacterial luciferase - Occurrence, mechanism and significance. *Archives of Microbiology*, 112 (1): 73–79.

Nemec, A., Krizova, L., Maixnerova, M., et al. (2011) Genotypic and phenotypic characterization of the *Acinetobacter calcoaceticus–Acinetobacter baumannii* complex with the proposal of *Acinetobacter pittii* sp. nov. (formerly *Acinetobacter* genomic species 3) and *Acinetobacter nosocomialis* sp. nov. (formerly *Acinetobacter* genomic species 13TU). *Research in Microbiology*, 162 (4): 393–404.

Ng, C.-K., How, K.-Y., Tee, K.-K., et al. (2019) Characterization and Transcriptome Studies of Autoinducer Synthase Gene from Multidrug Resistant *Acinetobacter baumannii* Strain 863. *Genes*, 10 (4): 282.

Niu, C., Clemmer, K.M., Bonomo, R.A., et al. (2008) Isolation and characterization of an autoinducer synthase from *Acinetobacter baumannii*. *Journal of Bacteriology*, 190 (9): 3386–3392.

Notredame, C., Higgins, D.G. and Heringa, J. (2000) T-Coffee: A novel method for fast and accurate multiple sequence alignment. *Journal of molecular biology*, 302 (1): 205–17.

Nowak, J., Zander, E., Stefanik, D., et al. (2017) High incidence of pandrug-resistant *Acinetobacter baumannii* isolates collected from patients with ventilator-associated pneumonia in Greece, Italy and Spain as part of the MagicBullet clinical trial. *The Journal of antimicrobial chemotherapy*, 72 (12): 3277–3282.

Nuccio, S.-P. and Bäumler, A.J. (2007) Evolution of the chaperone/usher assembly pathway: fimbrial classification goes Greek. *Microbiology and molecular biology reviews : MMBR*, 71 (4): 551–75.

O'Toole, G.A. (2011) Microtiter dish biofilm formation assay. *Journal of visualized experiments : JoVE*, (47).

O'Toole, G.A. and Kolter, R. (1998) Initiation of biofilm formation in *Pseudomonas fluorescens* WCS365 proceeds via multiple, convergent signalling pathways: a genetic analysis. *Molecular Microbiology*, 28 (3): 449–461.

O'Toole, G.A. and Wong, G.C. (2016) Sensational biofilms: surface sensing in bacteria. *Current Opinion in Microbiology*, 30: 139–146.

Ortori, C.A., Atkinson, S., Chhabra, S.R., et al. (2007) Comprehensive profiling of *N*-acylhomoserine lactones produced by *Yersinia pseudotuberculosis* using liquid chromatography coupled to hybrid quadrupole–linear ion trap mass spectrometry. *Analytical and Bioanalytical Chemistry*, 387 (2): 497–511.

Ortori, C.A., Dubern, J.-F., Chhabra, S.R., et al. (2011) Simultaneous quantitative profiling of *N*-acyl-L-homoserine lactone and 2-alkyl-4(1H)-quinolone families of quorum-sensing signaling molecules using LC-MS/MS. *Analytical and Bioanalytical Chemistry*, 399 (2): 839–850.

Ortori, C.A., Halliday, N., Cámara, M., et al. (2014) LC-MS/MS quantitative analysis of quorum sensing signal molecules. In *Humana Press*, New York, NY. pp. 255–270.

Pakharukova, N., Garnett, J.A., Tuittila, M., et al. (2015) Structural insight into archaic and alternative chaperone-usher pathways reveals a novel mechanism of pilus biogenesis. *PLoS Pathog*, 2015;11:e1005269

Pakharukova, N., Tuittila, M., Paavilainen, S., et al. (2018) Structural basis for *Acinetobacter baumannii* biofilm formation. *Proceedings of the National Academy of Sciences of the United States of America*, 115 (21): 5558–5563.

Palmer, J., Flint, S. and Brooks, J. (2007) Bacterial cell attachment, the beginning of a biofilm. *Journal of Industrial Microbiology & Biotechnology*, 34 (9): 577–588.

Papenfort, K. and Bassler, B.L. (2016) Quorum sensing signal-response systems in Gram-negative bacteria. *Nature reviews. Microbiology*, 14 (9): 576–88.

Peleg, A.Y., Jara, S., Monga, D., et al. (2009) *Galleria mellonella* as a model system to study *Acinetobacter baumannii* pathogenesis and therapeutics. *Antimicrobial Agents and Chemotherapy*, 53 (6): 2605.

Peleg, A.Y., Seifert, H. and Paterson, D.L. (2008) *Acinetobacter baumannii*: emergence of a successful pathogen. *Clinical microbiology reviews*, 21 (3): 538–82.

Pendleton, J.N., Gorman, S.P. and Gilmore, B.F. (2013) Clinical relevance of the ESKAPE pathogens. *Expert Review of Anti-infective Therapy*, 11 (3): 297–308.

Penwell, W.F., DeGrace, N., Tentarelli, S., et al. (2015) Discovery and characterization of new hydroxamate siderophores, Baumannoferrin A and B, produced by *Acinetobacter baumannii*. *ChemBioChem*, 16 (13): 1896–1904.

Pérez-Varela, M., Corral, J., Aranda, J., et al. (2019) Roles of efflux pumps from different superfamilies in the surface-associated motility and virulence of *Acinetobacter baumannii* ATCC 17978. *Antimicrobial Agents and Chemotherapy*, 63 (3).

Pérez-Varela, M., Corral, J., Vallejo, J.A., et al. (2017) Mutations in the ß-subunit of the RNA polymerase impair the surface-associated motility and virulence of *Acinetobacter baumannii*. *Infection and immunity*, 85 (8).

Pérez, A., Merino, M., Rumbo-Feal, S., et al. (2017) The FhaB/FhaC two-partner secretion system is involved in adhesion of *Acinetobacter baumannii* AbH12O-A2 strain. *Virulence*, 8 (6): 959–974.

Perez, F., Hujer, A.M., Hujer, K.M., et al. (2007) Global challenge of multidrug-resistant *Acinetobacter baumannii*. *Antimicrobial agents and chemotherapy*, 51 (10): 3471–84.

Del Pozo, J.L. (2018) Biofilm-related disease. *Expert Review of Anti-infective Therapy*, 16 (1): 51–65.

Proft, T. and Baker, E.N. (2009) Pili in Gram-negative and Gram-positive bacteria — structure, assembly and their role in disease. *Cellular and Molecular Life Sciences*, 66 (4): 613–635.

Proschak, A., Lubuta, P., Grün, P., et al. (2013) Structure and biosynthesis of Fimsbactins A-F, siderophores from *Acinetobacter baumannii* and *Acinetobacter baylyi*. *ChemBioChem*, 14 (5): 633–638.

Puri, A.W., Schaefer, A.L., Fu, Y., et al. (2017) Quorum sensing in a methane-oxidizing bacterium. *Journal of Bacteriology*, 199 (5).

Rabin, N., Zheng, Y., Opoku-Temeng, C., et al. (2015) Biofilm formation mechanisms and targets for developing antibiofilm agents. *Future Medicinal Chemistry*, 7 (4): 493–512.

Rampioni, G., Bertani, I., Zennaro, E., et al. (2006) The quorum-sensing negative regulator RsaL of *Pseudomonas aeruginosa* binds to the lasI promoter. *Journal of bacteriology*, 188 (2): 815–9.

Rampioni, G., Falcone, M., Heeb, S., et al. (2016) Unravelling the Genome-wide contributions of specific 2-alkyl-4-quinolones and PqsE to quorum sensing in *Pseudomonas aeruginosa*. Pesci, E. (ed.). *PLOS Pathogens*, 12 (11): e1006029.

Rampioni, G., Schuster, M., Greenberg, E.P., et al. (2007) RsaL provides quorum sensing homeostasis and functions as a global regulator of gene expression in *Pseudomonas aeruginosa*. *Molecular Microbiology*, 66 (6): 1557–1565.

Rather, P. (2019) "Regulation of a virulence switch in *Acinetobacter baumannii*." In *12th International Symposium on the biology of Acinetobacter*. Frankfurt (Germany), 2019.

Reboul, A., Lemaitre, N., Titecat, M., et al. (2014) *Yersinia pestis* requires the 2-component regulatory system OmpR-EnvZ to resist innate immunity during the early and late stages of plague. *Journal of Infectious Diseases*, 210 (9): 1367–1375.

Richmond, G.E., Evans, L.P., Anderson, M.J., et al. (2016) The *Acinetobacter baumannii* two-component system *adeRS* regulates genes required for multidrug efflux, biofilm formation, and virulence in a strain-specific manner. *mBio*, 7 (2): e00430-16.

Roca, I., Espinal, P., Vila-Farrés, X., et al. (2012) The *Acinetobacter baumannii* oxymoron: Commensal hospital dweller turned pan-drug-resistant menace. *Frontiers in microbiology*, 3: 148.

Rocha, I.V., Xavier, D.E., Almeida, K.R.H. de, et al. (2018) Multidrug-resistant *Acinetobacter baumannii* clones persist on hospital inanimate surfaces. *The Brazilian Journal of Infectious Diseases*, 22 (5): 438–441.

Römling, U. and Balsalobre, C. (2012) Biofilm infections, their resilience to therapy and innovative treatment strategies. *Journal of Internal Medicine*, 272 (6): 541–561.

Ronish, L.A., Lillehoj, E., Fields, J.K., et al. (2019) The structure of PilA from *Acinetobacter baumannii* AB5075 suggests a mechanism for functional specialization in *Acinetobacter* type IV pili. *Journal of Biological Chemistry*, 294 (1): 218–230.

Roux, D., Cywes-Bentley, C., Zhang, Y.-F., et al. (2015) Identification of poly- *N*- acetylglucosamine as a major polysaccharide component of the *Bacillus subtilis* Biofilm Matrix. *Journal of Biological Chemistry*, 290 (31): 19261–19272.

Rumbo-Feal, S., Gómez, M.J., Gayoso, C., et al. (2013) Whole transcriptome analysis of *Acinetobacter baumannii* assessed by RNA-sequencing reveals different mRNA expression profiles in biofilm compared to planktonic cells. *PloS one*, 8 (8): e72968.

Rumbo-Feal, S., Pérez, A., Ramelot, T.A., et al. (2017) Contribution of the *A. baumannii A1S_0114* gene to the interaction with eukaryotic cells and virulence. *Frontiers in Cellular and Infection Microbiology*, 7: 108.

Runci, F., Gentile, V., Frangipani, E., et al. (2019) Contribution of active iron uptake to *Acinetobacter baumannii* pathogenicity. *Infection and Immunity*, 87 (4).

Russo, T.A., Luke, N.R., Beanan, J.M., et al. (2010) The K1 capsular polysaccharide of *Acinetobacter baumannii* strain 307-0294 is a major virulence factor. *Infection and immunity*, 78 (9): 3993–4000.

Russo, T.A., Manohar, A., Beanan, J.M., et al. (2016) The response regulator BfmR is a potential drug target for *Acinetobacter baumannii*. *mSphere*, 1 (3): e00082-16.

Rutherford, S.T. and Bassler, B.L. (2012) Bacterial quorum sensing: its role in virulence and possibilities for its control. *Cold Spring Harbor perspectives in medicine*, 2 (11): a012427.

Sahu, P.K., Iyer, P.S., Oak, A.M., et al. (2012) Characterization of eDNA from the Clinical Strain *Acinetobacter baumannii* AIIMS 7 and Its Role in Biofilm Formation. *The Scientific World Journal*, 2012: 1–10.

Sakuragi, Y. and Kolter, R. (2007) Quorum-sensing regulation of the biofilm matrix genes (*pel*) of *Pseudomonas aeruginosa*. *Journal of bacteriology*, 189 (14): 5383–6.

Sanni, O., Chang, C.-Y., Anderson, D.G., et al. (2015) Bacterial attachment to polymeric materials correlates with molecular flexibility and hydrophilicity. *Advanced healthcare materials*, 4 (5): 695–701.

Schuster, M. and Greenberg, E.P. (2007) Early activation of quorum sensing in *Pseudomonas aeruginosa* reveals the architecture of a complex regulon. *BMC Genomics*, 8 (1): 287.

Schuster, M. and Peter Greenberg, E. (2006) A network of networks: quorum-sensing gene regulation in *Pseudomonas aeruginosa*. *International Journal of Medical Microbiology*, 296 (2–3): 73–81.

Shapiro, J.A. and Wencewicz, T.A. (2016) Acinetobactin isomerization enables adaptive iron acquisition in *Acinetobacter baumannii* through pH-triggered siderophore swapping. *ACS Infectious Diseases*, 2 (2): 157–168.

Shukla, S.K. and Rao, T.S. (2017) An Improved Crystal Violet Assay for Biofilm Quantification in 96-Well Microtitre Plate. *BioRxiv*.

Solano, C., Echeverz, M. and Lasa, I. (2014) Biofilm dispersion and quorum sensing. *Current Opinion in Microbiology*, 18: 96–104.

Soukarieh, F., Vico Oton, E., Dubern, J.-F., et al. (2018) In silico and in vitro-guided identification of inhibitors of alkylquinolone-dependent quorum sensing in *Pseudomonas aeruginosa*. *Molecules (Basel, Switzerland)*, 23 (2).

Thoendel, M., Kavanaugh, J.S., Flack, C.E., et al. (2011) Peptide signaling in the Staphylococci. *Chemical Reviews*, 111 (1): 117–151.

Tipton, K.A., Chin, C.-Y., Farokhyfar, M., et al. (2018) Role of capsule in resistance to disinfectants, host antimicrobials, and desiccation in *Acinetobacter baumannii*. *Antimicrobial agents and chemotherapy*, 62 (12).

Tipton, K.A., Dimitrova, D. and Rather, P.N. (2015) Phase-variable control of multiple phenotypes in *Acinetobacter baumannii* strain AB5075. *Journal of bacteriology*, 197 (15): 2593–9.

Tipton, K.A., Farokhyfar, M. and Rather, P.N. (2017) Multiple roles for a novel RND-type efflux system in *Acinetobacter baumannii* AB5075. *MicrobiologyOpen*, 6 (2).

Tipton, K.A. and Rather, P.N. (2017) An *ompR-envZ* two-component system ortholog regulates phase variation, osmotic tolerance, motility, and virulence in *Acinetobacter baumannii* strain AB5075. *Journal of bacteriology*, 199 (3).

Tomaras, A.P., Dorsey, C.W., Edelmann, R.E., et al. (2003) Attachment to and biofilm formation on abiotic surfaces by *Acinetobacter baumannii*: involvement of a novel chaperone-usher pili assembly system. *Microbiology*, 149 (12): 3473–3484.

Tomaras, A.P., Flagler, M.J., Dorsey, C.W., et al. (2008) Characterization of a two-component regulatory system from *Acinetobacter baumannii* that controls biofilm formation and cellular morphology. *Microbiology*, 154 (11): 3398–3409.

Tomlin, K.L., Malott, R.J., Ramage, G., et al. (2005) Quorum-sensing mutations affect attachment and stability of *Burkholderia cenocepacia* biofilms. *Applied and environmental microbiology*, 71 (9): 5208–18.

Di Tommaso, P., Moretti, S., Xenarios, I., et al. (2011) T-Coffee: a web server for the multiple sequence alignment of protein and RNA sequences using structural information and homology extension. *Nucleic acids research*, 39 (Web Server issue): W13-7.

Toyofuku, M., Inaba, T., Kiyokawa, T., et al. (2016) Environmental factors that shape biofilm formation. *Bioscience, Biotechnology, and Biochemistry*, 80 (1): 7–12.

Traglia, G.M., Place, K., Dotto, C., et al. (2018) Interspecies DNA acquisition by a naturally competent *Acinetobacter baumannii* strain. *bioRxiv*, p. 308833.

Uzelac, G., Patel, H.K., Devescovi, G., et al. (2017) Quorum sensing and RsaM regulons of the rice pathogen *Pseudomonas fuscovaginae*. *Microbiology*, 163 (5): 765–777.

Venturi, V. (2006) Regulation of quorum sensing in *Pseudomonas*. *FEMS Microbiology Reviews*, 30 (2): 274–291.

Vorregaard, M. (2008) Comstat2 - a modern 3D image analysis environment for biofilms, in Informatics and mathematical modelling. *University of Denmark: Kogens Lyngby, Denmark*.

Voth, W. and Jakob, U. (2017) Stress-activated chaperones: a first line of defense. *Trends in biochemical sciences*, 42 (11): 899–913.

Wan, B., Zhang, Q., Tao, J., et al. (2016) Global transcriptional regulation by H-NS and its biological influence on the virulence of Enterohemorrhagic *Escherichia coli*. *Gene*, 588 (2): 115–123.

Wand, M.E., Bock, L.J., Turton, J.F., et al. (2012) *Acinetobacter baumannii* virulence is enhanced in *Galleria mellonella* following biofilm adaptation. *Journal of Medical Microbiology*, 61 (Pt_4): 470–477.

Wang, X., Cole, C.G., DuPai, C.D., et al. (2020) Protein aggregation is associated with *Acinetobacter baumannii* desiccation tolerance. *Microorganisms*, 8 (3): 343.

Wang, Z., Gerstein, M. and Snyder, M. (2009) RNA-Seq: a revolutionary tool for transcriptomics. *Nature reviews. Genetics*, 10 (1): 57–63.

Weber, B.S., Harding, C.M. and Feldman, M.F. (2015a) Pathogenic *Acinetobacter*: from the cell surface to infinity and beyond. *Journal of bacteriology*, 198 (6): 880–7.

Weber, B.S., Ly, P.M., Irwin, J.N., et al. (2015b) A multidrug resistance plasmid contains the molecular switch for type VI secretion in *Acinetobacter baumannii*. *Proceedings of the National Academy of Sciences*, 112 (30): 9442–9447.

Weber, B.S., Miyata, S.T., Iwashkiw, J.A., et al. (2013) Genomic and functional analysis of the type VI secretion system in *Acinetobacter* Cascales, E. (ed.). *PLoS ONE*, 8 (1): e55142.

Wei, J.-R. and Lai, H.-C. (2006) *N*-Acylhomoserine lactone-dependent cell-to-cell communication and social behavior in the genus *Serratia*. *International Journal of Medical Microbiology*, 296 (2–3): 117–124.

Weinstein, R.A., Gaynes, R. and Edwards, J.R. (2005) Overview of nosocomial infections caused by Gram-negative bacilli. *Clinical Infectious Diseases*, 41 (6): 848–854.

Weintrob, A.C., Murray, C.K., Xu, J., et al. (2018) Early infections complicating the care of combat casualties from Iraq and Afghanistan. *Surgical infections*, 19 (3): 286–297.

Whitehead, N.A., Barnard, A.M.L., Slater, H., et al. (2001) Quorum-sensing in Gram-negative bacteria. *FEMS Microbiology Reviews*, 25 (4): 365–404.

Wieland, K., Chhatwal, P. and Vonberg, R.-P. (2018) Nosocomial outbreaks caused by *Acinetobacter baumannii* and *Pseudomonas aeruginosa*: Results of a systematic review. *American Journal of Infection Control*, 46 (6): 643–648.

Wilharm, G., Piesker, J., Laue, M., et al. (2013) DNA Uptake by the nosocomial pathogen *Acinetobacter baumannii* occurs during movement along wet surfaces. *Journal of Bacteriology*, 195 (18): 4146–4153.

Williams, P. and Cámara, M. (2009) Quorum sensing and environmental adaptation in *Pseudomonas aeruginosa*: a tale of regulatory networks and multifunctional signal molecules. *Current Opinion in Microbiology*, 12 (2): 182–191.

Williams, P., Winzer, K., Chan, W.C., et al. (2007) Look who's talking: communication and quorum sensing in the bacterial world. *Philosophical transactions of the Royal Society of London. Series B, Biological sciences*, 362 (1483): 1119–34.

Wilton, R., Ahrendt, A.J., Shinde, S., et al. (2018) A new suite of plasmid vectors for fluorescence-based imaging of root colonizing pseudomonads. *Frontiers in Plant Science*, 8: 2242.

Winson, M.K., Swift, S., Fish, L., et al. (1998) Construction and analysis of *luxCDABE* -based plasmid sensors for investigating *N*-acyl homoserine lactone-mediated quorum sensing. *FEMS Microbiology Letters*, 163 (2): 185–192.

Wisplinghoff, H., Bischoff, T., Tallent, S.M., et al. (2004) Nosocomial bloodstream infections in US hospitals: Analysis of 24,179 cases from a prospective nationwide surveillance study. *Clinical Infectious Diseases*, 39 (3): 309–317.

Withers, R., Doherty, G.P., Jordan, M., et al. (2014) AtfA, a new factor in global regulation of transcription in *A cinetobacter* spp. *Molecular Microbiology*, 93 (6)

World Health Organization (2017) *WHO publishes list of bacteria for which new antibiotics are urgently needed*. Available at: https://www.who.int/news-room/detail/27-02-2017-who-publishes-list-of-bacteria-for-which-new-antibiotics-are-urgently-needed (Accessed: 12 September 2019).

van der Woude, M.W. and Bäumler, A.J. (2004) Phase and antigenic variation in bacteria. *Clinical microbiology reviews*, 17 (3): 581–611.

www.comstat.dk

Xiao, J., Zhang, C. and Ye, S. (2019) *Acinetobacter baumannii* meningitis in children: a case series and literature review. *Infection*, 47 (4): 643–649.

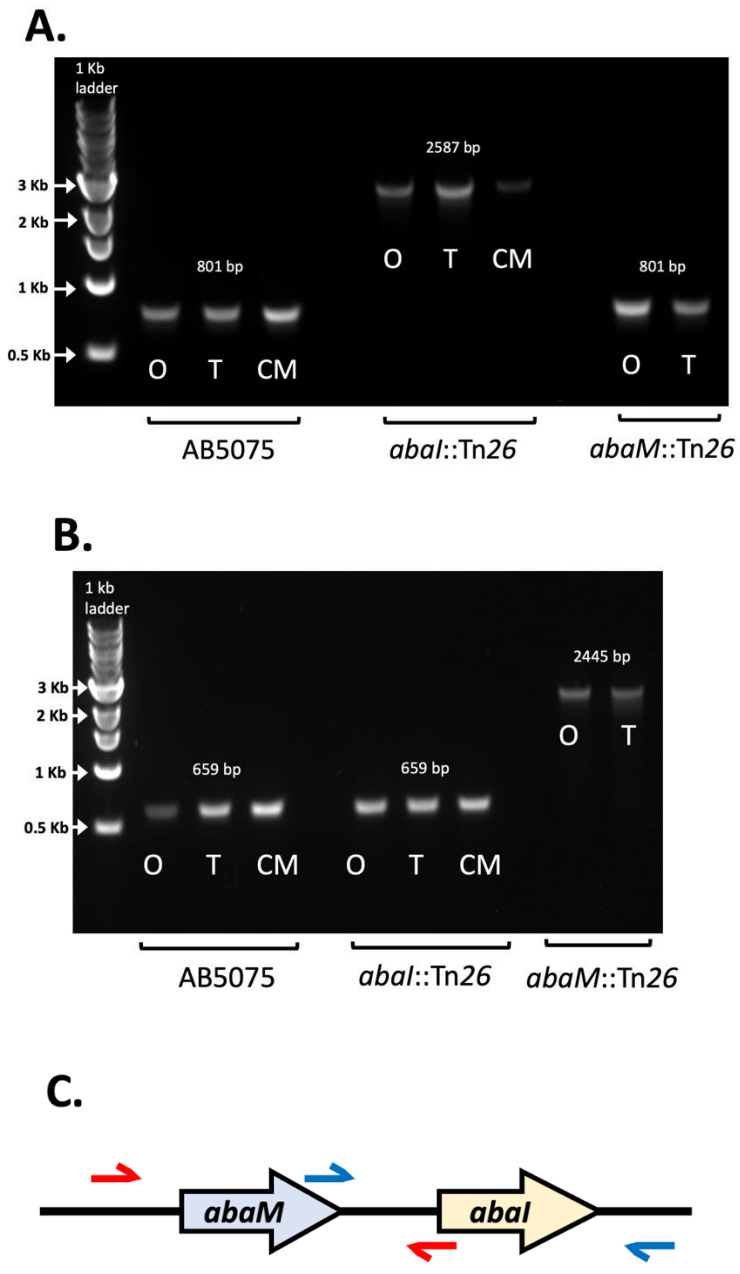
Yamamoto, S., Okujo, N. and Sakakibara, Y. (1994) Isolation and structure elucidation of acinetobactin, a novel siderophore from *Acinetobacter baumannii*. *Archives of Microbiology*, 162 (4): 249–254.

Yang, Y.-S., Chen, H.-Y., Hsu, W.-J., et al. (2019) Overexpression of AdeABC efflux pump associated with tigecycline resistance in clinical *Acinetobacter nosocomialis* isolates. *Clinical Microbiology and Infection*, 25 (4): 512.e1-512.e6.

Ye, J., Coulouris, G., Zaretskaya, I., et al. (2012) Primer-BLAST: a tool to design target-specific primers for polymerase chain reaction. *BMC bioinformatics*, 13: 134.

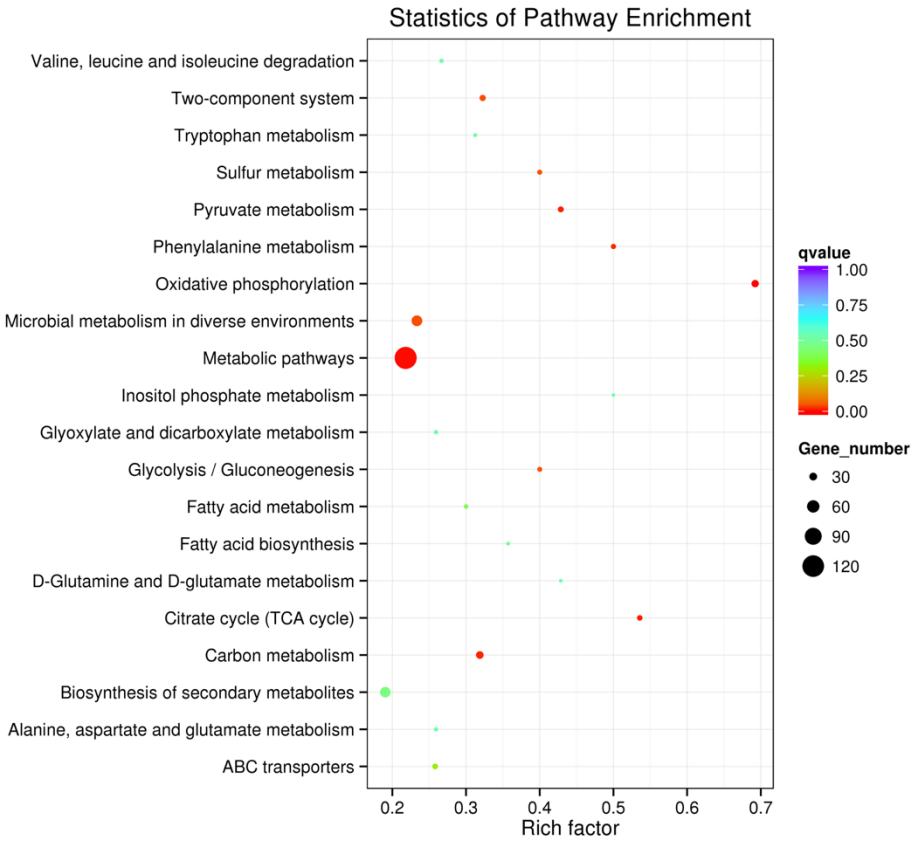
Zarrilli, R., Pournaras, S., Giannouli, M., et al. (2013) Global evolution of multidrug-resistant *Acinetobacter baumannii* clonal lineages. *International Journal of Antimicrobial Agents*. 41 (1) pp. 11–19.

8. Supplementary material

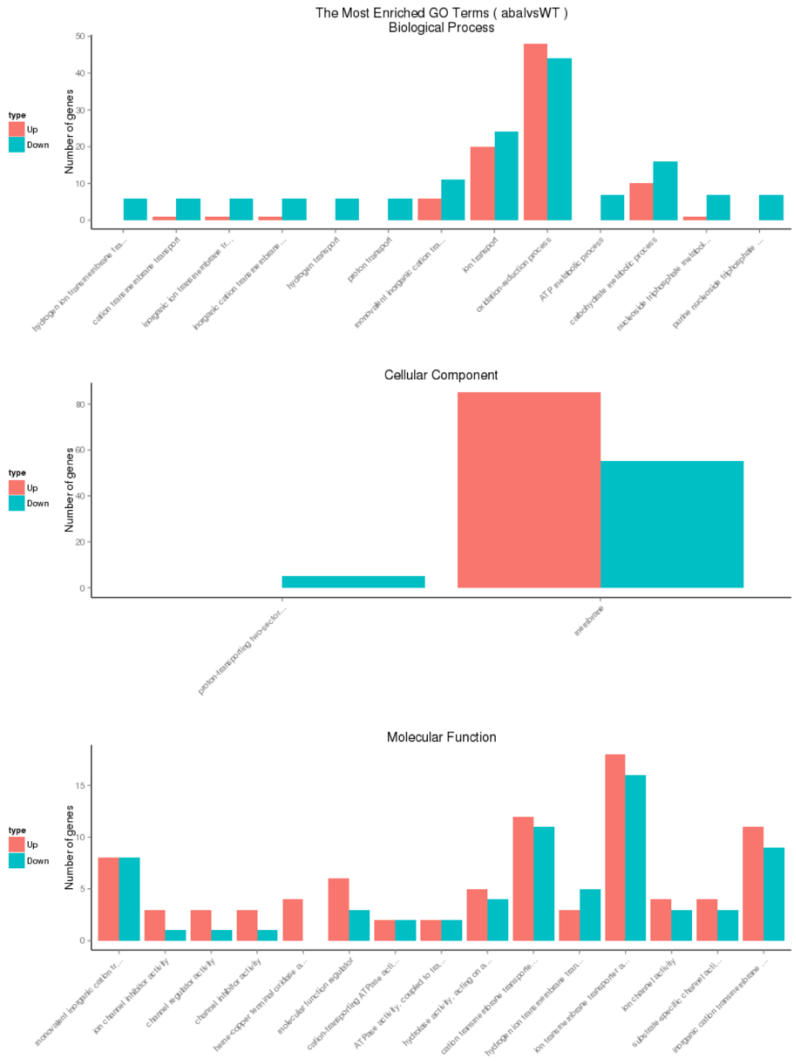


Supplementary Material Figure S1: Colony PCR of pure colony variants stocks. (A) PCR using primers amplifying the *abaI* locus. Only the *abaI* transposon mutants showed bands corresponding the the *abaI* locus amplicon (801 bp) plus the 1786 bp of the Tn*26* transposon (2587 bp band). **(B)** PCR using primers amplifying the *abaM* locus. Only the *abaM* transposon mutants showed bands corresponding the the wild-type *abaM* locus amplicon (659 bp) plus the 1786 bp of the Tn*26* transposon (2445 bp band). **(C)** QS locus with the hybridization sites of the *abaM* locus PCR (red) and the *abaI* locus PCR (blue). O = Opaque colony variant, T = Translucent colony variant, CM = Capsule mutant (isolated during the phase separation but not used in this project), bp = base pairs, Kb = kilobase pairs.

A.

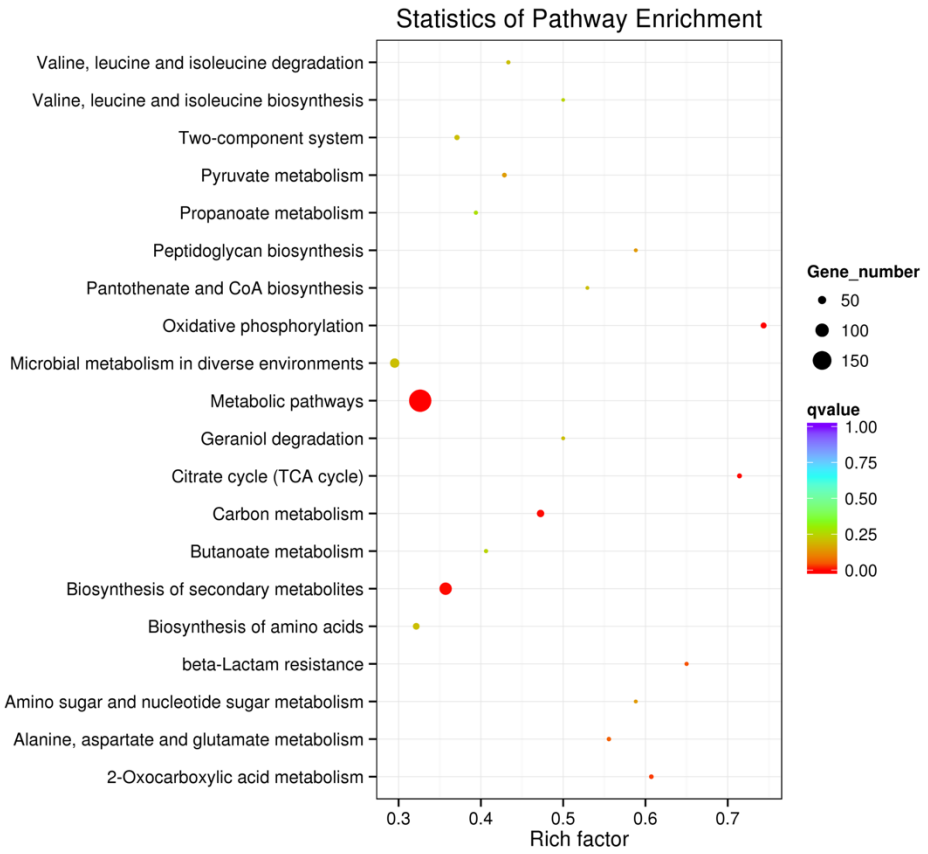

Statistics of Pathway Enrichment
Valine, leucine and isoleucine degradation
Two-component system
Tryptophan metabolism
Sulfur metabolism
Pyruvate metabolism
Phenylalanine metabolism
Oxidative phosphorylation
Microbial metabolism in diverse environments
Metabolic pathways
Inositol phosphate metabolism
Glyoxylate and dicarboxylate metabolism
Glycolysis / Gluconeogenesis
Fatty acid metabolism
Fatty acid biosynthesis
D-Glutamine and D-glutamate metabolism
Citrate cycle (TCA cycle)
Carbon metabolism
Biosynthesis of secondary metabolites
Alanine, aspartate and glutamate metabolism
ABC transporters
0.2
0.3
0.4
0.5
0.6
0.7
Rich factor
qvalue
1.00
0.75
0.50
0.25
0.00
Gene_number
30
60
90
120

B.

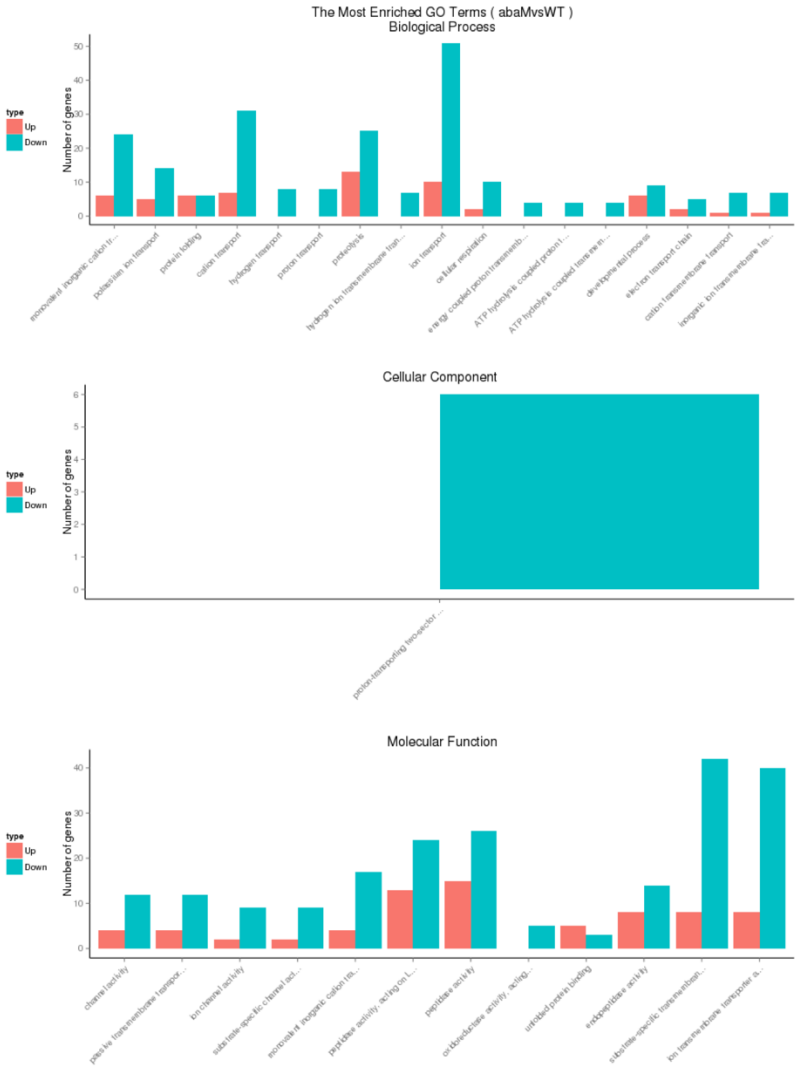


Supplementary Material Figure S2: *abaI*::Tn26/AB5075 differentially expressed genes enrichment analysis. (A) Scatter plot of KEGG pathway enrichment analysis. **(B)** Bar chart of GO terms enrichment analysis.

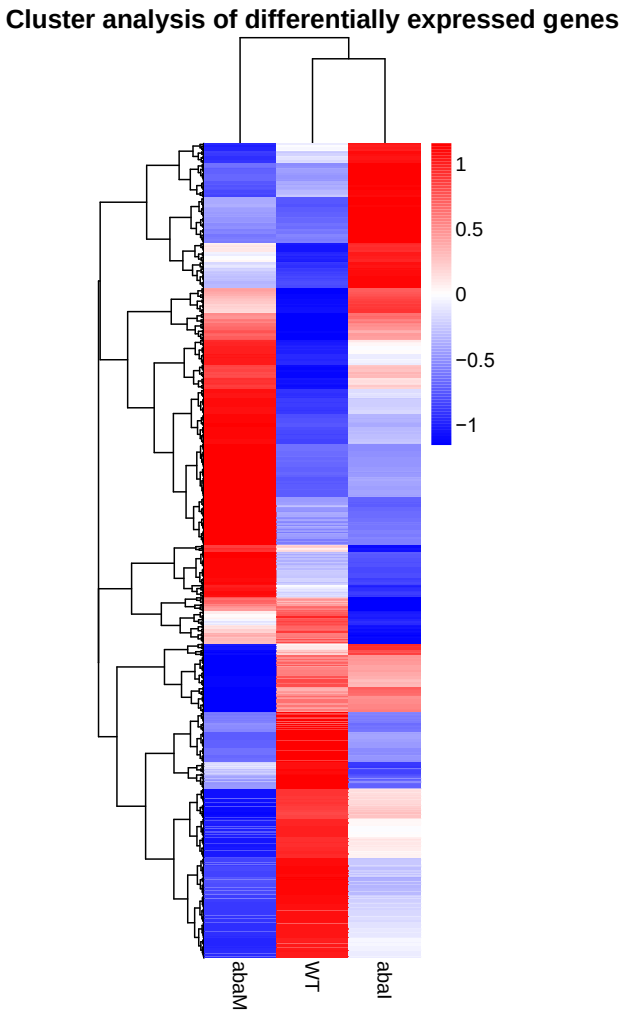
A.


Statistics of Pathway Enrichment
Valine, leucine and isoleucine degradation
Valine, leucine and isoleucine biosynthesis
Two-component system
Pyruvate metabolism
Propanoate metabolism
Peptidoglycan biosynthesis
Pantothenate and CoA biosynthesis
Oxidative phosphorylation
Microbial metabolism in diverse environments
Metabolic pathways
Geraniol degradation
Citrate cycle (TCA cycle)
Carbon metabolism
Butanoate metabolism
Biosynthesis of secondary metabolites
Biosynthesis of amino acids
beta-Lactam resistance
Amino sugar and nucleotide sugar metabolism
Alanine, aspartate and glutamate metabolism
2-Oxocarboxylic acid metabolism
0.3
0.4
0.5
0.6
0.7
Rich factor
Gene_number
50
100
150
qvalue
1.00
0.75
0.50
0.25
0.00

B.



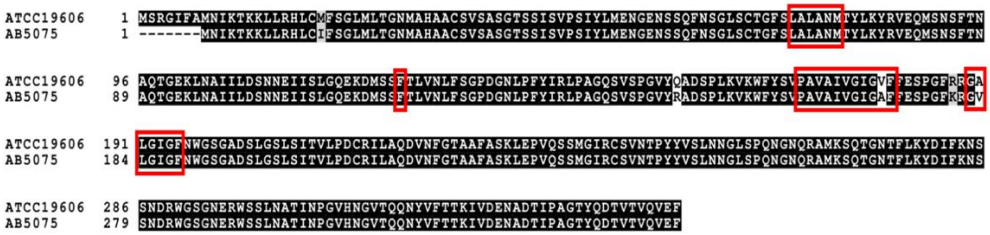
Supplementary Material Figure S3: *abaM*::Tn26/AB5075 differentially expressed genes enrichment analysis. (A) Scatter plot of KEGG pathway enrichment analysis. **(B)** Bar chart of GO terms enrichment analysis.



Supplementary Material Figure S4: Heat cluster of differentially expressed genes between AB5075 (WT), *abaI*::Tn26 (abaI) and *abaM*::Tn26 (abaM). Genes are clustered by expression pattern, revealing groups of genes with similar expression within a strain and between them. Colours represent the relative expression for each gene.



Supplementary Material Figure S5: AbaR protein sequence alignment between *A. baumannii* AB5075 and *A. nosocomialis* M2. Alignment created using T-Coffee and formatted using BoxShade (Notredame et al., 2000; Di Tommaso et al., 2011)**.** Amino acids with black background are conserved across the sequence. Amino acids with a grey background indicate a conservative substitution. Amino acids with white background indicate non-conservative substitution. Residues that are proposed to form hydrogen bonds with the ligand are indicated with red boxes (A38, N56, Q63, T131).



Supplementary Material Figure S6: CsuE protein sequence alignment of *A. baumannii* ATCC 19606 and *A. baumannii* AB5075. Alignment created using T-Coffee and formatted using BoxShade (Notredame et al., 2000; Di Tommaso et al., 2011)**.** Amino acids with black background are conserved across the sequence. Amino acids with a grey background indicate a conservative substitution. Amino acids with white background indicate non-conservative substitution. Conserved hydrophobic motifs present in the hydrophobic finger-like loops are indicated by red boxes.

Supplementary Table 1: Differentially expressed genes (log_2(fold change) ≥ 1) in *abaI*::Tn26 (compared with AB5075 wild-type).

Gene id	Log_2(Fold change)	Description	NCBI Protein Accession
ABUW_RS18385	4.3142	N-acylhomoserine lactone synthase	WP_001020940.1
ABUW_RS07260	4.2853	SCPU domain-containing protein	WP_000876475.1
ABUW_RS07255	4.1072	protein CsuA	WP_000577009.1
ABUW_RS07265	3.9262	molecular chaperone	WP_001065473.1
ABUW_RS07250	3.9062	SCPU domain-containing protein	WP_000790104.1
ABUW_RS07275	3.692	protein CsuE	WP_002017500.1
ABUW_RS07270	3.6287	fimbrial biogenesis outer membrane usher protein	WP_000603294.1
ABUW_RS07245	2.8129	TetR/AcrR family transcriptional regulator	WP_000590096.1
ABUW_RS07925	1.9432	alcohol dehydrogenase	WP_000874704.1
ABUW_RS01970	1.9355	flavohemoprotein	WP_000188888.1
ABUW_RS07910	1.9263	aldehyde dehydrogenase	WP_001269058.1
ABUW_RS07630	1.8189	hypothetical protein	WP_000783724.1
ABUW_RS07640	1.7361	hypothetical protein	WP_000772607.1
ABUW_RS07620	1.5361	hypothetical protein	WP_000020771.1
ABUW_RS07905	1.5245	ethanolamine permease	WP_001075439.1
ABUW_RS07625	1.4155	LLM class flavin-dependent oxidoreductase	WP_001257199.1
ABUW_RS07240	1.4129	hypothetical protein	WP_000637306.1
ABUW_RS08275	1.402	DNA methylase	WP_000652017.1
ABUW_RS06205	1.3599	DNA helicase	WP_000106166.1
ABUW_RS07280	1.3354	hypothetical protein	WP_000821199.1
ABUW_RS08025	1.3233	hypothetical protein	WP_001092426.1
ABUW_RS07895	1.3225	ethanolamine ammonia-lyase subunit EutC	WP_000774022.1
ABUW_RS19740	1.3116	hypothetical protein	WP_002017532.1
ABUW_RS08010	1.3043	hypothetical protein	WP_001243508.1
ABUW_RS07980	1.2832	glutathione S-transferase family protein	WP_001279985.1
ABUW_RS07800	1.2821	membrane protein	WP_001228338.1

ABUW_RS08160	1.2796	3-oxoacyl-ACP reductase	WP_000132115.1
ABUW_RS07445	1.2788	dicarboxylate/amino acid:cation symporter	WP_000347180.1
ABUW_RS08155	1.2734	acetyl-CoA C-acyltransferase	WP_000047940.1
ABUW_RS05005	1.2604	alpha/beta hydrolase	WP_000149921.1
ABUW_RS08165	1.2485	hypothetical protein	WP_001097352.1
ABUW_RS08145	1.2425	LysR family transcriptional regulator	WP_001024733.1
ABUW_RS19150	1.2359	hypothetical protein	WP_001024502.1
ABUW_RS11580	1.2324	taurine ABC transporter permease	WP_001092656.1
ABUW_RS07985	1.2211	short-chain dehydrogenase	WP_000135428.1
ABUW_RS08190	1.2166	phospholipase C%2C phosphocholine-specific	WP_000633003.1
ABUW_RS07715	1.2132	2-amino-4-hydroxy-6-hydroxymethyldihydropteridine pyrophosphokinase	WP_000993407.1
ABUW_RS08170	1.2116	esterase	WP_000588779.1
ABUW_RS19155	1.2107	hypothetical protein	WP_000241707.1
ABUW_RS07725	1.2067	K(+)-transporting ATPase subunit B	WP_001097170.1
ABUW_RS07435	1.186	MFS transporter	WP_001066110.1
ABUW_RS11590	1.1859	taurine ABC transporter substrate-binding protein	WP_000105187.1
ABUW_RS19145	1.1712	transcriptional regulator	WP_000096600.1
ABUW_RS07920	1.1707	alpha/beta hydrolase	WP_001098135.1
ABUW_RS07955	1.1695	aminopeptidase N	WP_001017234.1
ABUW_RS05010	1.1572	sulfate ABC transporter substrate-binding protein	WP_001212600.1
ABUW_RS07845	1.1519	tRNA (adenosine(37)-N6)-threonylcarbamoyltransferase complex ATPase subunit type 1 TsaE	WP_031944287.1
ABUW_RS08125	1.1426	membrane protein	WP_001169538.1
ABUW_RS07465	1.1379	methionine ABC transporter ATP-binding protein	WP_000614025.1
ABUW_RS19770	1.1377	hypothetical protein	-
ABUW_RS08255	1.132	hypothetical protein	WP_001238662.1
ABUW_RS19165	1.1273	toxic anion resistance protein	WP_000933769.1
ABUW_RS07360	1.123	acyl-CoA desaturase	WP_000032710.1

ABUW_RS19170	1.1197	hypothetical protein	WP_001093570.1
ABUW_RS07935	1.1175	5-carboxymethyl-2-hydroxymuconate isomerase	WP_001120984.1
ABUW_RS07460	1.1162	ABC transporter permease	WP_001205190.1
ABUW_RS07505	1.1138	tRNA uridine-5-carboxymethylaminomethyl(34) synthesis enzyme MnmG	WP_000559187.1
ABUW_RS08225	1.1107	alpha/beta hydrolase	WP_001290021.1
ABUW_RS19105	1.1103	hypothetical protein	WP_001070890.1
ABUW_RS19075	1.1051	hypothetical protein	WP_001012847.1
ABUW_RS19080	1.1038	thermonuclease	WP_000861205.1
ABUW_RS07735	1.1031	sensor histidine kinase KdpD	WP_001191611.1
ABUW_RS07660	1.0966	peptide chain release factor N(5)-glutamine methyltransferase	WP_001017509.1
ABUW_RS07605	1.0929	poly-beta-1%2C6-N-acetyl-D-glucosamine N-deacetylase PgaB	WP_001061302.1
ABUW_RS07775	1.0919	hypothetical protein	WP_000756505.1
ABUW_RS07650	1.0916	type 1 glutamine amidotransferase domain-containing protein	WP_000735895.1
ABUW_RS07395	1.0911	DNA-binding response regulator	WP_000526534.1
ABUW_RS08035	1.0891	TonB-dependent siderophore receptor	WP_000527015.1
ABUW_RS07720	1.0799	potassium-transporting ATPase subunit KdpA	WP_000891202.1
ABUW_RS07305	1.0773	TetR/AcrR family transcriptional regulator	WP_000792929.1
ABUW_RS19160	1.0754	hypothetical protein	WP_000661588.1
ABUW_RS08095	1.0722	universal stress protein	WP_001109442.1
ABUW_RS07785	1.0593	hypothetical protein	WP_000920881.1
ABUW_RS08250	1.0587	MFS transporter	WP_071543520.1
ABUW_RS08235	1.0544	PepSY domain-containing protein	WP_000075461.1
ABUW_RS08280	1.0528	nitrate transporter	WP_000039924.1
ABUW_RS07235	1.052	FadR family transcriptional regulator	WP_000572518.1
ABUW_RS07840	1.05	pseudouridylate synthase	WP_000097958.1
ABUW_RS07990	1.0454	oxidoreductase	WP_000920714.1
ABUW_RS08110	1.0389	RDD family protein	WP_000221476.1
ABUW_RS07710	1.0383	dihydroneopterin aldolase	WP_000338779.1

ABUW_RS07600	1.0353	poly-beta-1%2C6 N-acetyl-D-glucosamine export porin PgaA	WP_000913301.1
ABUW_RS07560	1.035	protoheme IX farnesyltransferase	WP_000915319.1
ABUW_RS19300	1.0227	aminoglycoside O-phosphotransferase APH(3'')-Ib	WP_025464697.1
ABUW_RS07930	1.0224	helicase	WP_000808297.1
ABUW_RS08090	1.0174	ABC transporter ATP-binding protein	WP_000193596.1
ABUW_RS08185	1.0159	DNA polymerase III subunit gamma/tau	WP_045887671.1
ABUW_RS07815	0.99981	DUF441 domain-containing protein	WP_000880863.1
ABUW_RS15330	-1.016	hypothetical protein	WP_001001666.1
ABUW_RS09690	-1.0661	zonular occludens toxin	WP_032017212.1
ABUW_RS13220	-1.0776	hypothetical protein	WP_001037898.1
ABUW_RS15280	-1.1274	hypothetical protein	WP_000206132.1
ABUW_RS09695	-1.1693	hypothetical protein	WP_032017213.1
ABUW_RS01270	-1.1982	sulfate permease	WP_001111063.1
ABUW_RS09700	-1.2079	hypothetical protein	WP_032017215.1
ABUW_RS01160	-1.2284	aquaporin Z	WP_001045986.1
ABUW_RS12990	-1.4531	hypothetical protein	WP_001034729.1

Supplementary Table 2: Differentially expressed genes (log_2(fold change) ≥ 1) in *abaM*::Tn26 (compared with AB5075 wild-type).

Gene id	Log_2(Fold change)	Description	NCBI Protein Accession
ABUW_RS07245	2.9052	TetR/AcrR family transcriptional regulator	WP_000590096.1
ABUW_RS07260	2.878	SCPU domain-containing protein	WP_000876475.1
ABUW_RS18365	2.8531	acyl-CoA dehydrogenase	WP_000060267.1
ABUW_RS11870	2.7441	hypothetical protein	WP_000108365.1
ABUW_RS18350	2.6991	RND transporter	WP_000256252.1
ABUW_RS18355	2.6293	non-ribosomal peptide synthetase	WP_001060991.1
ABUW_RS18375	2.554	LuxR family transcriptional regulator	WP_000446790.1
ABUW_RS07265	2.5191	molecular chaperone	WP_001065473.1
ABUW_RS07250	2.4684	SCPU domain-containing protein	WP_000790104.1
ABUW_RS18385	2.4087	N-acylhomoserine lactone synthase	WP_001020940.1
ABUW_RS18370	2.3341	acyl-CoA synthetase	WP_000279948.1
ABUW_RS07255	2.323	protein CsuA	WP_000577009.1
ABUW_RS07270	2.2652	fimbrial biogenesis outer membrane usher protein	WP_000603294.1
ABUW_RS07275	2.1508	protein CsuE	WP_002017500.1
ABUW_RS07145	1.8615	DUF2171 domain-containing protein	WP_001094391.1
ABUW_RS11840	1.7989	stress-induced protein	WP_000024222.1
ABUW_RS08050	1.7574	hypothetical protein	WP_001123841.1
ABUW_RS11875	1.7165	hypothetical protein	WP_000132046.1
ABUW_RS19150	1.5586	hypothetical protein	WP_001024502.1
ABUW_RS19060	1.4374	hypothetical protein	WP_000910917.1
ABUW_RS19165	1.4373	toxic anion resistance protein	WP_000933769.1
ABUW_RS19145	1.4181	transcriptional regulator	WP_000096600.1
ABUW_RS03420	1.4179	tRNA-Asp	-
ABUW_RS01970	1.4088	flavohemoprotein	WP_000188888.1
ABUW_RS19155	1.3734	hypothetical protein	WP_000241707.1
ABUW_RS19115	1.3711	hypothetical protein	WP_001057663.1
ABUW_RS19170	1.3708	hypothetical protein	WP_001093570.1

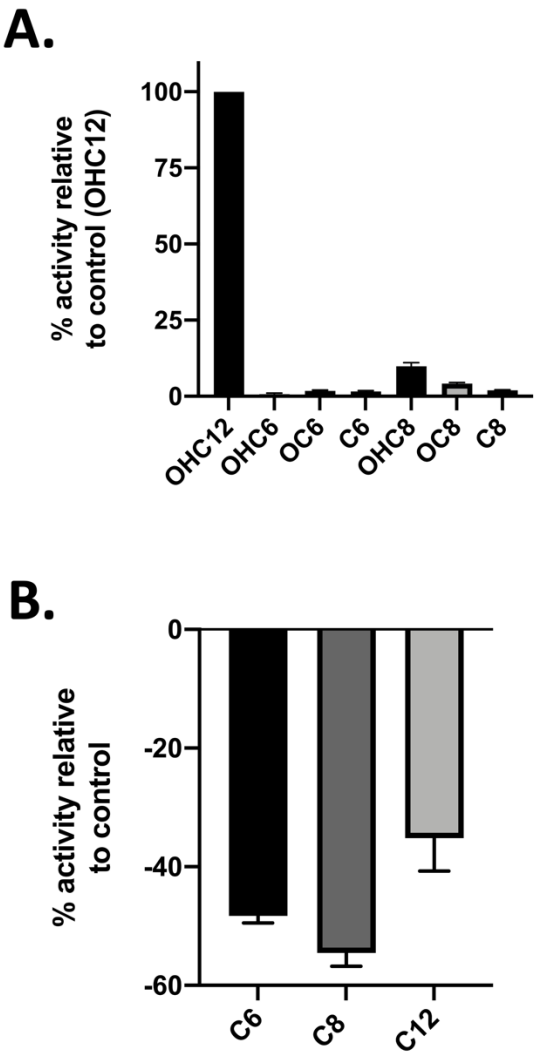
ABUW_RS19140	1.3556	ParA family protein	WP_000724905.1
ABUW_RS13115	1.3406	hypothetical protein	WP_000980495.1
ABUW_RS19080	1.2162	thermonuclease	WP_000861205.1
ABUW_RS19240	1.202	hypothetical protein	-
ABUW_RS19305	1.1854	ANT(3'')-Ia family aminoglycoside nucleotidyltransferase AadA2	WP_001261740.1
ABUW_RS20015	1.1825	hypothetical protein	-
ABUW_RS19065	1.1742	hypothetical protein	WP_000095825.1
ABUW_RS12220	1.1605	hypothetical protein	WP_000008105.1
ABUW_RS19105	1.1574	hypothetical protein	WP_001070890.1
ABUW_RS11885	1.1476	hypothetical protein	WP_001136759.1
ABUW_RS13925	1.1447	23S rRNA (pseudouridine(1915)-N(3))-methyltransferase RlmH	WP_000702193.1
ABUW_RS20020	1.1374	transposition protein TniB	WP_001381192.1
ABUW_RS19595	1.0943	DNA-binding protein	WP_001096616.1
ABUW_RS19110	1.0805	DUF2786 domain-containing protein	WP_000389915.1
ABUW_RS19200	1.0625	hypothetical protein	WP_000790084.1
ABUW_RS19820	1.0579	hypothetical protein	-
ABUW_RS19190	1.0498	hypothetical protein	WP_000701003.1
ABUW_RS19235	1.0446	hypothetical protein	WP_000654348.1
ABUW_RS19180	1.0398	hypothetical protein	WP_000443897.1
ABUW_RS10070	1.0279	Fur family transcriptional regulator	WP_000207886.1
ABUW_RS13010	1.0165	DUF4142 domain-containing protein	WP_000644336.1
ABUW_RS19345	1.0122	molecular chaperone DnaJ	WP_000758689.1
ABUW_RS08580	1.009	DUF159 family protein	WP_000332547.1
ABUW_RS19300	1.0071	aminoglycoside O-phosphotransferase APH(3'')-Ib	WP_025464697.1
ABUW_RS11975	1.003	PaaI family thioesterase	WP_000445634.1
ABUW_RS10685	-0.99885	HU family DNA-binding protein	WP_001043034.1
ABUW_RS14775	-1.0208	outer membrane protein	WP_001202415.1
ABUW_RS17210	-1.0241	Na+/H+ antiporter subunit E	WP_001177202.1
ABUW_RS18725	-1.045	thiol:disulfide interchange protein DsbA/DsbL	WP_000737570.1
ABUW_RS15925	-1.0539	integration host factor subunit alpha	WP_000126166.1
ABUW_RS03825	-1.0607	hypothetical protein	WP_001278744.1

ABUW_RS15280	-1.0657	hypothetical protein	WP_000206132.1
ABUW_RS18190	-1.0826	ATP synthase subunit C	WP_000424060.1
ABUW_RS08725	-1.0884	hypothetical protein	WP_000179560.1
ABUW_RS02765	-1.0913	carbapenem-hydrolyzing class D beta-lactamase OXA-23	WP_001046004.1
ABUW_RS03465	-1.0935	alanine:cation symporter family protein	WP_001005337.1
ABUW_RS09695	-1.0973	hypothetical protein	WP_032017213.1
ABUW_RS17205	-1.1655	monovalent cation/H+ antiporter subunit D	WP_000459267.1
ABUW_RS04295	-1.1868	succinyl-CoA ligase subunit beta	WP_001048573.1
ABUW_RS01270	-1.2922	sulfate permease	WP_001111063.1
ABUW_RS13140	-1.3221	heavy metal-associated domain protein	WP_000770719.1
ABUW_RS14740	-1.3499	hemerythrin	WP_000782976.1
ABUW_RS15385	-1.35	NADH-quinone oxidoreductase subunit K	WP_000529822.1
ABUW_RS17440	-1.4553	membrane protein	WP_000472947.1
ABUW_RS03380	-1.5003	entericidin%2C EcnA/B family	WP_000757214.1
ABUW_RS17200	-1.5374	Na+/H+ antiporter subunit C	WP_000624229.1
ABUW_RS02775	-1.8507	phage tail assembly protein	WP_001071615.1
ABUW_RS12990	-2.1063	hypothetical protein	WP_001034729.1
ABUW_RS00585	-2.1307	hypothetical protein	WP_000770763.1

8.1. Additional experimental results

This section contains some experimental work performed after the thesis submission (September 30th, 2019) and discussed during the *viva voce* examination realized on January 27th, 2020. The data consists in additional agonist/antagonists assays with the *abaI*::Tn*26* P*abaM*::*lux* bioreporter using shorter acyl chain AHLs (6 and 8 carbons length, respectively) that were not available when performing the previous assays (see 4.3.2). For the agonist assay, the 3-hydroxy (OHC6 and OHC8), 3-oxo (OC6 and OC8) and unmodified (C6 and C8) *N*-hexanoyl-L-homoserine lactones and *N*-octanoyl-L-homoserine lactones, respectively, were used. For the antagonist assays, only the unmodified C6 and C8 were used. Materials and methods for these assays are detailed in sections 2.4.6.1 for the agonist assay and 2.4.6.2 for the antagonist assay. General structure of AHLs molecules can be found in section 4.3.1.3 (**Figure 4.3**).

As it can be observed in **Additional Figure 1**, none of the C6 and C8 AHLs were capable of activating AbaR, while both unmodified C6 and C8 were potent competitive antagonists of OHC12, reducing the activity of the promoter fusion by 48% and 54%, respectively, compared to the 35% displayed by the unmodified C12 used as a reference.



Additional Figure 1: Agonist (A) and antagonist (B) assays using medium-length AHLs. (A) Data expressed as % activity relative to the native ligand, OHC12. **(B)** Data expressed as % decreased activity relative to the control (*abaI*::Tn*26* P*abaM*::*lux* + 500 nM OHC12). Strains were grown to an OD600 = 0.5, diluted 1:10 in 96-well plates. AHLs were added to a 1 μM concentration for the agonist (A) assay. OHC12 was added at 500 nM final concentration and the AHL to be tested at 100 μM for the antagonist (B) assay. Plates were incubated at 37°C for 24 h. The RLUs and OD600 were measured every 30 min and the maximum normalized (RLUs/OD600) value was used for the statistical analysis. Error bars indicate standard deviation between three biological replicates.